

12-2011

DETERMINING TRANSVERSE DESIGN FORCES FOR A NEXT-D BRIDGE USING 3D FINITE ELEMENT MODELING

Robert Funcik

Clemson University, rfuncik@g.clemson.edu

Follow this and additional works at: https://tigerprints.clemson.edu/all_theses



Part of the [Civil Engineering Commons](#)

Recommended Citation

Funcik, Robert, "DETERMINING TRANSVERSE DESIGN FORCES FOR A NEXT-D BRIDGE USING 3D FINITE ELEMENT MODELING" (2011). *All Theses*. 1280.

https://tigerprints.clemson.edu/all_theses/1280

This Thesis is brought to you for free and open access by the Theses at TigerPrints. It has been accepted for inclusion in All Theses by an authorized administrator of TigerPrints. For more information, please contact kokeefe@clemson.edu.

DETERMINING TRANSVERSE DESIGN FORCES FOR A NEXT-D BRIDGE
USING 3D FINITE ELEMENT MODELING

A Thesis
Presented to
the Graduate School of
Clemson University

In Partial Fulfillment
of the Requirements for the Degree
Master of Science in
Civil Engineering

by
Robert Michael Funcik
December 2011

Accepted by:
Dr. Scott D. Schiff, Committee Chair
Dr. Bryant G. Nielson
Dr. WeiChiang Pang

ABSTRACT

The South Carolina Department of Transportation (SCDOT) has been building short-span bridges using adjacent precast concrete beams for years in order to decrease construction time for bridges. Concerns have been raised about the durability of the hollow-core bridges that are currently used for this purpose throughout the state. Adjacent beams in a precast concrete bridge are typically connected by grouted shear keys, and many of these bridges experience longitudinal reflective cracking throughout their lifetime. The loss of load sharing between adjacent beams because of these cracks is a concern. As a result of these issues, the SCDOT has decided to pursue an alternative bridge design that utilizes precast components. For this project, the use of a modified version of the Northeast Extreme Tee with integral deck (NEXT-D) has been selected as a viable alternative to the hollow core box beams bridges. However, there are concerns about the distribution of transverse deck forces for the NEXT-D bridge system, which was proposed by the Northeast Chapter of the Precast/Prestressed Concrete Institute (PCINE). This study attempts to address those concerns.

The American Association of State Highway and Transportation Officials (AASHTO) Load and Resistance Factor Design (LRFD) Bridge Design Specifications do not specify a design procedure for the deck of a NEXT-D bridge. Therefore, the objective of this study is to identify the appropriate design forces for this bridge deck. In order to achieve this objective, three dimensional

(3D) finite element models of 40-foot span NEXT-D beam bridges were created using SAP2000. Finite element modeling is a sensitive process, so results from a model made of 3D eight-node solid elements and another model built with four-node shell elements and frame elements were compared in order to check the appropriateness of the results. The models took the stiffness of the shear keys into account by utilizing a frame element that was calibrated to provide appropriate stiffness properties.

Design live loads defined by the AASHTO LRFD Bridge Design Specifications were applied to the bridge models in order to determine the transverse design shear, positive moment, and negative moment for the shear keys and bridge deck. Dead load demands for the bridge were also determined. Through the comparison of the solid and shell models, the shell model was proven to be an acceptable representation of a NEXT-D bridge. The live load demands for the shear key and deck in the six-foot and eight-foot section NEXT-D bridges are shown in Abstract Tables 1 and 2.

Abstract Table 1: Unfactored live load demand in the shear keys and deck for a six-foot section NEXT-D bridge normalized for strip width

	Shear key	Point A/E	Point B/D	Point C	Units
Max shear:	2.8	2.8	1.7	1.1	kip/ft
Max positive moment:	24.8	34.6	46.6	46.8	(kip-in)/ft
Max negative moment:	16.4	27.1	30.9	21.4	(kip-in)/ft

Abstract Table 2: Unfactored live load demand in the shear keys and deck for an eight-foot section NEXT-D bridge normalized for strip width

	Shear key	Point A/E	Point B/D	Point C	Units
Max shear:	2.8	3.3	2.1	1.6	kip/ft
Max positive moment:	34.4	47.4	62.3	56.2	(kip-in)/ft
Max negative moment:	16.8	48.9	51.2	35.0	(kip-in)/ft

These Tables show that the shear key live load demands for the six-foot and eight-foot section were very close for shear and negative moment. However, the shear key live load demand for positive moment in the eight-foot section was significantly higher than for the six-foot section. The live load demands in the deck were significantly higher for the eight-foot section than the eight-foot section for shear, positive moment, and negative moment.

The distribution of force effects throughout the length of the bridge was also explored in order to recommend a design strip width to the SCDOT for the design of NEXT-D bridges. The shear and moment were distributed very well throughout the entire length of the bridge, so strip widths were recommended based on the geometry of the loads. Strip widths were defined for each load so that the strip was equal to the tributary length of one design load. This was done to account for the possibility of having multiple design loads in one lane. Accounting for strip width, the design tandem load specified by AASHTO was found to be the most critical load case. The recommended strip width for the design tandem is ten feet. The values given in Abstract Tables 1 and 2 were found using this strip width. The entire length of the NEXT-D bridge should be designed so that the shear

keys and bridge deck have the capacity to resist the demands given in these Tables.

ACKNOWLEDGEMENTS

First of all, I would like to thank God for leading me to where I am today and for always supporting me.

I would also like the South Carolina Department of Transportation for their making this project (SPR 682 Accelerated Bridge Construction – Precast Alternate for Flat Slab Spans) possible.

I would like to thank my research advisors, Dr. Bryant G. Nielson, Dr. Scott D. Schiff, and Dr. WeiChiang Pang for giving me the opportunity to work on this research team and for always pushing me to complete this project to the best of my ability. I could not have asked for a group of more patient and helpful advisors.

Thank you to my research teammates, Armando Flores Duron, Rob Stevenson, and Huan Sheng as well. It was a pleasure working with them throughout the duration of the project.

I also thank my parents, Thomas Funcik and Christine Donovan for providing the support and encouragement to lead me to this point in my life. Last, but certainly not least, I cannot thank my wife, Emily Funcik, enough for the incredible patience, support, and love that she has shown throughout this entire process.

TABLE OF CONTENTS

	Page
TITLE PAGE	i
ABSTRACT.....	ii
ACKNOWLEDGEMENTS.....	vi
TABLE OF CONTENTS.....	vii
LIST OF TABLES.....	x
LIST OF FIGURES	xvii
CHAPTER	
1. INTRODUCTION.....	1
Project Overview	1
Scope and Objectives.....	1
Outline of Thesis.....	3
2. LITERATURE REVIEW.....	4
NEXT-D Beam Selection	4
AASHTO Deck Design	7
3D Modeling	13
Shear Key Stiffness	20
Conclusions.....	25

Table of Contents (Continued)

	Page
3. ANALYSIS OF 3D NEXT-D BRIDGE MODELS	27
Introduction.....	27
Shear Key Modeling	29
Solid Model.....	34
Shell Model.....	42
Load Application.....	54
Conclusions.....	58
4. RESULTS AND DISCUSSION.....	60
Shear Key Live Load Analysis.....	60
Deck Live Load Analysis	91
Dead Load Analysis.....	98
AASHTO Deck Design	102
Sensitivity Studies	112
5. CONCLUSIONS.....	125
Design Conclusions.....	125
Recommendations for Future Work.....	132

Table of Contents (Continued)

	Page
APPENDICES.....	134
A: Abbreviations Used in this Thesis	134
B: Shear Key Calibration spreadsheet.....	136
C: Shear Key Influence Lines	137
D: Demand Distribution and Accumulation Plots	158
E: Bridge Deck Influence Lines.....	161
REFERENCES	174

LIST OF TABLES

Table	Page
2-1: Equations for calculating equivalent strips for concrete bridge decks (AASHTO 2010).....	9
2-2: Shear key stiffness matrix for a 3 inch section	24
3-1: Frame element stiffness matrix for a six-inch section of shear key	30
3-2: Shear key section properties	33
3-3: Properties of six-ksi Concrete Used in the NEXT-D Models	35
3-4: Parapet section properties.....	45
3-5: Stem section properties.....	47
3-6: Rigid link section properties.....	49
4-1: Maximum shear key demands for a six-foot section NEXT-D bridge under the design tandem loading	67
4-2: Maximum shear key demands for a six-foot section NEXT-D bridge under the single-axle loading.....	67
4-3: Maximum shear key demands for a six-foot section NEXT-D bridge under the two-axle loading.....	68
4-4: Maximum shear key demands for an eight-foot section NEXT-D bridge under the design tandem loading	68

List of Tables (Continued)

Table	Page
4-5: Maximum shear key demands for an eight-foot section NEXT-D bridge under the single-axle loading	69
4-6: Maximum shear key demands for an eight-foot section NEXT-D bridge under the two-axle loading	69
4-7: Maximum shear key demands for a six-foot section NEXT-D bridge without parapets under the design tandem loading	73
4-8: Maximum shear key demands for an eight-foot section NEXT-D bridge without parapets under the design tandem loading.....	74
4-9: Demand per foot for a six-foot NEXT-D bridge based on recommended strip widths	89
4-10: Demand per foot for an eight-foot NEXT-D bridge based on recommended strip widths	89
4-11: Unfactored shear key design live loads for a forty-foot NEXT-D bridge	91
4-12: Unfactored deck design live loads for a six-foot section NEXT-D bridge forty feet in length.....	95

List of Tables (Continued)

Table	Page
4-13: Unfactored deck design live loads for an eight-foot section NEXT-D bridge forty feet in length.....	95
4-14: Unfactored deck design live loads for the outer beams in a six-foot section NEXT-D bridge forty feet in length	97
4-15: Unfactored deck design live loads for the middle beams in a six-foot section NEXT-D bridge forty feet in length	97
4-16: Unfactored deck design live loads for the outer beams in an eight-foot section NEXT-D bridge forty feet in length	97
4-17: Unfactored deck design live loads for the middle beams in an eight-foot section NEXT-D bridge forty feet in length	97
4-18: Dead load and future wearing surface demand for the shear keys in a six-foot section NEXT-D bridge.....	100
4-19: Dead load and future wearing surface demand for the shear keys in an eight-foot section NEXT-D bridge.....	100

List of Tables (Continued)

Table	Page
4-20: Dead load demand for the deck in a six-foot section NEXT-D bridge	101
4-21: Future wearing surface demand for the deck in a six-foot section NEXT-D bridge.....	101
4-22: Dead load demand for the deck in an eight-foot section NEXT-D bridge	101
4-23: Future wearing surface demand for the deck in a six-foot section NEXT-D bridge.....	102
4-24: Unfactored live load demand in the shear keys of a six-foot section NEXT-D bridge.....	105
4-25: Unfactored live load demand in the shear keys of an eight-foot section NEXT-D bridge	105
4-26: Unfactored live load demand in the shear keys of a six-foot section NEXT-D bridge normalized for strip width.....	107
4-27: Unfactored live load demand in the shear keys of an eight-foot section NEXT-D bridge normalized for strip width	107
4-28: Unfactored live load demand in the shear keys and deck for a six-foot section NEXT-D bridge.....	108

List of Tables (Continued)

Table	Page
4-29: Unfactored live load demand in the shear keys and deck for an eight-foot section NEXT-D bridge.....	108
4-30: Unfactored live load demand in the shear keys and deck for a six-foot section NEXT-D bridge normalized for strip width.....	109
4-31: Unfactored live load demand in the shear keys and deck for an eight-foot section NEXT-D bridge normalized for strip width.....	109
4-32: Unfactored dead load demand in the shear keys and deck for a six-foot section NEXT-D bridge normalized for strip width.....	111
4-33: Unfactored dead load demand in the shear keys and deck for an eight-foot section NEXT-D bridge normalized for strip width.....	111
4-34: Unfactored future wearing surface demand in the shear keys and deck for a six-foot section NEXT-D bridge normalized for strip width.....	111
4-35: Unfactored future wearing surface demand in the shear keys and deck for an eight-foot section NEXT-D bridge normalized for strip width.....	111

List of Tables (Continued)

Table	Page
4-36: Unfactored live load shear key demand for eight-foot section NEXT-D bridges of various span lengths	121
5-1: Recommended strip widths in feet	127
5-2: Unfactored live load demand in the shear keys and deck for a six-foot section NEXT-D bridge normalized for strip width	127
5-3: Unfactored live load demand in the shear keys and deck for an eight-foot section NEXT-D bridge normalized for strip width	127
5-4: Unfactored live load demand in the shear keys of a six-foot section NEXT-D bridge normalized for strip width.....	128
5-5: Unfactored live load demand in the shear keys of an eight-foot section NEXT-D bridge normalized for strip width.....	128
5-6: Unfactored dead load demand in the shear keys and deck for a six-foot section NEXT-D bridge normalized for strip width	130

List of Tables (Continued)

Table	Page
5-7: Unfactored dead load demand in the shear keys and deck for an eight-foot section NEXT-D bridge normalized for strip width	130
5-8: Unfactored future wearing surface demand in the shear keys and deck for a six-foot section NEXT-D bridge normalized for strip width	130
5-9: Unfactored future wearing surface demand in the shear keys and deck for an eight-foot section NEXT-D bridge normalized for strip width.....	130

LIST OF FIGURES

Figure	Page
2-1: NEXT-D beam proposed by PCINE (PCI Northeast 2010).....	5
2-2: Revised NEXT-D beam (Deery 2010)	6
2-3: AASHTO HS20 design truck (AASHTO 2010)	11
2-4: AASHTO design tandem (AASHTO 2010)	12
2-5: SAP2000 solid definition window.....	15
2-6: SAP2000 material definition window	16
2-7: Frame to solid connection in SAP2000 using rigid links.....	17
2-8: Frame to solid connection in SAP2000 using body constraints	17
2-9: ANSYS model of the NEXT-D shear key (Flores Duron 2011).....	20
2-10: Boundary conditions and applied displacements for the transverse direction (δ_x) (Flores Duron 2011)	22
2-11: Boundary conditions and applied displacements for the vertical direction (δ_y) (Flores Duron 2011).....	22
2-12: Boundary conditions and applied displacements for the longitudinal direction (δ_z) (Flores Duron 2011).....	22

List of Figures (Continued)

Figure	Page
2-13: Boundary conditions and applied displacements for the rotation about the longitudinal direction (θ_z) (Flores Duron 2011).....	23
2-14: Force versus displacement curve for transverse	23
2-15: Definition of shear key local axes	24
3-1: Dimensions for the six-foot NEXT-D bridge model.....	28
3-2: Dimensions for the eight-foot NEXT-D bridge model.....	29
3-3: Definition of shear key local axes for 3D model.....	30
3-4: Element stiffness matrix for beam elements with inclusion of shear deformations (Nielson 2011)	31
3-5: Simple shear key test model	33
3-6: Shear key connection in solid model	34
3-7: Parapet dimensions (SCDOT 2008).....	36
3-8: Restraints for solid model.....	38
3-9: SAP2000 8' NEXT-D solid model.....	39
3-10: Legend for Figure 3-11 and Figure 3-12.....	39
3-11: Solid modeling layout for eight-foot NEXT-D section.....	40
3-12: Solid modeling layout for six-foot NEXT-D section	41
3-13: Shear key connection in shell model	42

List of Figures (Continued)

Figure	Page
3-14: Parapet in section designer	45
3-15: NEXT beam with stem highlighted	46
3-16: Stem in section designer	47
3-17: Restraints for shell model	50
3-18: SAP2000 eight-foot NEXT-D shell model	51
3-19: Legend for Figure 3-20 and Figure 3-21	52
3-20: Shell modeling layout for eight-foot NEXT-D section.....	52
3-21: Shell modeling layout for six-foot NEXT-D section	53
3-22: Design tandem transverse load placement	55
3-23: Design tandem longitudinal load placement.....	56
3-24: Critical locations for deck demand.....	57
4-1: Uniformly distributed area load.....	61
4-2: Legend for shear key influence lines	62
4-3: Shear influence line for the shear keys in a six-foot section NEXT-D bridge under a design tandem loading at mid-span	63
4-4: Moment influence line for the left side of the shear keys in a six-foot section NEXT-D bridge under a design tandem loading at mid-span	63

List of Figures (Continued)

Figure	Page
4-5: Moment influence line for the right side of the shear keys in a six-foot section NEXT-D bridge under a design tandem loading at mid-span	64
4-6: Shear influence line for the shear keys in an eight-foot section NEXT-D bridge under a design tandem loading at mid-span.....	65
4-7: Moment influence line for the left side of the shear keys in an eight-foot section NEXT-D bridge under a design tandem loading at mid-span	66
4-8: Shear influence line for the shear keys in a six-foot section NEXT-D bridge without parapets under a design tandem loading at mid-span	71
4-9: Moment influence line for the left side of the shear keys in a six-foot section NEXT-D bridge without parapets bridge under a design tandem loading at mid-span	71
4-10: Shear influence line for the shear keys in an eight-foot section NEXT-D bridge without parapets under a design tandem loading at mid-span.....	72

List of Figures (Continued)

Figure	Page
4-11: Moment influence line for the left side of the shear keys in an eight-foot section NEXT-D bridge with no parapets bridge under a design tandem loading at mid-span	72
4-12: Critical load location for shear for a six-foot section NEXT-D bridge	76
4-13: Shear influence line for the shear keys in a six-foot section NEXT-D bridge without parapets under a design tandem loading at the critical shear location	76
4-14: Critical load location for positive moment for a six-foot section NEXT-D bridge	77
4-15: Moment influence line for the shear keys in a six-foot section NEXT-D bridge without parapets under a design tandem loading at the critical positive moment location	77
4-16: Critical load location for negative moment for a six-foot section NEXT-D bridge	78

List of Figures (Continued)

Figure	Page
4-17: Moment influence line for the shear keys in a six-foot section NEXT-D bridge without parapets under a design tandem loading at the critical negative moment location.....	78
4-18: Critical load location for shear for an eight-foot section NEXT-D bridge.....	79
4-19: Shear influence line for the shear keys in an eight-foot section NEXT-D bridge without parapets under a design tandem loading at the critical shear location.....	79
4-20: Critical load location for positive moment for an eight-foot section NEXT-D bridge.....	80
4-21: Moment influence line for the shear keys in an eight-foot section NEXT-D bridge without parapets under a design tandem loading at the critical positive moment location.....	80
4-22: Critical load location for negative moment for an eight-foot section NEXT-D bridge.....	81

List of Figures (Continued)

Figure	Page
4-23: Moment influence line for the shear keys in an eight-foot section NEXT-D bridge without parapets under a design tandem loading at the critical negative moment location.....	81
4-24: Shear in each shear key element of Key 5 along the length of an eight-foot section NEXT-D bridge with load at the critical shear location	83
4-25: Shear accumulation plot for Key 5 of an eight-foot section NEXT-D bridge with load at the critical shear location	83
4-26: Moment in each shear key element of Key 4 along the length of an eight-foot section NEXT-D bridge with load at the critical positive moment location	84
4-27: Moment accumulation plot for Key 4 of an eight-foot section NEXT-D bridge with load at the critical positive moment location	84
4-28: Moment in each shear key element of Key 5 along the length of an eight-foot section NEXT-D bridge with load at the critical negative moment location.....	85

List of Figures (Continued)

Figure	Page
4-29: Moment accumulation plot for Key 5 of an eight-foot section NEXT-D bridge with load at the critical negative moment location.....	85
4-30: Moment accumulation plot for an eight-foot section NEXT-D bridge under the design tandem loading at the critical positive moment case	86
4-31: Design tandem strip width determination.....	87
4-32: Single-axle strip width determination.....	88
4-33: Two-axle strip width determination	88
4-34: Critical slab locations.....	92
4-35: Shear influence line for the critical deck locations in the third beam from the left in an eight-foot section NEXT-D bridge	94
4-36: Moment influence line for the critical deck locations in the third beam from the left in an eight-foot section NEXT-D bridge	94
4-37: Shear influence lines for the shear keys in a six-foot section NEXT-D bridge using the AASHTO strip width method	103

List of Figures (Continued)

Figure	Page
4-38: Moment influence lines for the shear keys in a six-foot section NEXT-D bridge using the AASHTO strip width method.....	104
4-39: Shear influence lines for the shear keys in an eight-foot section NEXT-D bridge using the AASHTO strip width method.....	104
4-40: Moment influence lines for the shear keys in an eight-foot section NEXT-D bridge using the AASHTO strip width method.....	105
4-41: Transverse shear in shear key vs. shear key stiffness for critical shear load location	113
4-42: Transverse moment in shear key vs. shear key stiffness for critical positive moment load location	114
4-43: Transverse moment in shear key vs. shear key stiffness for critical negative moment load location.....	114
4-44: Transverse shear in shear key vs. stem stiffness for critical shear load location.....	116
4-45: Transverse moment in shear key vs. stem stiffness for critical positive moment load location	117

List of Figures (Continued)

Figure	Page
4-46: Transverse moment in shear key vs. stem stiffness for critical negative moment load location	117
4-47: Span length research model.....	119
4-48: Total transverse moment vs. span length.....	119
4-49: Unfactored live load shear demand in the shear key vs. span length for an eight-foot section NEXT-D bridge.....	122
4-50: Unfactored live load positive moment demand in the shear key vs. span length for an eight-foot section NEXT-D bridge	122
4-51: Unfactored live load negative moment demand in the shear key vs. span length for an eight-foot section NEXT-D bridge	123

Chapter 1

INTRODUCTION

Project Overview

For years, the SCDOT has been using precast concrete bridges to speed up the construction process. In the past, hollow-core box beam bridges have been used to build such bridges, but concerns have been raised about the durability of these bridges. In precast bridges, the adjacent beams are typically connected by grouted shear keys. Many of these bridges experience longitudinal reflective cracking throughout their lifetime. This causes a concern about their ability to maintain load sharing between adjacent beams in addition to the resulting water infiltration. As a result of these issues, the SCDOT has decided to pursue an alternative bridge design that utilizes precast components and has identified the NEXT-D beam as a viable alternative (Deery 2010). NEXT-D bridges are characterized by precast double-tee sections connected together using a full depth, cast-in-place shear key.

Scope and Objectives

The AASHTO LRFD Bridge Design Specifications does not currently address the design of NEXT-D beams (AASHTO 2010), so the South Carolina Department of Transportation (SCDOT) requires a method for designing NEXT-D bridges.

Therefore, the primary objective of this study is to analyze 3D NEXT-D bridge models in SAP2000 (Computers and Structures 2011b) to determine the shear and moment demand in the shear key and the slab for short-span NEXT-D bridges (between 22 feet and 40 feet).

A previous study utilized finite element modeling to determine the predicted stiffness properties of the proposed shear key (Flores Duron 2011). This project implements those results into the full-scale 3D finite element models. The use of a six-foot NEXT-D section and an eight-foot NEXT-D section were investigated because selections of these widths allow the SCDOT versatility in the overall width of their bridges.

The bridge was modeled using two different methods in order to verify the results of the study. One model was built using 3D eight-node solid elements for the NEXT-D beam and the parapets. The other model used four-node shell elements to represent the slab and frame elements to represent the stem and the parapets. The slab was connected to the stems and the parapets using rigid links. In both models, the shear key was represented by a frame element that was calibrated to the stiffness values proposed by Flores Duron (2011). Once the two types of models were calibrated to produce the same results, the shell model was used to gather data because it is more computationally efficient and less time consuming to work with than the solid element model.

The HS20 design truck and design tandem loads specified in the AASHTO LRFD Bridge Design Specifications (AASHTO 2010) were applied to the bridge models in order to determine the transverse shear, positive moment, and negative moment in the shear keys and deck of a 40-foot NEXT-D bridge. Dead load demands were also determined for the bridge. The distribution of transverse forces throughout the length of the bridge was also monitored so that a design strip width could be recommended to the SCDOT. Recommendations are provided for both the six-foot and eight-foot NEXT-D sections.

Outline of Thesis

The research and work performed in this project are presented in Chapters 2 through 5. Chapter 2 discusses the current method provided by the AASHTO LRFD Bridge Design Specifications for designing bridge decks, 3D modeling techniques for bridges, and the stiffness of the grouted shear key used in this project. Chapter 3 describes the modeling parameters used to model the NEXT-D bridge in SAP2000 along with the techniques used to determine design forces in the shear keys and bridge deck. Chapter 4 provides the results of the 3D models and a comparison with the current AASHTO deck design method. Chapter 5 discusses the most important results of the project including the live load, dead load, and future wearing surface demands that the keys and deck of a NEXT-D bridge should be designed for. It also discusses recommendations for future work regarding this project.

Chapter 2

LITERATURE REVIEW

NEXT-D Beam Selection

Adjacent precast, prestressed concrete beam bridges are a very important component of the arsenal of Departments of Transportation (DOTs) across the country. Today, the Federal Highway Administration (FHWA) places a large emphasis on building bridges as quickly and safely as possible. Building bridges quickly limits the disruptions and costs associated with temporarily closing roads or reducing the number of available traffic lanes. However, the FHWA understands that speed is not worth sacrificing quality and durability, so they have adopted the slogan of “Get in, Get out, and Stay out” (AASHTO Technology Implementation Group 2002). The main technology driving this philosophy is the development of prefabricated elements. The SCDOT has built precast bridges in the past, but concerns have been raised about their durability and service-level performance. Up until this point, precast bridges built in South Carolina have mainly consisted of flat slab or hollow core sections. One of the main issues with these bridges has been the longitudinal reflective cracks that have been forming along the shear key. A shear key is a section of cast in place grout between adjacent precast beams that is designed to transfer loads between beams. Cracks can also lead to the infiltration of water and deicing salts between the members of the bridge which can lead to corrosion of the reinforcing steel in the

bridge. As a result of these issues, the SCDOT has decided to pursue an alternative bridge design that utilizes precast components. For this project, the use of a modified version of the Northeast Extreme Tee with integral deck (NEXT-D) has been selected as a viable substitute to the hollow-core box beams bridges (Deery 2010). The NEXT-D beam is a double tee beam that is connected to adjacent beams using a full-depth grouted keyway that is located between the stems of adjacent beams. It was originally proposed by the Northeast Chapter of the Precast/Prestressed Concrete Institute (PCINE) (PCI Northeast 2010). The NEXT-D beam proposed by PCINE is shown below in Figure 2-1.

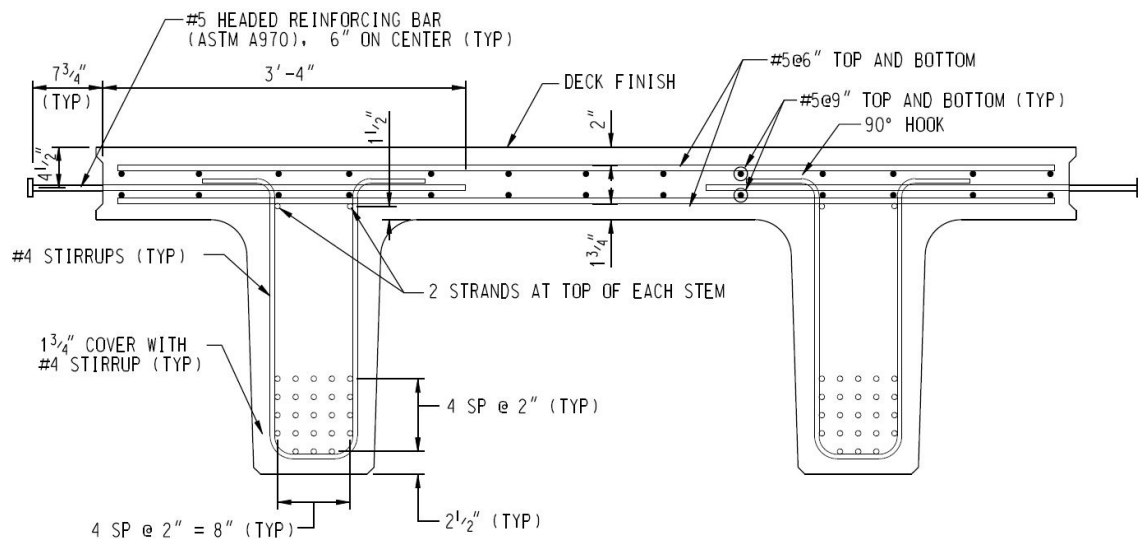


Figure 2-1: NEXT-D beam proposed by PCINE (PCI Northeast 2010)

The NEXT-D beam was chosen by an SCDOT steering committee as the best alternative to the current solutions based on several factors. The NEXT-D beam reduces complications for fabricators because it does not require void material or shear studs, both of which increase fabrication cost. Also, on low volume roads, a NEXT-D bridge will not require any overlay. The keys can simply be filled with grout, then the entire surface can be ground smooth and the bridge can be opened for traffic. For high volume roads, an overlay can be placed and used as the wearing surface. The NEXT-D section is also a wide section, thus requiring fewer sections to build a bridge which results in shorter construction times. One drawback of the NEXT-D beam is that it was heavier than the other alternatives. This would mean that the contractors responsible for building the bridges would need access to large cranes, and bridges may be more difficult to construct. However, the fact that the NEXT-D beam does not require a cast-in-place deck and that the key is very simple to grout outweighed the disadvantage of being such a heavy section (Deery 2010).

AASHTO Deck Design

Introduction

The design of the bridge deck is a vital portion of the design of a bridge. Bridge design typically follows a top-down approach, meaning that the deck is often the first component of the bridge that is designed. The AASTHO LRFD Bridge Design Specifications provide standard measures for designing bridge decks for

common bridge types used throughout the country (Tonias and Zhao 2007). However, the 2010 edition does not address issues that arise with NEXT-D bridges. The Design Specifications allow for finite element analysis of bridges to determine design loads, but this is not a practical method for the SCDOT to design NEXT-D bridges. These bridges are intended to be used for short span bridges throughout the state, so modeling each of these bridges would be time consuming, and many engineers do not have the experience necessary to create such a model. Therefore, 3D models of NEXT-D bridges were created using SAP2000 and analyzed to determine a proper yet simplified design procedure for NEXT-D bridge decks.

AASHTO Strip Width Method

The most common way that slabs are designed is the Approximate, or Strip Width Method specified in Section 4.6.2.1 of the AASHTO LRFD Bridge Design Specifications (AASHTO 2010). In this method, the deck is divided into strips perpendicular to the supporting components. In the case of a NEXT-D bridge, the supporting components are the stems of the precast sections. The equivalent strip width is a function of the spacing of the supporting components. For this project, a six-foot NEXT-D beam and an eight-foot NEXT-D beam were analyzed. In the case of the 8-foot section, the stem spacing was not uniform, and the AASHTO LRFD Bridge Design Specifications do not address this issue. Table 2-1 shows the equations for calculating the equivalent strip widths for concrete bridge decks where X is the distance from load to point of support in feet, S is the

spacing of supporting components in feet, and the $+M$ or $-M$ defines whether the equation applies to the positive or negative moment (AASHTO 2010).

Table 2-1: Equations for calculating equivalent strips for concrete bridge decks (AASHTO 2010)

Type of Deck	Direction of Primary Strip Relative to Traffic	Width of Primary Strip (in)
Cast-in-place	Overhang	$45.0 + 10.0X$
	Either Parallel or Perpendicular	$+M: 26.0 + 6.6S$ $-M: 48.0 + 3.0S$
Cast-in-place with stay-in-place concrete formwork	Either Parallel or Perpendicular	$+M: 26.0 + 6.6S$ $-M: 48.0 + 3.0S$
Precast, post-tensioned	Either Parallel or Perpendicular	$+M: 26.0 + 6.6S$
		$-M: 48.0 + 3.0S$

The developer of the NEXT beam has brought up concerns about what dimension should be used for the spacing of supporting components for NEXT beams that do not have uniform stem spacing (Culmo 2011). Furthermore, AASHTO states that, “Values provided for equivalent strip widths and strength requirements in the secondary direction are based on past experience. Practical experience and future research work may lead to refinement” (AASHTO 2010). In this study, the strip width method will be tested by the 3D models of NEXT-D bridges and a recommendation will be made addressing the issue of calculating strip widths for NEXT-D bridges.

Once the equivalent strip width has been determined, the strip is treated as a continuous beam, with the supporting components acting as infinitely rigid supports (AASHTO 2010). The live loads defined in the AASHTO LRFD Bridge Design Specifications are then moved across the deck laterally in order to determine the maximum positive and negative moment demands.

The assumption that the strip is a continuous beam is not actually true for bridges built using NEXT-D beams because the shear key does not provide the same stiffness as the rest of the slab. Furthermore, the stems do not provide infinitely rigid supports for the slab. In fact, the stiffness of the stem decreases at points further away from the ends of the bridge, and the stiffness of the stem will also decrease as the span of the bridge increases. The effect of these assumptions on the calculated force effects on the slab and shear key will also be investigated by analysis of the 3D models.

AASHTO Live Loads

The live loads that are used to determine the demand in the slab are given in Chapter Three of the AASHTO LRFD Bridge Specifications (AASHTO 2010). The deck is to be designed for either an HS20 design truck or a design tandem. The HS20 design truck consists of an eight-kip front axle and a 32-kip rear axle on the tractor, and a 32-kip axle load on the trailer. The axle loads are split evenly between the driver's side and passenger's side of the truck and the tires on an axle are spaced six feet apart. The spacing between axles on the tractor is 14

feet and the spacing between the rear axle of the tractor and the trailer axle is a minimum of 14 feet but not more than 30 feet. The spacing used should maximize the demand of the design. The HS20 design truck is shown in Figure 2-3. The design tandem consists of two 25-kip axles with six feet between each tire on an axle and four feet between axles. The design tandem is shown in Figure 2-4.

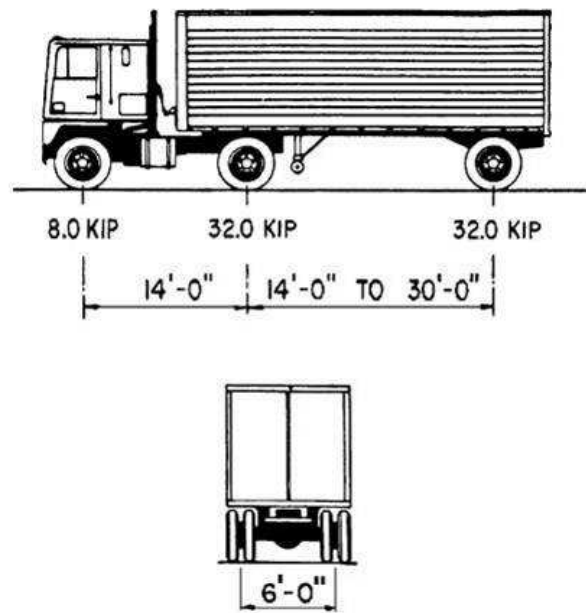


Figure 2-3: AASHTO HS20 design truck (AASHTO 2010)

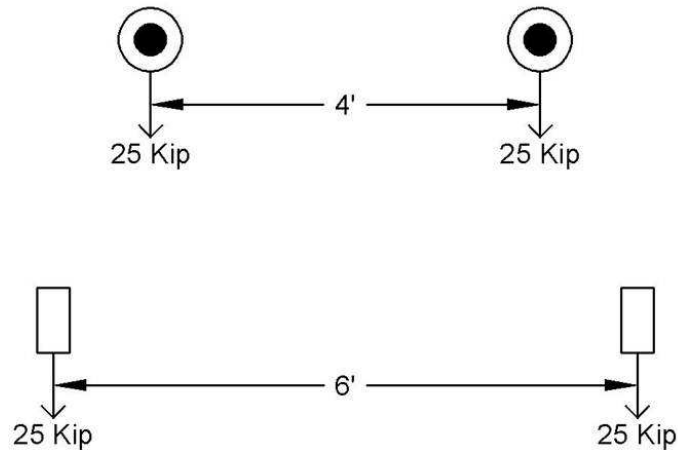


Figure 2-4: AASHTO design tandem (AASHTO 2010)

The tires for both cases are specified to have an effective contact area with a width of 20 inches and a length of ten inches. The force of the tire is to be uniformly distributed over the contact area (AASHTO 2010). The AASHTO LRFD Bridge Specifications state that only the HS20 design truck and design tandem need to be considered in the design of the deck, meaning that the design lane load does not need to be considered. This is because the lane load is specified for the design of elements that are impacted by a continuous line of traffic and the lane load would not produce the critical demand on the deck. It also states that the amplification of the wheel loads from centrifugal and braking forces can be ignored (AASHTO 2010).

3D Modeling

Introduction

For this project, NEXT-D bridges were modeled three dimensionally in order to determine the shear and moment demands for the key and slab based on the AASHTO design loads specified in the AASHTO LRFD Bridge Design Specifications. As per the request of the SCDOT, this project is to focus on bridge spans of 22 to 40 feet which led to the selection of bridge dimensions for 3D modeling. The FHWA provides guidelines for the refined analysis of deck slabs. They state that plate, shell, or solid elements may be used to model a bridge deck for refined deck analysis. However, plates cannot be used as part of 3D models that include decks and girders because they do not account for in plane forces in the deck. Shell and solid elements are both acceptable methods of modeling bridge decks, although shell elements are easier to work with because the output for the deck forces is more convenient for design (Federal Highway Administration 2011).

Finite element modeling is very sensitive to the model inputs, so it is important to establish certain checks in order to ensure that results come as close as possible to representing reality. For this project, one 3D model was build using solid elements to represent the NEXT-D sections and parapets, and another type of model was built using shell elements to represent the bridge deck and frame elements to represent the stems and parapets. Once the shell model was proven

to provide the same results as the solid model, the shell model was used going forward to analyze the NEXT-D bridge due to the numerical simplicity of the shell model compared to the solid model. SAP2000 was used as the structural analysis finite element modeling software for this project, and the simplicity of the shell model allowed for much faster run times in analyzing various load cases compared to the solid model.

Solid Modeling

For the solid model, solid elements were used to represent the entire NEXT-D section along with the parapets. “The solid element is an eight-node element that is based on an isoparametric formulation that includes nine optional incompatible bending modes” (Computers and Structures 2011a). It is very important to ensure that the incompatible bending modes option is turned on to achieve accurate results. This feature is selected during the definition of a solid section. The material is also specified in the solid element definition. Material properties include modulus of elasticity (E), shear modulus (G), Poisson’s ratio (ν), coefficient of thermal expansion (α), and mass density (m) or weight density (w). E , G , ν , and α can all be defined as direction specific (Computers and Structures 2011a). However, because concrete is assumed to be isotropic, this option was not utilized for the solid model used in this project. SAP2000 has built in material

properties for different concrete mixes of various strengths, so these predefined materials were utilized to define the material for the solid elements used in the model. Figure 2-5 shows the SAP2000 solid definition window, while the material definition window is shown in Figure 2-6.

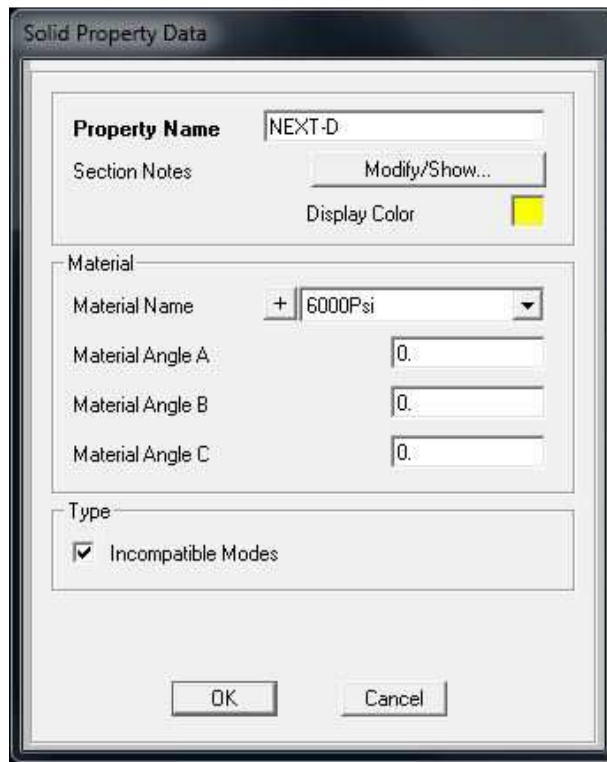


Figure 2-5: SAP2000 solid definition window

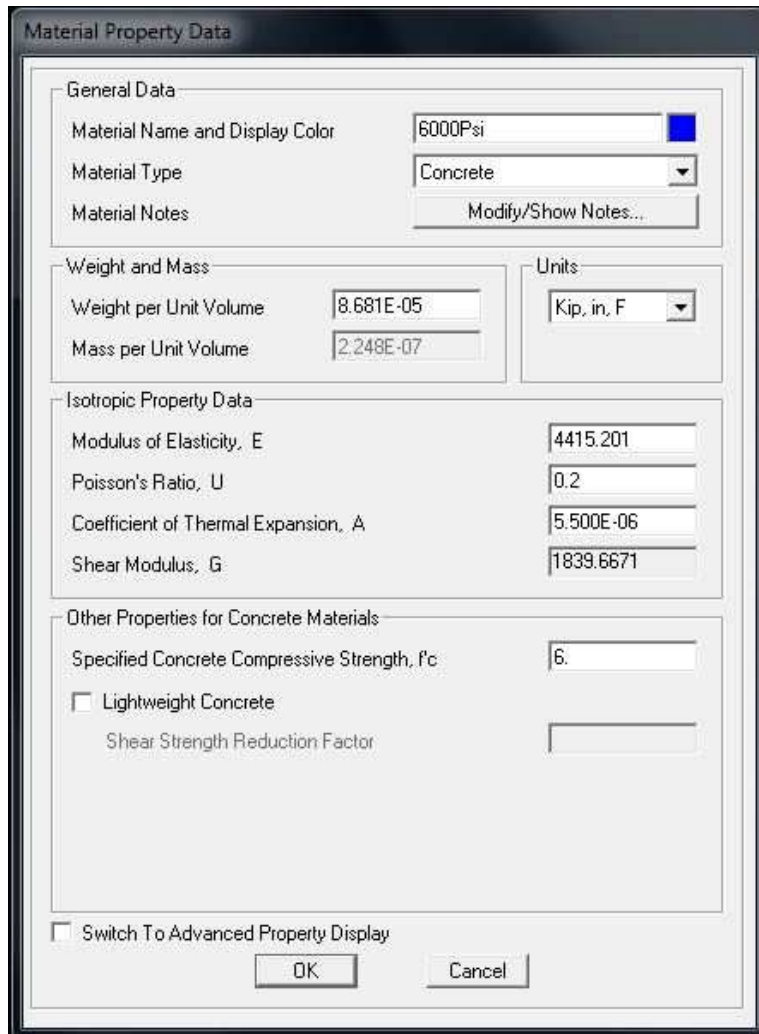


Figure 2-6: SAP2000 material definition window

One of the problems with modeling the bridge using solid elements arises from the fact that the solid elements in SAP2000 only have translational degrees of freedom at the nodes (Computers and Structures 2011a). For this model, it was necessary to connect a frame element to the nodes of solid elements and obtain internal moments from the frames because the shear keys were modeled using

frame elements. When a frame element is connected to a node on a solid element, no moment or torsion is transferred. This problem can be avoided through the use of rigid links or body constraints (CSI Wiki Knowledge Base 2011). These two possible solutions are shown in Figures 2-7 and 2-8.

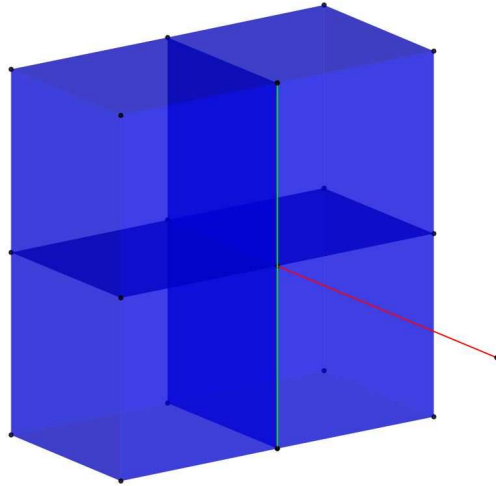


Figure 2-7: Frame to solid connection in SAP2000 using rigid links

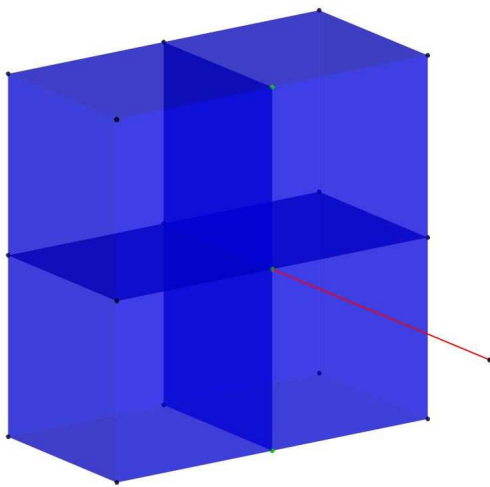


Figure 2-8: Frame to solid connection in SAP2000 using body constraints

In Figure 2-7, the green frame member represents the rigid link used to connect the red frame member to the node shared by the four solid elements. A rigid link is a member that is defined to be extremely rigid so it does not contribute to any additional deformation to a structure. In Figure 2-8, the green dots represent the body constraints. Body constraints require the nodes that are constrained to rotate and translate together. Using body constraints reduces the number of degrees of freedom in a model, which makes the model less computationally complex. However, the rigid link solution is much easier to implement because constraints cannot be replicated and a separate body constraint would have to be defined for each shear key member (CSI Wiki Knowledge Base 2011). For these reasons, the rigid link solution was chosen for the solid model used in this project.

Shell Modeling

In the formulation of the shell model, shell elements were used to represent the bridge deck, while frame elements were used to represent the stems and the parapets. “The shell element is a three- or four-node formulation that combines membrane and plate-bending behavior” (Computers and Structures 2011a). Shell elements are often used to model floor systems, wall systems, and bridge decks. In order to ensure accurate results, it is important to keep the aspect ratio of the longest side to the shortest side of a rectangular shell element as close to unity as possible, and the ratio should at least be less than four, and never greater

than ten. A shell element in SAP2000 has all six degrees of freedom at each node (Computers and Structures 2011a).

There are two different shell formulations. There is the thick-plate (Mindlin/Reissner) formulation, which includes the effects of transverse shear deformation, and the thin-plate (Kirchhoff) formulation, which ignores the contributions of shearing deformation. In general, the thick-plate formulation is more accurate, but it is more sensitive to large aspect ratios and can result in inaccurate results in such cases. In this study, both formulations were used and compared to the solid model in order to determine which formulation is better suited for this application. In general, the solid element is assumed to provide the most realistic results (CSI Wiki Knowledge Base 2011).

The main problem that arises with the use of shell elements for modeling a 3D bridge is accurately modeling the geometry of the different members in relation to each other. This problem was solved through the use of rigid links. When a shell member is drawn in SAP2000, it is depicted as a plane, and when a frame member is drawn, it is depicted as a line. In reality, the shell and the frame actually possess three dimensional geometries. For example, for a NEXT-D bridge, the centroid of the bridge slab and the bridge stem are separated. In order to model this geometric relationship, members can be drawn at their centroid, and then connected using rigid links (Computers and Structures 2011a).

Shear Key Stiffness

The stiffness properties of the shear key used in the 3D analyses of the NEXT-D bridges for this project were based on previous research (Flores Duron 2011). Flores Duron (2011) used the finite element software ANSYS 12.0 (ANSYS 2009) to model the shear key to be used in this project and determined its translational and rotational stiffness, which were needed in order to create an accurate 3D model of the entire bridge. A depiction of this model is shown in Figure 2-9.

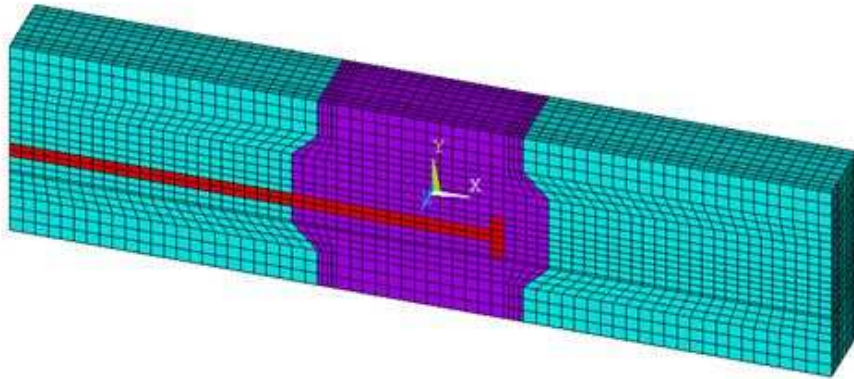


Figure 2-9: ANSYS model of the NEXT-D shear key (Flores Duron 2011)

Once the key had been modeled and calibrated, load-displacement and moment-rotation relationships were determined to attain the required stiffness properties of the shear key. Figures 2-10 through 2-13 show the applied loads and displacements that were used to determine the translational and rotational stiffness of the shear key. Based on the load-displacement curves for the above

configurations, a stiffness matrix was determined for the proposed shear key. An example of one of the force-deformation plots is shown in Figure 2-14 (Flores Duron 2011).

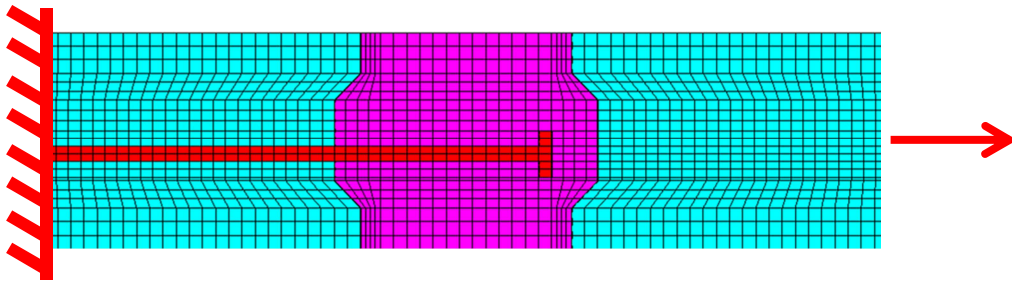


Figure 2-10: Boundary conditions and applied displacements for the transverse direction (δ_x) (Flores Duron 2011)

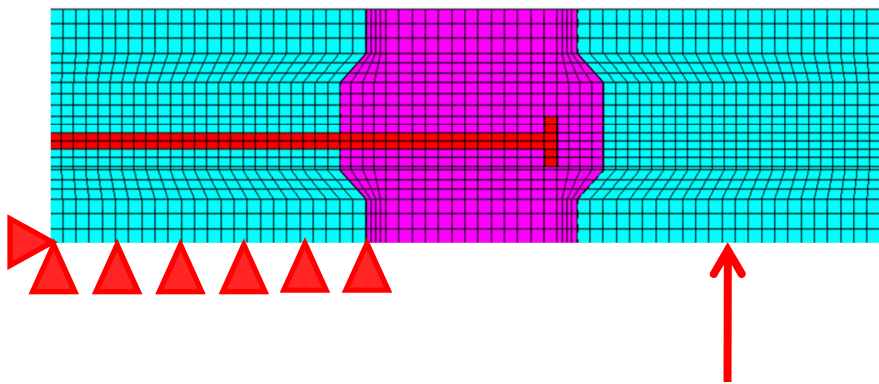


Figure 2-11: Boundary conditions and applied displacements for the vertical direction (δ_y) (Flores Duron 2011)

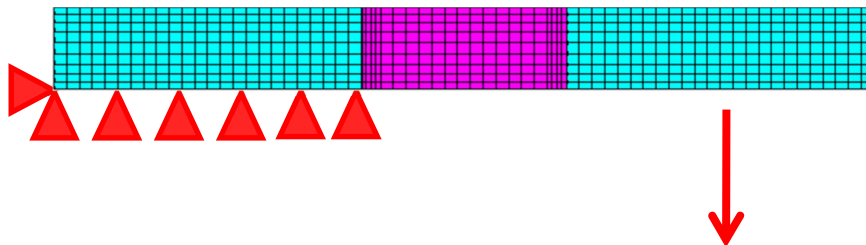


Figure 2-12: Boundary conditions and applied displacements for the longitudinal direction (δ_z) (Flores Duron 2011)

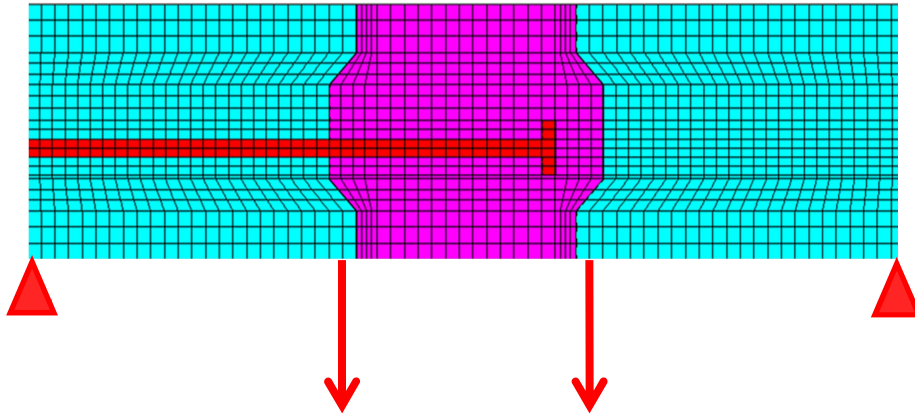


Figure 2-13: Boundary conditions and applied displacements for the rotation about the longitudinal direction (θ_z) (Flores Duron 2011)

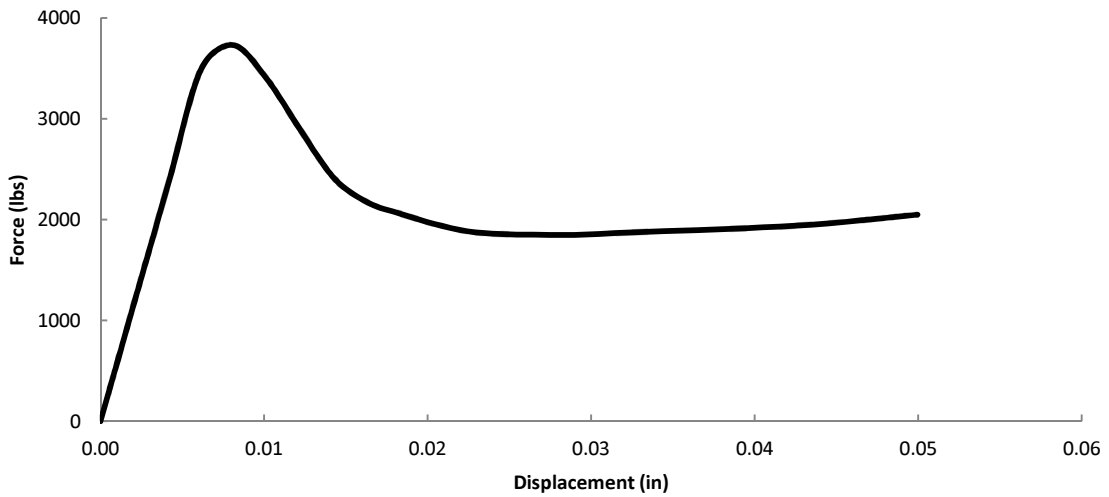


Figure 2-14: Force versus displacement curve for transverse translation (δ_x) (Flores Duron 2011)

From the initial slope of the load-displacement and moment-rotation curves, Flores Duron (2011) was able to propose the stiffness matrix in Table 2-2 which represents a three inch wide section of the shear key. The shear key local axes which correspond to the stiffness labels are identified in Figure 2-15.

Table 2-2: Shear key stiffness matrix for a 3 inch section of shear key (Flores Duron 2011)

	δ_x	δ_y	δ_z	θ_z
δ_x	1201 kip/in	0	0	0
δ_y		110.1 kip/in	0	256.8 kip/rad
δ_z		(Symmetric)	408.5 kip/in	0
θ_z				2952.7 (kip-in)/rad

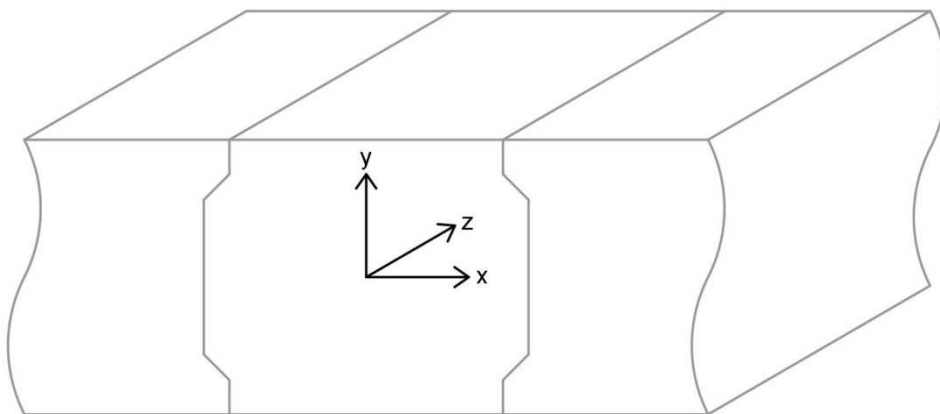


Figure 2-15: Definition of shear key local axes

Flores Duron (2011) determined that the pre-cracking stiffness of the shear key was based primarily on the bond strength between the grout and the concrete deck. Therefore, the 3D models in this project utilized the stiffness values for the shear key proposed in this work, even though the shear key configuration to be used in the testing is currently being updated to include reinforcement details different than those modeled by Flores Duron (2011). However, it is recommended that the new shear key configuration be modeled and analyzed in ANSYS 12.0. The 3D bridge models should then be updated with the new shear and rotational stiffness values based on the new configuration. It is important to note that Flores Duron's (2011) ANSYS model depicted a three-inch section of shear key. In the bridge models used in this project, the shear key members were spaced at six inches, so the stiffness properties that were used in the bridge models were double suggested values.

Conclusions

The deck design and shear key design of a bridge are vital for the safety and durability of a bridge. The NEXT-D beam has been suggested as an alternative to the current precast sections being used by the SCDOT today as a way to improve the durability, cost, and construction time of bridges in the state. The AASHTO LRFD Bridge Design Specifications contain a design procedure for the decks of many standard bridges, but the NEXT-D beam is not included in these specifications. In order to establish the demand in the shear key and deck of a

NEXT-D bridge, 3D models using either solid elements or shell and frame elements were created using SAP2000. The two types of models were compared as a check on the accuracy of the models. The design forces recommended in the AASHTO LRFD Bridge Design Specifications were applied to the bridge in order to obtain these design values. In order to model the bridge accurately, the section proposed by Deery (2010) was used along with the shear key stiffness proposed by Flores Duron (2011).

Chapter 3

ANALYSIS OF 3D NEXT-D BRIDGE MODELS

Introduction

In order to provide recommendations to the SCDOT for the design of NEXT-D bridges, it was necessary to create three dimensional models of bridges built with NEXT-D beams. The finite element structural analysis software used to model the bridges was SAP2000 (Computers and Structures 2011b). Finite element modeling is very sensitive to many different parameters that go into the building of a model, so two different types of models were created in order to compare results to ensure realistic analysis of the bridge. One of the models used solid elements to represent the parapets, deck, and stems. The other type of model used shell elements to represent the bridge deck and frame elements to represent the parapets and stems. The shell elements were connected to the stems and parapets using rigid links. In both types of models, the shear keys were represented by frame elements that were designed to exhibit the properties recommended by Flores Duron (2011). AASHTO design loads were applied to the bridge, and then the shear keys and slab were analyzed to determine the shear and moment demand for the shear keys and various locations in the slab. The design values from the 3D model were compared to a 2D model which used the assumptions provided by the AASHTO strip width method. Several sensitivity studies were also performed for various parameters. These parameters included

shear key stiffness, stem stiffness, and span length. The main bridge analyzed in this project was 40 feet long and 47 feet and four inches wide. The bridge was supported six inches in from each end which was considered to be the center of bearing. The six-foot NEXT-D bridge model consists of eight NEXT-D beams and seven shear keys. The eight-foot NEXT-D model consists of six NEXT-D beams and five shear keys. The dimensions of the six-foot and eight-foot models are shown in Figures 3-1 and 3-2.

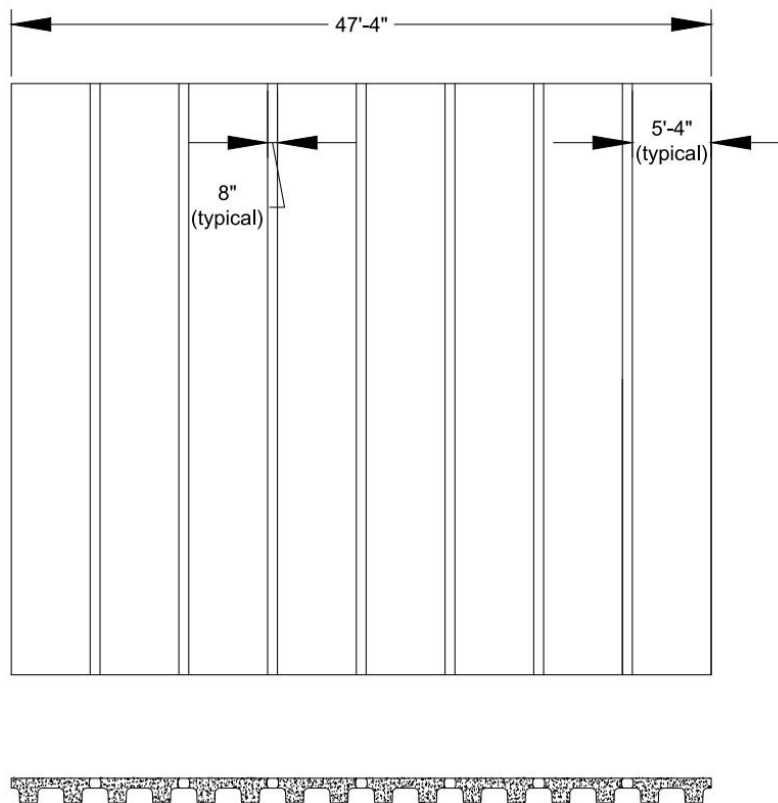


Figure 3-1: Dimensions for the six-foot NEXT-D bridge model

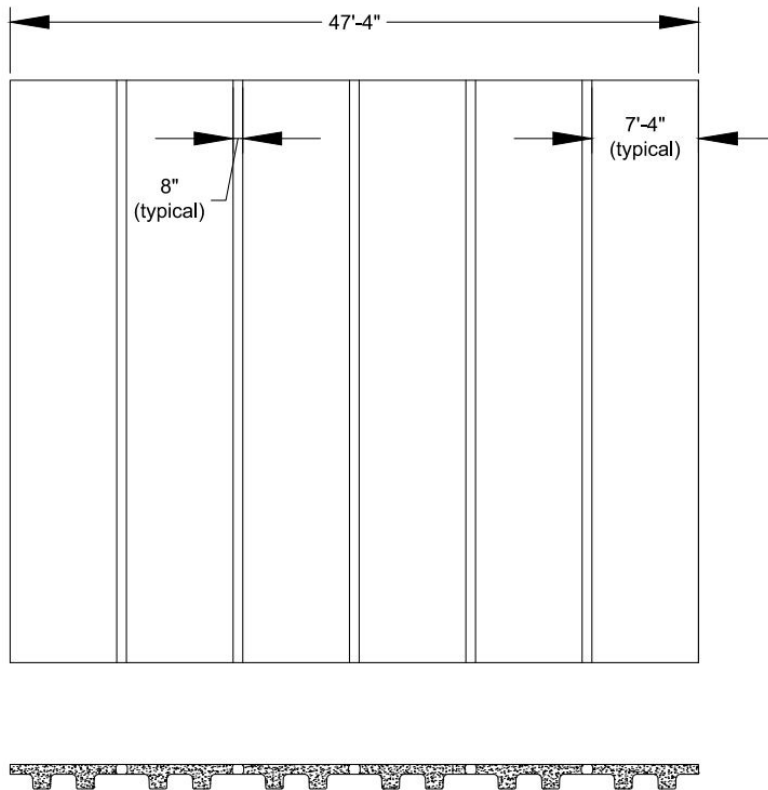


Figure 3-2: Dimensions for the eight-foot NEXT-D bridge model

Shear Key Modeling

Frame Calibration

The modeling of the shear key was a very important component in the 3D modeling of the NEXT-D bridges. The goal was to use an element that possessed all of the stiffness properties proposed by Flores Duron (2011). For the models used in this project, a shear key spacing of six inches was chosen in order to ensure accurate results and to allow for investigation as to how

transverse moment and shear are distributed throughout the length of the bridge. The proposed stiffness values for a three-inch spacing were doubled to convert them into the values for a six-inch section of shear key. For this project, a frame element was defined and assigned section properties so that it would accurately represent the shear key. The target stiffness properties for the frame are shown in Table 3-1. In SAP2000, U1-U3 denote translational degrees of freedom, and R1-R3 denote rotational degrees of freedom. The local axes for the shear key frame elements in the bridge models are shown in Figure 3-3.

Table 3-1: Frame element stiffness matrix for a six-inch section of shear key

	U1	U2	U3	R1	R2	R3
U1	201 kip/in	0	0	0	0	0
U2		220 kip/in	0	0	0	513 kip/rad
U3			817 kip/in	0	1905 kip/rad	0
R1				381 (kip-in)/rad	0	0
R2		(Symmetric)			21929 (kip-in)/rad	0
R3						5905 (kip-in)/rad

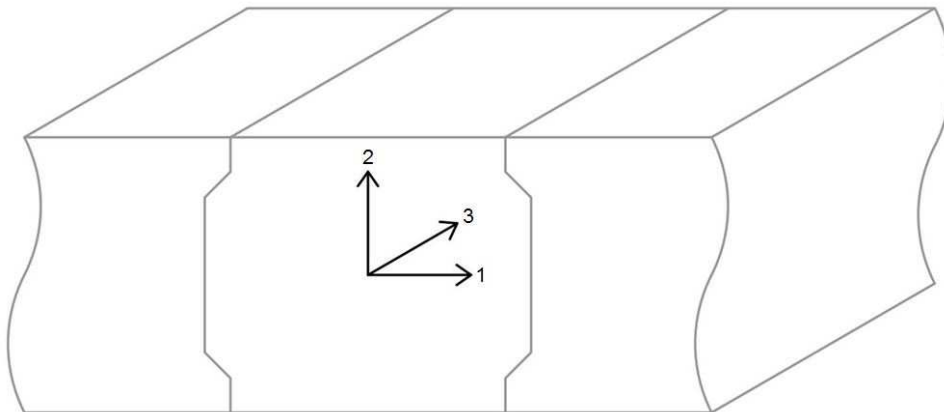


Figure 3-3: Definition of shear key local axes for 3D model

In order to achieve all of the desired stiffness properties for the shear key frame section, the element stiffness matrix for beam elements with inclusion of shear deformations shown in Figure 3-4 was utilized.

$$k_{w/shear} = \frac{EI}{L^3(1+\beta_s)} \begin{bmatrix} 12 & 6L & -12 & 6L \\ 6L & L^2(4+\beta_s) & -6L & L^2(2-\beta_s) \\ -12 & -6L & 12 & -6L \\ 6L & L^2(2-\beta_s) & -6L & L^2(4+\beta_s) \end{bmatrix}$$


$$\beta_s = \frac{12EIf_s}{GAL^2}$$


Figure 3-4: Element stiffness matrix for beam elements with inclusion of shear deformations (Nielson 2011)

The above stiffness matrix formulation is for a 2D beam element. This formulation was used for both directions to develop a frame member with the stiffness properties shown in Table 3-1. In Figure 3-4, E stands for modulus of elasticity, I stands for moment of inertia, f_s is the shape factor, G is the shear modulus, A is the cross sectional area, and L is the length of the element. It should be noted that axial stiffness is equal to $\frac{AE}{L}$ and torsional stiffness is equal to $\frac{JG}{L}$ where J is the torsional constant. As seen in the above stiffness matrix formulation, there are several inputs that can be adjusted in order to manipulate

a frame element to achieve the desired stiffness properties in each direction. However, the coupled stiffness term is related to rotational stiffness term by a factor of $L/2$. This created a problem because in order to define a frame element with all of the correct stiffness properties, a specific member length was required. The length of the member required to achieve the desired relationship of stiffness values for the shear key was 4.66 inches $\left(\frac{\delta_{U2-R3}}{\delta_{U2-U2}} = \frac{513kip/rad}{220kip/in} = 4.66\ inches\right)$. However, in order to properly model the geometry of the NEXT-D bridge there needs to be a gap of eight inches between adjacent precast sections that represents the shear key. This problem was solved through the use of body constraints. One end of the shear key frame element was attached to the shear key-precast slab interface of a NEXT-D beam and the shear key frame element was assigned a length of 4.66 inches. This left the other end of the shear key free in space, so it was constrained to the adjacent NEXT-D beam using six separate body constraints (one for each translational and rotational degree of freedom).

The properties of the frame element were then defined so that it possessed the stiffness properties shown in Table 3-1. The properties that were used to achieve this included the material properties of modulus of elasticity (E), shear modulus (G), and Poisson’s ratio (ν). Section properties that were used included cross sectional area (A), torsional constant (J), moment of inertia about both axes (I_2 , I_3), and shear area in both directions. This method was checked by creating a very simple model of a 4.66-inch long frame element that was fixed at one end and free at the other. The free end was constrained with a fixed node that was 3.44 inches away from the end of the frame element. Unit displacements and rotations were applied to both the fixed end of the frame and the fixed node. When the unit displacements and rotations were applied at both ends to all six degrees of

freedom, the reactions at the fixed end of the beam and the fixed node were equal to the desired stiffness terms from Table 3-1. This model is shown in

Figure 3-5.

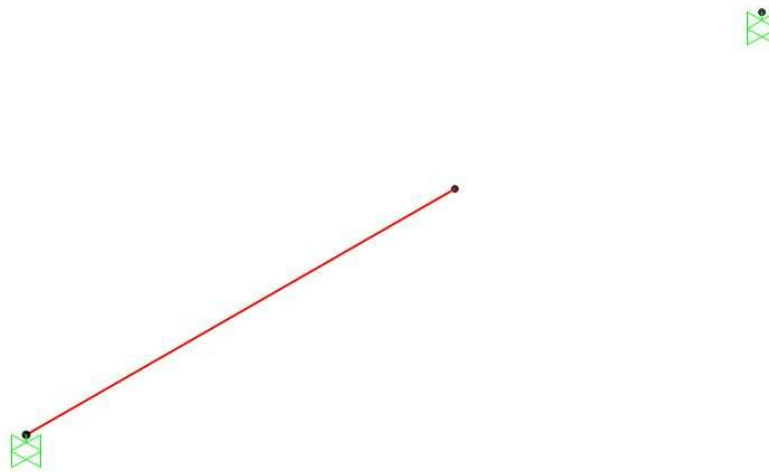


Figure 3-5: Simple shear key test model

The section properties that were assigned to the shear key to achieve the stiffness values from Table 3-1 are shown in Table 3-2. The shear key was assigned a modulus of elasticity of 4415.2-ksi and a Poisson's ratio of 0.3 which results in a shear modulus of 1698.2-ksi. The spreadsheet used to determine the required properties can be found in Appendix B.

Table 3-2: Shear key section properties

Cross Sectional Area:	1.269 in ²
Torsional Constant:	1.046 in ⁴
Moment of Inertia about 3-axis:	4.974 in ⁴

Moment of Inertia about 2-axis:	18.471 in ⁴
Shear Area in 2-direction:	0.660 in ²
Shear Area in 3-direction:	2.451 in ²

Solid Model

Shear Key

The shear key was connected to the adjacent NEXT-D sections as described in the Frame Calibration section above. The shear key to deck connection in the solid model is shown in Figure 3-6. The green dots show the body constraints for the shear keys. The rigid links are the red vertical lines on the edge of the solid face.

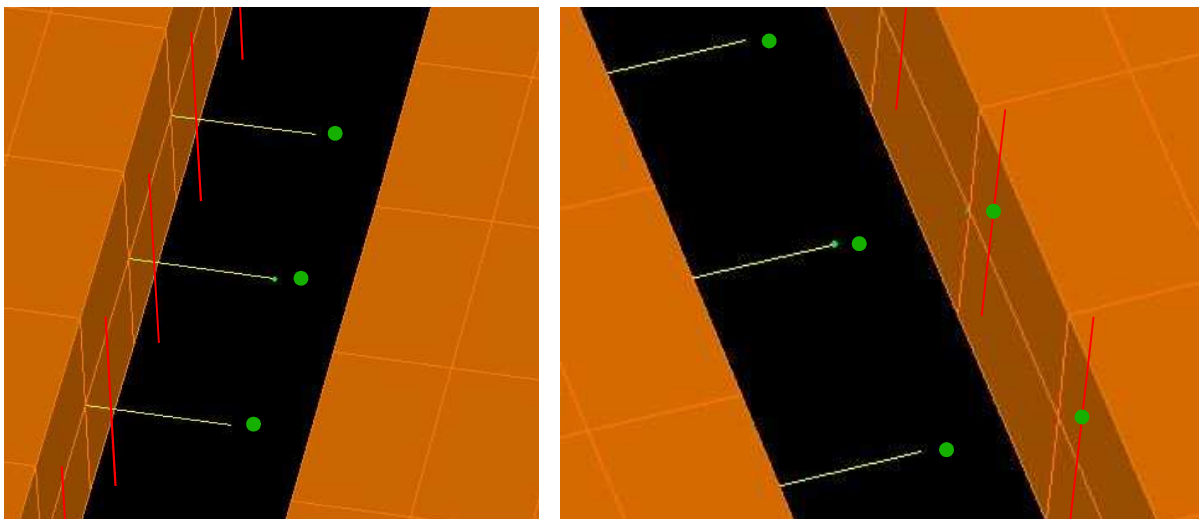


Figure 3-6: Shear key connection in solid model

NEXT-8 Beams and Parapets

For the solid model, the entire NEXT-D section and the parapets were all represented by solid elements. The material of the solids was defined as six-ksi concrete. The properties of six-ksi concrete are shown in Table 3-3.

Table 3-3: Properties of six-ksi Concrete Used in the NEXT-D Models

Property	Value	Units
Compressive Strength	6	ksi
Weight per Unit Volume	150	lb/ft ³
Modulus of Elasticity	4415.2	ksi
Poisson's Ratio	0.2	-
Shear Modulus	1839.7	ksi

The incompatible bending modes option was turned on for all solid elements in order to ensure the most accurate results. The spacing of the shear keys was specified to be six inches along the length of the bridge, so the solid elements were given a longitudinal dimension of six inches as well so that the joints would match up with the location of the shear keys. The solid elements in the bridge deck were divided in the transverse direction into sections between 3.25 and 3.75 inches so that wheel loads could be applied at various locations along the bridge. The deck was divided vertically into two layers of four inches each. The FHWA (2011) states that the deck could be modeled by one layer and still achieve accurate results (Federal Highway Administration 2011). The stem was divided into four solid elements transversely and three solid elements vertically. The fillet between the deck and the stem was modeled using two six-node

triangular solid elements. It is important to keep the aspect ratio of the longest side to the shortest side of a solid element as close to unity as possible in order to achieve accurate results (Computers and Structures 2011a), so the largest aspect ratio for the rectangular solids in the model is $6:3.25=1.85$. For the triangular solids, the largest aspect ratio was $6:1.58=3.80$. The parapet was also broken up into smaller solid elements in order to match the nodes up with the nodes of the bridge deck. The parapet was modeled with the dimensions given in Figure 3-7.

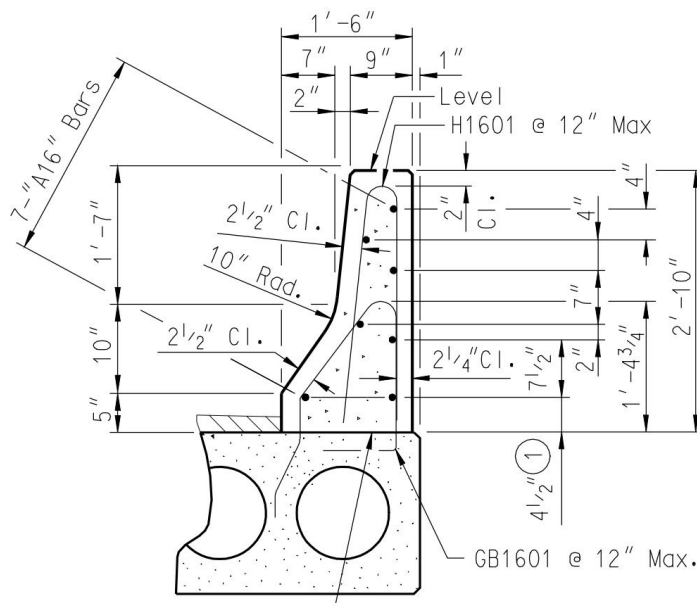


Figure 3-7: Parapet dimensions (SCDOT 2008)

Restraints

In order to ensure a symmetric response and avoid Poisson effect induced stresses at the supports for the bridge, special attention was paid to the restraints placed on the bridge. For the solid model, the bridge was supported six inches in from both ends which was considered to be the center of bearing. All of the nodes at this location on the bottom of the stems were restrained for translation in the z (vertical) direction. At one end of the bridge, one node on the far side of the bridge was restrained for translation in all three directions. On the opposite end and side of the bridge, one node was restrained for translation in the x (transverse) direction in order to keep the bridge from rotating about the z-axis. All of the supported nodes were unrestrained for rotation. The configuration of the supports is shown in Figure 3-8.

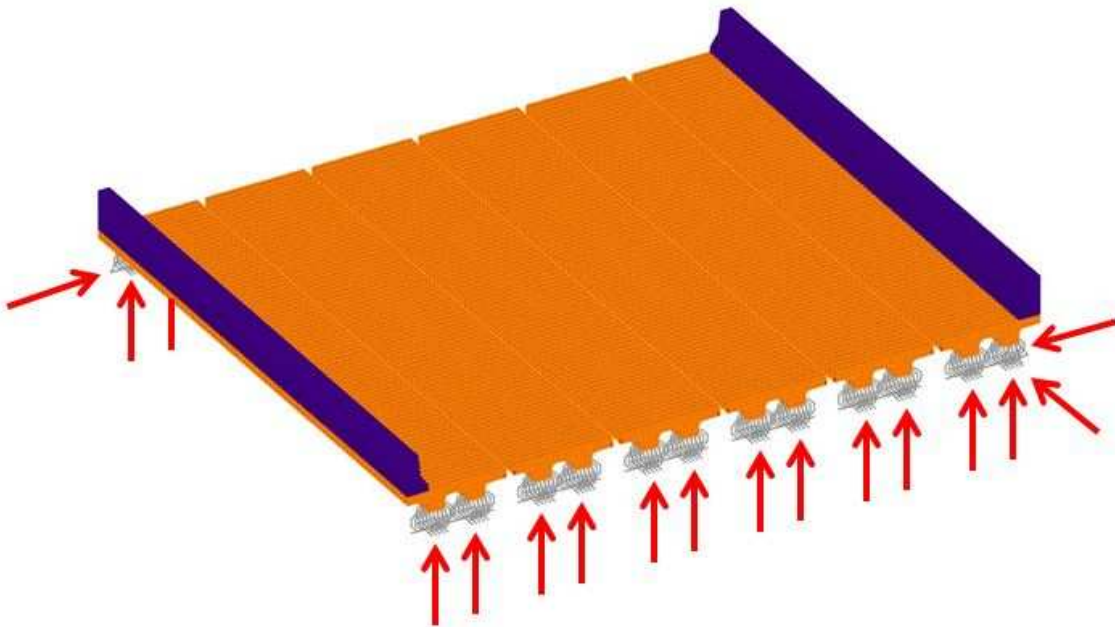


Figure 3-8: Restraints for solid model

Conclusions

The NEXT-D sections and parapets for the solid model were represented by solid elements. The shear keys were represented by frame elements which were calibrated to provide stiffness properties equal to those recommended by Flores Duron (2011). They were spaced at six inches along the longitudinal length of the bridge. The solids were divided into six inch sections in the longitudinal direction in order to match up with the nodes of the shear keys. They were also divided in the transverse direction in order to keep aspect ratios within an acceptable range. The deck solids were divided into two layers vertically, and the stem solids were divided into three layers vertically. The SAP2000 solid model for the eight-foot NEXT-D section can be seen in Figure 3-9. Figures 3-11 and 3-12 show the modeling breakdown for a NEXT-D section used in the solid model for the eight-foot and six-foot sections respectively. For Figures 3-11 and 3-12, refer to the legend in Figure 3-10.

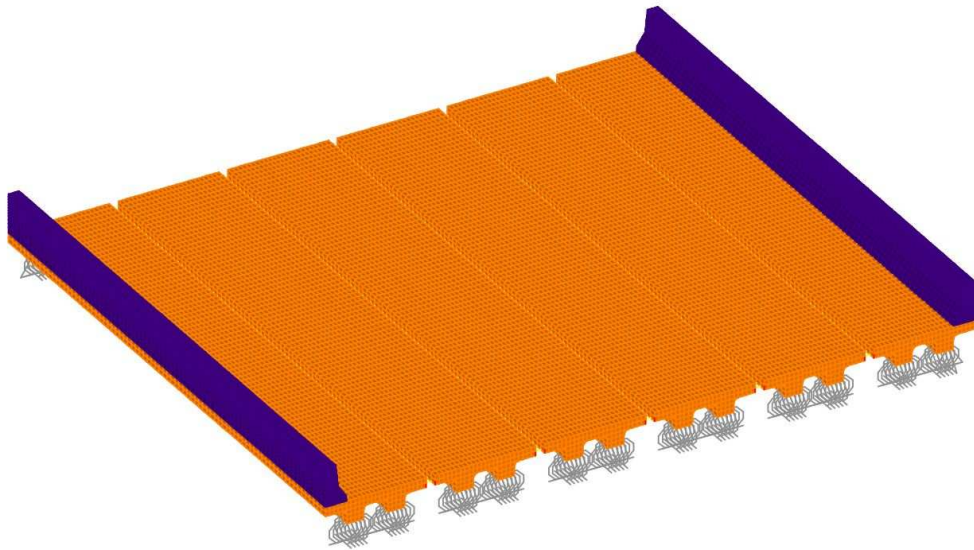


Figure 3-9: SAP2000 8' NEXT-D solid model

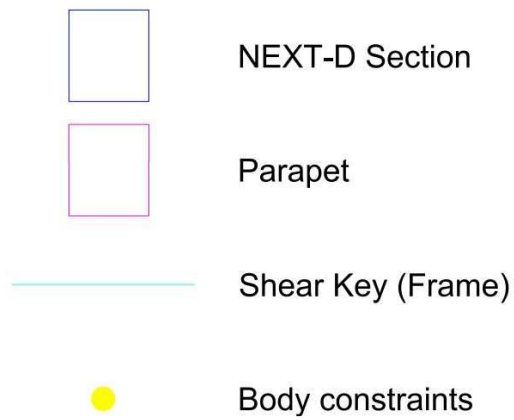


Figure 3-10: Legend for Figure 3-11 and Figure 3-12

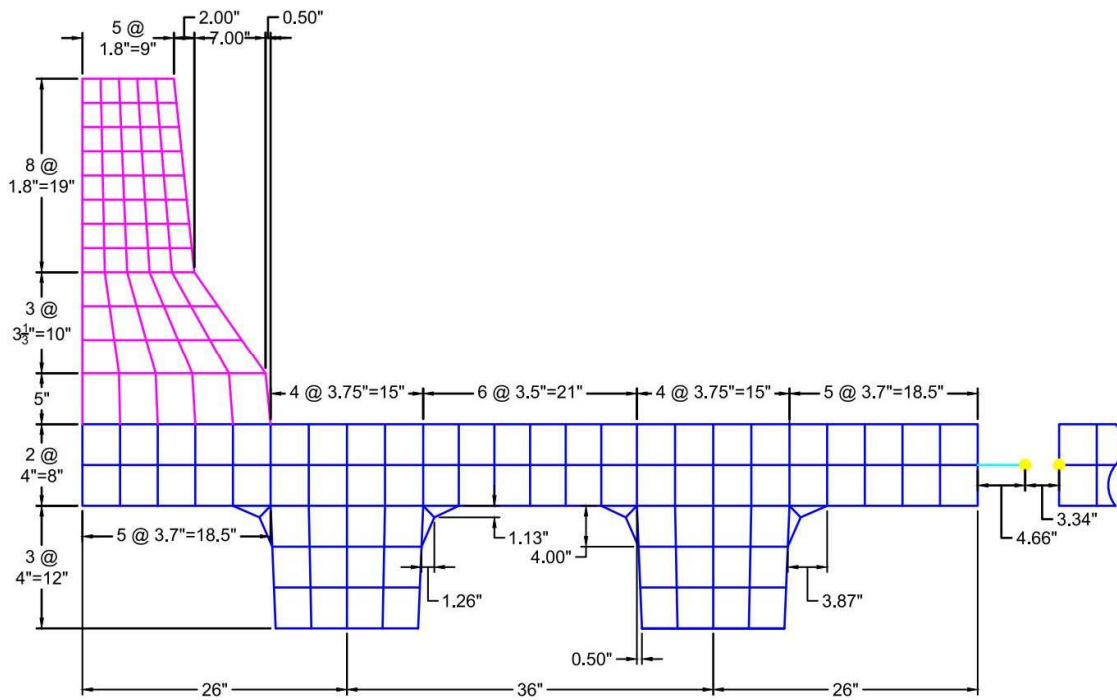


Figure 3-11: Solid modeling layout for eight-foot NEXT-D section

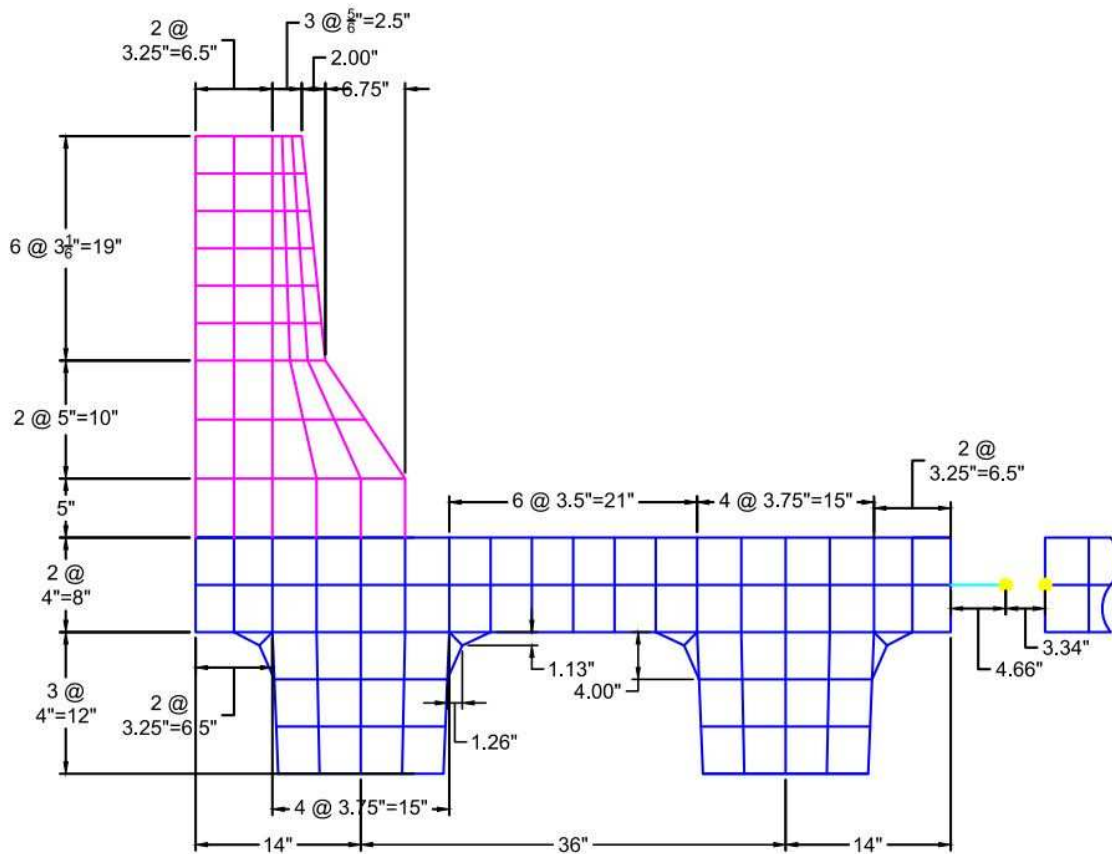


Figure 3-12: Solid modeling layout for six-foot NEXT-D section

Shell Model

Shear Key

The shear key was connected to adjacent NEXT-D sections as described in the Frame Calibration section above. The shear key to deck connection in the shell model is shown in Figure 3-13. The green dots show the body constraints for the shear keys.

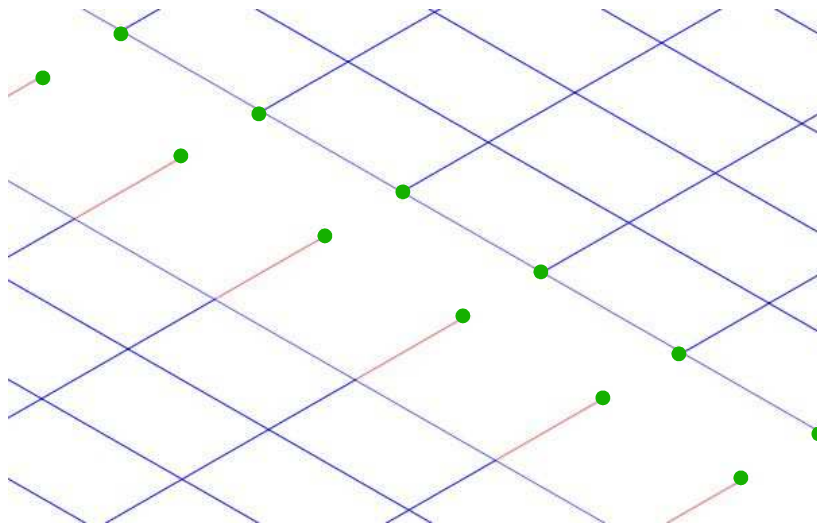


Figure 3-13: Shear key connection in shell model

Deck

The deck for the shell model was modeled using both thin shells and thick shells. Thick shells take shear deformation into account, while thin shells ignore the contributions of shear deformations (Computers and Structures 2011a). Both formulations were used as checks for one another. Although the thin shells

ignore shear deformations, the results are expected to be similar. The shells were assigned a thickness of eight inches, which is representative of the thickness of the slab for the NEXT-D beam used for this project. The shells were specified to be six-ksi concrete. The spacing of the shear keys was specified to be six inches along the length of the bridge. This allowed the shells' nodes to match up with the location of the shear keys' nodes. The shells were divided in the transverse direction into sections between 3.25 and 3.75 inches so that wheel loads could be applied at various locations along the bridge. It is important to keep the aspect ratio of the longest side to the shortest side of a rectangular shell element below four to achieve accurate results (Computers and Structures 2011a). The largest aspect ratio for the shells in the model is $6:3.25 = 1.85$. The shells over the stems of the bridge were assigned a modifier for bending due to the fact that in a real NEXT-D beam, the deck and the stems are integral, and the deck would have the stiffness of the entire depth of the section in these locations. This was accomplished by applying a stiffness modifier of 15.625 for the bending in the transverse direction because the entire depth of the deck and stem is twenty inches, while the depth of the slab is eight inches, and $I = \frac{bh^3}{12}$. Therefore,

$$I_{total} = \frac{6in*(20in)^3}{12} = 4000 in^4 \text{ and } I_{deck} = \frac{6in*(8in)^3}{12} = 256 in^4 \text{ and } \frac{4000in^4}{256in^4} = 15.625.$$

Parapet

The parapet was modeled as a frame element using the section designer feature of SAP2000. A screen capture of the parapet shown in the section designer feature is shown in Figure 3-14. The parapet was assigned to be made of six-ksi concrete and its section properties are shown in Table 3-4.

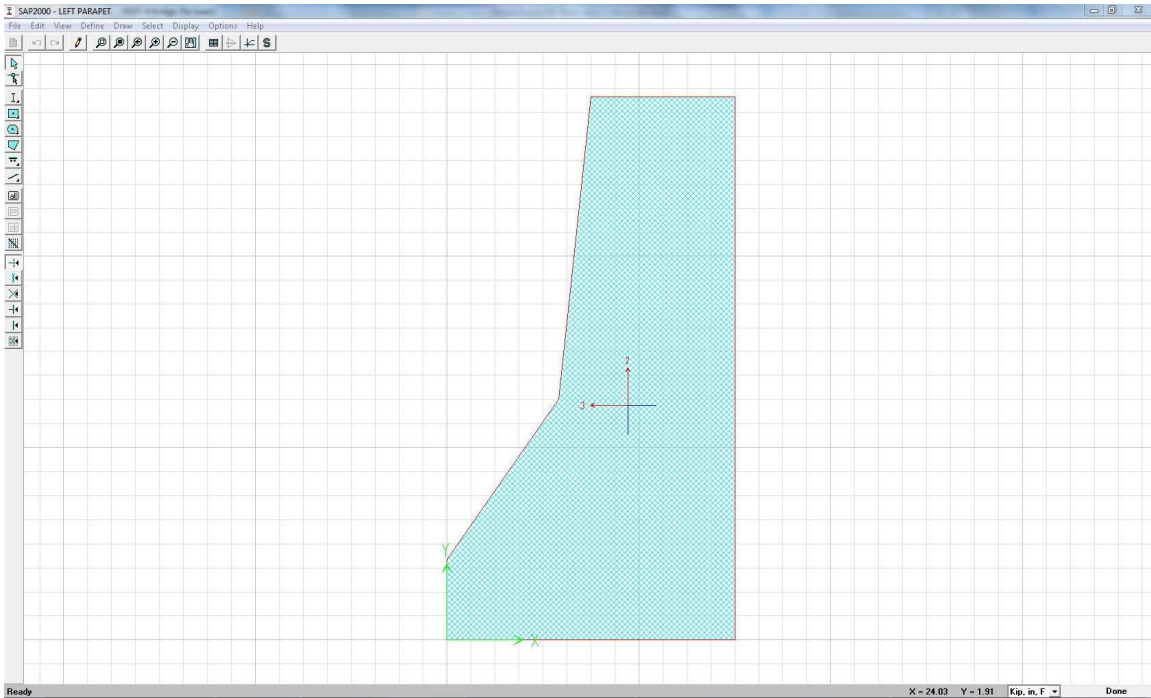


Figure 3-14: Parapet in section designer

Table 3-4: Parapet section properties

Cross Sectional Area:	347.0 in ²
Torsional Constant:	12622.2 in ⁴
Moment of Inertia about 3-axis:	33740.9 in ⁴
Moment of Inertia about 2-axis:	6500.9 in ⁴
Shear Area in 2-direction:	253.9 in ²
Shear Area in 3-direction:	319.9 in ²

The parapet was connected to the deck using rigid links. The links allowed the centroid of the parapet to be located properly in space relative to the rest of the bridge. Each parapet member was six inches long in order to correspond with the shear key spacing.

Stem

The stem of the bridge was also modeled as a frame element using section designer. The stem was taken to be the entire section of concrete below the eight inches considered to be the bridge deck as highlighted in

Figure 3-15. A screen capture of the stem section in section designer is shown in Figure 3-16, and the section properties of the stem are shown in Table 3-5.

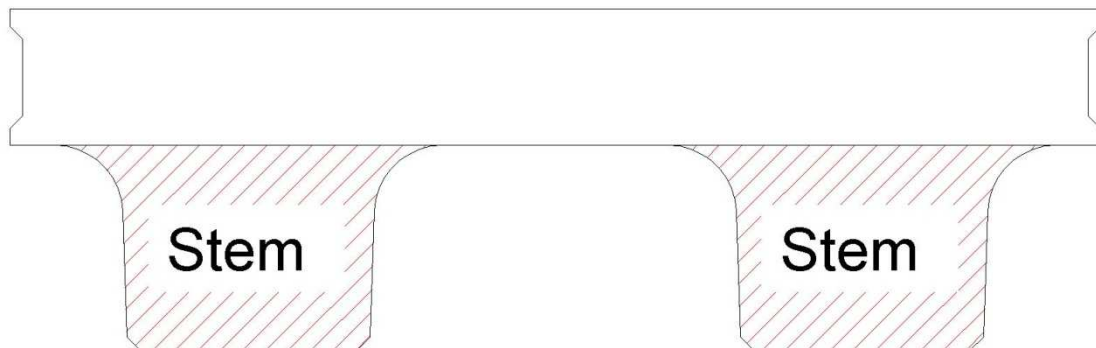


Figure 3-15: NEXT beam with stem highlighted

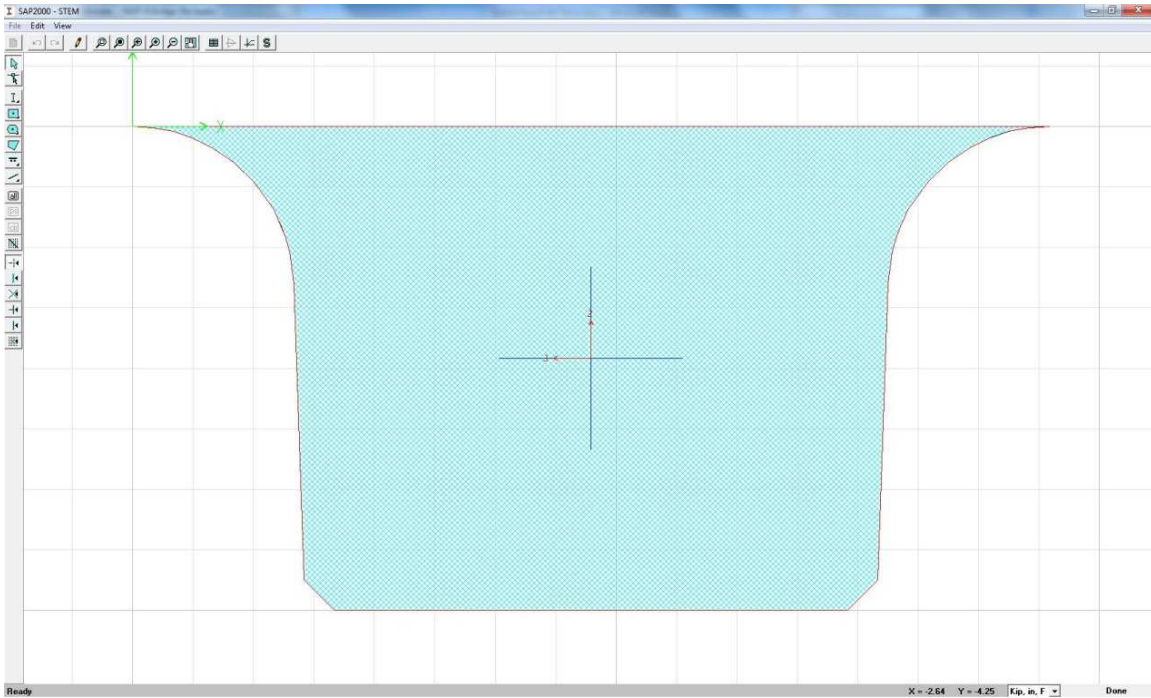


Figure 3-16: Stem in section designer

Table 3-5: Stem section properties

Cross Sectional Area:	147.9 in ²
Torsional Constant:	3509.0 in ⁴
Moment of Inertia about 3-axis:	1834.6 in ⁴
Moment of Inertia about 2-axis:	2895.0 in ⁴
Shear Area in 2-direction:	122.2 in ²
Shear Area in 3-direction:	127.1 in ²

The stems were also connected to the slab using rigid links so that the geometry of the bridge could accurately be represented in three dimensional space. The material of the stems was assigned to be 6-ksi concrete. Each parapet member was six inches long in order to correspond with the shear key spacing.

Rigid Links

The rigid links were created to connect the various elements of the bridge so that their relative geometry could accurately be represented in a 3D model. The parapets and stems were connected to the deck at their centroids. The links were assigned properties to prevent any additional deflection to the bridge. If elements in a model have properties that are too stiff, SAP2000 will generate an ill-conditioned stiffness matrix, so the analysis details were monitored to be sure that this was not the case. The shear area of the rigid links was assigned to be zero because this causes SAP2000 to ignore the contributions of shear deformation. The properties of the rigid links are shown in Table 3-6.

Table 3-6: Rigid link section properties

Cross Sectional Area:	1000000.0	in ²
Torsional Constant:	1000000.0	in ⁴
Moment of Inertia about 3-axis:	1000000.0	in ⁴
Moment of Inertia about 2-axis:	1000000.0	in ⁴
Shear Area in 2-direction:	0.0	in ²
Shear Area in 3-direction:	0.0	in ²

Restraints

The shell model was restrained using the same process as the solid model. Again, the bridge was supported six inches in from the ends of the bridge at the stems which was considered to be the center of bearing. The only difference was that for the shell model, there was only one node at the bottom of the stem, which is where the rigid links and the stem frame member come together. All of the stems at this location were restrained in the z (vertical) direction. On one end of the bridge, the stem closest to the side of the bridge was restrained for translation in all three directions. On the opposite end and side of the bridge, one node was restrained for translation in the y (transverse) direction in order to keep the bridge from rotating. All of the supported nodes were unrestrained for rotation. The configuration of the support restraints is shown in Figure 3-17.

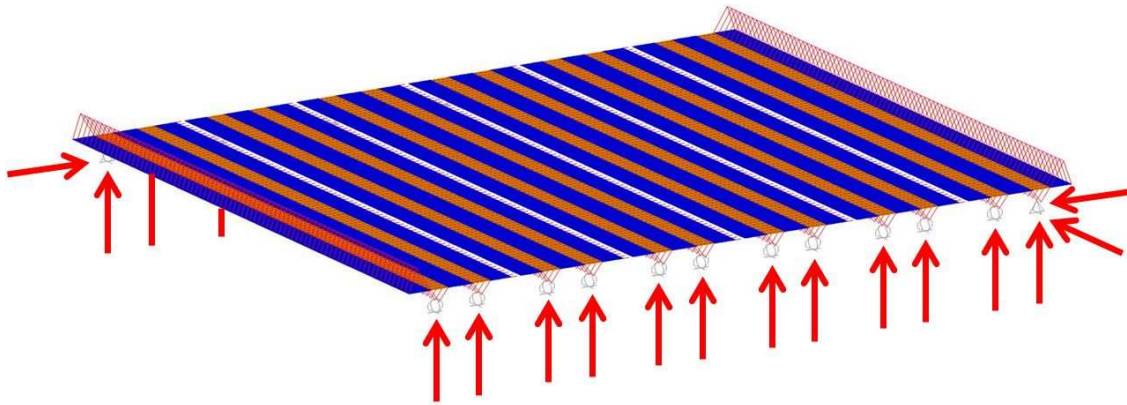


Figure 3-17: Restraints for shell model

Conclusions

The bridge deck was modeled using thin and thick shells to determine which shells provide results closest to those of the solid model. The parapet and stems were modeled using frame elements. These frame elements were then connected to the shell elements using rigid links. The shear keys were represented by frame elements which were calibrated to provide stiffness properties equal to those recommended by Flores Duron (2011). They were spaced at six inches along the longitudinal length of the bridge. The stem, parapet, and deck members were connected every six inches as well, so that they would match up with the nodes of the shear keys. Shell members were six inches in the longitudinal direction and were divided in the transverse direction in order to apply wheel loads at various locations across the bridge and to keep aspect ratios within an acceptable range. The SAP2000 shell model for the eight-

foot NEXT-D section can be seen in Figure 3-18. Figure 3-20 and 3-21 show the modeling breakdown for the shell model of a NEXT-D section used in the shell model for the eight-foot and six-foot sections, respectively. For Figure 3-20 and 3-21, refer to the legend in Figure 3-19.

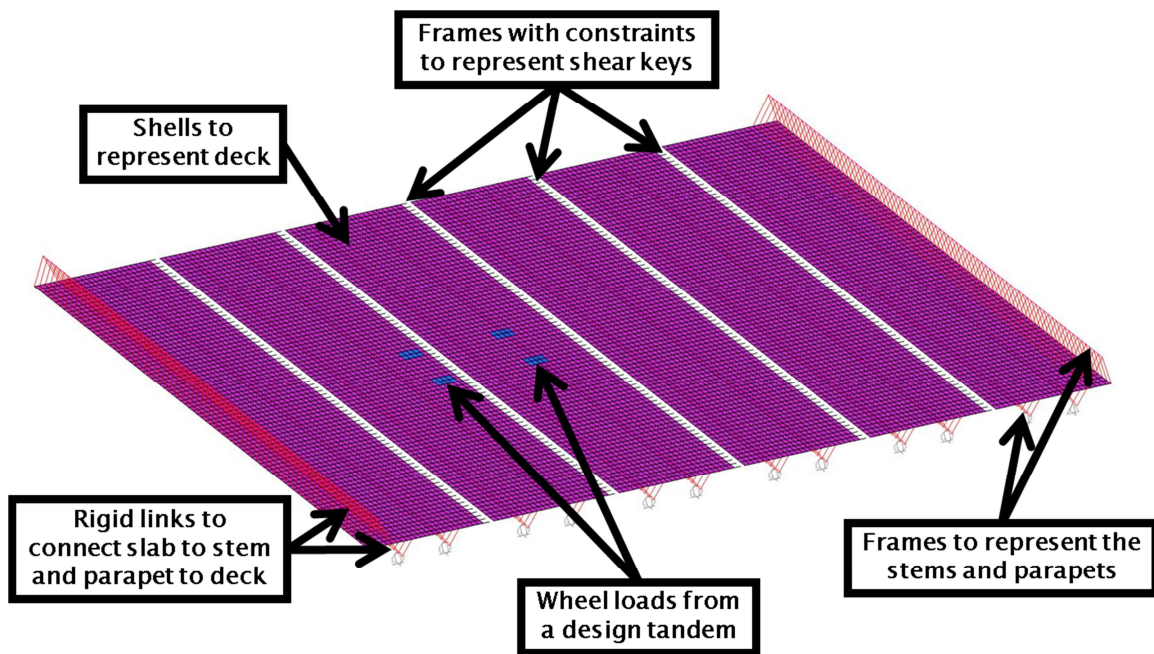


Figure 3-18: SAP2000 eight-foot NEXT-D shell model

- Outline of actual NEXT-D section
- Shell with 8" thickness
- Shell with 8" thickness and stiffness modifier applied
- Rigid Link (Frame)
- Shear Key (Frame)
- Parapet (Frame)
- Stem (Frame)
- Body constraints

Figure 3-19: Legend for Figure 3-20 and Figure 3-21

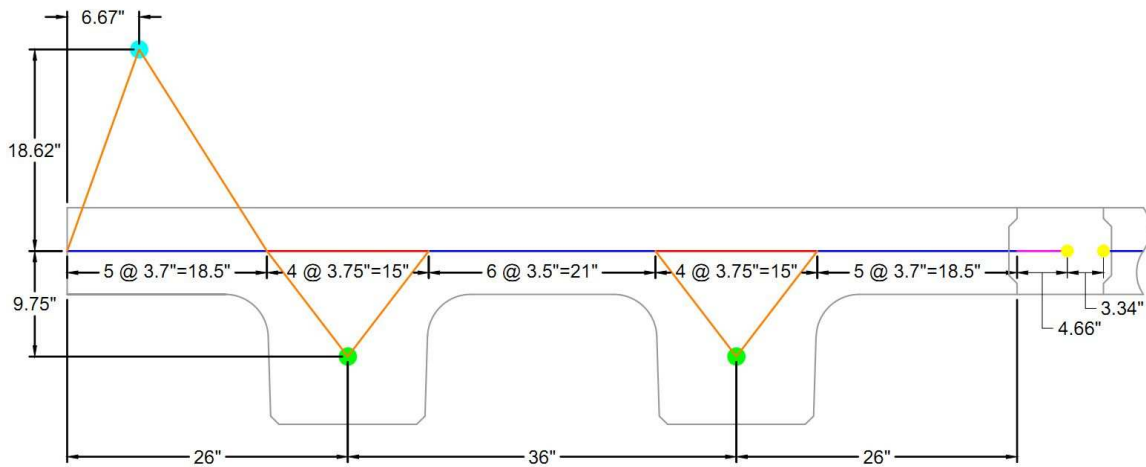


Figure 3-20: Shell modeling layout for eight-foot NEXT-D section

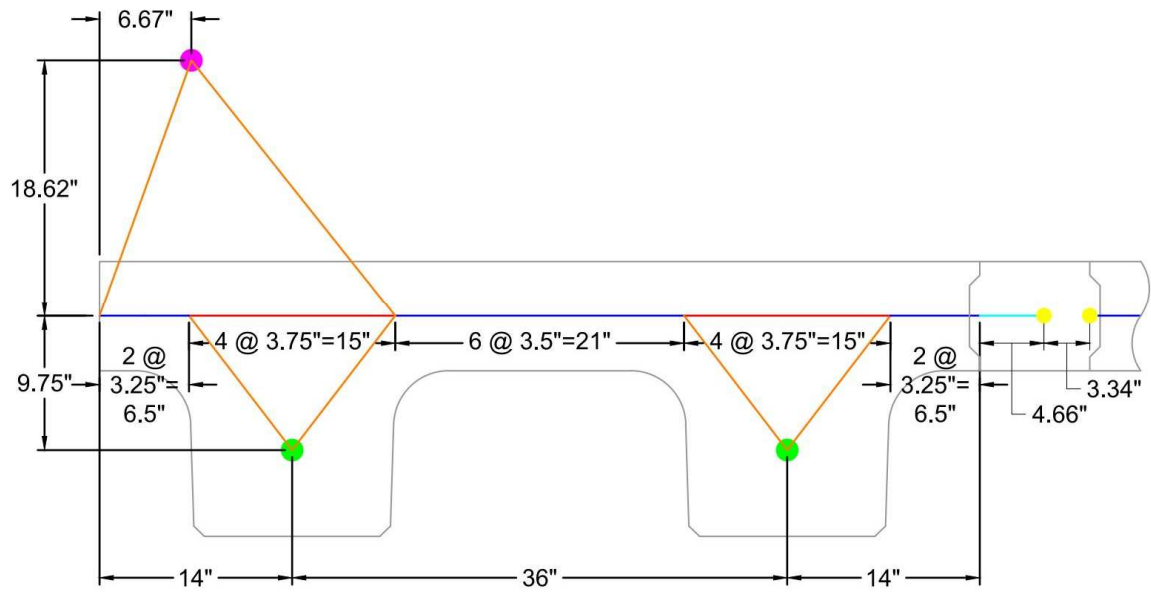


Figure 3-21: Shell modeling layout for six-foot NEXT-D section

Load Application

Live Loads

In order to determine the design shear and moment demands on the shear key and slab, the AASHTO LRFD Bridge Specifications HS20 design truck and design tandem loads were applied to the bridge. According to AASHTO, the wheels are to be applied as concentrated loads or patch loads. The patch loads are to be 20 inches wide by ten inches long (AASHTO 2010). For this project, the wheel loads were applied as patch loads with widths between 14 and 15 inches and a length of 12 inches. This was done to avoid any unrealistic stress concentrations caused by a mathematical point load. The dimensions of the wheel load were driven by the dimensions of the shell and solid elements represented the deck in the models. The widths were chosen to be smaller than 20 inches as a smaller area results in a more conservative model. The three different load cases that were investigated were a single 32-kip axle, two 32-kip axles spaced 14 feet apart, and the design tandem. The design tandem consists of two 25 kip axles that are four feet apart (AASHTO 2010).

As an initial study of the moment and shear distributions throughout the bridge, the three truck loads were applied at three points along the length of the bridge: above the supports, at quarter-span of the bridge, and at mid-span of the bridge. At each location along the length of the bridge, the loads were moved across the

bridge laterally from parapet to parapet as shown in Figure 3-22. Note that wheel loads were modeled as area loads, not point loads as the Figure implies.

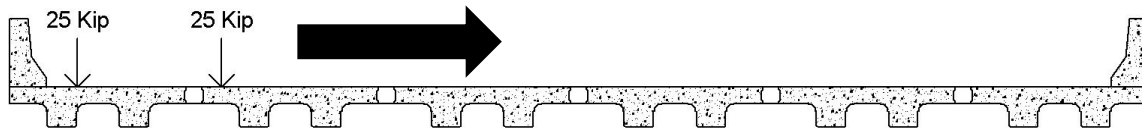


Figure 3-22: Design tandem transverse load placement

For each of these load locations, the moment and shear in each key was monitored. The shear and moments reported included the shear or moment in the entire length of the key. From these values, the critical locations for shear, positive moment, and negative moment were determined. Each load was then moved across the bridge longitudinally at the critical transverse locations in order to ensure that the maximum responses occurred with the load centered over mid-span of the bridge. This is shown in Figure 3-23.

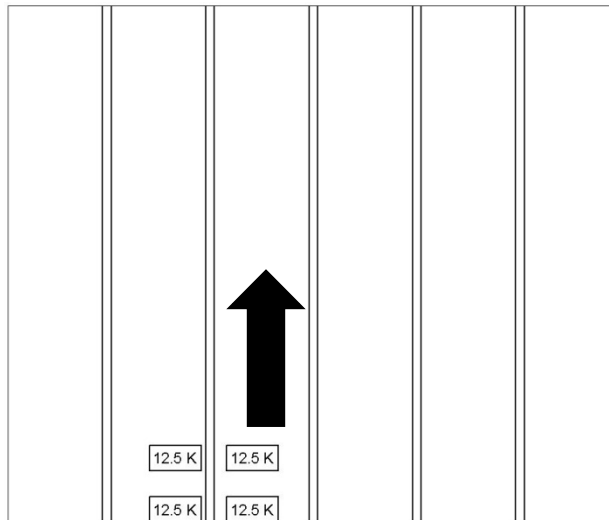


Figure 3-23: Design tandem longitudinal load placement

The accumulation of shear and moment in the shear keys was also monitored in order to determine a recommended strip width to be used for the design of the shear key. Once all of the load cases were run, the results of the shell model were compared to the results of the solid model in order to verify that the results were similar and to determine if it was necessary to continue using the solid model. It was decided that if the shell model provided close enough results to the solid model, that it would be used to determine slab forces in the bridge due to the computational overhead of the solid models and complications with determining shear and moments in the deck from the solid elements. Once the demand in the shear key was established, and the critical load location was determined to be centered over mid-span of the bridge, the maximum shear, positive moment, and negative moment as a result of the truck loads at mid-span

were monitored at various location in the deck of the bridge. The locations monitored are shown in Figure 3-4. All five locations were checked in each NEXT-D section in order to determine design forces in the slab.

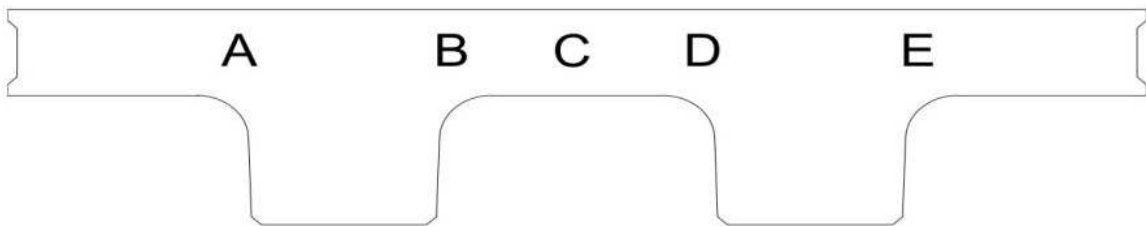


Figure 3-24: Critical locations for deck demand

Dead Load

Once the live load demands for the shear key and slab were determined, the dead load demand for the shear key was investigated. Due to the construction process that will be used to build a NEXT-D bridge, the self-weight of the NEXT-D sections were neglected in calculating the dead load demand in the shear keys. When the bridge is being built, the NEXT-D sections will already be put in place and supporting themselves before the shear keys are cast. Therefore, the only superimposed dead load that will be applied to the shear keys is the weight of the parapets.

For the slab, the dead load demand was determined by modeling one simply supported NEXT-D section and determining the shear and moment demand for the slab due to the self-weight of the section. Next, the demand in the slab due to

the self-weight of the parapet was determined, and this was added to the demand due to the self-weight of the NEXT-D section itself in order to determine the dead load demand for the deck.

In addition to the dead loads due to self-weight, a super-imposed dead load due to a future wearing surface was applied to the entire bridge deck. The future wearing surface was assigned a thickness of three inches and was applied to the bridge deck in the form of a uniformly distributed area load. Separate demands for the dead load due to self-weight and due to the future wearing surface because in design, these demands will be factored by different amounts prescribed by the AASHTO LRFD Bridge Design Specifications (AASHTO 2010).

Conclusions

The purpose of this project was to determine the design demand for the shear key and deck for a NEXT-D bridge. The AASHTO LRFD Bridge Design Specs do not provide a recommendation as to how to find these demands, so SAP2000 was used to create 3D models of NEXT-D bridges. Models were created for bridges using six-foot and eight-foot NEXT-D sections. There were two types of models built for this study. One of the models mainly used solid elements, and the other used shell and frame elements to model the bridge. For both types of models, the shear key was modeled using a frame element that was calibrated to possess the stiffness properties specified by Flores Duron (2011). Each model was subjected to the HS20 design truck and design tandem loads defined in the

AASHTO LRFD Bridge Design Specs at various locations in order to determine the critical design values for shear, positive moment, and negative moment in the key and the slab. These values were compared to the values determined using the AASHTO strip width method. Several modeling parameters including shear key stiffness, stem stiffness, and span length were also investigated through sensitivity studies.

Chapter 4

RESULTS AND DISCUSSION

Shear Key Live Load Analysis

Transverse Load Analysis

The HS20 design truck and design tandem load cases specified in the AASHTO LRFD Bridge Design Specifications (AASHTO 2010) and the SAP2000 (Computers and Structures 2011b) models were used to determine the moment and shear demand on the shear key and bridge deck. Each wheel load was applied to the shell or solid elements as a uniform area load spread out over eight elements. This load covered two elements in the longitudinal direction for a length of twelve inches and four elements in the transverse direction for widths ranging between fourteen and fifteen inches depending on the width of the elements at that location. Uniform loads were calculated by dividing the wheel load specified by AASHTO by the loaded area. One uniformly distributed wheel load is shown in Figure 4-1. This figure shows a design tandem wheel applied to eight solid elements that totaled 14.5 inches wide and 12 inches long, resulting in an area of $14.5in * 12in = 168in^2$, and a uniformly distributed area load of

$$\frac{12,500lbs}{174in^2} = 71.84psi.$$

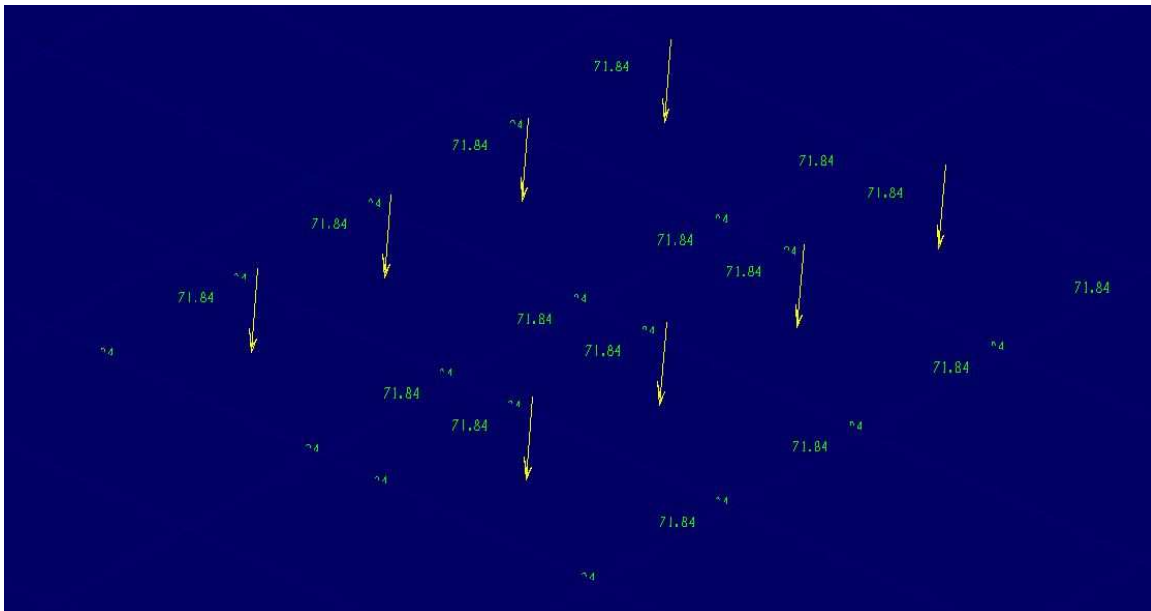


Figure 4-1: Uniformly distributed area load

Three different load configurations were applied to the bridge: One axle of the HS20 design truck (single-axle), two axles of the HS20 design truck (two-axle), and the design tandem. The two-axle load configuration used the minimum axle spacing allowed by the AASHTO LRFD Bridge Design Specifications (AASHTO 2011). The three load types were moved across the bridge laterally, and shear and moment were monitored in each shear key for each load location in order to create influence lines for the shear keys. The shear and moment values plotted are the total shears and moments in the entire forty-foot long shear key. Moment influence lines were produced for the left and right sides of the shear key. This process was repeated over the supports of the bridge, at quarter-span of the bridge, and at mid-span of the bridge. This entire procedure was carried out for

both the six-foot and eight-foot models. Furthermore, for both the six-foot and eight-foot models, the shell and solid models were investigated.

Influence lines for the shear keys of a six-foot NEXT-D bridge under the design tandem loading at mid-span are shown in Figures 4-3 through 4-5. The location of the load on the x-axis refers to the point midway between the left and right wheels. Each figure shows the influence lines for all seven shear keys in the model built with six-foot NEXT-D sections. Figure 4-2 shows the legend for the shear key influence lines. The keys are labeled in sequence from one side of the bridge to the other.



Figure 4-2: Legend for shear key influence lines

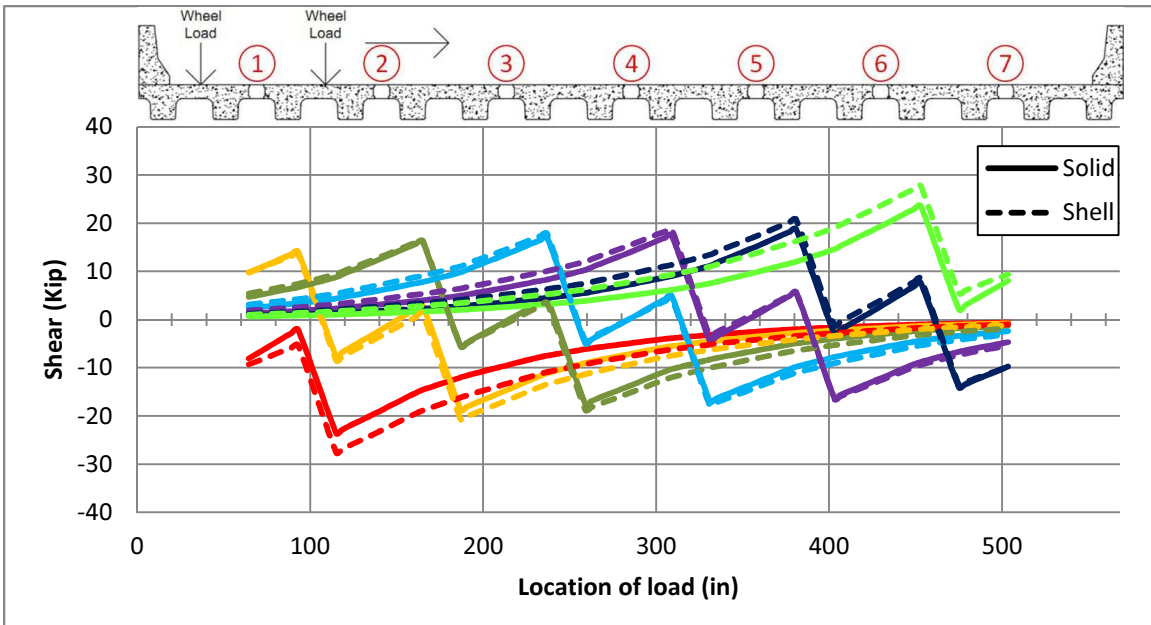


Figure 4-3: Shear influence line for the shear keys in a six-foot section NEXT-D bridge under a design tandem loading at mid-span

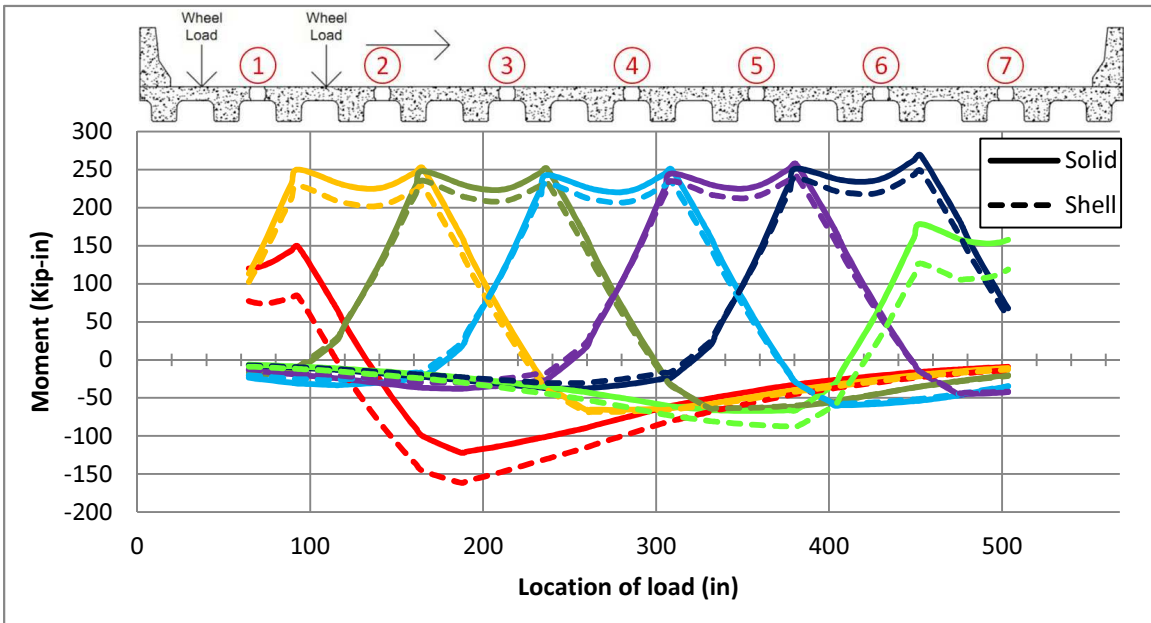


Figure 4-4: Moment influence line for the left side of the shear keys in a six-foot section NEXT-D bridge under a design tandem loading at mid-span

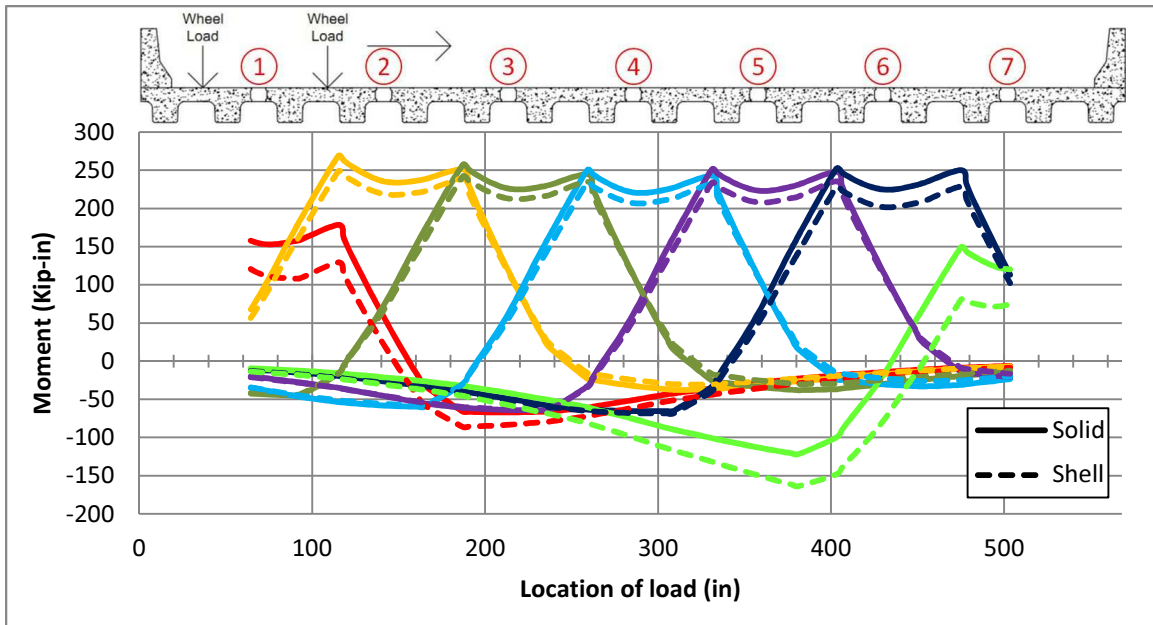


Figure 4-5: Moment influence line for the right side of the shear keys in a six-foot section NEXT-D bridge under a design tandem loading at mid-span

Figures 4-4 and 4-5 show that the moments at the right edge of the shear key mirror the moments in the left edge of the shear key. For this reason, moment influence lines will only be shown for one side of the key from this point forward. The shear and moment influence lines for the solid model and shell model closely resemble each other with the exception of the outermost keys. Also, the greatest shear and negative moment demands clearly exist in Keys one and seven, while the greatest positive moment demands exist in Keys two through six.

Influence lines for the shear keys of an eight-foot NEXT-D bridge under the design tandem loading at mid-span are shown in Figure 4-6 and 4-7. Influence

lines for the single-axle and two-axle loadings for the six-foot and eight-foot NEXT-D bridges are shown in Appendix C. Appendix C also includes the influence lines for each of the loadings at the quarter-span and support locations for all three loadings.

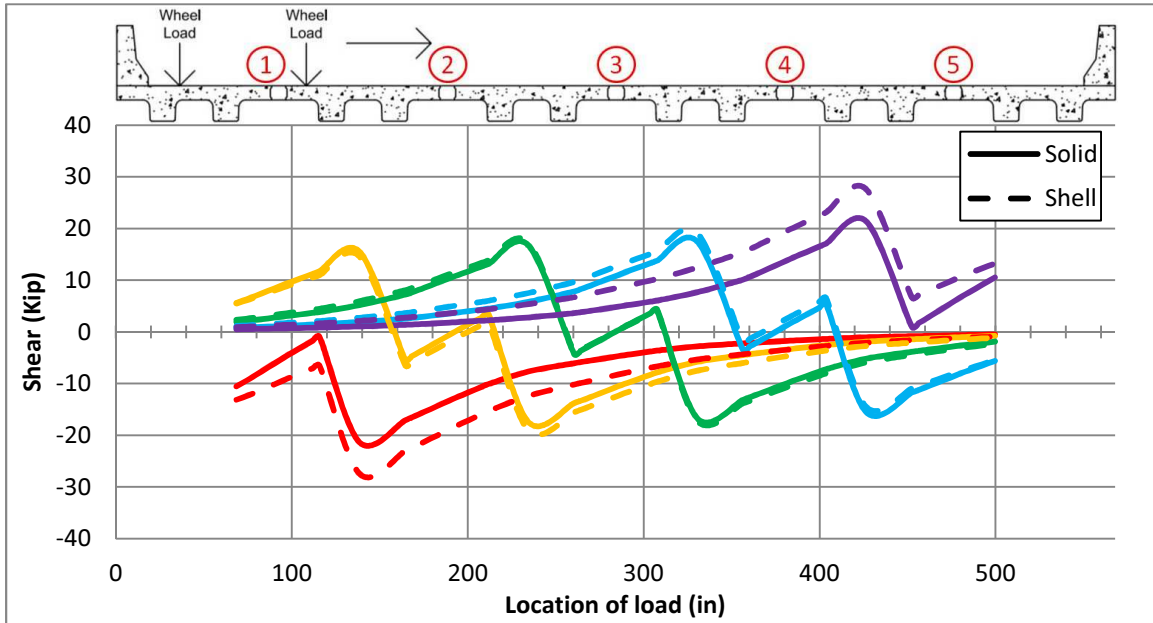


Figure 4-6: Shear influence line for the shear keys in an eight-foot section NEXT-D bridge under a design tandem loading at mid-span

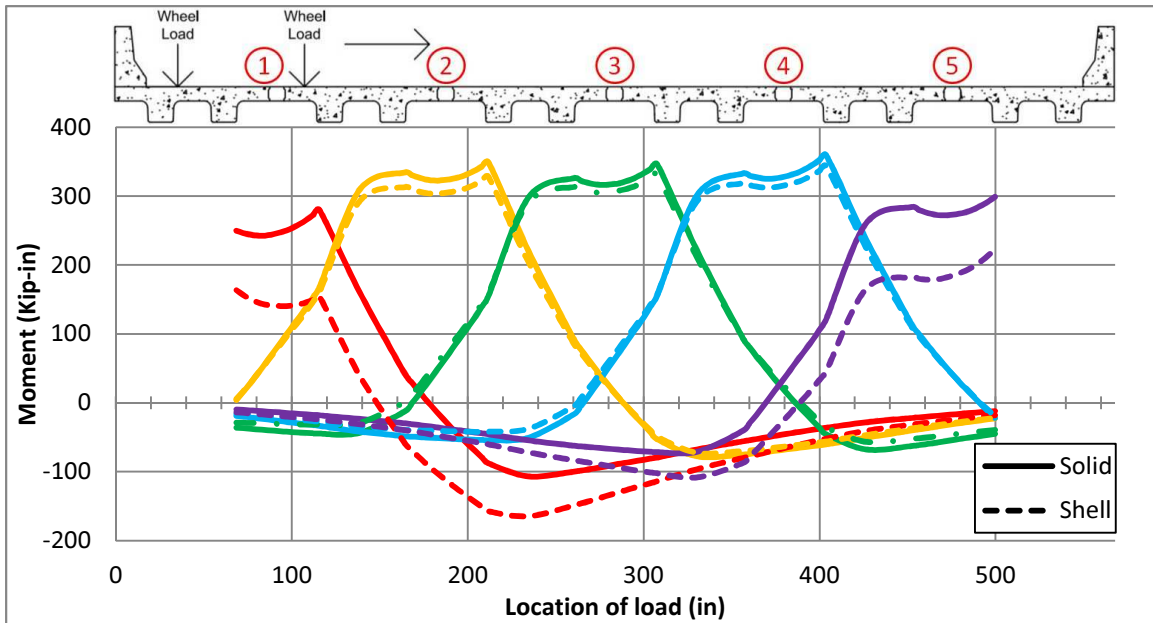


Figure 4-7: Moment influence line for the left side of the shear keys in an eight-foot section NEXT-D bridge under a design tandem loading at mid-span

Similarly to the six-foot model, the greatest shear and negative moment demands clearly exist in the outermost keys (Keys one and five), while the greatest positive moment demands exist in middle keys.

Once all of the influence lines were created, the maximum values of shear, positive moment, and negative moment were compared for each loading scenarios described above. The results for the six-foot section NEXT-D bridge are shown in Tables 4-1 through 4-3. The results for the eight-foot section NEXT-D bridge are shown in Tables 4-4 through 4-6. The percent error calculation assumes that the solid model provides the “theoretical results” in the percent

error equation ($\%Error = \frac{Experimental\ value - Theoretical\ value}{Theoretical\ value}$) because the solid modeling technique is accepted as being more accurate than the shell method.

Table 4-1: Maximum shear key demands for a six-foot section NEXT-D bridge under the design tandem loading

Location	Criterion	Units	Solid	Shell	% Error
Mid-span	Max shear	kip	26.6	27.8	4.6%
	Max (+) moment	kip-in	268.6	248.4	-7.5%
	Max (-) moment	kip-in	-126.4	-164.1	29.8%
	+/- ratio	-	2.12	1.51	-
Quarter-span	Max shear	kip	22.4	24.2	8.0%
	Max (+) moment	kip-in	200.9	185.8	-7.5%
	Max (-) moment	kip-in	-91.8	-118.2	28.8%
	+/- ratio	-	2.19	1.57	-
Support	Max shear	kip	9.5	10.5	9.8%
	Max (+) moment	kip-in	71.9	66.2	-7.9%
	Max (-) moment	kip-in	-28.3	-35.8	26.5%
	+/- ratio	-	2.54	1.85	-

Table 4-2: Maximum shear key demands for a six-foot section NEXT-D bridge under the single-axle loading

Location	Criterion	Units	Solid	Shell	% Error
Mid-span	Max shear	kip	17.1	17.8	4.4%
	Max (+) moment	kip-in	173.7	160.6	-7.5%
	Max (-) moment	kip-in	-81.8	-106.2	29.8%
	+/- ratio	-	2.12	1.51	-
Quarter-span	Max shear	kip	14.6	15.7	7.8%
	Max (+) moment	kip-in	130.2	120.4	-7.5%
	Max (-) moment	kip-in	-59.6	-76.8	28.8%
	+/- ratio	-	2.18	1.57	-
Support	Max shear	kip	2.5	2.4	-4.0%
	Max (+) moment	kip-in	15.5	14.0	-9.5%
	Max (-) moment	kip-in	-4.2	-4.9	19.0%
	+/- ratio	-	3.73	2.84	-

Table 4-3: Maximum shear key demands for a six-foot section NEXT-D bridge under the two-axle loading

Location	Criterion	Units	Solid	Shell	% Error
Mid-span	Max shear	kip	31.8	33.8	6.3%
	Max (+) moment	kip-in	304.5	281.6	-7.5%
	Max (-) moment	kip-in	-141.9	-183.5	29.3%
	+/- ratio	-	2.15	1.53	-
Quarter-span	Max shear	kip	22.9	25.2	9.7%
	Max (+) moment	kip-in	217.9	201.5	-7.5%
	Max (-) moment	kip-in	-98.3	-126.9	29.1%
	+/- ratio	-	2.22	1.59	-
Support	Max shear	kip	17.8	19.8	11.1%
	Max (+) moment	kip-in	178.2	164.5	-7.7%
	Max (-) moment	kip-in	-80.4	-103.8	29.0%
	+/- ratio	-	2.22	1.59	-

Table 4-4: Maximum shear key demands for an eight-foot section NEXT-D bridge under the design tandem loading

Location	Criterion	Units	Solid	Shell	% Error
Mid-span	Max shear	kip	24.8	28.0	12.8%
	Max (+) moment	kip-in	359.6	343.6	-4.4%
	Max (-) moment	kip-in	-113.0	-167.8	48.4%
	+/- ratio	-	3.18	2.05	-
Quarter-span	Max shear	kip	21.0	24.0	14.5%
	Max (+) moment	kip-in	269.9	257.0	-4.8%
	Max (-) moment	kip-in	-81.7	-119.7	46.5%
	+/- ratio	-	3.30	2.15	-
Support	Max shear	kip	9.8	11.8	20.0%
	Max (+) moment	kip-in	107.8	101.3	-6.0%
	Max (-) moment	kip-in	-25.7	-36.1	40.4%
	+/- ratio	-	4.20	2.81	-

Table 4-5: Maximum shear key demands for an eight-foot section NEXT-D bridge under the single-axle loading

Location	Criterion	Units	Solid	Shell	% Error
Mid-span	Max shear	kip	16.3	18.0	10.8%
	Max (+) moment	kip-in	222.6	222.2	-0.2%
	Max (-) moment	kip-in	-71.0	-108.6	53.0%
	+/- ratio	-	3.14	2.05	-
Quarter-span	Max shear	kip	13.6	15.6	14.5%
	Max (+) moment	kip-in	174.9	166.5	-4.8%
	Max (-) moment	kip-in	-53.1	-77.7	46.4%
	+/- ratio	-	3.30	2.14	-
Support	Max shear	kip	3.9	4.5	14.9%
	Max (+) moment	kip-in	33.0	30.2	-8.5%
	Max (-) moment	kip-in	-4.3	-5.2	21.1%
	+/- ratio	-	7.65	5.78	-

Table 4-6: Maximum shear key demands for an eight-foot section NEXT-D bridge under the two-axle loading

Location	Criterion	Units	Solid	Shell	% Error
Mid-span	Max shear	kip	29.8	33.9	13.7%
	Max (+) moment	kip-in	408.0	389.3	-4.6%
	Max (-) moment	kip-in	-126.6	-186.7	47.5%
	+/- ratio	-	3.22	2.09	-
Quarter-span	Max shear	kip	22.0	25.7	17.0%
	Max (+) moment	kip-in	297.3	283.0	-4.8%
	Max (-) moment	kip-in	-88.0	-129.3	46.8%
	+/- ratio	-	3.38	2.19	-
Support	Max shear	kip	17.4	21.6	24.1%
	Max (+) moment	kip-in	250.9	238.3	-5.0%
	Max (-) moment	kip-in	-72.4	-106.0	46.4%
	+/- ratio	-	3.46	2.25	-

These Tables show that the maximum responses in the shear key all occur with the loading applied over the mid-span of the bridge. For the design tandem and two-axle loadings, this meant that the two axles for either design vehicle were centered over the mid-span of the bridge. For both the six-foot and eight-foot section bridges, the percent errors for the maximum positive moments were under ten percent. For the six-foot section bridge, the percent errors for the shear demand in the keys were all within ten percent with the exception of the two-axle loading at the support of the bridge. However, for the shear demand in the keys for the eight-foot section bridge and the negative moment demand in the keys for the six-foot and eight-foot section bridges, the percent errors were significantly higher. These differences can be attributed to the difference between the connection of the parapet to the bridge for the solid model and the shell model. The effect of the parapet is demonstrated in the above influence lines by the fact that the maximum demands in the solid and shell models are most significant in the outermost keys, which are connected to the NEXT-D girder that supports the parapet. This theory was tested by building six-foot and eight-foot bridge models without the parapets and comparing the results for the shell and solid models. The influence lines for these models with the design tandem load applied at mid-span are shown in Figures 4-8 through 4-11. The influence lines for the design tandem load applied at quarter-span and over the supports are found in Appendix C.

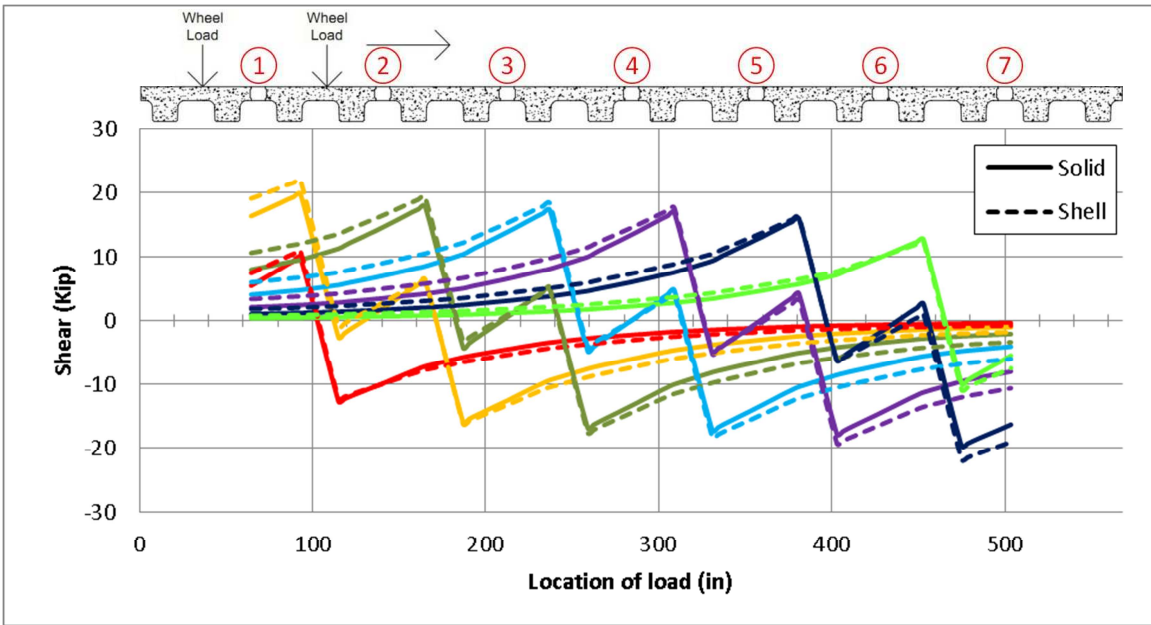


Figure 4-8: Shear influence line for the shear keys in a six-foot section NEXT-D bridge without parapets under a design tandem loading at mid-span

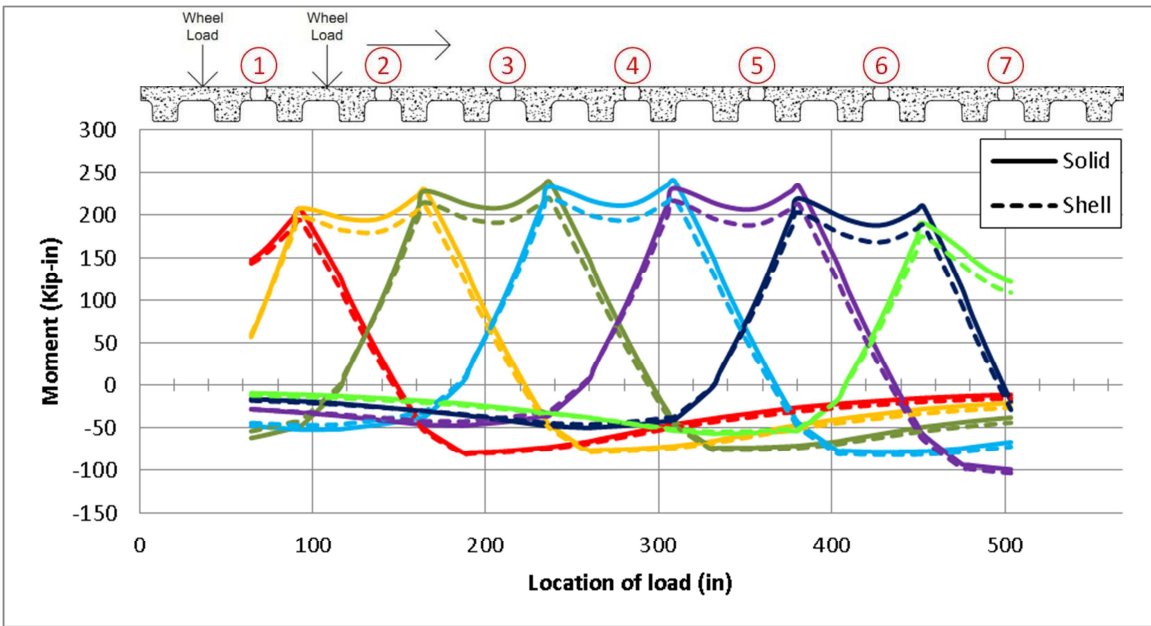


Figure 4-9: Moment influence line for the left side of the shear keys in a six-foot section NEXT-D bridge without parapets bridge under a design tandem loading at mid-span

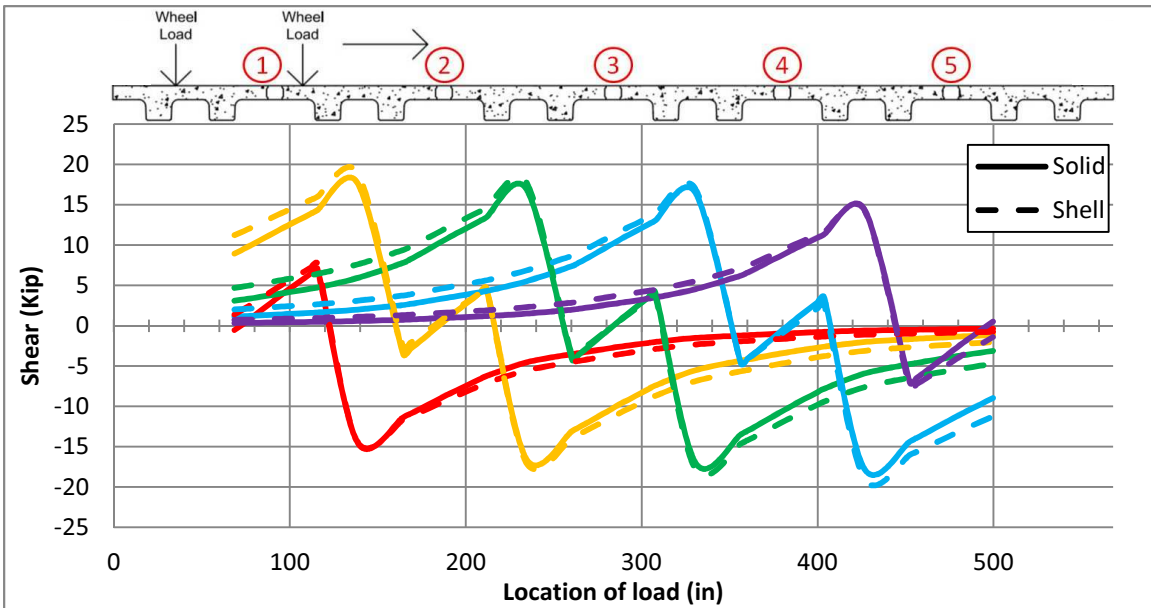


Figure 4-10: Shear influence line for the shear keys in an eight-foot section NEXT-D bridge without parapets under a design tandem loading at mid-span

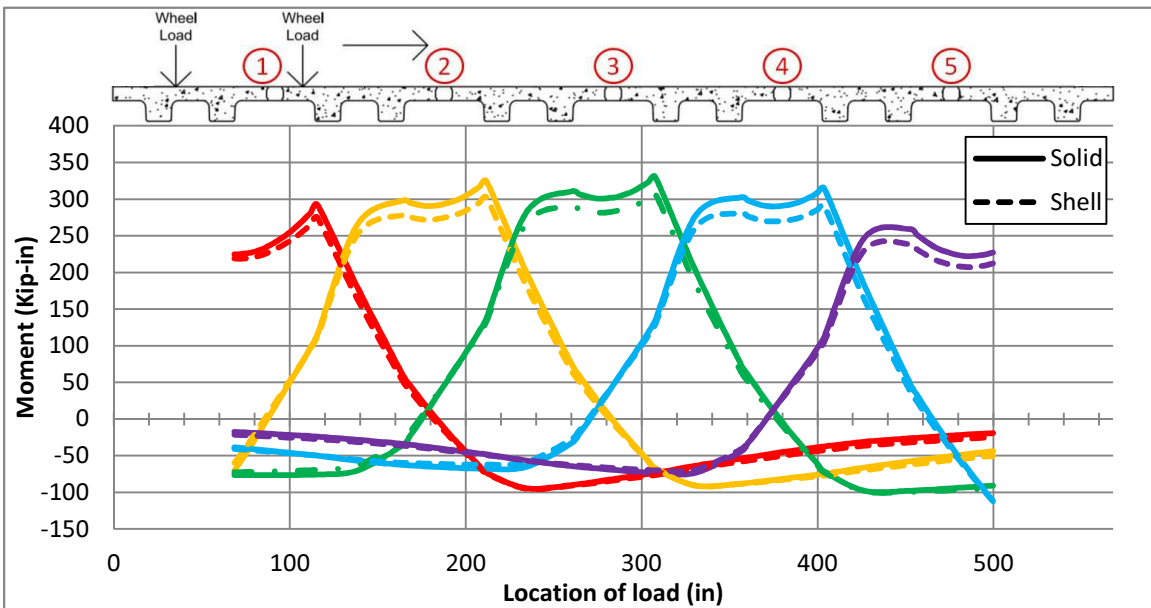


Figure 4-11: Moment influence line for the left side of the shear keys in an eight-foot section NEXT-D bridge with no parapets bridge under a design tandem loading at mid-span

In the figures above, the influence lines for the outermost keys for the solid and shell models align much more closely with each other than the influence lines for the bridge models with parapets. The maximum demands in the shear key for the six-foot and eight-foot NEXT-D models without parapets are shown in Tables 4-7 and 4-8.

Table 4-7: Maximum shear key demands for a six-foot section NEXT-D bridge without parapets under the design tandem loading

Location	Criterion	Units	Solid	Shell	% Error
Mid-span	Max shear	kip	23.8	25.2	6.1%
	Max (+) moment	kip-in	239.9	219.5	-8.5%
	Max (-) moment	kip-in	-106.0	-109.3	3.1%
	+/- ratio	-	2.26	2.01	-
Quarter-span	Max shear	kip	20.1	21.4	6.4%
	Max (+) moment	kip-in	180.5	164.9	-8.7%
	Max (-) moment	kip-in	-75.7	-78.3	3.5%
	+/- ratio	-	2.38	2.10	-
Support	Max shear	kip	8.6	9.1	5.1%
	Max (+) moment	kip-in	65.8	60.0	-8.9%
	Max (-) moment	kip-in	-22.5	-23.3	3.7%
	+/- ratio	-	2.92	2.57	-

Table 4-8: Maximum shear key demands for an eight-foot section NEXT-D bridge without parapets under the design tandem loading

Location	Criterion	Units	Solid	Shell	% Error
Mid-span	Max shear	kip	21.2	22.3	5.2%
	Max (+) moment	kip-in	330.4	307.6	-6.9%
	Max (-) moment	kip-in	-122.0	-122.3	0.3%
	+/- ratio	-	2.71	2.52	-
Quarter-span	Max shear	kip	18.8	19.3	2.7%
	Max (+) moment	kip-in	249.6	231.9	-7.1%
	Max (-) moment	kip-in	-89.7	-90.1	0.5%
	+/- ratio	-	2.78	2.57	-
Support	Max shear	kip	9.1	9.7	7.1%
	Max (+) moment	kip-in	101.9	94.0	-7.8%
	Max (-) moment	kip-in	-29.7	-28.3	-5.0%
	+/- ratio	-	3.43	3.33	-

All of the percent errors for the shell model in Tables 4-7 and 4-8 are under ten percent, proving that the cause for the large variations in the solid and shell models for shear and negative moment demand stemmed from the difference between the connections of the parapet to the bridge deck. In the solid model, the parapet is connected to the bridge deck at each shared node between the solids at the base of the parapet and the bridge deck solids. In the shell model, the parapet is only connected to the bridge deck by rigid links where the left edge of the parapet and the right edge of the parapet would be located. The way that the parapet is modeled in the shell model is more representative of the real-life parapet to deck connection because in reality, the parapet is not integral with the bridge deck across its entire width. Based on the closeness of the shear key demands in the solid and shell bridge models without parapets and the more

accurate representation of the parapet to deck connection utilized in the shell model, the shell model was determined to be an adequate solution for determining the shear and moment demands in a NEXT-D bridge. From this point forward, results will be given for the shell model only. This was an important conclusion to make because the solid model was more computationally intense than the shell model and slab forces were easier to extract from the shell model than the solid model.

Longitudinal Load Analysis

Once the shell model was chosen as an accurate representation of the bridge, the design tandem loading was moved across the six-foot and eight-foot bridge models longitudinally at each of the critical locations for shear, positive moment, and negative moment in the key to ensure that the maximum demands occurred with the load centered over the mid-span of the bridge. The critical load locations and corresponding longitudinal influence lines for the six-foot NEXT-D bridge are shown in Figures 4-12 through 4-17. The same figures are shown for the eight-foot NEXT-D bridge in Figures 4-18 through 4-23. The shear key that is subjected to the critical demand is highlighted in each figure. The Figures clearly indicate that the critical demands for shear, positive moment, and negative moment all occur when the loading is at the mid-span of the bridge.

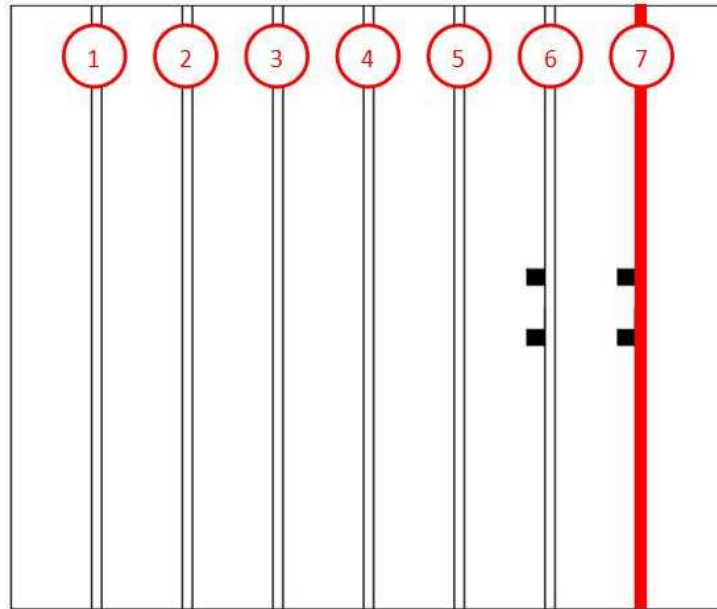


Figure 4-12: Critical load location for shear for a six-foot section NEXT-D bridge

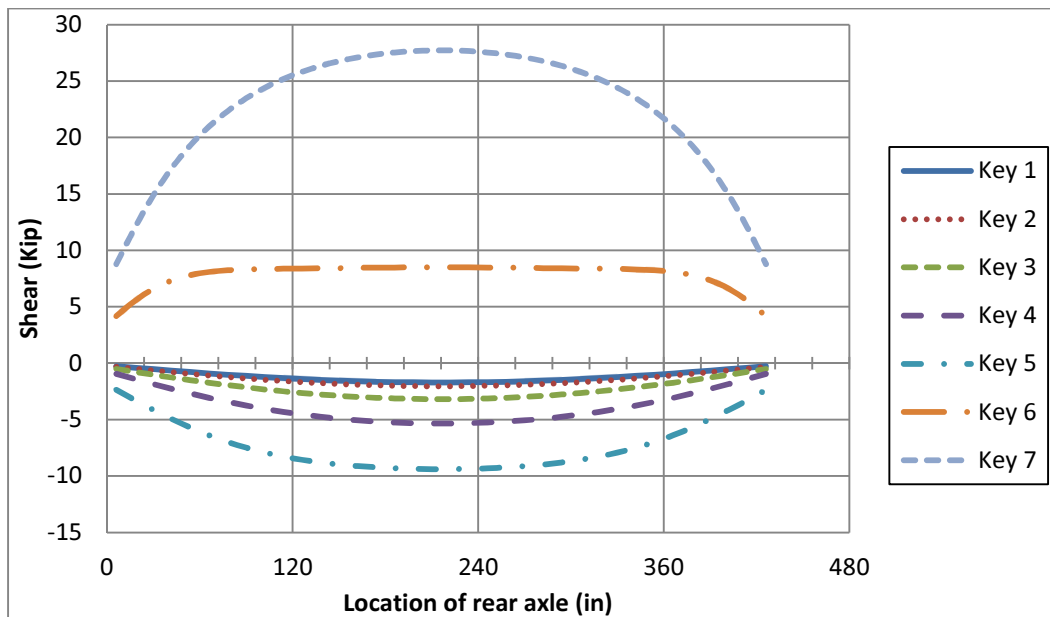


Figure 4-13: Shear influence line for the shear keys in a six-foot section NEXT-D bridge without parapets under a design tandem loading at the critical shear location

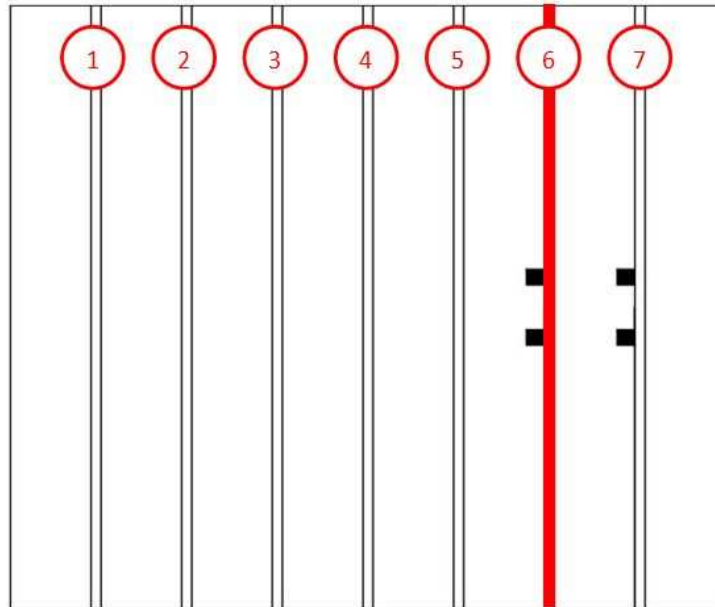


Figure 4-14: Critical load location for positive moment for a six-foot section NEXT-D bridge

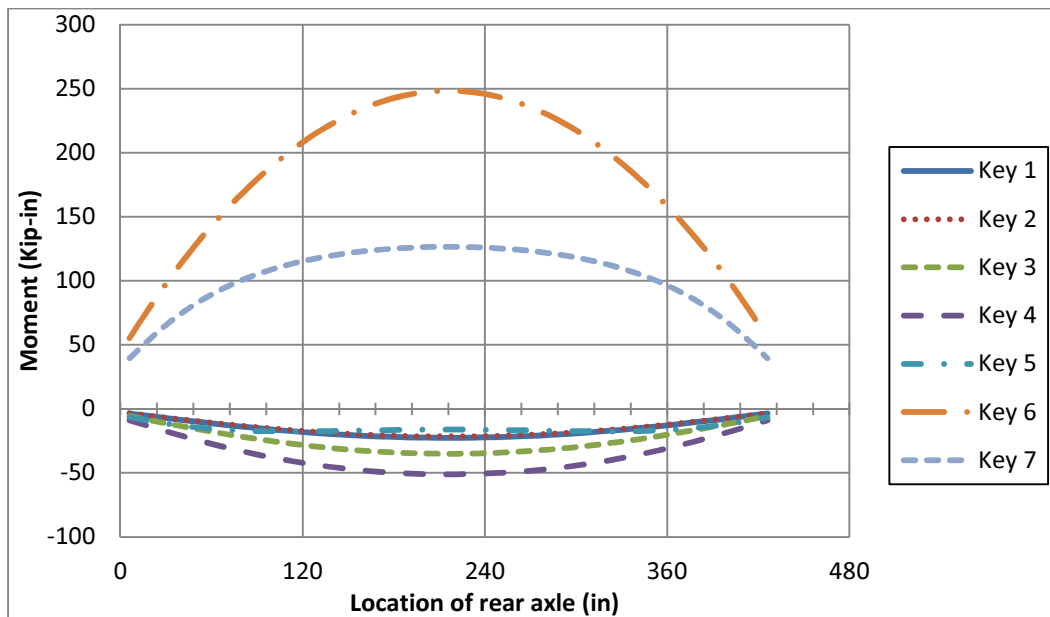


Figure 4-15: Moment influence line for the shear keys in a six-foot section NEXT-D bridge without parapets under a design tandem loading at the critical positive moment location

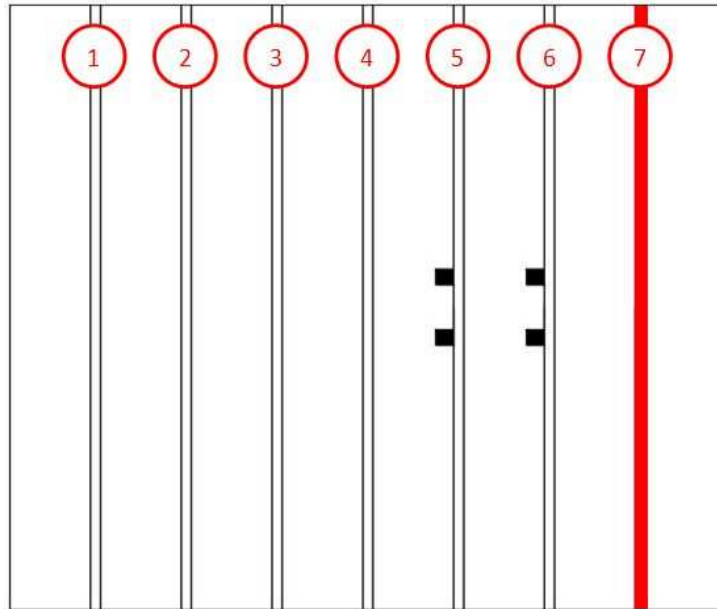


Figure 4-16: Critical load location for negative moment for a six-foot section NEXT-D bridge

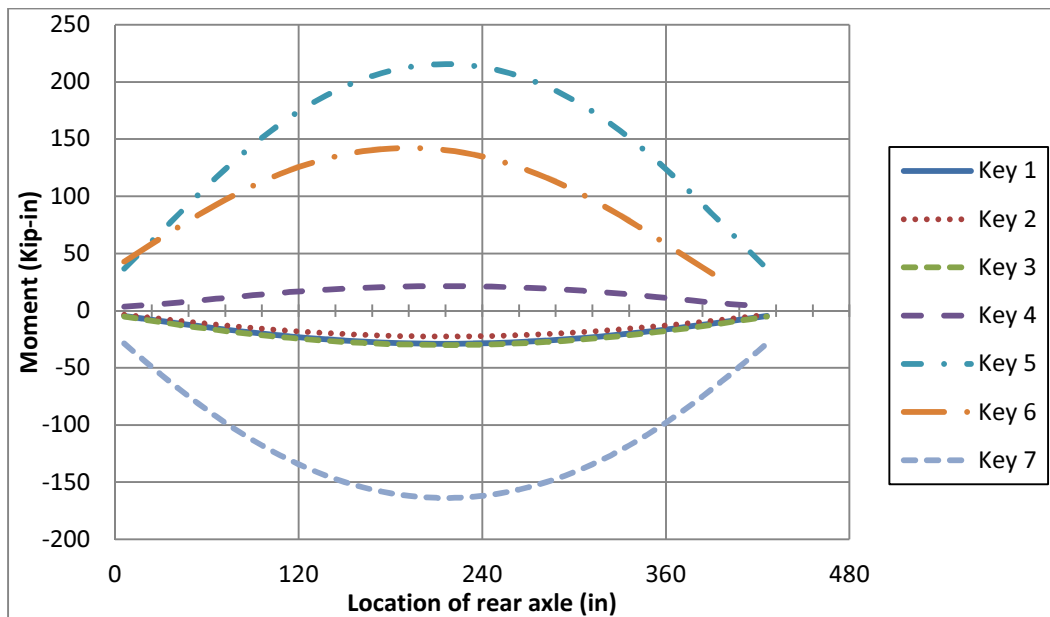


Figure 4-17: Moment influence line for the shear keys in a six-foot section NEXT-D bridge without parapets under a design tandem loading at the critical negative moment location

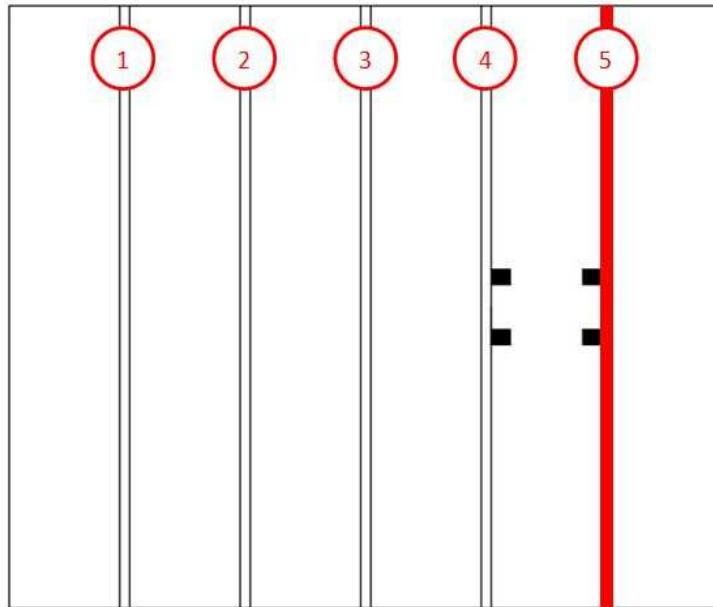


Figure 4-18: Critical load location for shear for an eight-foot section NEXT-D bridge

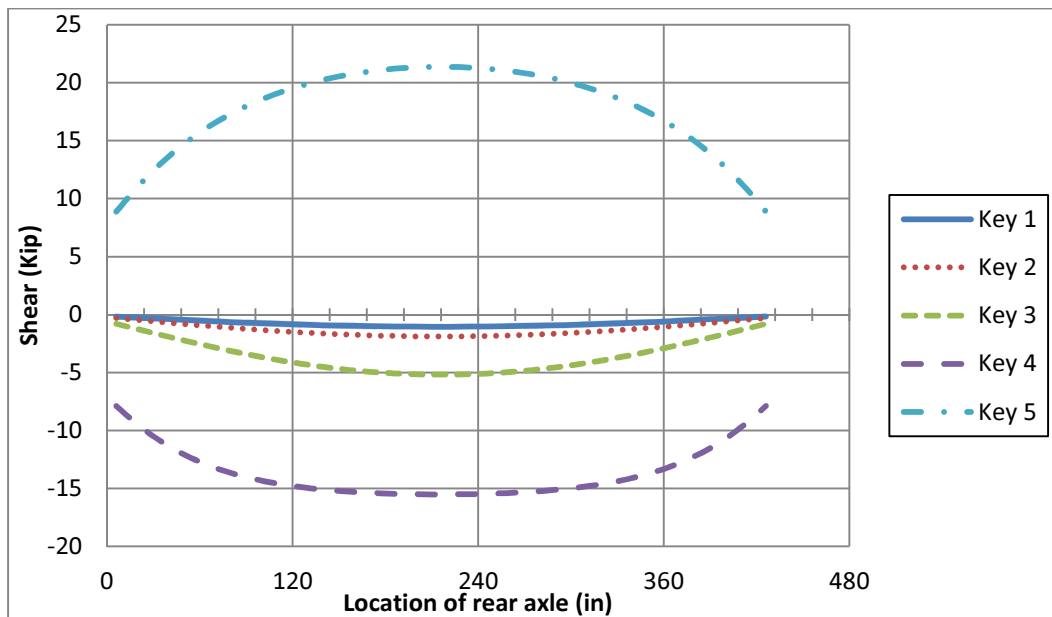


Figure 4-19: Shear influence line for the shear keys in an eight-foot section NEXT-D bridge without parapets under a design tandem loading at the critical shear location

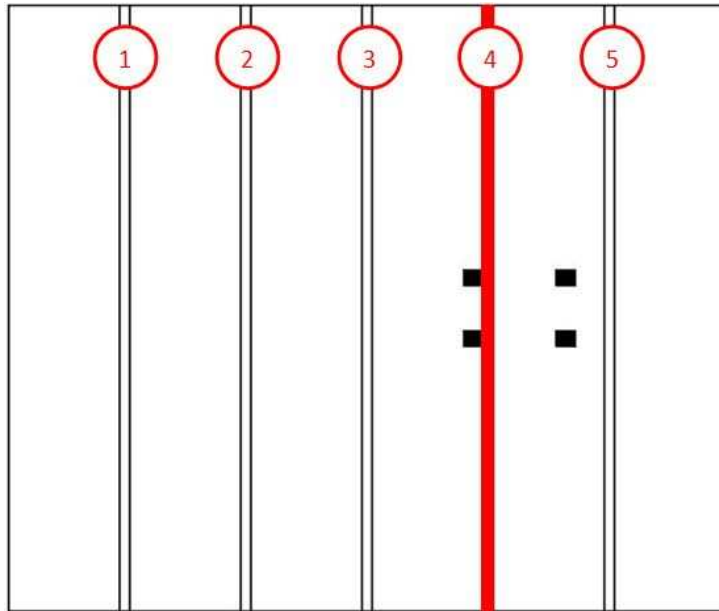


Figure 4-20: Critical load location for positive moment for an eight-foot section NEXT-D bridge

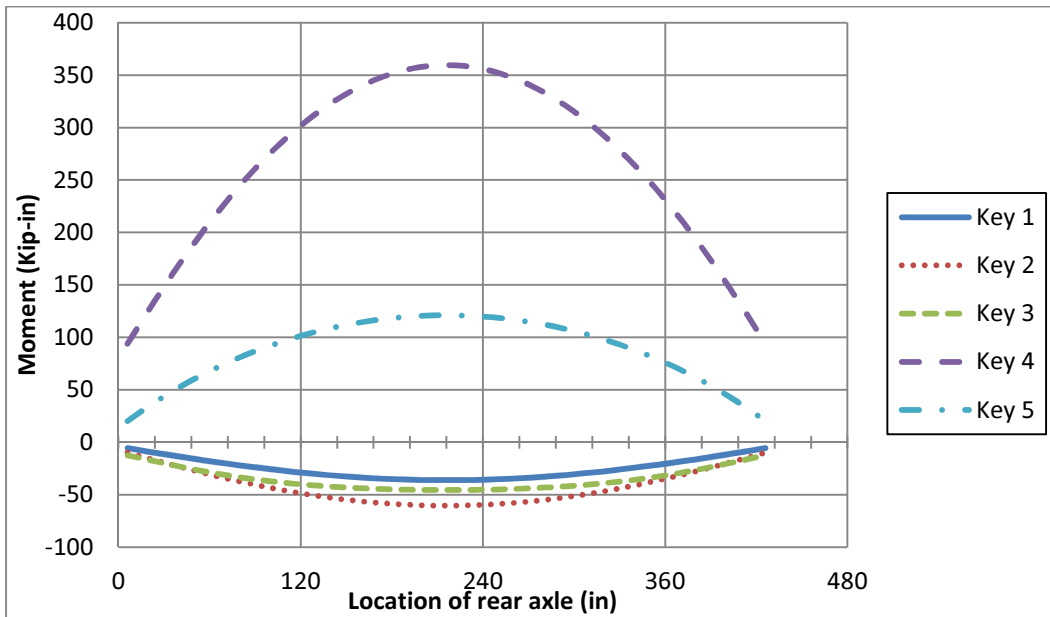


Figure 4-21: Moment influence line for the shear keys in an eight-foot section NEXT-D bridge without parapets under a design tandem loading at the critical positive moment location

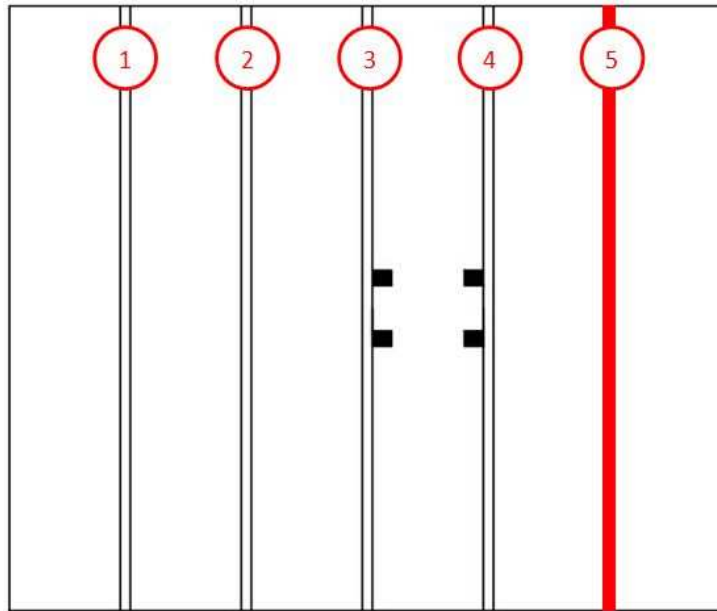


Figure 4-22: Critical load location for negative moment for an eight-foot section NEXT-D bridge

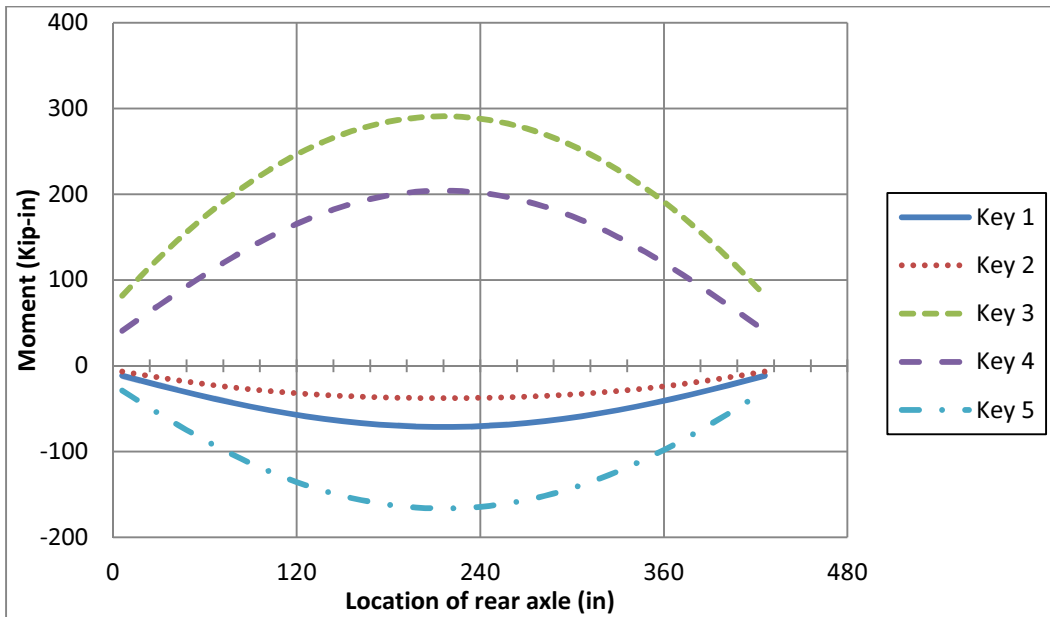


Figure 4-23: Moment influence line for the shear keys in an eight-foot section NEXT-D bridge without parapets under a design tandem loading at the critical negative moment location

Strip Width Recommendation

In order to determine a recommended strip width for the NEXT-D shear key, the distribution of shear and moment throughout the length of the shear key was investigated for the three loadings. Plots were created for all three loadings showing the shear or moment in each individual shear key element in the model and the elements location on the bridge for the critical cases shown above. Plots were also created showing the accumulated shear or moment in the key for various strip widths starting with a width of six inches (using only the shear key element at the mid-span of the bridge) all the way up to a strip width of four hundred and eighty inches (using the accumulated shear in all of the shear key elements in a row). These plots for the eight-foot section NEXT-D bridge are shown below in Figures 4-24 through 4-29. The same plots for the six-foot section NEXT-D bridge can be found in Appendix D.

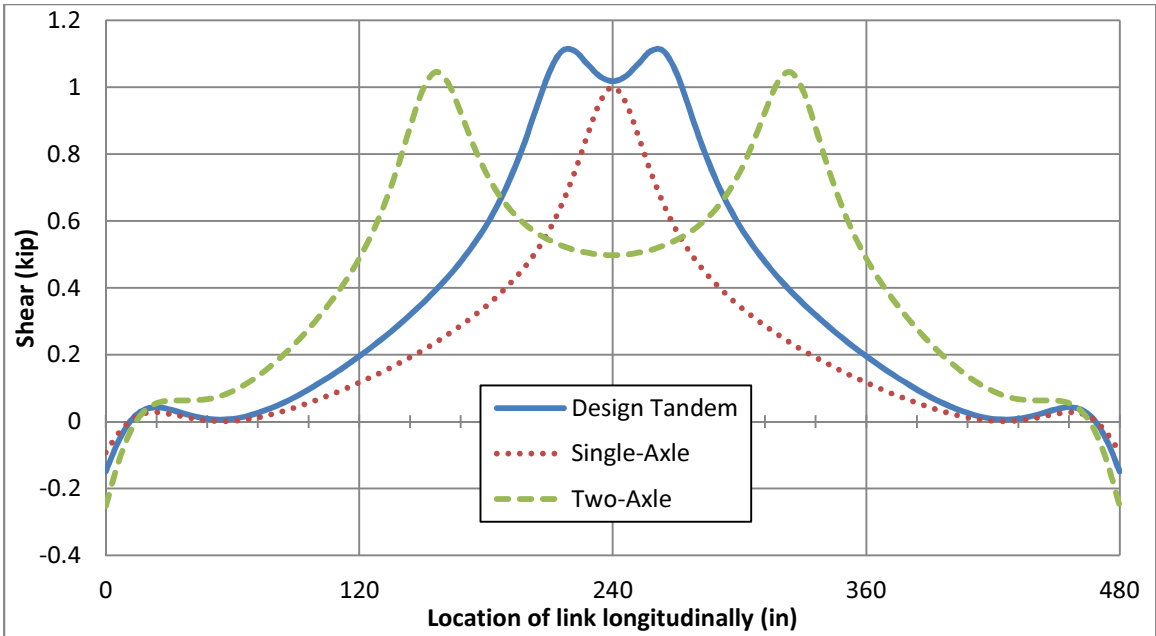


Figure 4-24: Shear in each shear key element of Key 5 along the length of an eight-foot section NEXT-D bridge with load at the critical shear location

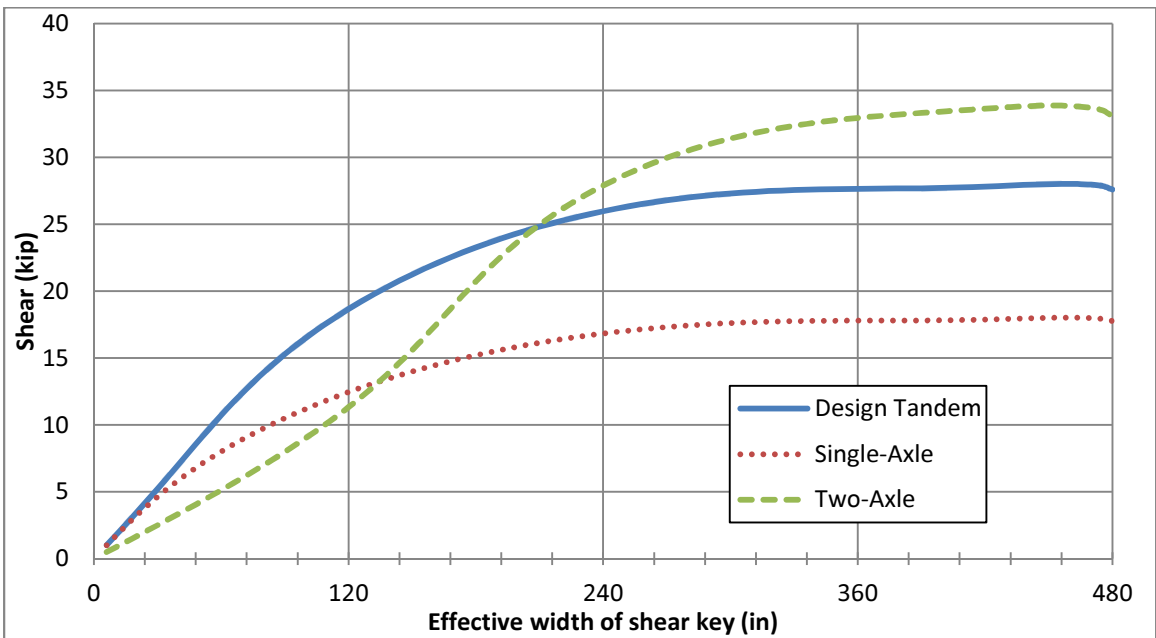


Figure 4-25: Shear accumulation plot for Key 5 of an eight-foot section NEXT-D bridge with load at the critical shear location

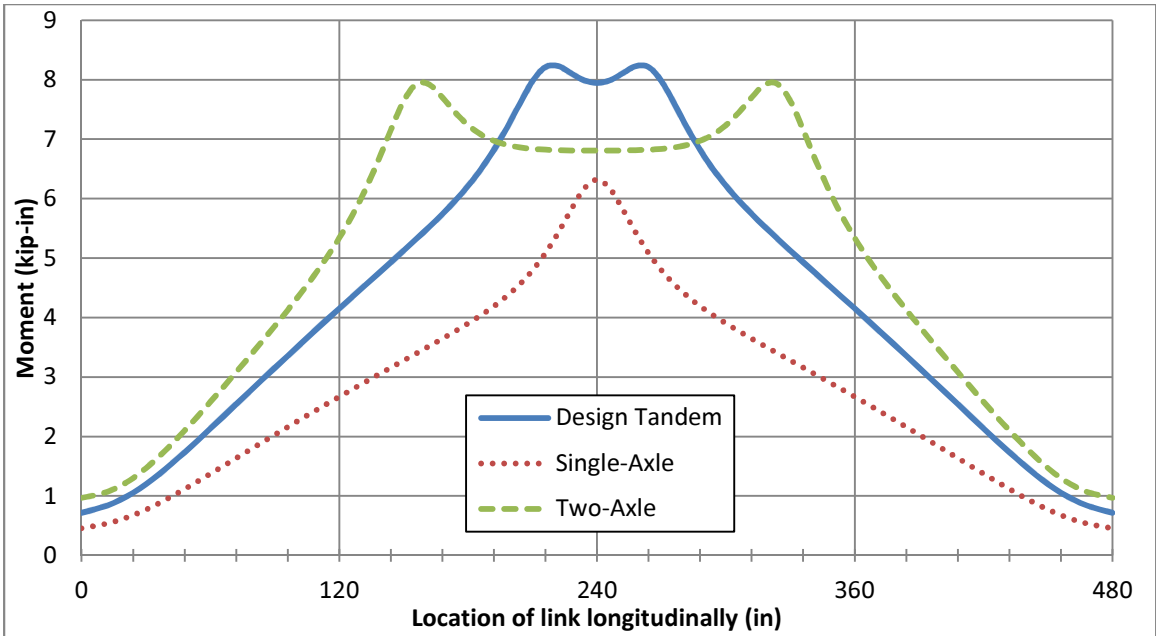


Figure 4-26: Moment in each shear key element of Key 4 along the length of an eight-foot section NEXT-D bridge with load at the critical positive moment location

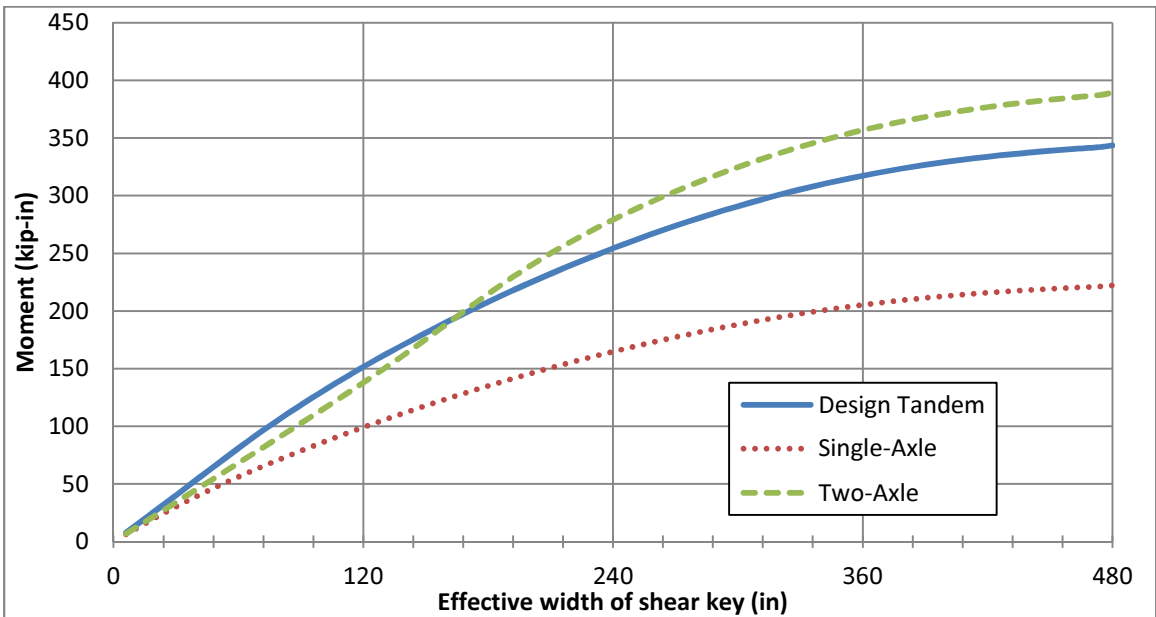


Figure 4-27: Moment accumulation plot for Key 4 of an eight-foot section NEXT-D bridge with load at the critical positive moment location

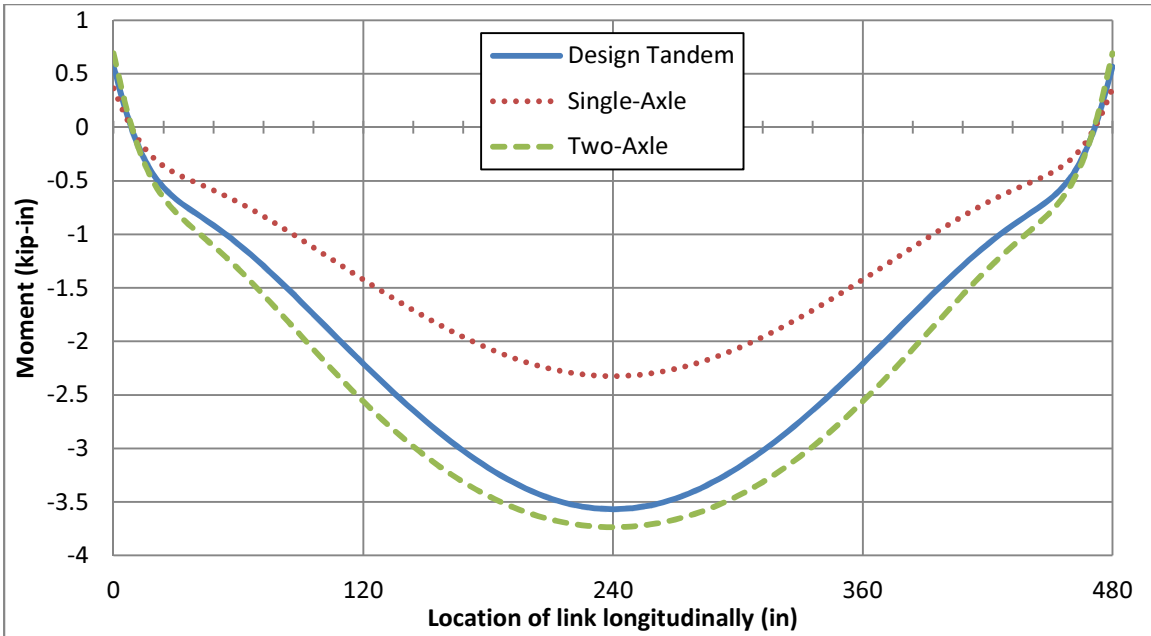


Figure 4-28: Moment in each shear key element of Key 5 along the length of an eight-foot section NEXT-D bridge with load at the critical negative moment location

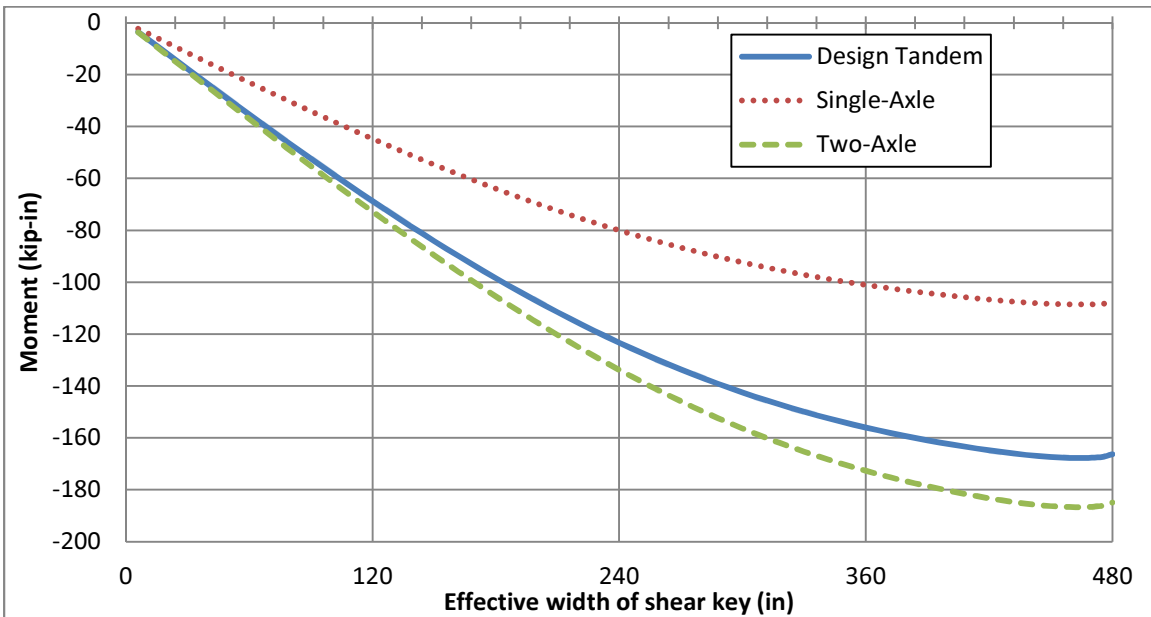


Figure 4-29: Moment accumulation plot for Key 5 of an eight-foot section NEXT-D bridge with load at the critical negative moment location

The previous figures show that the shear and moment demand in the shear key is spread out throughout the entire length of the key. For example, Figure 4-30 shows that in order to accumulate ninety percent of the maximum moment in the shear key, a strip width of twenty eight feet would need to be used. To accumulate seventy-five percent of the maximum moment, a strip width of twenty feet is required.

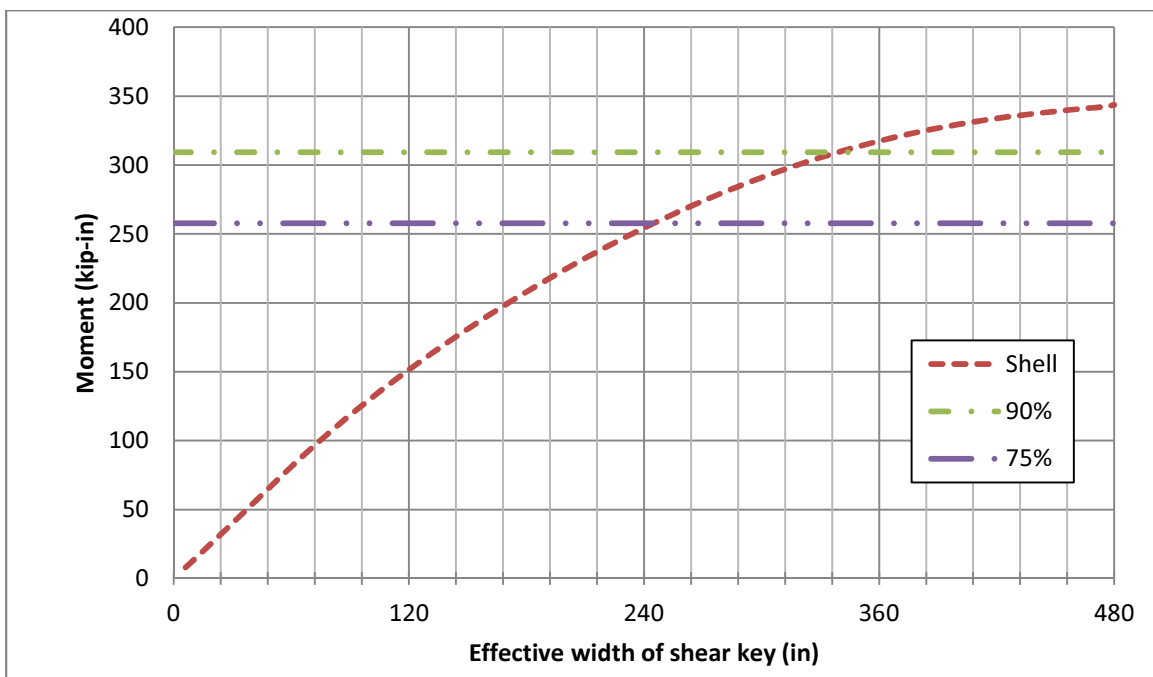


Figure 4-30: Moment accumulation plot for an eight-foot section NEXT-D bridge under the design tandem loading at the critical positive moment case

Because the shear and moments were distributed throughout the key so well, the geometry of the live loads was used to recommend a strip width. For the design tandem, the recommended strip width is ten feet. For the single-axle load, the

recommended strip width is 14 feet. The recommended strip width for the two-axle load is 28 feet. These widths were determined based on the spacing of the axles and the closest possible spacing of an additional axle. By only allowing a strip width equal to the tributary length of one truck, the presence of multiple design vehicles in a lane is easily accounted for. If each strip width is designed to be able to withstand the demand created in the entire 40-foot length of the shear key, then even if more than one truck is in a lane at a time, the bridge will be ensured to have enough capacity to function without failure. The possibility of multiple side-by-side trucks was not considered in this study because previous research showed that the presence of one truck is more conservative than the presence of multiple trucks (Deery 2010). This is because a 1.2 multiple presence factor must be used if only one truck is considered, and this factor decreases as more trucks are considered (AASHTO 2010). This strip width determination for all three loads is shown in Figures 4-31 through 4-33.

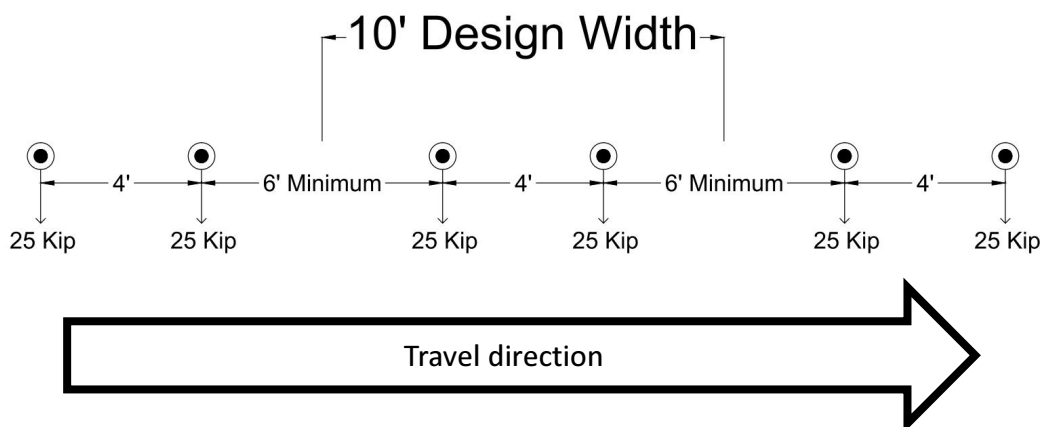


Figure 4-31: Design tandem strip width determination

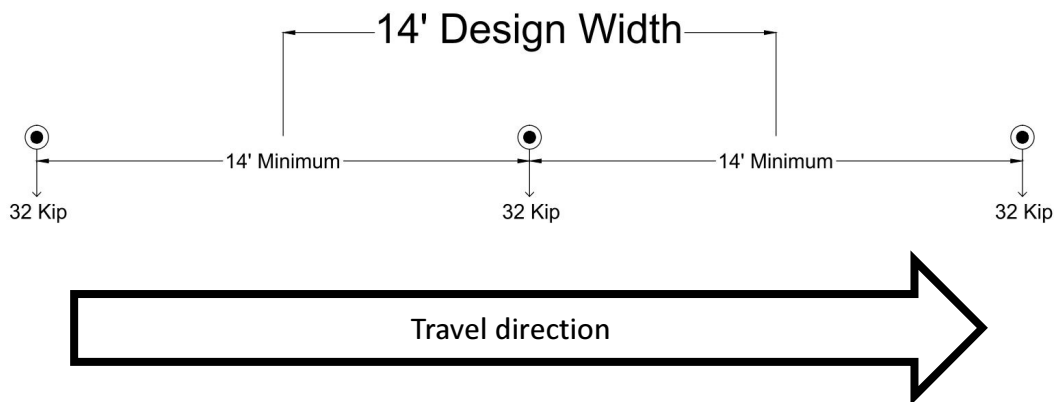


Figure 4-32: Single-axle strip width determination

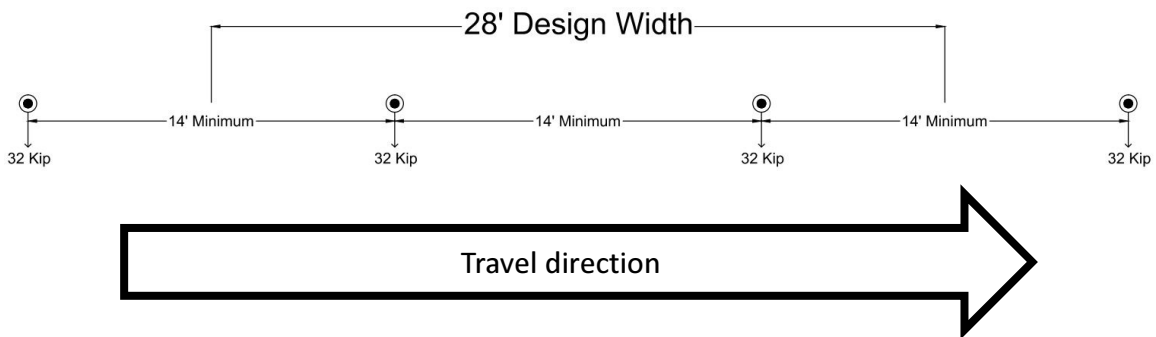


Figure 4-33: Two-axle strip width determination

The critical demands determined by the influence lines were then divided by the recommended strip widths for each load in order to determine which load case controlled based on a demand per foot basis. These results are shown in Tables 4-9 and 4-10 for the six-foot and eight-foot section NEXT-D beams.

Table 4-9: Demand per foot for a six-foot NEXT-D bridge based on recommended strip widths

	Design Tandem	Single Axle	Two Axles	Units
Strip width:	10	14	28	ft
Max shear:	2.78	1.27	1.21	kip/ft
Max positive moment:	24.84	11.47	10.06	(kip-in)/ft
Max negative moment:	-16.41	-7.58	-6.55	(kip-in)/ft

Table 4-10: Demand per foot for an eight-foot NEXT-D bridge based on recommended strip widths

	Design Tandem	Single Axle	Two Axles	Units
Strip width:	10	14	28	ft
Max shear:	2.80	1.29	1.21	kip/ft
Max positive moment:	34.36	15.87	13.90	(kip-in)/ft
Max negative moment:	-16.78	-7.76	-6.67	(kip-in)/ft

Based on the recommended strip widths, the design tandem was the most critical loading for both the six-foot and eight-foot NEXT-D bridges by a large margin. The shear, positive moment, and negative moment demand per foot of the design tandem load exceeded that of the single-axle and double-axle load by a factor greater than two.

Conclusions

The HS20 design truck and the design tandem were moved across the six-foot and eight-foot NEXT-D bridge models transversely in order to determine the maximum shear, positive moment, and negative moment in the shear keys. Both the solid models and the shell models were analyzed to determine the maximum

demands in the shear keys. The shell and solid model results were compared, and provided very similar results with the exception of the outermost shear keys. This difference was caused by the different methods of connecting the parapet to the bridge deck. The method used in the shell model was deemed the more accurate of the two, so the shell model was concluded to provide an accurate representation of a NEXT-D bridge. Loads were moved across the bridge longitudinally at the critical shear, positive moment, and negative moment locations in order to prove that the maximum demand occurred in the keys with the loading over the mid-span of the bridge.

Once maximum demands in the bridge were found, for each loading, the distribution of shear and moment throughout the forty-foot length of the key was investigated. The model showed that the forces were well distributed throughout the entire length of the bridge, so a strip width was recommended for each loading based on the geometry of the design trucks to facilitate multiple-presence more easily. Shear and moment demands were determined on a per-foot basis for each loading and its respective strip width. The design tandem loading caused the highest shear, positive moment, and negative moment demand in the shear keys. The unfactored design values for the transverse forces for the shear keys in a six-foot and eight-foot NEXT-D bridge forty feet in length are shown in Table 4-11. The shear key should be designed so that any ten-foot section of key has enough capacity for these demands.

Table 4-11: Unfactored shear key design live loads for a forty-foot NEXT-D bridge

	Six-foot sections	Eight-foot sections	Units
Max shear:	27.8	28.0	kip
Max positive moment:	248.4	343.6	kip-in
Max negative moment:	-164.1	-167.8	kip-in

Table 4-11 shows that the six-foot and eight-foot section NEXT-D bridges result in similar demands for shear and negative moment, but that the eight-foot sections result in a significantly greater demand for positive moment.

Deck Live Load Analysis

Procedure

After the demands were determined for the shear keys in a NEXT-D bridge, the demands for the eight-inch deep section of the NEXT-D beams that composes the deck were found. A process similar to that of the shear keys was followed in order to determine the maximum demands in the deck. The deck live load analysis was performed under the assumption that the design tandem at mid-span produces the maximum transverse demand in the bridge based on the results of the shear key study. Also, only the shell model was analyzed for transverse deck forces. The design tandem loading was moved laterally across the mid-span of the bridge in order to create influence lines for various locations on the NEXT-D beams. Shear and moment influence lines were created for five points on each NEXT-D section. These points included both faces of the two

stems and the mid-point between the two stems as shown in Figure 4-34. The maximum shear, positive moment, and negative moment demands were found for each point for the six-foot and eight-foot NEXT-D models.

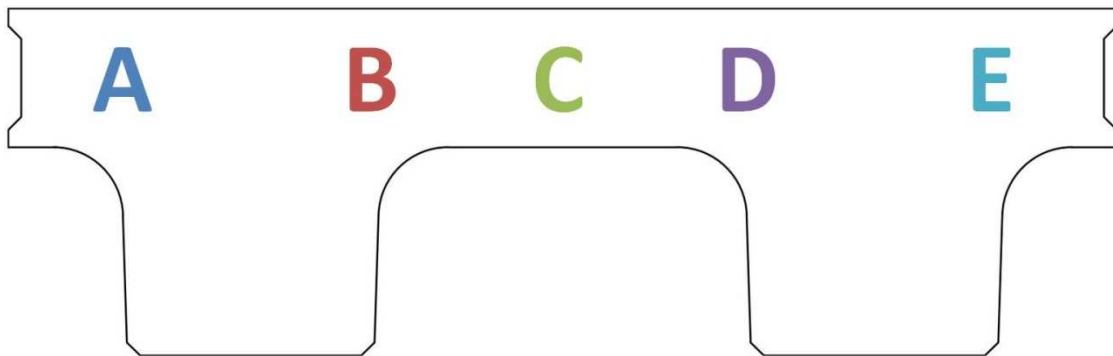


Figure 4-34: Critical slab locations

SAP2000 Shell Joint Forces

SAP2000 (Computers and Structures 2011b) shell elements provide joint forces at each node for all six degrees of freedom: forces in the direction of all three joint local axis and moments about all three axes. With the exception of the shell elements on the edge of the bridge, each shell element node is shared by four shell elements. In order to maintain equilibrium, whenever multiple elements share a node, the joint forces for the shared node from all of the elements must sum to zero. For the nodes at Point C in Figure 4-34, the joint forces for the joints located at Point C from the shell elements to the left of the point are equal and opposite to those from those from the shell elements to the right of the point. Therefore, for Point C, the deck forces could be taken from the shells on either

side of the point. For Points A, B, D, and E there is also a rigid link that shares the node with the corners of the shell elements located at these points. Therefore, the joint force from the end of the rigid link must be included in the shell joint forces to maintain equilibrium at the node. At these points, the shell joint forces to the left of the point of interest are not equal to the shell joint forces to the right of the point of interest. For this reason, it was important to use the shell joint forces in the shell elements to the left of Points A and D, and the shell joint forces in the shell elements to the right of Points B and E because the demand in the eight-inch section of the NEXT-D beams is needed to determine the required capacity for the bridge deck. Careful attention was paid to the sign of the joint moments to ensure that moments were reported with the correct sign.

Results and Conclusions

Typical shear and moment influence lines for the critical deck locations in one NEXT-D beam from the eight-foot section bridge are shown in Figures 4-35 and 4-36. The rest of the influence lines can be found in Appendix E.

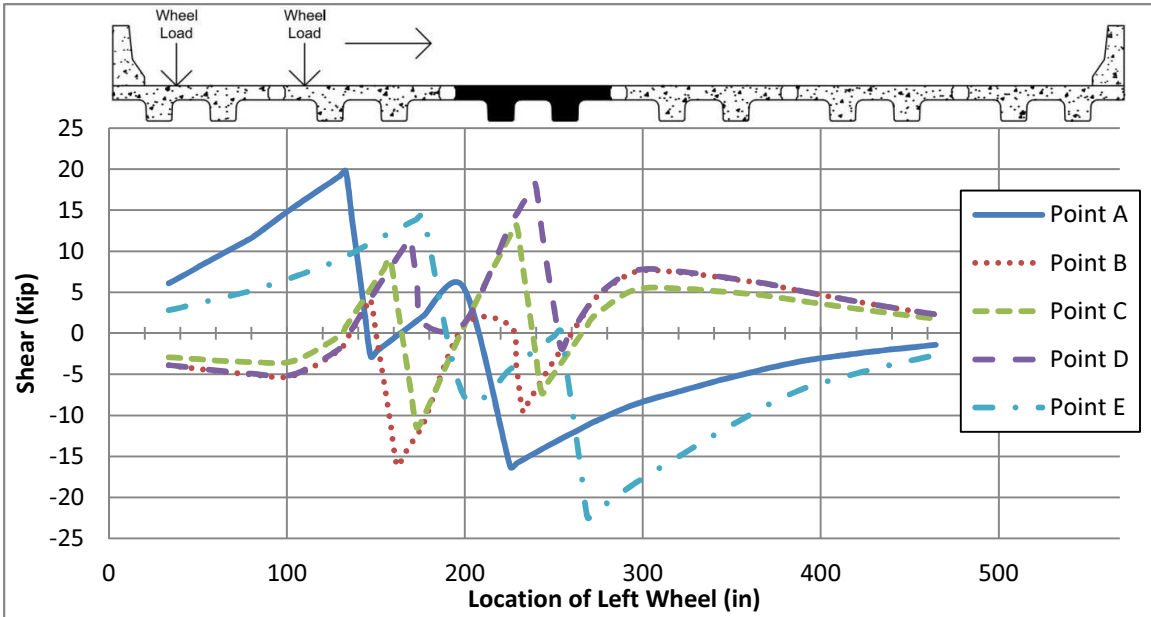


Figure 4-35: Shear influence line for the critical deck locations in the third beam from the left in an eight-foot section NEXT-D bridge

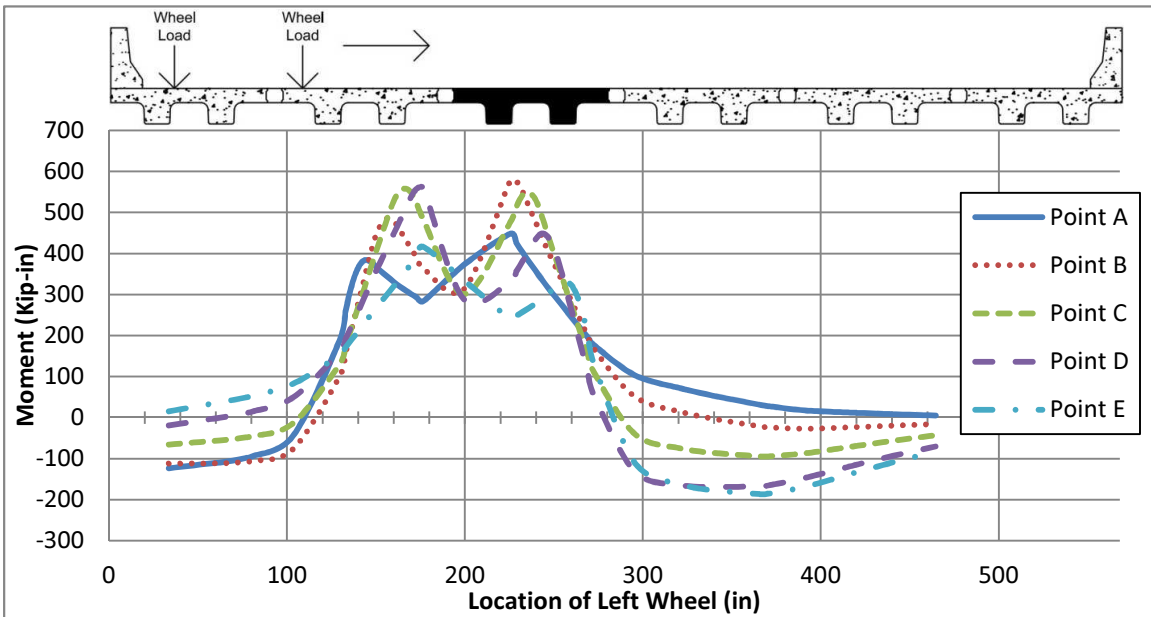


Figure 4-36: Moment influence line for the critical deck locations in the third beam from the left in an eight-foot section NEXT-D bridge

From these influence lines, the maximum shear, positive moment, and negative moment in the decks were found for all five critical points for both the six-foot and eight-foot NEXT-D bridge models. Based on the above Figures, the maximum shear demand occurs in Points A and E, while the maximum moment demand occurs in Points B, C, and D.

The unfactored deck design loads for each critical point for the six-foot section NEXT-D bridge are shown in Table 4-12 and the unfactored deck design loads for each critical point for the eight-foot section NEXT-D bridge are shown in Table 4-13. The bridge deck should be designed so that a ten-foot section of deck has enough capacity for these demands.

Table 4-12: Unfactored deck design live loads for a six-foot section NEXT-D bridge forty feet in length

	A/E	B/D	C	Units
Max shear:	28.2	16.9	11.2	Kip
Max positive moment:	345.6	466.2	467.8	Kip-in
Max negative moment:	-271.2	-309.3	-213.7	Kip-in

Table 4-13: Unfactored deck design live loads for an eight-foot section NEXT-D bridge forty feet in length

	A/E	B/D	C	Units
Max shear:	33.3	21.2	15.6	Kip
Max positive moment:	474.0	623.4	562.3	Kip-in
Max negative moment:	-488.9	-511.5	-349.6	Kip-in

As shown in Tables 4-12 and 4-13, the maximum shear demand exists in Points A and E while the maximum positive moment demand exists in Points B, C, and D. The maximum negative moment demand exists in points B and D. The deck demand for the eight-foot sections are significantly higher than the demands for the six-foot section.

In order to save costs on reinforcement, the outer NEXT-D beams could be designed differently than the middle NEXT-D beams. This would allow the deck in the outer beams to be designed for much smaller positive moments and the deck in the middle beams to be designed for much smaller negative moments. However, the savings in reinforcing steel may not be worth the extra fabrication costs of making two separate NEXT-D sections for the same bridge. Furthermore, if different outer and middle beams were utilized, the potentially catastrophic result of placing outer beams in the middle and vice versa would be introduced into the construction process. The unfactored deck design loads for the six-foot section NEXT-D bridge broken up into outside and middle girders are shown in Table 4-14 and 4-15. The unfactored deck design loads for the eight-foot section NEXT-D bridge broken up into outside and middle girders are shown in Tables 4-16 and 4-17.

Table 4-14: Unfactored deck design live loads for the outer beams in a six-foot section NEXT-D bridge forty feet in length

	A/E	B/D	C	Units
Max shear:	28.2	15.5	10.4	Kip
Max positive moment:	44.3	104.0	152.7	Kip-in
Max negative moment:	-271.2	-309.3	-213.7	Kip-in

Table 4-15: Unfactored deck design live loads for the middle beams in a six-foot section NEXT-D bridge forty feet in length

	A/E	B/D	C	Units
Max shear:	26.6	16.9	11.2	Kip
Max positive moment:	345.6	466.2	467.8	Kip-in
Max negative moment:	-143.6	-149.6	-85.4	Kip-in

Table 4-16: Unfactored deck design live loads for the outer beams in an eight-foot section NEXT-D bridge forty feet in length

	A/E	B/D	C	Units
Max shear:	33.3	16.4	11.7	Kip
Max positive moment:	53.5	61.8	97.9	Kip-in
Max negative moment:	-488.9	-511.5	-349.6	Kip-in

Table 4-17: Unfactored deck design live loads for the middle beams in an eight-foot section NEXT-D bridge forty feet in length

	A/E	B/D	C	Units
Max shear:	24.8	21.2	15.6	Kip
Max positive moment:	474.0	623.4	562.3	Kip-in
Max negative moment:	-230.8	-199.4	-105.0	Kip-in

As Tables 4-14 through 4-17 show, by separating the NEXT-D beams into the outer beams and middle beams, the outer beams can be designed for considerably lower positive moment demands than the middle beams and the middle beams can be designed for significantly lower negative moments than the outer beams. For the six-foot section bridge, the maximum positive moment in the middle beams is about three times greater than the maximum positive moment in the outer beams. The maximum negative moment in the outer beams is about twice as high as the maximum negative moment in the middle beams. The difference between the outer beams and middle beams of the eight-foot section bridge is even greater. For the eight-foot section bridge, the maximum positive moment in the middle beams is over six times greater than the maximum positive moment in the outer beams, while the maximum negative moment in the outer beams is over twice as high as that of the middle beams.

Dead Load Analysis

Shear Key Dead Loads

The self-weight of the shear keys was ignored in the calculations of the dead loads for the bridge. This is because in the transverse direction, the length of the shear key is only eight inches, so the contribution of its self-weight is negligible. The self-weight of the key becomes even less significant once the design loads are factored because the self-weight is multiplied by a factor of 1.25, while the live loads are multiplied by a 1.75 live load factor, a 1.2 multiple presence factor,

and a 1.33 impact load factor for a total factor of 2.8 (AASHTO 2010). Also, the length of the shear key in the model is only 4.66 inches and the shear key elements are not centered between adjacent NEXT-D sections, so including the dead load would throw off the symmetry of the model. In order to determine the dead load demand for the shear keys, the self-weight of the NEXT-D sections were turned off, so the only dead load due to self-weight acting on the shear keys was the self-weight of the parapets. This was done because of the construction process of a NEXT-D bridge. When the bridge is built, the NEXT-D beams will already be in place before the shear keys are poured. Therefore, the self-weight of the beams will not contribute to the dead load demand on the shear keys.

In addition to the self-weight of the parapet, a super-imposed dead load of 37.5 pounds per square foot was applied to the entire bridge deck to represent a future wearing surface on the bridge. The maximum shear, moment, and negative moment demands were found for a ten-foot section of bridge based on these dead loads. A ten-foot section was chosen to correspond with the strip width recommendation. The maximum dead load demand for a ten-foot section of shear key would be factored and added to the factored live load demands on the shear keys in order to determine the required shear key capacity. This is a very conservative method because it assumes that the maximum dead load demand in the key occurs at the same location as the maximum live load demand. The maximum dead load and future wearing surface demand for the shear keys in a six-foot section NEXT-D bridge are shown in Table 4-18. The

maximum dead load and future wearing surface demand for the shear keys in an eight-foot section NEXT-D bridge are shown in Table 4-19. The demand due to the self-weight of the parapet is given separately than the demand due to the future wearing surface because AASHTO specifies a different load factor for the two demands (AASHTO 2010).

Table 4-18: Dead load and future wearing surface demand for the shear keys in a six-foot section NEXT-D bridge

	Dead load	Future wearing surface	Units
Max shear:	1.1	2.8	Kip
Max positive moment:	1.7	14.8	Kip-in
Max negative moment:	-4.8	-11.2	Kip-in

Table 4-19: Dead load and future wearing surface demand for the shear keys in an eight-foot section NEXT-D bridge

	Dead load	Future wearing surface	Units
Max shear:	0.8	2.7	Kip
Max positive moment:	0.1	20.9	Kip-in
Max negative moment:	-3.3	-7.8	Kip-in

Slab Dead Loads

For the slab, the dead load demand was determined by modeling one simply supported NEXT-D section and determining the shear and moment demand for the slab due to the self-weight of the section. Next, the demand in the slab due to the self-weight of the parapet was determined, and this was added to the demand due to the self-weight of the NEXT-D section itself in order to determine the dead load demand for the deck. The future wearing surface load was also

considered for the slab dead load demand. The maximum dead load and future wearing surface demand for the critical locations in the deck for a six-foot section NEXT-D bridge are shown in Table 4-20 and 4-21. The maximum dead load and future wearing surface demand for the critical locations in the deck for an eight-foot section NEXT-D bridge are shown in Tables 4-22 and 4-23.

Table 4-20: Dead load demand for the deck in a six-foot section NEXT-D bridge

	Point A/E	Point B/D	Point C	Units
Max shear:	1.7	4.9	3.7	Kip
Max positive moment:	6.0	34.9	24.8	Kip-in
Max negative moment:	-10.3	-74.1	-31.6	Kip-in

Table 4-21: Future wearing surface demand for the deck in a six-foot section NEXT-D bridge

	Point A/E	Point B/D	Point C	Units
Max shear:	2.4	4.3	4.4	Kip
Max positive moment:	22.6	70.6	28.1	Kip-in
Max negative moment:	-27.6	-97.0	-63.6	Kip-in

Table 4-22: Dead load demand for the deck in an eight-foot section NEXT-D bridge

	Point A/E	Point B/D	Point C	Units
Max shear:	2.6	10.9	8.8	Kip
Max positive moment:	28.4	-2.2	-36.9	Kip-in
Max negative moment:	-29.9	-245.2	-148.4	Kip-in

Table 4-23: Future wearing surface demand for the deck in a six-foot section NEXT-D bridge

	Point A/E	Point B/D	Point C	Units
Max shear:	2.6	5.1	5.4	Kip
Max positive moment:	39.7	76.4	26.6	Kip-in
Max negative moment:	-56.0	-127.9	-91.7	Kip-in

AASHTO Deck Design

Results and Discussions

The equivalent strip width method prescribed by AASHTO was also used to determine the demand for the shear key. This was done by using SAP2000 to create models of a continuous beam with rigid supports at the location of each stem for both the six-foot and eight-foot sections. The design tandem load was moved across the beam laterally and shear and moment influence lines were created. The shear, positive moment, and negative moment live load demands in the shear key were determined using this method and then compared to the results of the 3D model to test the adequacy of the AASHTO strip width method in determining design forces in the key. The shear and moment influence lines for the six-foot section NEXT-D bridge are shown in Figures 4-37 and 4-38. The shear and moment influence lines for the eight-foot section NEXT-D bridge are shown in Figures 4-39 and 4-40. The maximum demands in the shear key based on the AASHTO model are compared with the demands provided by the 3D

model in Tables 4-24 and 4-25. Percent errors are calculated based on the assumption that the 3D model provides the “theoretical results.”

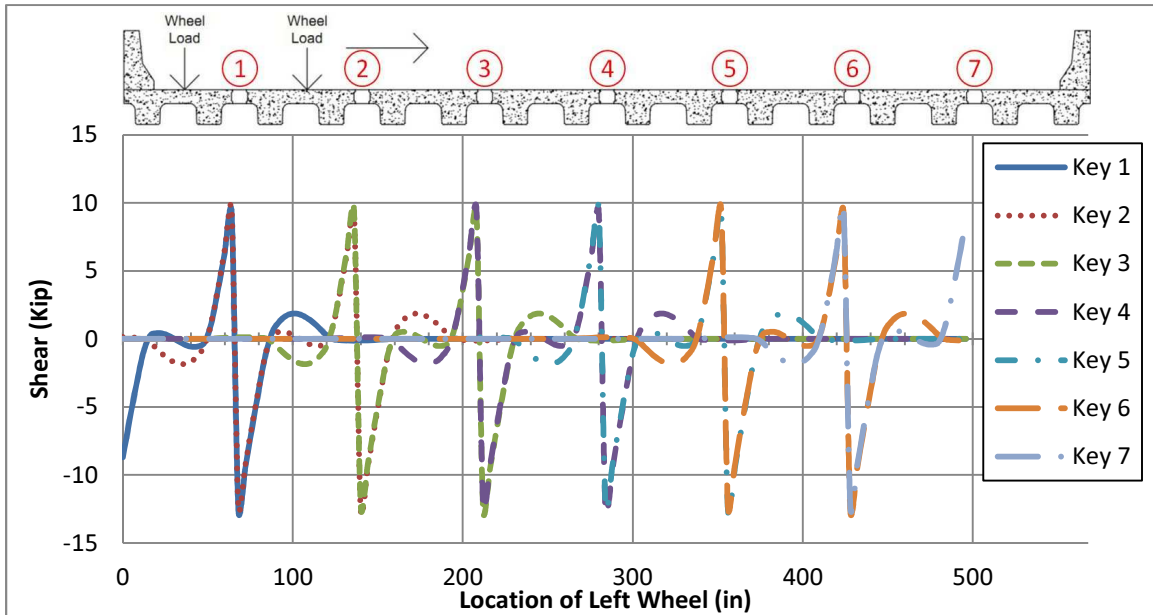


Figure 4-37: Shear influence lines for the shear keys in a six-foot section NEXT-D bridge using the AASHTO strip width method

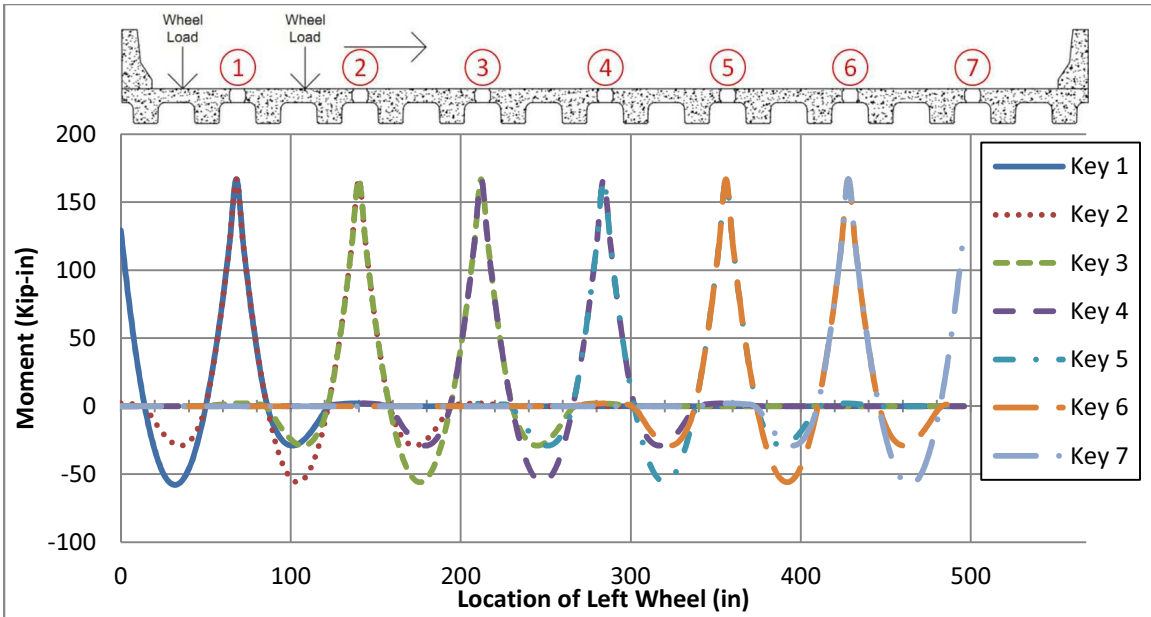


Figure 4-38: Moment influence lines for the shear keys in a six-foot section NEXT-D bridge using the AASHTO strip width method

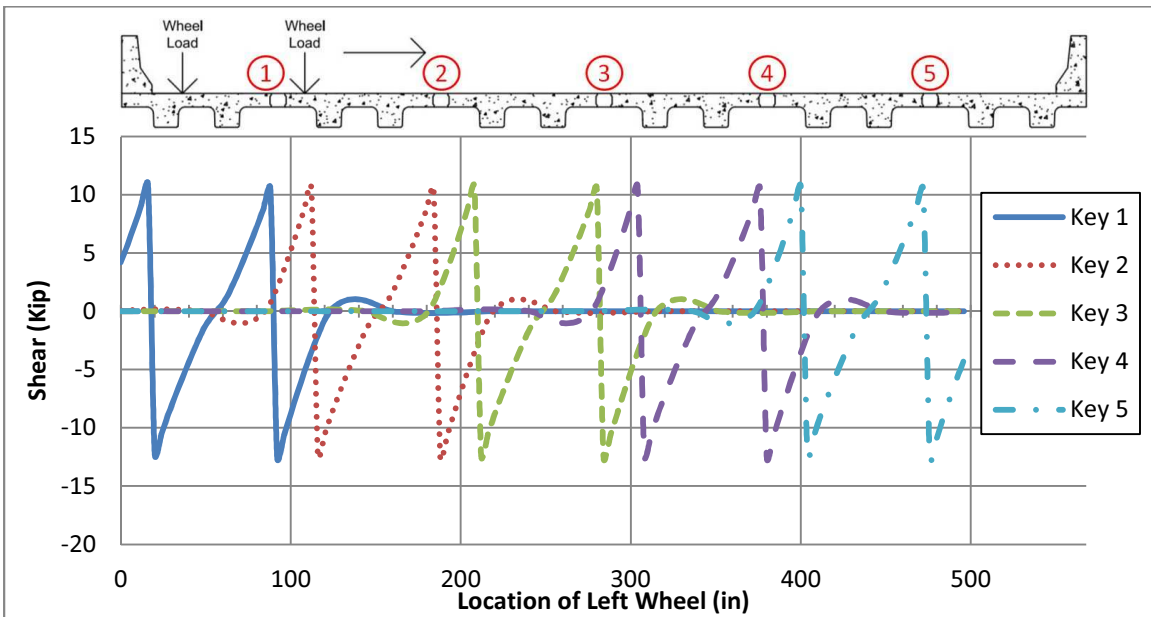


Figure 4-39: Shear influence lines for the shear keys in an eight-foot section NEXT-D bridge using the AASHTO strip width method

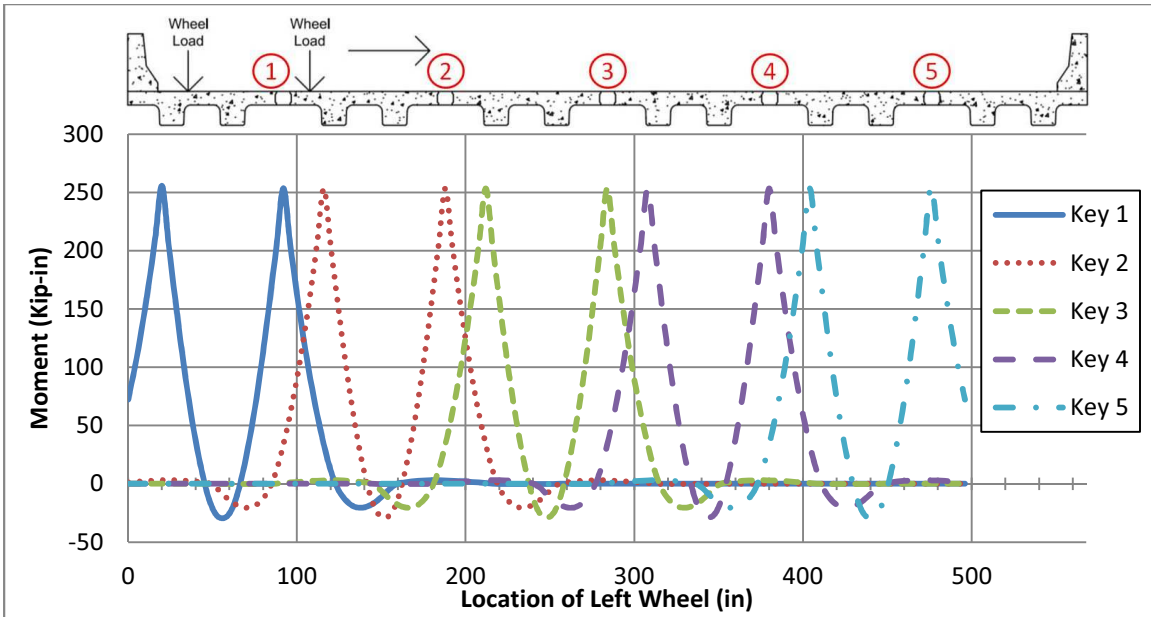


Figure 4-40: Moment influence lines for the shear keys in an eight-foot section NEXT-D bridge using the AASHTO strip width method

Table 4-24: Unfactored live load demand in the shear keys of a six-foot section NEXT-D bridge

	AASHTO model	3D model	Units	% Error
Max shear:	12.6	27.8	kip	-54.5%
Max positive moment:	166.9	248.4	kip-in	-32.8%
Max negative moment:	-58.5	-164.1	kip-in	-64.3%

Table 4-25: Unfactored live load demand in the shear keys of an eight-foot section NEXT-D bridge

	AASHTO model	3D model	Units	% Error
Max shear:	12.7	28.0	kip	-54.7%
Max positive moment:	255.6	343.6	kip-in	-25.6%
Max negative moment:	-29.6	-167.8	kip-in	-82.4%

Figures 4-37 through 4-40 show that unlike the results of the 3D models, the shear and moment demands in the outer shear keys and middle shear keys are the same. Based on the values in Tables 4-24 and 4-25, the AASHTO strip width method is very unconservative. However, the equivalent strip width for the six-foot NEXT-D bridge based on the AASHTO equations shown in Table 2-1 is 45.8 inches for the positive moment design ($26.0in + 6.6 \frac{in}{ft} * 3ft = 45.8in$) and 57 inches ($48 + 3.0 \frac{in}{ft} * 3ft = 57in$) for the negative moment design. There is no equation given in AASHTO to determine a strip width for shear design, so the positive moment strip width will be used because it is conservative compared to the negative moment strip width. The equivalent strip width for the eight-foot NEXT-D bridge cannot be determined from the AASHTO LRFD Bridge Design Specs because they do not address bridges where the supporting components of the deck have variable spacings. For the purpose of comparing the results from the AASHTO model to the results from the 3D model, an S of four feet, which is the average spacing of the stems of a bridge built with eight-foot NEXT-D sections. This results in a strip width of 52.4 inches for positive moment design and 60 inches for negative moment design (AASHTO 2010). The shear, positive moment, and negative moment demand normalized for the strip width for both the AASHTO beam model and the 3D bridge model are shown in Tables 4-26 and 4-27.

Table 4-26: Unfactored live load demand in the shear keys of a six-foot section NEXT-D bridge normalized for strip width

	AASHTO model	3D model	Units	% Error
Max shear:	3.3	2.8	kip/ft	19.2%
Max positive moment:	43.7	24.8	(kip-in)/ft	76.0%
Max negative moment:	-12.3	-16.4	(kip-in)/ft	-24.9%

Table 4-27: Unfactored live load demand in the shear keys of an eight-foot section NEXT-D bridge normalized for strip width

	AASHTO model	3D model	Units	% Error
Max shear:	2.9	2.8	kip/ft	3.8%
Max positive moment:	58.5	34.4	(kip-in)/ft	70.4%
Max negative moment:	-5.9	-16.8	(kip-in)/ft	-64.7%

Tables 4-26 and 4-27 show that the AASHTO strip width method is not as unconservative as was originally indicated. The AASTHO method is actually conservative for the shear and positive moment design. However, the method is still significantly unconservative for the negative moment design, particularly for the eight-foot section NEXT-D bridge. The differences between the results of the 3D model and the AASHTO method are likely explained by the fact that the AASHTO model does not account for the settlement of the stems or the difference in stiffness between the shear keys and the bridge deck.

Conclusions

Because of the large percent errors between the demands given by AASHTO strip width method and the 3D models, it is recommended that the results of the 3D analysis be used in lieu of the results of the AASHTO method. For the forty-foot bridges analyzed in this study, the design tandem load provided the critical demands on the shear keys and deck. The recommended strip width for the design tandem is ten feet. The total live load demands in the shear key and deck for the six-foot section NEXT-D bridge are shown in Table 4-28. The total demands in the shear key and deck for the eight-foot section NEXT-D bridge are shown in Table 4-29.

Table 4-28: Unfactored live load demand in the shear keys and deck for a six-foot section NEXT-D bridge

	Shear key	Point A/E	Point B/D	Point C	Units
Max shear:	27.8	28.2	16.9	11.2	Kip
Max positive moment:	248.4	345.6	466.2	467.8	kip-in
Max negative moment:	-164.1	-271.2	-309.3	-213.7	kip-in

Table 4-29: Unfactored live load demand in the shear keys and deck for an eight-foot section NEXT-D bridge

	Shear key	Point A/E	Point B/D	Point C	Units
Max shear:	27.8	33.3	21.2	15.6	Kip
Max positive moment:	248.4	474	623.4	562.3	kip-in
Max negative moment:	-164.1	-488.9	-511.5	-349.6	kip-in

If a load other than the design tandem is desired to be used for the design of the bridge, further analysis would be required. If the load has an axle spacing greater than the four-foot spacing of the design tandem, the demands could be multiplied by the factor of the total weight of the “new loading” over the total weight of the design tandem (50 kips). As long as the axle spacing is greater than four feet, this method will be conservative. If the axle spacing is less than four feet or if more refined demands are desired, further analysis will be required. Each ten-foot strip of shear key or deck for a NEXT-D bridge should be designed to withstand total demands in Tables 4-28 and 4-29. In order to design the shear key and bridge deck, the demands should be divided by ten feet in order to determine a required capacity per foot. The unfactored live load demands normalized for strip width for the shear key and deck of a 40-foot NEXT-D bridge are shown in Tables 4-30 and 4-31 for the six-foot and eight-foot section bridges.

Table 4-30: Unfactored live load demand in the shear keys and deck for a six-foot section NEXT-D bridge normalized for strip width

	Shear key	Point A/E	Point B/D	Point C	Units
Max shear:	2.8	2.8	1.7	1.1	kip/ft
Max positive moment:	24.8	34.6	46.6	46.8	(kip-in)/ft
Max negative moment:	-16.4	-27.1	-30.9	-21.4	(kip-in)/ft

Table 4-31: Unfactored live load demand in the shear keys and deck for an eight-foot section NEXT-D bridge normalized for strip width

	Shear key	Point A/E	Point B/D	Point C	Units
Max shear:	2.8	3.3	2.1	1.6	kip/ft
Max positive moment:	34.4	47.4	62.3	56.2	(kip-in)/ft
Max negative moment:	-16.8	-48.9	-51.2	-35.0	(kip-in)/ft

The six-foot and eight-foot shear and negative moment demand in the shear key are similar. However, for all other demands, the demand for the eight-foot section is greater than that of the six-foot section. This would seem to indicate that the six-foot section is a better section to use for the SCDOT because less reinforcing will be required. However, this may not be the case because the eight-foot section would require placing fewer precast elements and fewer cast-in-place shear keys, which would decrease construction time in the field.

The dead load and future wearing surface demands must also be considered in the design of the shear keys and deck. The unfactored dead load demands for the shear keys and bridge deck normalized for a ten-foot strip width are shown in Tables 4-32 and 4-33. Tables 4-34 and 4-35 show the unfactored future wearing surface demands for the shear keys and bridge deck normalized for a strip width of ten feet.

Table 4-32: Unfactored dead load demand in the shear keys and deck for a six-foot section NEXT-D bridge normalized for strip width

	Shear key	Point A/E	Point B/D	Point C	Units
Max shear:	0.11	0.17	0.49	0.37	kip/ft
Max positive moment:	0.17	0.60	3.49	2.48	(kip-in)/ft
Max negative moment:	-0.48	-1.03	-7.41	-3.16	(kip-in)/ft

Table 4-33: Unfactored dead load demand in the shear keys and deck for an eight-foot section NEXT-D bridge normalized for strip width

	Shear key	Point A/E	Point B/D	Point C	Units
Max shear:	0.08	0.26	1.09	0.88	kip/ft
Max positive moment:	0.01	2.84	-0.22	-3.69	(kip-in)/ft
Max negative moment:	-0.33	-2.99	-24.52	-14.84	(kip-in)/ft

Table 4-34: Unfactored future wearing surface demand in the shear keys and deck for a six-foot section NEXT-D bridge normalized for strip width

	Shear key	Point A/E	Point B/D	Point C	Units
Max shear:	0.28	0.24	0.43	0.44	kip/ft
Max positive moment:	1.48	2.26	7.06	2.81	(kip-in)/ft
Max negative moment:	-1.12	-2.76	-9.70	-6.36	(kip-in)/ft

Table 4-35: Unfactored future wearing surface demand in the shear keys and deck for an eight-foot section NEXT-D bridge normalized for strip width

	Shear key	Point A/E	Point B/D	Point C	Units
Max shear:	0.27	0.26	0.51	0.54	kip/ft
Max positive moment:	2.09	3.97	7.64	2.66	(kip-in)/ft
Max negative moment:	-0.78	-5.60	-12.79	-9.17	(kip-in)/ft

The demands given in Tables 4-30 through 4-35 should be multiplied by the appropriate factors provided in the AASHTO LRFD Bridge Specifications and then the entire shear key and bridge deck should be designed to withstand this factored demand. The live load demands on the bridge are much greater than the dead load and future wearing surface demands on the bridge. Furthermore, the live loads are multiplied by much larger factors than the dead load or future wearing surface load because of their unpredictability. Therefore, the live loads are the driving force for the design of the shear keys and deck.

Sensitivity Studies

Shear Key Stiffness Sensitivity Study

One of the assumptions in the AASHTO LRFD Bridge Design Specs is that the bridge deck is treated as a continuous beam. This assumption is not true for a NEXT-D bridge because the stiffness of the shear key is different than that of the deck. In order to determine the effect of the stiffness of the shear key on the demand in the shear key, the eight-foot NEXT-D bridge model was run using various stiffness modifiers for the moment of inertia of the shear key about the major axis. The critical load cases for shear, positive moment, and negative moment in the shear key were applied to the model for each stiffness modifier and the total shear and moment were monitored. Plots showing the effect of the shear key stiffness on the maximum demands in the shear key are shown in Figures 4-41 through 4-43. All of the figures show the shear key demand based

on a single axle loading at mid-span of the bridge. Each figure also shows the actual demand based on the 3D model highlighted by the red dot.

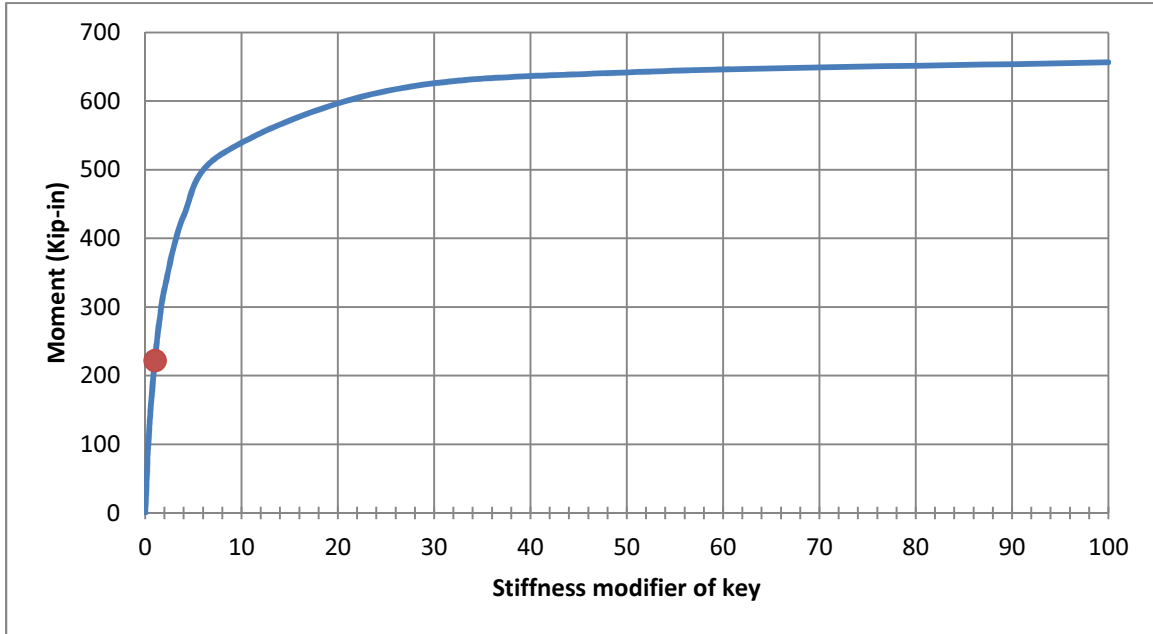


Figure 4-41: Transverse shear in shear key vs. shear key stiffness for critical shear load location

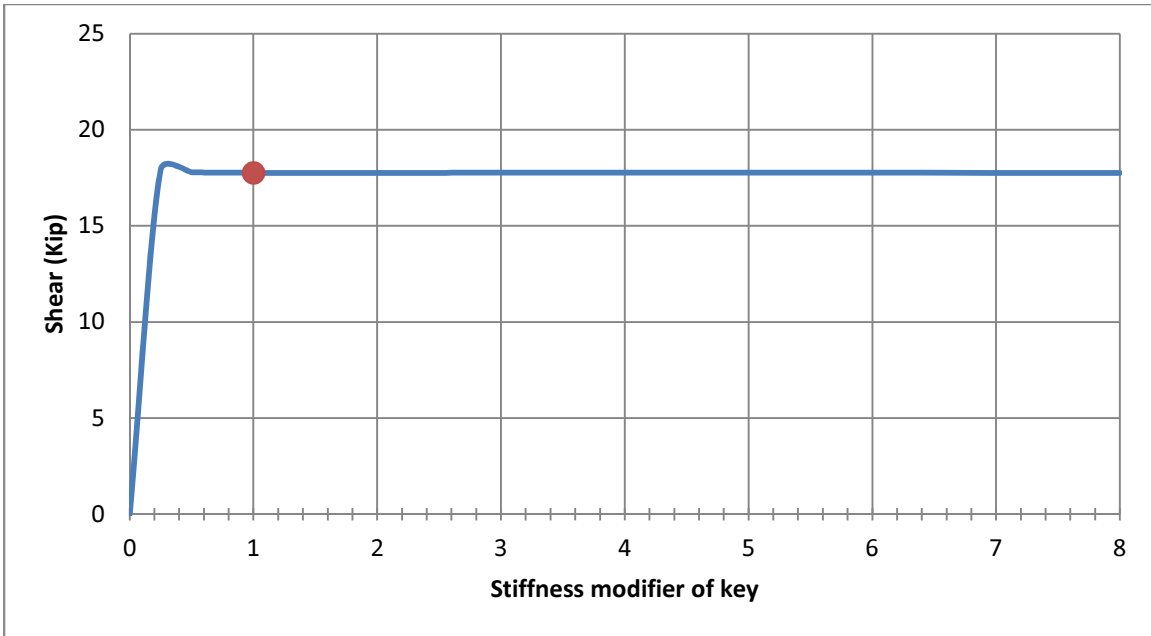


Figure 4-42: Transverse moment in shear key vs. shear key stiffness for critical positive moment load location

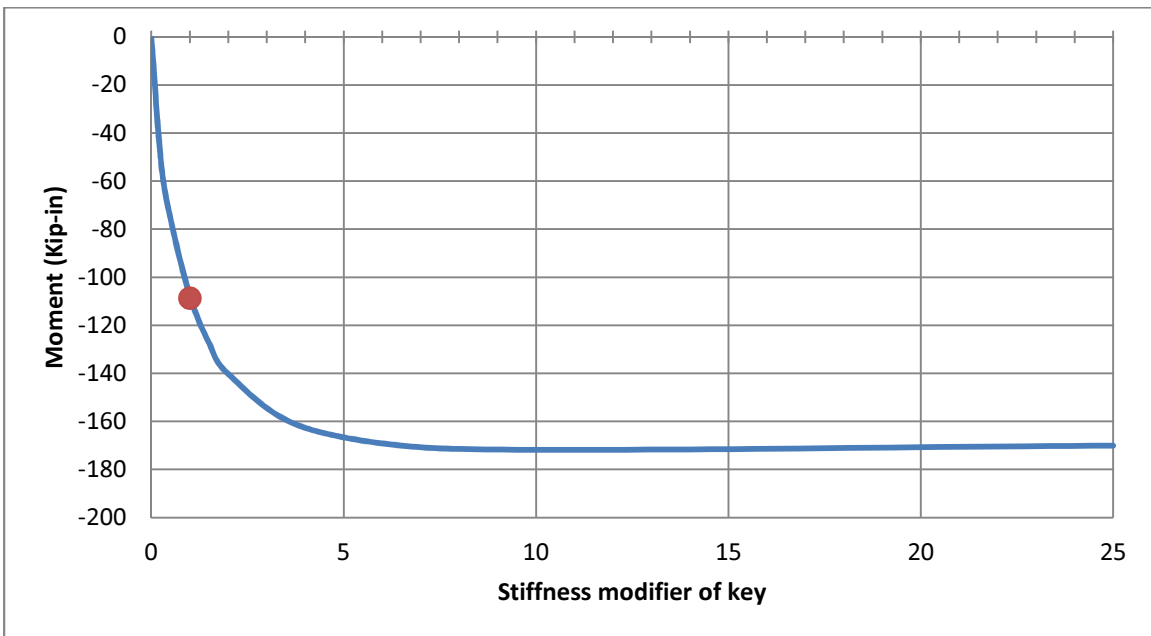


Figure 4-43: Transverse moment in shear key vs. shear key stiffness for critical negative moment load location

The previous figures show that shear key stiffness has a large effect on the demand in the shear key. As the stiffness of the shear key increases, the demand in the shear key also increases. Therefore, it is vital that the stiffness of the shear key used in the 3D model is representative of the actual detail which will be used. The actual shear key demand corresponds with a stiffness modifier of one, and this is in a very sensitive region for the shear key stiffness. If the stiffness of the key is underestimated, the shear key demands predicted by the 3D models will be lower than the actual demands. The shear and moment demand in the shear keys reached an asymptote once the shear keys reached a certain stiffness. The AASHTO continuous beam model used for the deck design is actually conservative in this regard when compared with the 3D model because the AASHTO method assumption assumes that the shear keys are equally as stiff as the rest of the bridge deck.

Stem Stiffness Sensitivity Study

The AASHTO LRFD Bridge Design Specs assumes that the deck is supported by the stems of the NEXT-D beam and that these supports are rigid. This assumption is not true for a NEXT-D bridge because the stem is not infinitely stiff. In order to determine the effect of the stiffness of the stem on the demand in the shear key, the same process used in the Shear Key Stiffness Sensitivity Study was followed, except that the stiffness modifier was applied to the major axis moment of inertia of the stem instead of the shear key. Plots showing the effect of the stem stiffness on the maximum demands in the shear key are shown in

Figures 4-44 through 4-46. All of the figures show the shear key demand based on a single axle loading at mid-span of the bridge. Each figure also shows the actual demand based on the 3D model highlighted by the red dot.

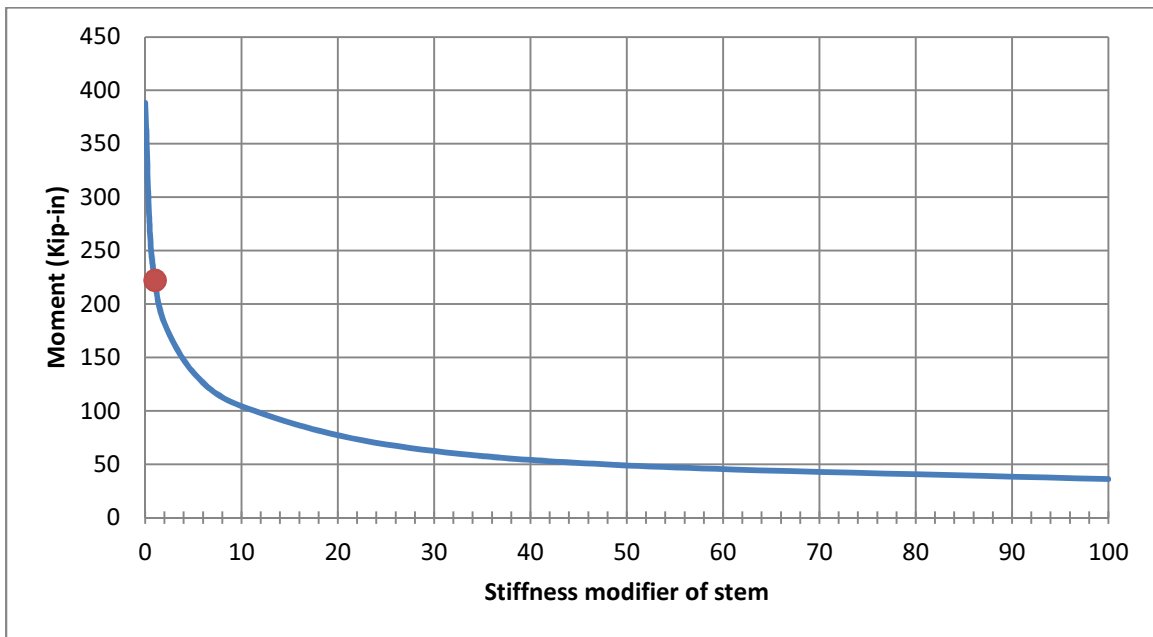


Figure 4-44: Transverse shear in shear key vs. stem stiffness for critical shear load location

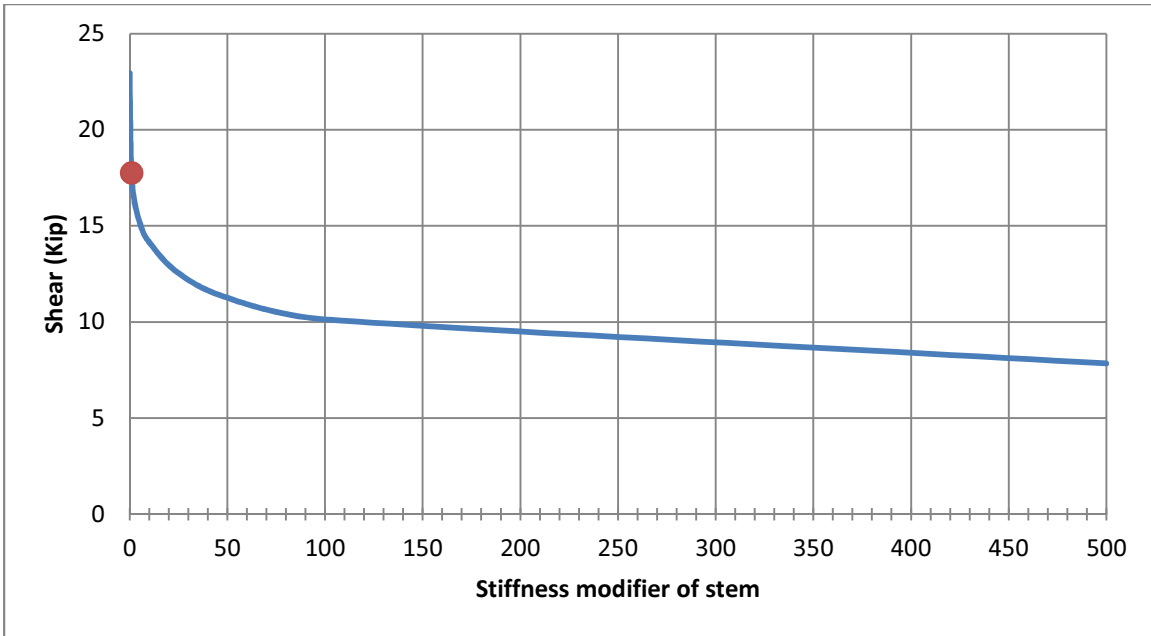


Figure 4-45: Transverse moment in shear key vs. stem stiffness for critical positive moment load location

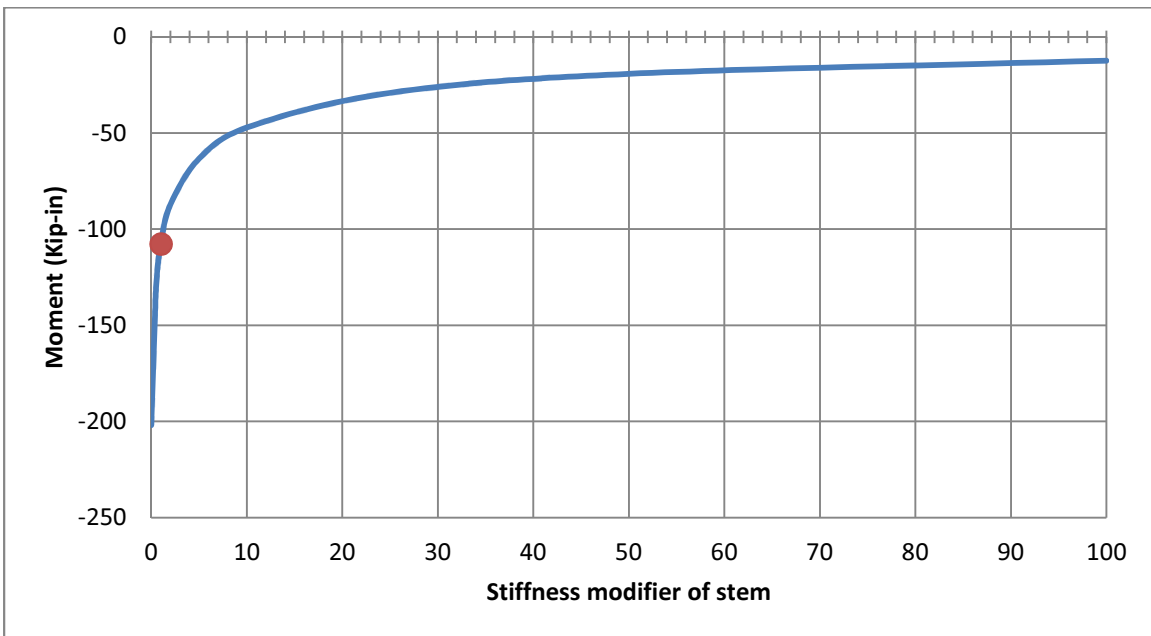


Figure 4-46: Transverse moment in shear key vs. stem stiffness for critical negative moment load location

Similar to the shear key stiffness studies, the stem stiffness has a large effect on the demand in the shear key. In this case, the demand in the shear key decreases as the stiffness of the stem increases. The shear key demand did not reach as clear of an asymptote as in the shear key stiffness study, but the demand did level off to some extent as the stem stiffness increased. The actual shear key demand corresponds with a stiffness modifier of one for the stem. This is in a very sensitive region for the stem stiffness, meaning that the stem must be modeled accurately to achieve accurate results. The AASHTO beam model assumes infinitely rigid supports, so it is unconservative in comparison with the 3D model.

Simplified Span Length Sensitivity Study

Another study was performed to determine the effect of span length on the transverse shear and moment in a bridge deck. This was a simplified study using only a flat slab made up of eight-inch thick shell elements that was supported at both ends in the same manner as the shell model of the NEXT-D bridge. A point load was applied at the center of the bridge and the transverse moment was tracked on the centerline of the bridge. This was repeated for various span lengths in order to determine the effects of span length on transverse deck forces. Each model was 47 feet and 4 inches wide. An example of one of the models used for this study is shown in Figure 4-47. The plot showing the effect of span length on the transverse moment is shown in Figure 4-48.

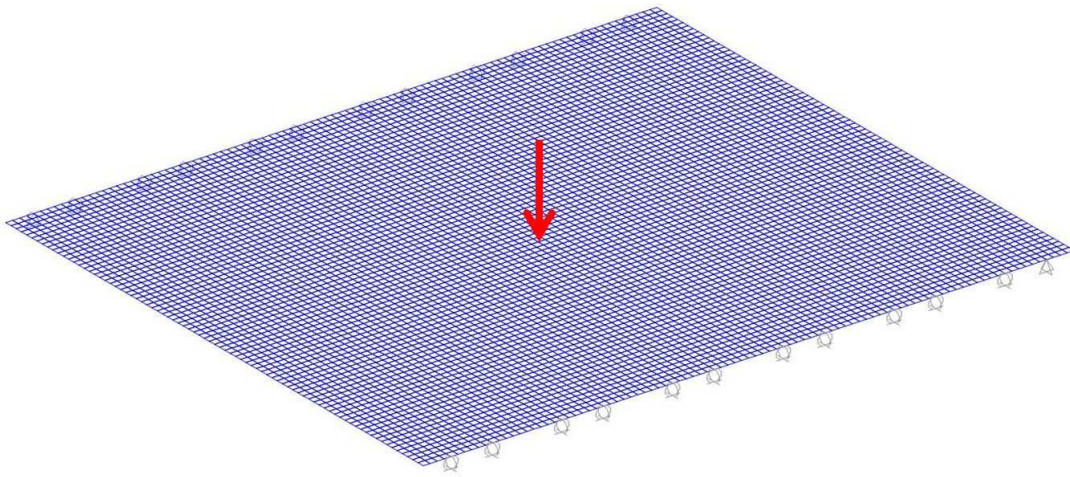


Figure 4-47: Span length research model

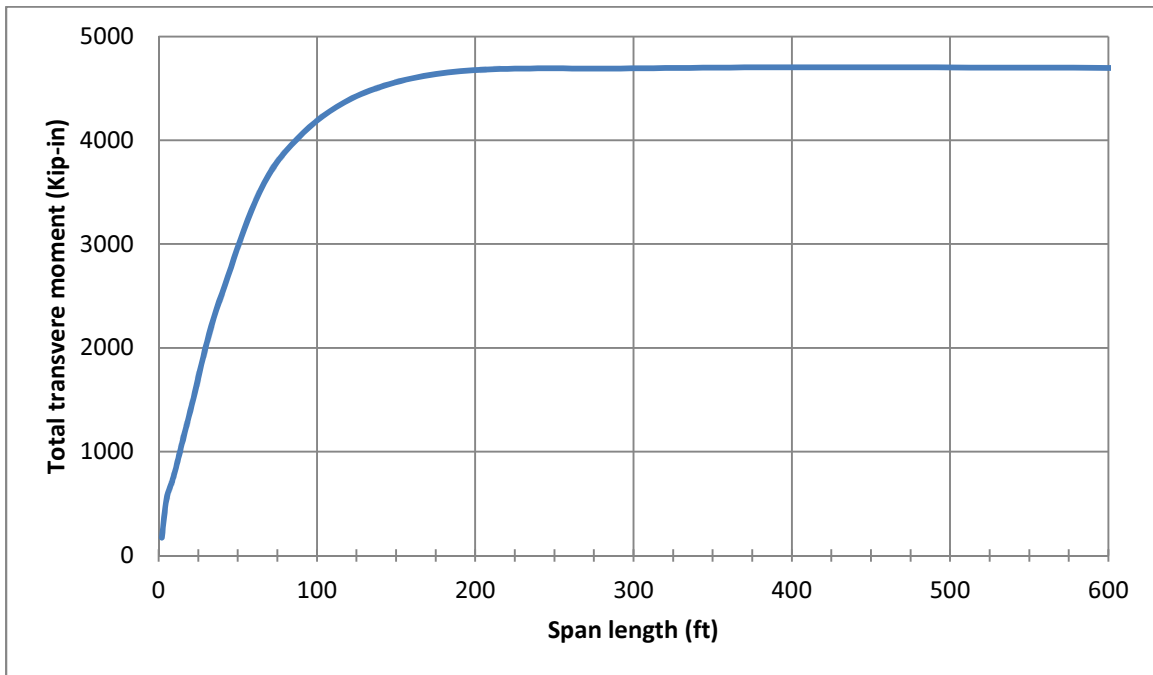


Figure 4-48: Total transverse moment vs. span length

Figure 4-48 shows that as the span length increases, the transverse moment in the slab also increases until it reaches an asymptote. This figure supports the proposed shear and moment demands for a NEXT-D bridge provided in this study for the use of the SCDOT. The SCDOT wishes to use this research project to design NEXT-D bridges with spans ranging from 22 to 40 feet. This span length study proves that bridges with spans shorter than the 40-foot bridge modeled in this study will have shear and moment demands less than those recommend in this study. It should be noted that this was only a simplified model, so a span length study using the full 3D bridge models was performed to provide better insight into the effect of span length on the demand in the shear keys and deck.

Detailed Span Length Sensitivity Study

For this study was performed in a similar manner to the Simplified Span Length Sensitivity Study, but the eight-foot section 3D bridge model was used to determine the effect of span length on transverse shear key live load demand. For this study, ten bridge models were built with spans ranging from 22 to 200 feet. The design tandem load was applied to the mid-span of each bridge at the critical locations for shear, positive moment, and negative moment and the resulting shear key demands were monitored. The shear, positive moment, and negative moment demands for the various span lengths are shown in Table 4-36. Plots showing the effect of span length on the shear key demand are shown in Figures 4-49 through 4-51. The maximum span length analyzed for this study

was 200 feet because longer span lengths became too computationally intense to analyze due to the amount of elements in the model.

Table 4-36: Unfactored live load shear key demand for eight-foot section NEXT-D bridges of various span lengths

Span (ft)	Shear (kip)	Positive moment (kip-in)	Negative moment (kip-in)
22	19.5	103.4	-34.8
30	24.1	195.7	-85.5
40	27.6	343.6	-166.3
50	28.5	469.7	-234.2
60	28.1	549.2	-274.6
70	27.2	596.5	-296.1
80	26.0	620.5	-307.6
90	24.6	635.2	-315.3
100	23.3	650.3	-319.8
200	14.8	814.6	-348.0

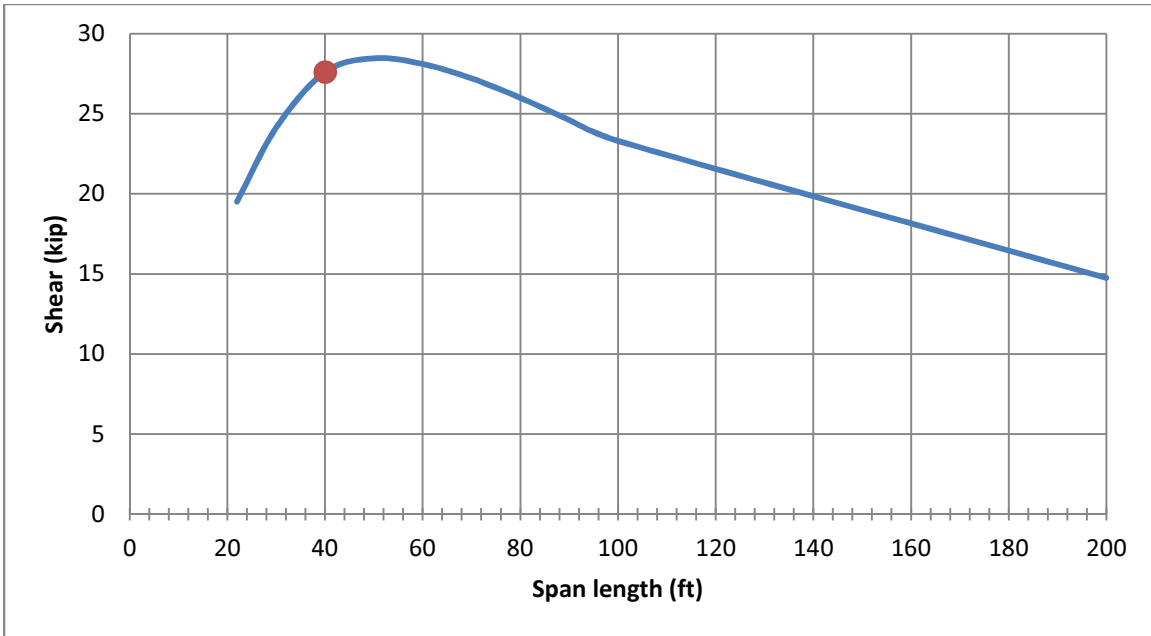


Figure 4-49: Unfactored live load shear demand in the shear key vs. span length for an eight-foot section NEXT-D bridge

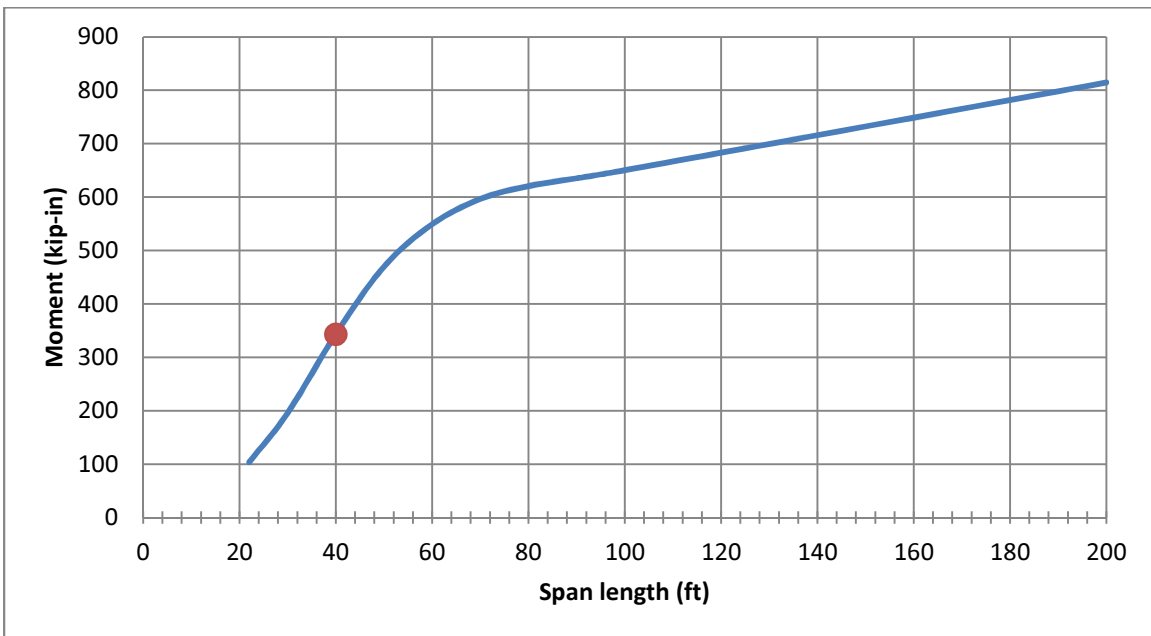


Figure 4-50: Unfactored live load positive moment demand in the shear key vs. span length for an eight-foot section NEXT-D bridge

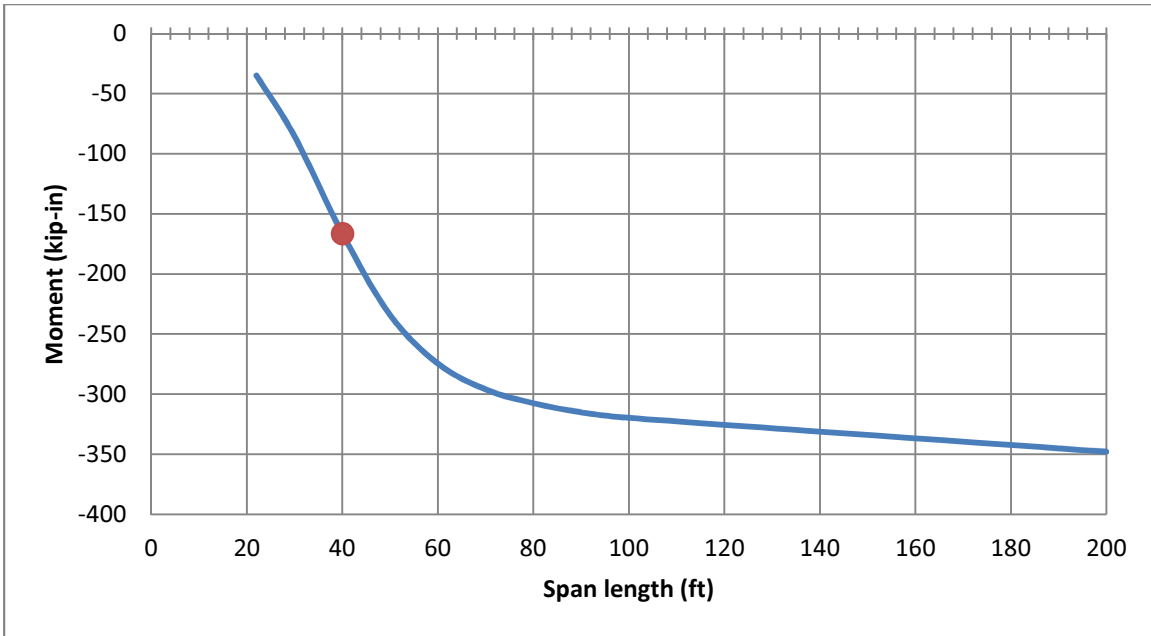


Figure 4-51: Unfactored live load negative moment demand in the shear key vs. span length for an eight-foot section NEXT-D bridge

The Figures above confirm the conclusion that the results of the 40-foot model are conservative for bridges of shorter spans. The shear, positive moment, and negative moment demands all decrease for bridges shorter than 40 feet. The shear moment demand peaks at a span length of 50 feet, and then decreases for bridges longer than that. The positive and negative moment demands continue to increase as span length increases all the way up to the maximum 200-foot span analyzed in this study. In order to design NEXT-D sections for shorter spans, the live load demands could be determined for 3D bridge models of shorter spans. However, designing all NEXT-D sections based on the demand of a 40-foot bridge would be adequate for all shorter spans and would allow fabricators to

keep the same setups for all short-span NEXT-D bridges. This would decrease fabrication cost and avoid the possibility of accidentally using a girder on a bridge with a longer span than what the girder was designed for, which could result in catastrophic bridge failures.

Conclusions

Based on the above sensitivity studies, the demands for the shear keys and deck for NEXT-D bridges provided in Tables 4-30 through 4-35 are acceptable values for the design of a NEXT-D bridge provided the shear key properties used in the model are accurate. The shear key should be tested in order to confirm the results of Flores Duron (2011) and ensure the accuracy of the 3D models. The Simplified Span Length Sensitivity Study showed that the provided positive moment demands are conservative for any bridge with a length shorter than 40 feet because these demands were based on 40-foot bridge models. The study shows that as span length decreases, the transverse demands in the deck decrease. This conclusion was confirmed for the shear and negative moment demands as well in the Detailed Span Length Sensitivity Study. Therefore, the recommended demands will allow the SCDOT to build bridges in the 22 to 40-foot range targeted by this study.

Chapter 5

CONCLUSIONS

Design Conclusions

This research was performed to determine the transverse design demands for the shear key and bridge deck for bridges built using NEXT-D beams. Six-foot and eight-foot NEXT-D sections were considered in this study. In order to establish shear key and deck demands, 3D finite element models of NEXT-D bridges were created using SAP2000 (Computers and Structures 2011b). The bridges were 40 feet long and 47 feet and four inches wide. Two different types of models were built. One type utilized primarily eight-node solid elements, and the other utilized a combination of four-node shell elements and frame elements. For both models, the shear key was represented by a frame element that was calibrated to possess the stiffness properties recommended by Flores Duron (2011). With the parapets removed from the models, the solid and shell models yielded very similar results. With the parapets included, the solid and shell models generated different results in the outermost deck and keys, so this variability was attributed to differences in the parapet to deck connection between the two models. The parapet to deck connection in the shell model was deemed to be a more accurate representation of the actual connection that would be used to connect the parapet to the bridge, thus the results from the shell

model were used to provide recommended design demands for the shear keys and the bridge deck.

In order to predict the critical transverse live load design demands in the shear keys and the deck, one axle of the HS20 design truck, two axles of the HS20 design truck, and the design tandem loads (AASHTO 2010) were moved across the bridge transversely and longitudinally in order to create influence lines for the shear keys and deck. Once the critical live load demands were determined, the distribution of the shear and moment throughout the length of the bridge was investigated in order to recommend a design strip width for the shear key and bridge deck. The demand in the shear key was distributed very well throughout the entire length of the bridge, so strip widths were determined based on the geometry of the design load. Strip widths were chosen so that the width was equal to the tributary length of one truck to account for the possibility of more than one truck in a lane. It was recommended that each strip width be designed to be able to carry the capacity of the demand created on the entire 40-foot length due to a design load at mid-span, which was proven to be the critical load location. By following this recommendation, the bridge deck and shear key will have enough capacity to function without failure even if more than one truck is in a lane at a time. The recommended strip widths for each load type are shown in Table 5-1.

Table 5-1: Recommended strip widths in feet

Load type	Axle spacing	Strip width
Single-axle	14	14
Two-axle	14	28
Design tandem	4	10

Using the strip widths given in Table 5-1, the live load demands normalized for strip width for each load case were determined by dividing the total demand in the shear key and deck over the length of the bridge by the recommend strip width for the corresponding load type. These results proved that the design tandem case was the most critical for design. The unfactored live loads for the design tandem load are shown in Tables 5-2 and 5-3.

Table 5-2: Unfactored live load demand in the shear keys and deck for a six-foot section NEXT-D bridge normalized for strip width

	Shear key	Point A/E	Point B/D	Point C	Units
Max shear:	2.8	2.8	1.7	1.1	kip/ft
Max positive moment:	24.8	34.6	46.6	46.8	(kip-in)/ft
Max negative moment:	-16.4	-27.1	-30.9	-21.4	(kip-in)/ft

Table 5-3: Unfactored live load demand in the shear keys and deck for an eight-foot section NEXT-D bridge normalized for strip width

	Shear key	Point A/E	Point B/D	Point C	Units
Max shear:	2.8	3.3	2.1	1.6	kip/ft
Max positive moment:	34.4	47.4	62.3	56.2	(kip-in)/ft
Max negative moment:	-16.8	-48.9	-51.2	-35.0	(kip-in)/ft

These results were compared to the results provided by the AASHTO strip width method (AASHTO 2010). The comparison between shear key demands based on the AASHTO strip width method and the recommended shear key demands based on the 3D analysis are shown in Tables 5-4 and 5-5.

Table 5-4: Unfactored live load demand in the shear keys of a six-foot section NEXT-D bridge normalized for strip width

	AASHTO model	3D model	Units	% Error
Max shear:	3.3	2.8	kip/ft	19.2%
Max positive moment:	43.7	24.8	(kip-in)/ft	76.0%
Max negative moment:	-12.3	-16.4	(kip-in)/ft	-24.9%

Table 5-5: Unfactored live load demand in the shear keys of an eight-foot section NEXT-D bridge normalized for strip width

	AASHTO model	3D model	Units	% Error
Max shear:	2.9	2.8	kip/ft	3.8%
Max positive moment:	58.5	34.4	(kip-in)/ft	70.4%
Max negative moment:	-5.9	-16.8	(kip-in)/ft	-64.7%

Tables 5-4 and 5-5 show that the differences between the AASHTO strip width method and the results of the 3D analysis were significant for both the six-foot and eight-foot section bridges. The strip width method provided similar results as the 3D model in predicting the shear demand in the keys. However, the method was significantly conservative for positive moment demand and significantly unconservative for the negative moment demand. Due to these major disagreements with the 3D model, the AASHTO method was not recommended for the determination of live load demand in the shear keys or deck.

Once the strip width of ten feet was chosen for the design of the NEXT-D bridges, the dead load demands were determined for both the six-foot and eight-foot section NEXT-D bridges. For the shear keys, this demand was determined by ignoring the self-weight of the NEXT-D beams due to the construction process for precast bridges. Therefore, the only self-weight considered was the self-weight of the parapet. For the deck, the transverse demand due to the dead load of one simply supported NEXT-D beam was determined, and this was added to the demand created by the self-weight of the parapets in order to accurately portray the construction process. The maximum dead load demand for a ten foot section of bridge was used to recommend the unfactored design demands for the shear keys and deck of a NEXT-D bridge. In addition to the dead load demand due to self-weight, a future wearing surface load was applied to the entire deck of the bridge in order to account for the presence of such a surface. Once again, the maximum demand in a ten-foot section of bridge was used to recommend the unfactored demand on the shear keys and deck as a result of a future wearing surface load. The future wearing surface considered in this project was three inches in depth. The unfactored demand on a ten-foot section of bridge due to self-weight is shown in Tables 5-6 and 5-7. The unfactored demand on a ten-foot section of bridge due to the presence of a three-inch future wearing surface is shown in Tables 5-8 and 5-9.

Table 5-6: Unfactored dead load demand in the shear keys and deck for a six-foot section NEXT-D bridge normalized for strip width

	Shear key	Point A/E	Point B/D	Point C	Units
Max shear:	0.11	0.17	0.49	0.37	kip/ft
Max positive moment:	0.17	0.60	3.49	2.48	(kip-in)/ft
Max negative moment:	-0.48	-1.03	-7.41	-3.16	(kip-in)/ft

Table 5-7: Unfactored dead load demand in the shear keys and deck for an eight-foot section NEXT-D bridge normalized for strip width

	Shear key	Point A/E	Point B/D	Point C	Units
Max shear:	0.08	0.26	1.09	0.88	kip/ft
Max positive moment:	0.01	2.84	-0.22	-3.69	(kip-in)/ft
Max negative moment:	-0.33	-2.99	-24.52	-14.84	(kip-in)/ft

Table 5-8: Unfactored future wearing surface demand in the shear keys and deck for a six-foot section NEXT-D bridge normalized for strip width

	Shear key	Point A/E	Point B/D	Point C	Units
Max shear:	0.28	0.24	0.43	0.44	kip/ft
Max positive moment:	1.48	2.26	7.06	2.81	(kip-in)/ft
Max negative moment:	-1.12	-2.76	-9.70	-6.36	(kip-in)/ft

Table 5-9: Unfactored future wearing surface demand in the shear keys and deck for an eight-foot section NEXT-D bridge normalized for strip width

	Shear key	Point A/E	Point B/D	Point C	Units
Max shear:	0.27	0.26	0.51	0.54	kip/ft
Max positive moment:	2.09	3.97	7.64	2.66	(kip-in)/ft
Max negative moment:	-0.78	-5.60	-12.79	-9.17	(kip-in)/ft

In order to determine the factored design demand for the shear keys and deck for a 40-foot long NEXT-D bridge, the demands provided in Tables 5-2 through 5-9 should be multiplied by the appropriate factors provided by the AASHTO LRFD Bridge Design Specifications (AASHTO 2010). The shear key and deck should be designed to be able to withstand these factored demands on a per foot basis along the entire length of the bridge.

Sensitivity studies were also carried out to determine the effect of the stiffness of the shear key and the stem on the demands in the shear key. The Shear Key Stiffness Sensitivity Study showed that the demand in the shear keys increases as the stiffness of the shear keys increases. The Stem Stiffness Sensitivity Study showed that the demand in the shear key decreases as the stem stiffness increases. For this reason, it is very important to ensure that the stiffness of each of these elements is accurately represented in the 3D models. Testing should be carried out to determine the actual stiffness of the shear key in order to verify the results of the model. A preliminary study was also done to determine the effect of span length on the transverse demand in the bridge. The Detailed Span Length Sensitivity Study showed that as span length decreases from 40 feet, the transverse shear, positive moment, and negative moment demands in the deck also decrease. Based on this conclusion, the demands given in Tables 5-2 through 5-9 would be conservative for any bridge with a span length less than 40 feet. Therefore, these recommended demands could be used to determine the

detail for the NEXT-D beams used by the SCDOT for bridge spans between 22 and 40 feet.

Recommendations for Future Work

- The stiffness of the shear key should be experimentally validated to determine the amount of shear and moment that will actually be transferred between adjacent beams. Once this testing has been carried out, the models should be updated to include the actual shear key stiffness. This should be done because the stiffness of the shear keys has a very large effect on the transverse demands in the key.
- The models reported some concentrated stresses near the supports of the bridge, so further research into this phenomenon should be performed in order to see if special design considerations need to be taken into account for these regions of the bridge.
- A greater variety of models with different span lengths and widths should be analyzed in order to establish a more general method of determining the demand in the shear keys and deck of NEXT-D bridges. The recommendations of this study apply only to bridges that are 40 feet or shorter and 47 feet and 6 inches wide.

- Different beam sections should be investigated in order to determine the effect that the relative stiffness of the stem compared to the slab and shear key has on the shear key and deck demands.
- It would be best if some method similar to the AASHTO strip width method could be devised so that various bridge geometries and bridge loadings could be used to design the details for the NEXT-D beams and shear keys.

APPENDICES

Appendix A: Abbreviations Used in this Thesis

2D: Two Dimensional

3D: Three Dimensional

A: Cross-sectional area

AASHTO: American Association of State Highway and Transportation Officials

CSI: Computers and Structures Incorporated

DOT: Department of Transportation

E: Modulus of elasticity

FHWA: Federal Highway Administration

f_s : Shape factor

ft: Feet

G: Shear modulus

I: Moment of inertia

in: Inches

J: Torsional constant

ksi: kips per square inch

L: Length

LRFD: Load Resistance Factor Design

M: Moment

NEXT-D: Northeast Extreme Tee with Integral Deck

PCINE: Northeast Chapter of the Precast/Prestressed Concrete Institute

R: Rotational degree of freedom

S: Spacing of supporting components in feet

SCDOT: South Carolina Department of Transportation

U: Translational degree of freedom

X: The distance from load to point of support in feet

α : Coefficient of thermal expansion

ν : Poisson's ratio

Appendix B: Shear Key Calibration spreadsheet

Inputs		
Property	Value	Units
f_c'	6000	psi
ν	0.3	-

Calculated Values		
Property	Value	Units
E =	4415.2	psi $E = 57 \sqrt{f_c'}$
G =	1698.2	psi $G = \frac{E}{2(1+\nu)}$
L =	4.664	in $L = 2 \cdot \left(\frac{\delta_{U2_R3}}{\delta_{U2_U2}} \right)$
J =	1.046	in ⁴ $J = \frac{\delta_{R1_R1} \cdot L}{G}$
A =	1.269	in ² $A = \frac{\delta_{U1_U1} \cdot L}{E}$
β_s =	10.809	- $\beta_s = \frac{12 \cdot \delta_{R3_R3}}{L^2 \cdot \delta_{U2_U2}} - 4$
I_3 =	4.974	in ⁴ $I_3 = \frac{L^3 \cdot \delta_{U2_U2} \cdot (1 + \beta_s)}{12 \cdot E}$
$f_{s,2}$ =	1.922	- $f_{s,2} = \frac{\beta_s \cdot G \cdot A \cdot L^2}{12 \cdot E \cdot I_3}$
$A_{v,2}$ =	0.660	in ² $A_{v,2} = \frac{A}{f_{s,2}}$
I_2 =	18.471	in ⁴ $I_2 = \frac{L^3 \cdot \delta_{U3_U3} \cdot (1 + \beta_s)}{12 \cdot E}$
$f_{s,3}$ =	0.518	- $f_{s,3} = \frac{\beta_s \cdot G \cdot A \cdot L^2}{12 \cdot E \cdot I_2}$
$A_{v,3}$ =	2.451	in ² $A_{v,3} = \frac{A}{f_{s,3}}$

Targeted Stiffness Matrix (δ) (Flores Duron 2011)						
--	--	--	--	--	--	--

***Units are kips, inches, and radians

	U1	U2	U3	R1	R2	R3
U1	1201	0	0	0	0	0
U2	0	220	0	0	0	513
U3	0	0	817	0	1905	0
R1	0	0	0	381	0	0
R2	0	0	1905	0	21929	0
R3	0	513	0	0	0	5905

Stiffness Matrix (δ) Based on Inputs						
---	--	--	--	--	--	--

***Units are kips, inches, and radians

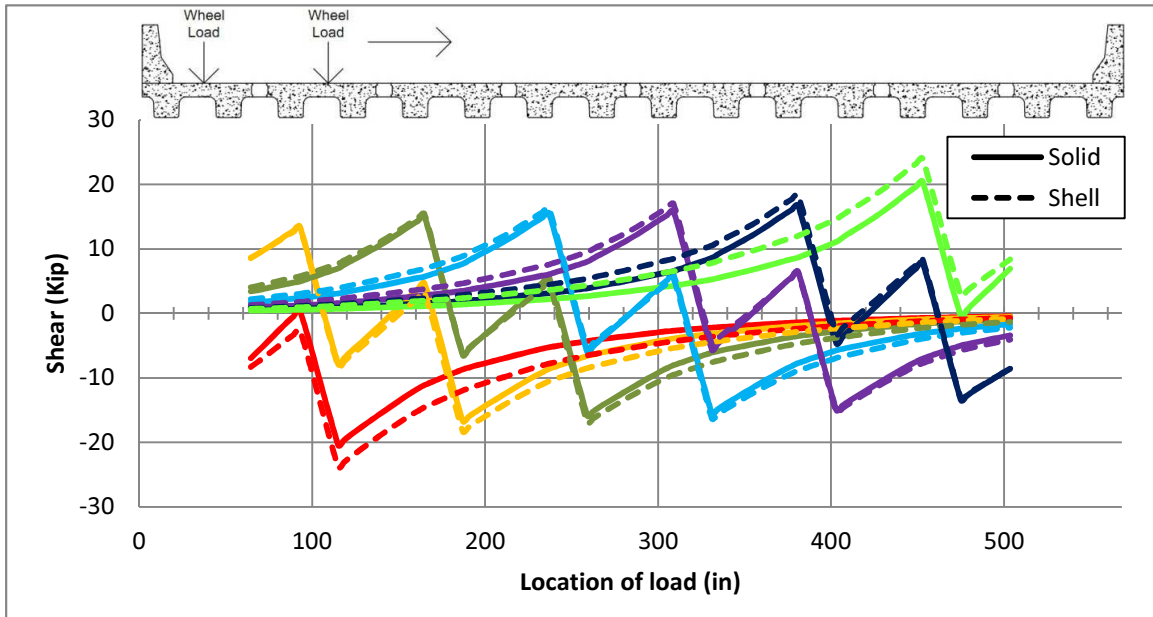
	U1	U2	U3	R1	R2	R3
U1	1201	0	0	0	0	0
U2	0	220	0	0	0	513
U3	0	0	817	0	1905	0
R1	0	0	0	381	0	0
R2	0	0	1905	0	21929	0
R3	0	513	0	0	0	5905

	U1	U2	U3	R1	R2	R3
U1	=A*E/L	0	0	0	0	0
U2	0	=12*X ₃	0	0	0	=6*L*X ₃
U3	0	0	=12*X ₂	0	=6*L*X ₂	0
R1	0	0	0	=J*G/L	0	0
R2	0	0	=6*L*X ₂	0	=2*(4+β _s)*	0
R3	0	=6*L*X ₃	0	0	0	=L ² *(4+β _s)*X ₂

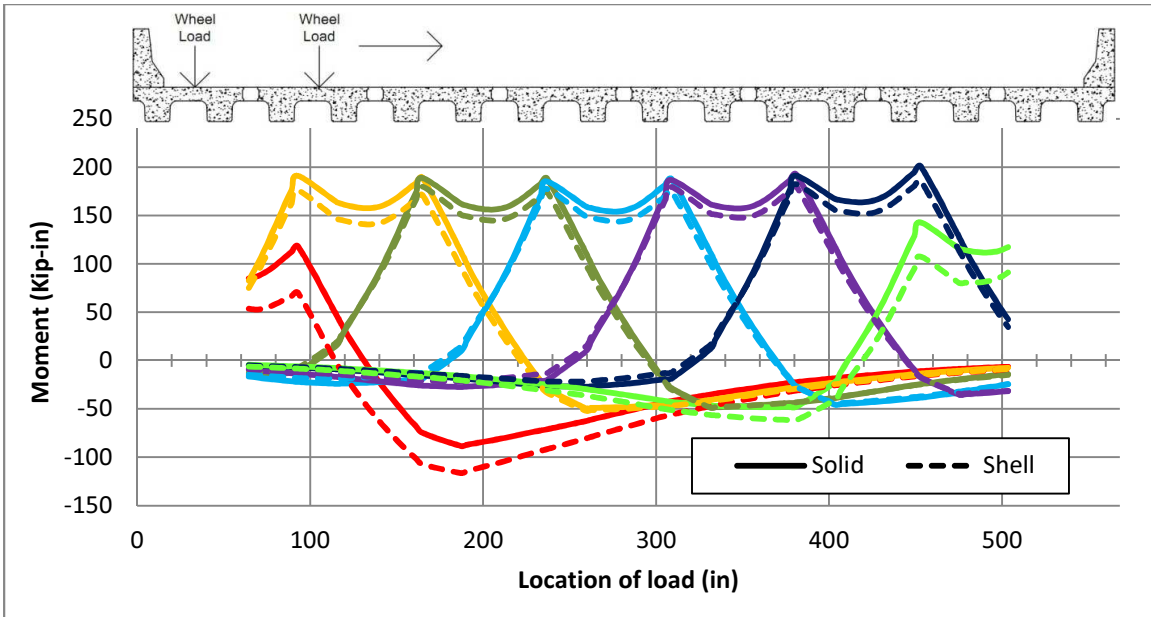
$X_3 = 18.33 \quad X_3 = EI_3 / (L^3 * (1 + \beta_s))$
 $X_2 = 68.08 \quad X_2 = EI_2 / (L^3 * (1 + \beta_s))$

Appendix C: Shear Influence Lines

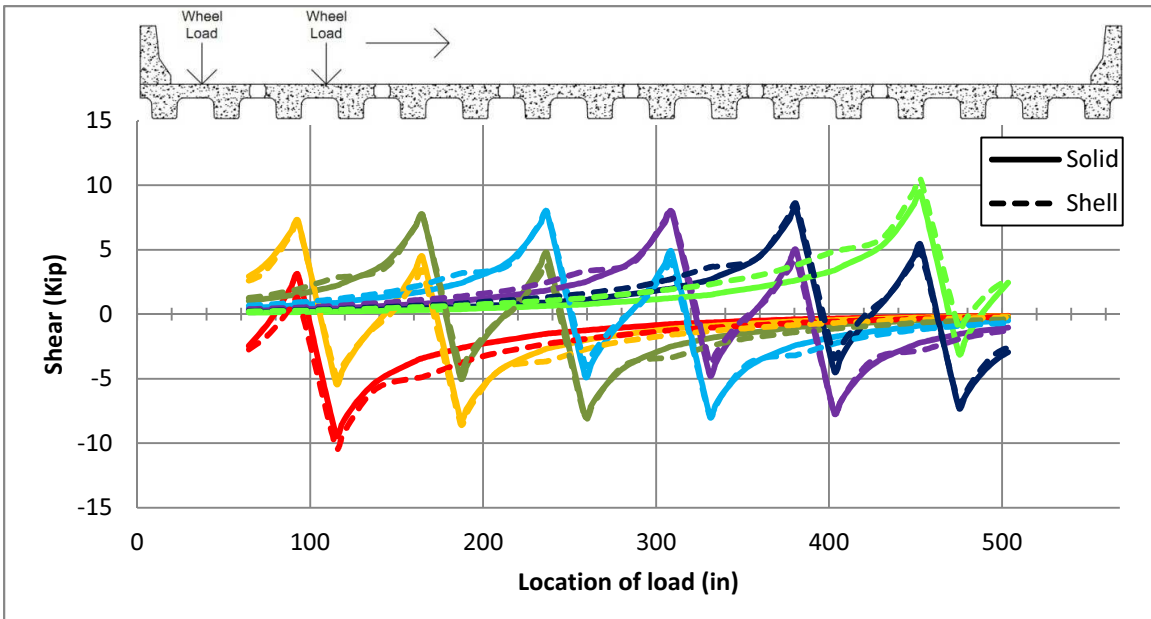
Design Tandem Influence Lines for the 6-Foot Section Bridge with Parapets



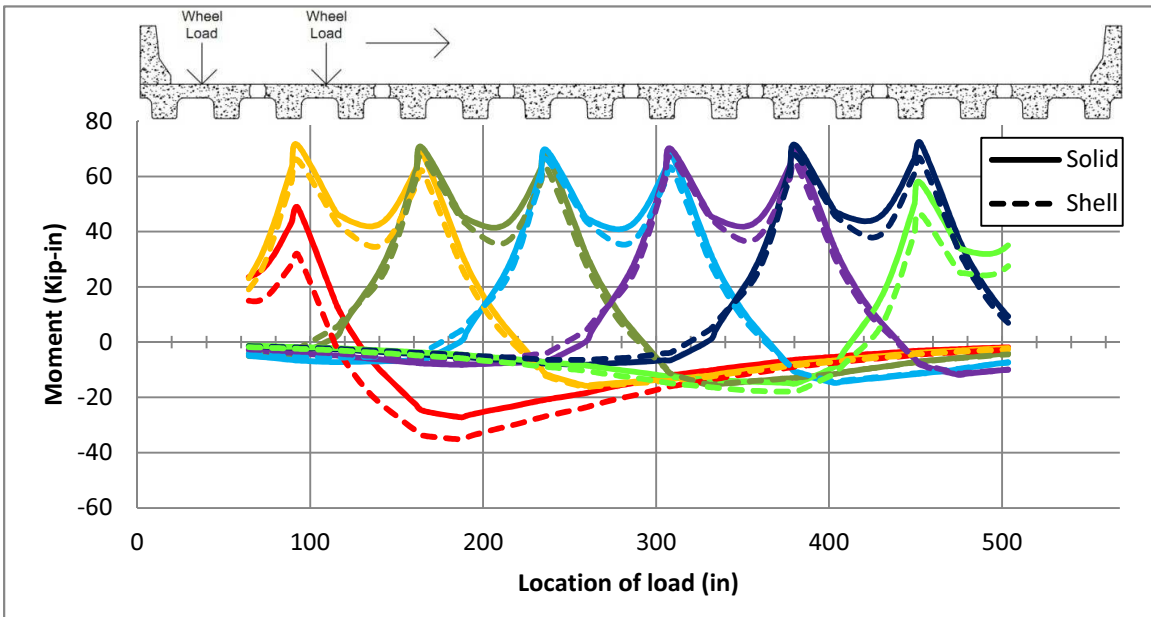
Appendix Figure 1: Shear influence line for the shear keys in a six-foot section NEXT-D bridge under a design tandem loading at quarter-span



Appendix Figure 2: Moment influence line for the left side of the shear keys in a six-foot section NEXT-D bridge under a design tandem loading at quarter-span

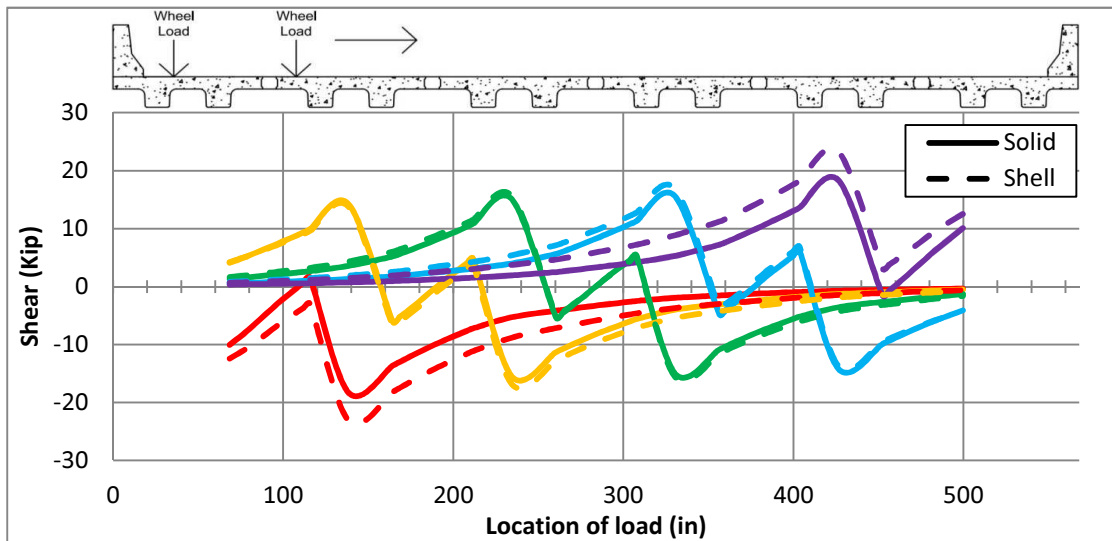


Appendix Figure 3: Shear influence line for the shear keys in a six-foot section NEXT-D bridge under a design tandem loading at the supports

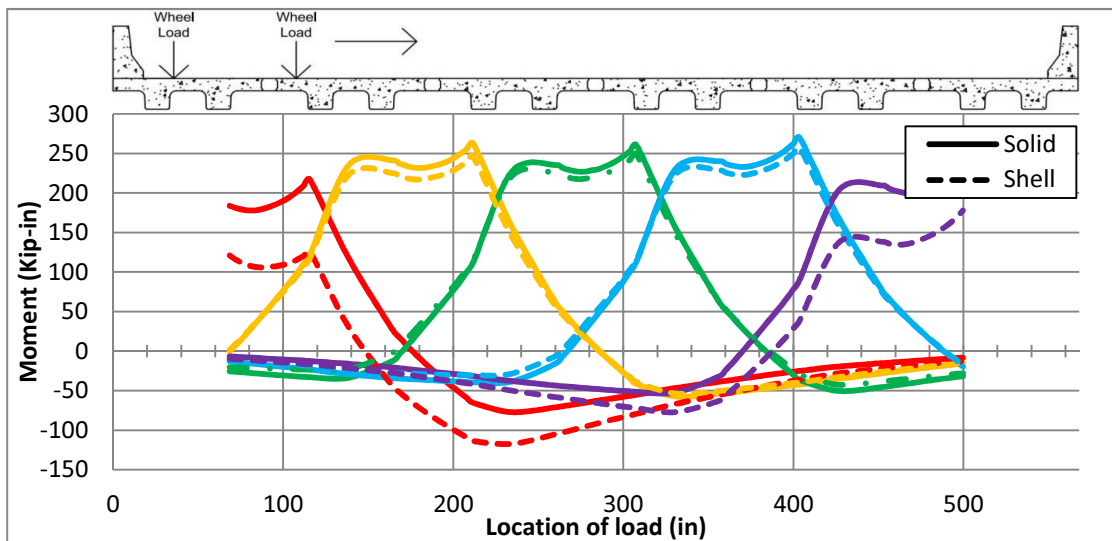


Appendix Figure 4: Moment influence line for the left side of the shear keys in a six-foot section NEXT-D bridge under a design tandem loading at the supports

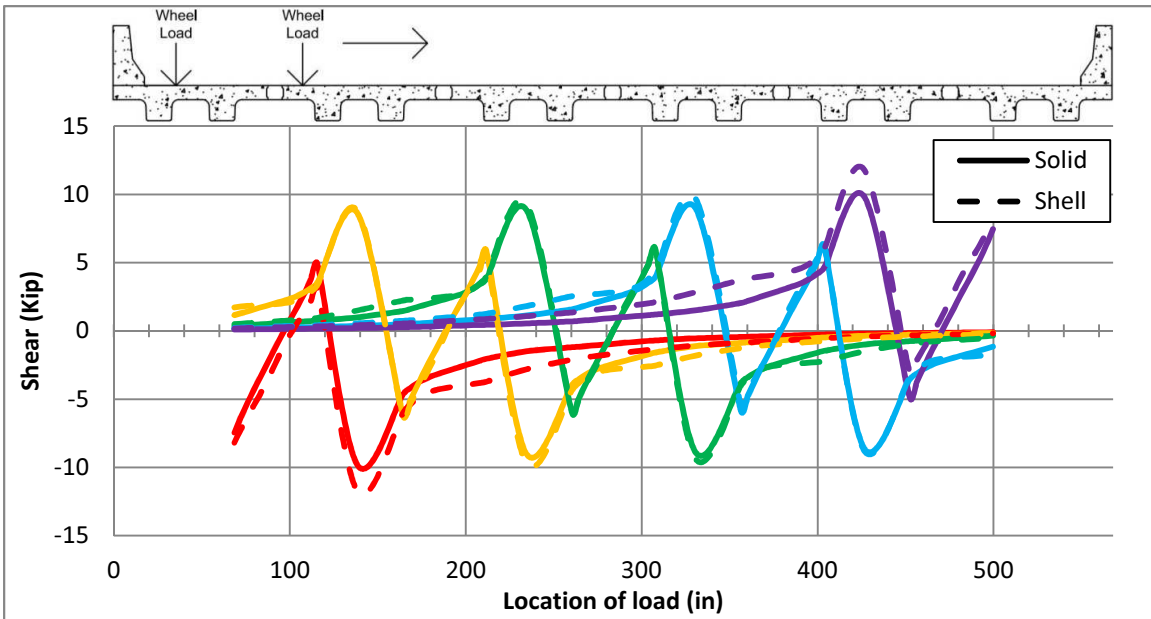
Design Tandem Influence Lines for the 8-Foot Section Bridge with Parapets



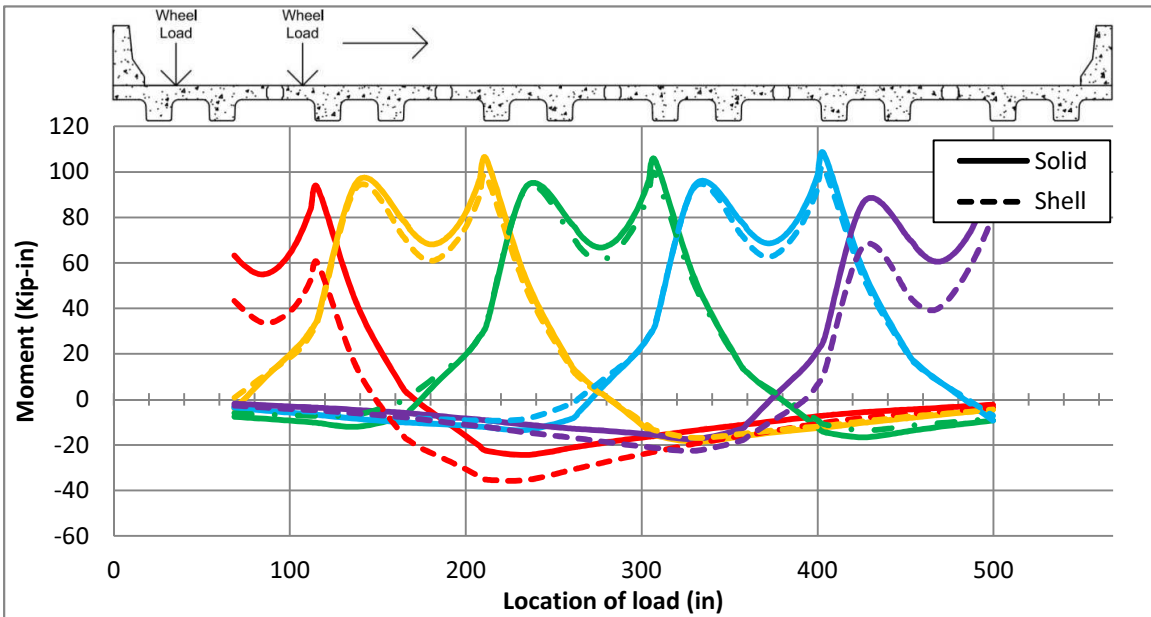
Appendix Figure 5: Shear influence line for the shear keys in an eight-foot section NEXT-D bridge under a design tandem loading at quarter-span



Appendix Figure 6: Moment influence line for the left side of the shear keys in an eight-foot section NEXT-D bridge under a design tandem loading at quarter-span

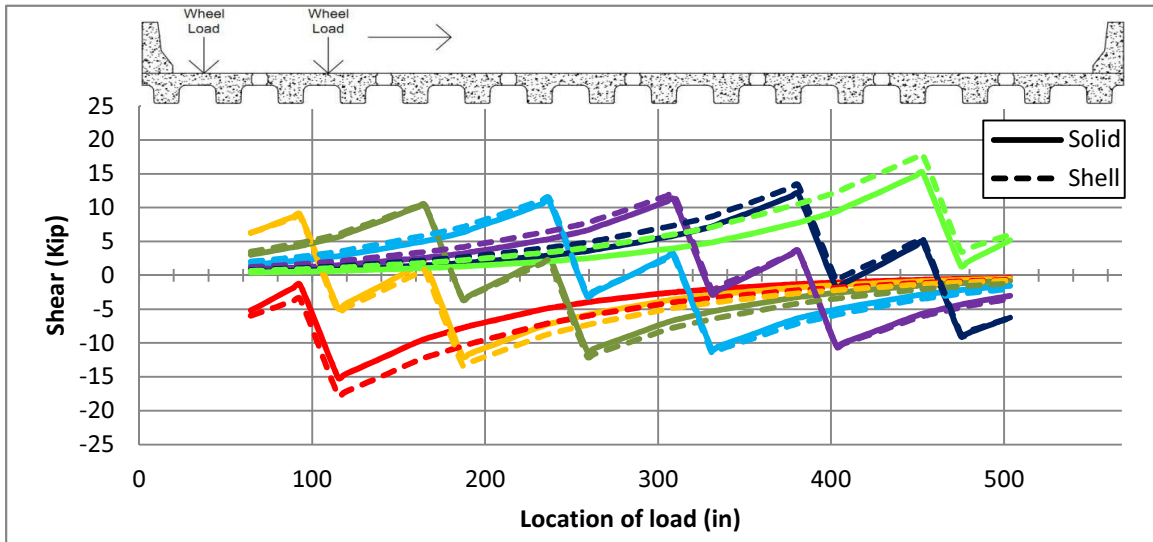


Appendix Figure 7: Shear influence line for the shear keys in an eight-foot section NEXT-D bridge under a design tandem loading at the supports

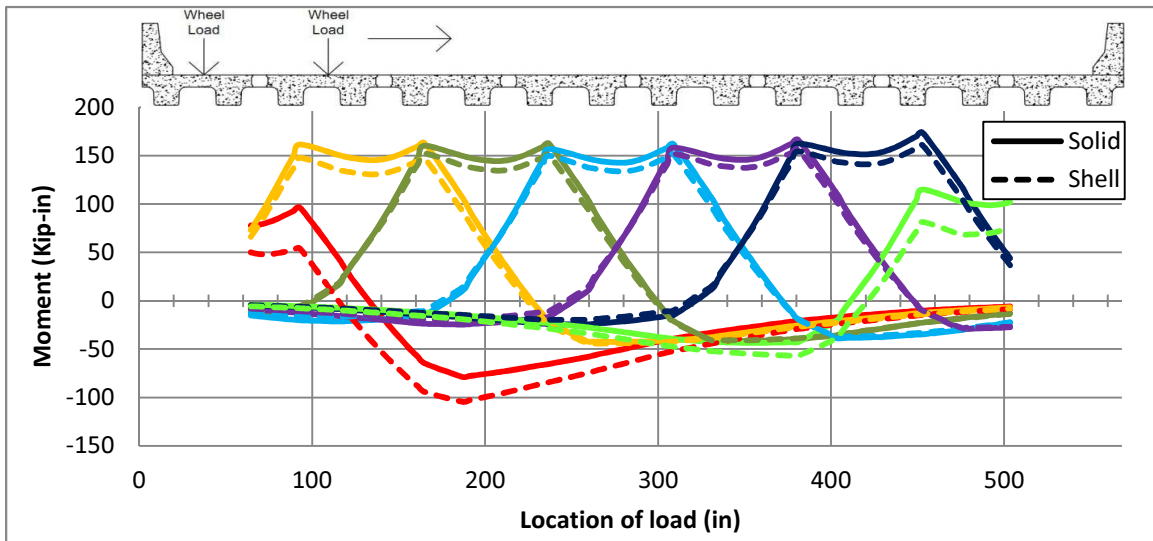


Appendix Figure 8: Moment influence line for the left side of the shear keys in an eight-foot section NEXT-D bridge under a design tandem loading at the supports

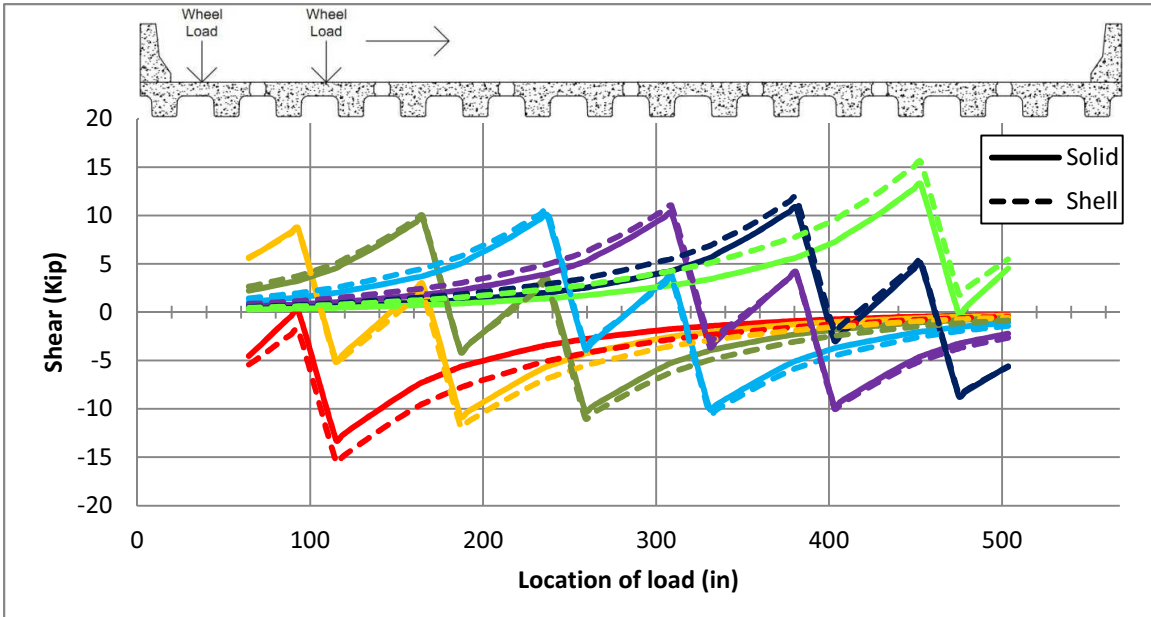
Single-Axle Influence Lines for the 6-Foot Section Bridge with Parapets



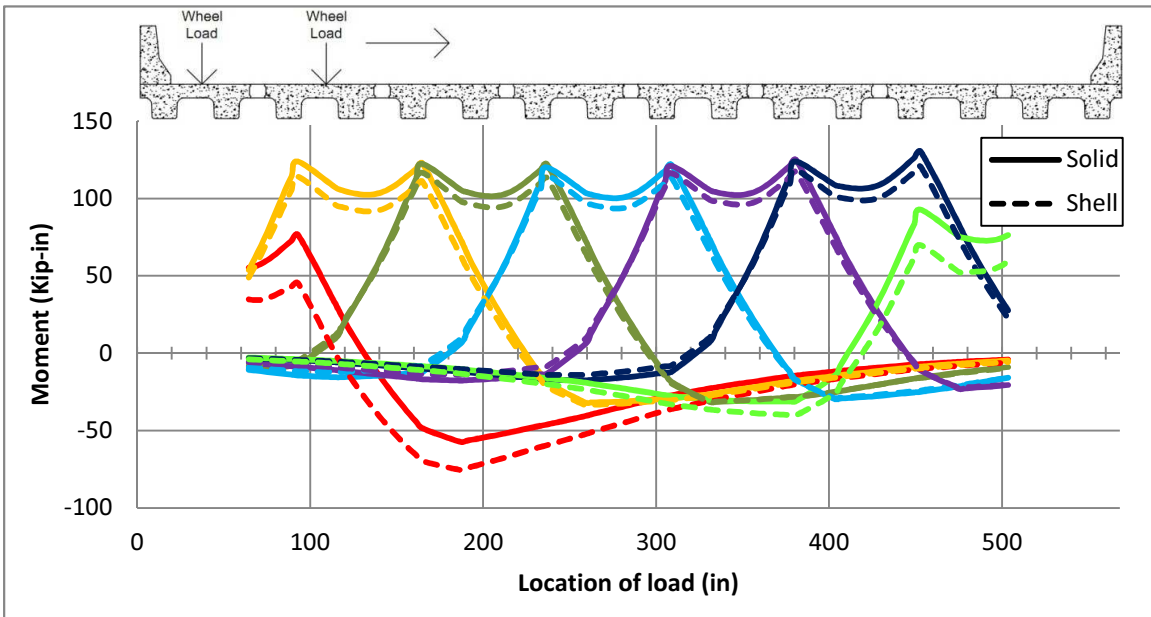
Appendix Figure 9: Shear influence line for the shear keys in a six-foot section NEXT-D bridge under a single-axle loading at mid-span



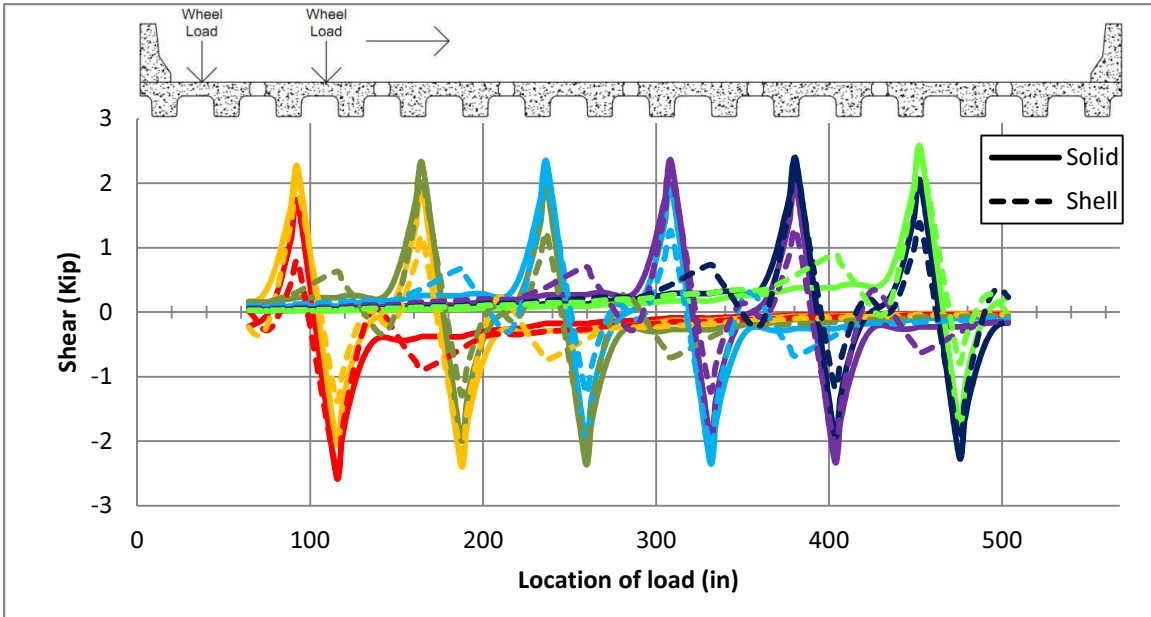
Appendix Figure 10: Moment influence line for the left side of the shear keys in a six-foot section NEXT-D bridge under a single-axle loading at mid-span



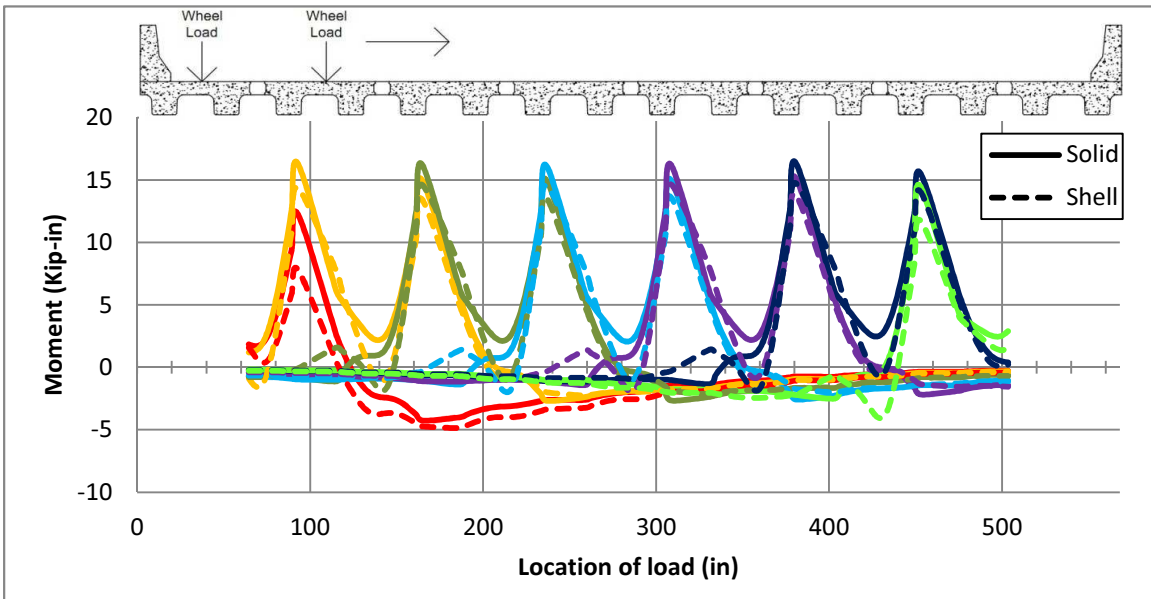
Appendix Figure 11: Shear influence line for the shear keys in a six-foot section NEXT-D bridge under a single-axe loading at quarter-span



Appendix Figure 12: Moment influence line for the left side of the shear keys in a six-foot section NEXT-D bridge under a single-axe loading at quarter-span

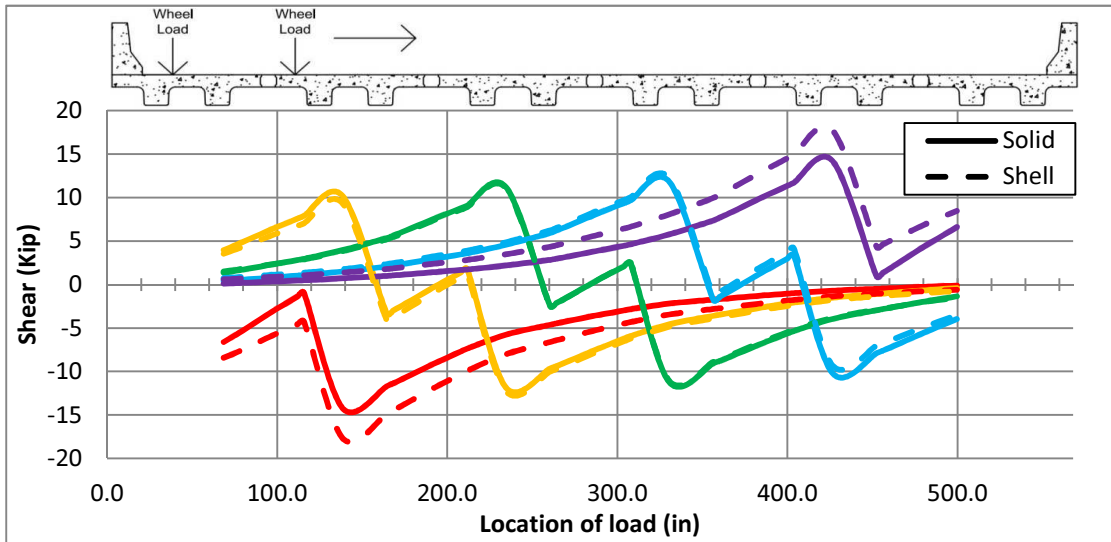


Appendix Figure 13: Shear influence line for the shear keys in a six-foot section NEXT-D bridge under a single-axle loading at the supports

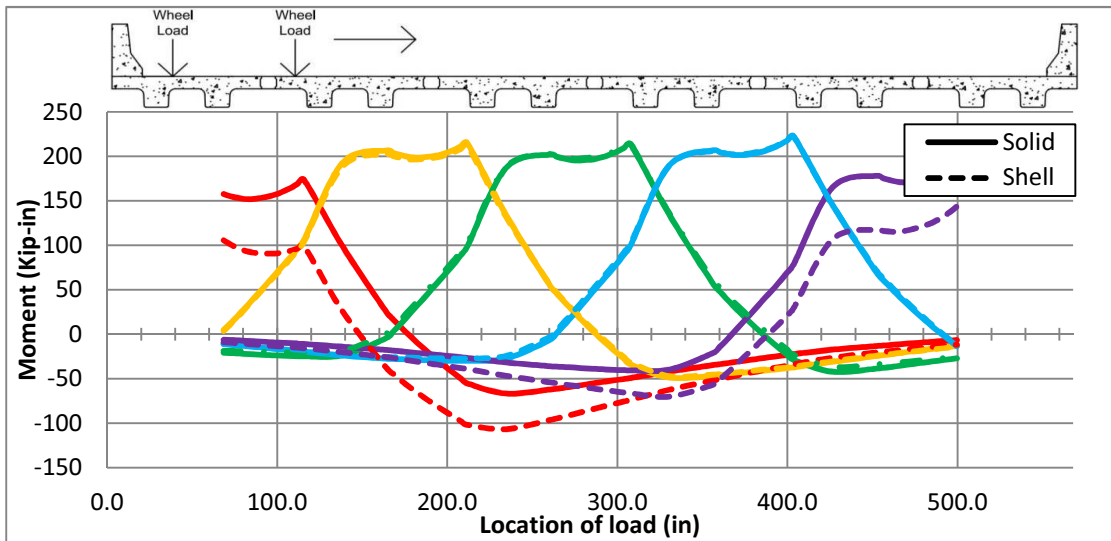


Appendix Figure 14: Moment influence line for the left side of the shear keys in a six-foot section NEXT-D bridge under a single-axle loading at the supports

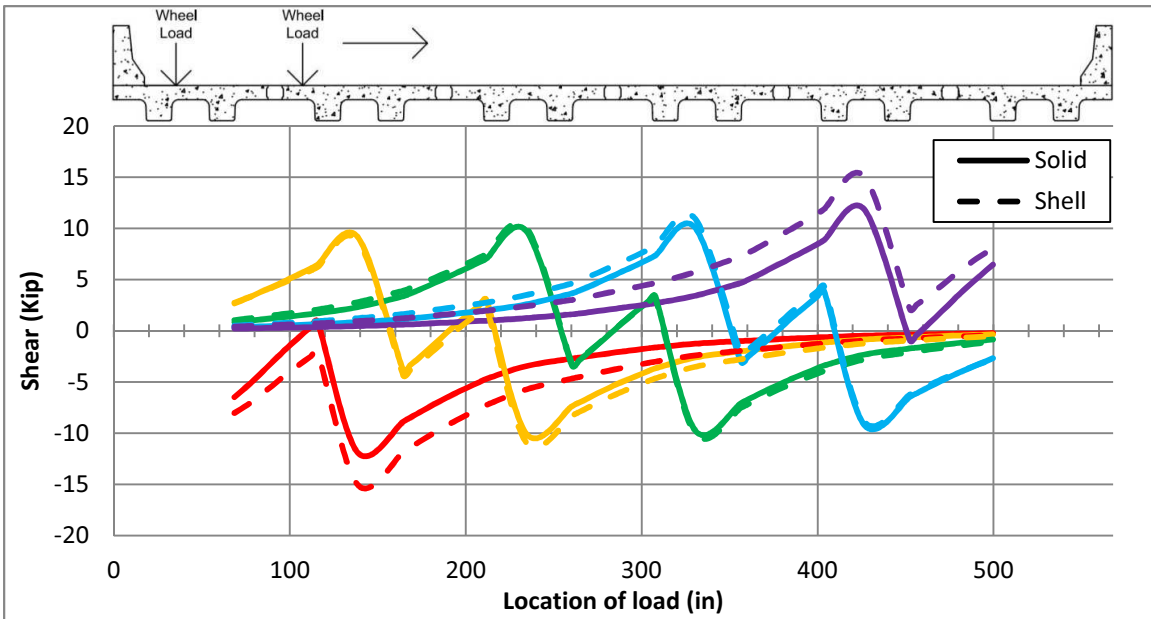
Single-Axle Influence Lines for the 8-Foot Section Bridge with Parapets



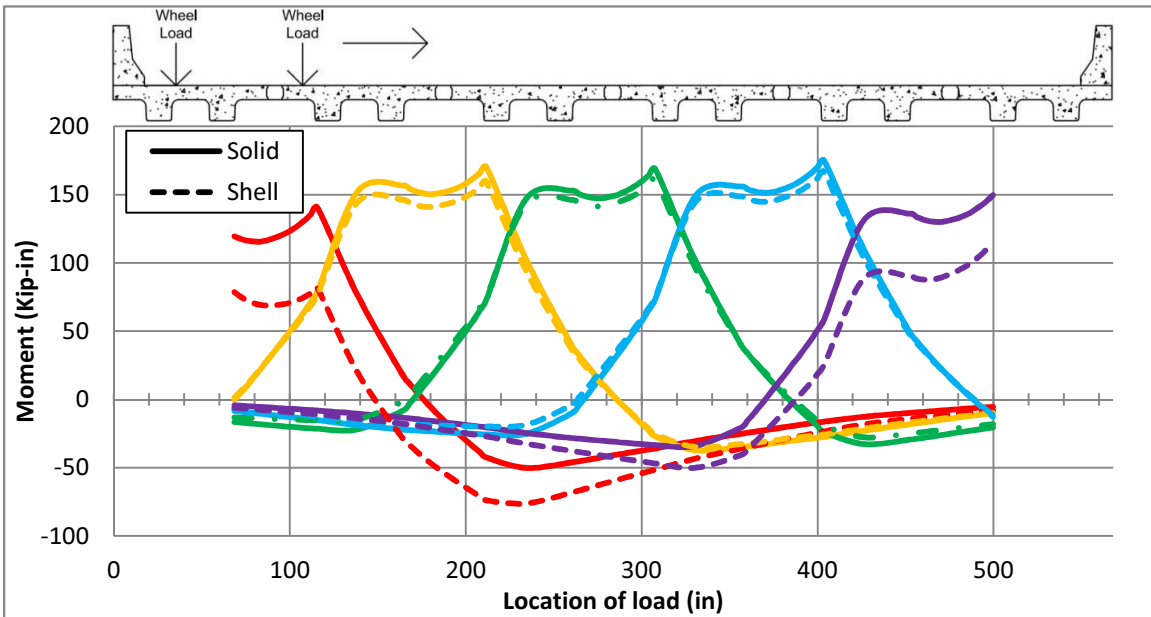
Appendix Figure 15: Shear influence line for the shear keys in an eight-foot section NEXT-D bridge under a single-axle loading at mid-span



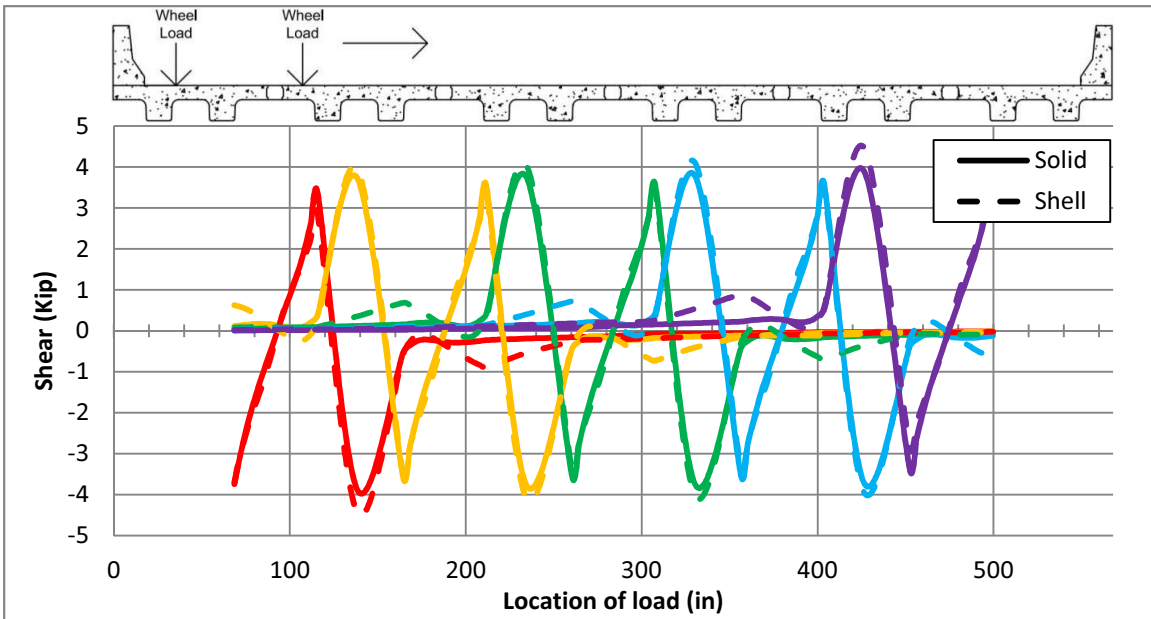
Appendix Figure 16: Moment influence line for the left side of the shear keys in an eight-foot section NEXT-D bridge under a single-axle loading at mid-span



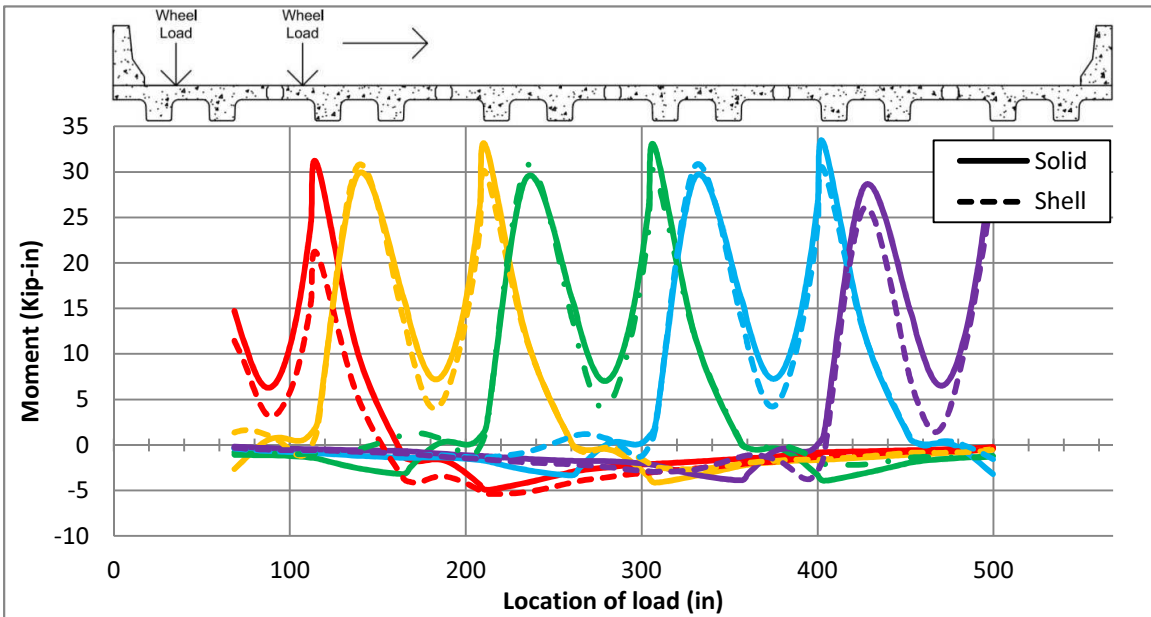
Appendix Figure 17: Shear influence line for the shear keys in an eight-foot section NEXT-D bridge under a single-axle loading at quarter-span



Appendix Figure 18: Moment influence line for the left side of the shear keys in an eight-foot section NEXT-D bridge under a single-axle loading at quarter-span

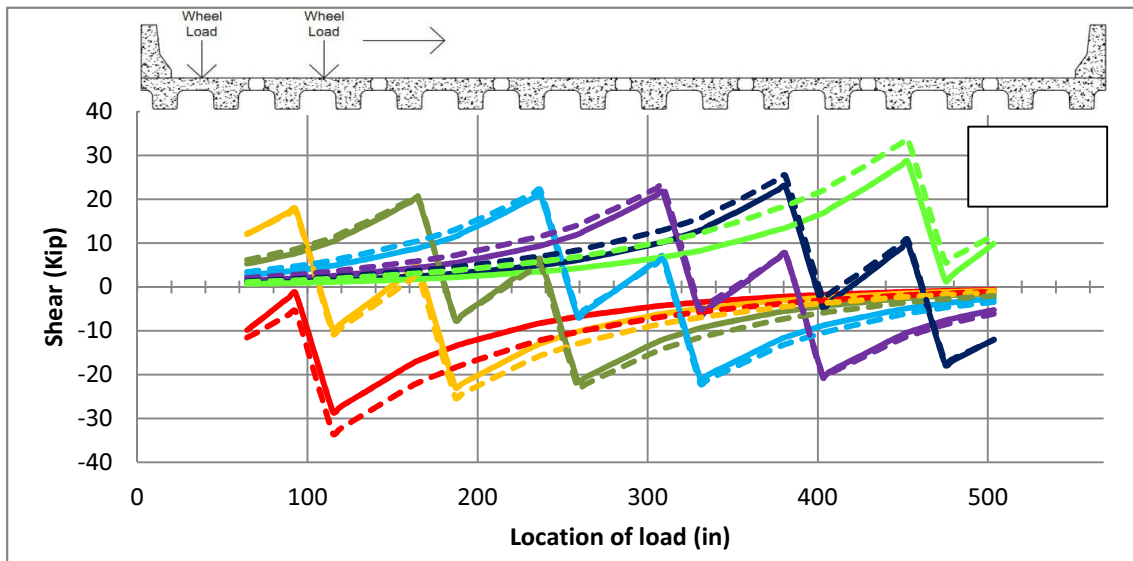


Appendix Figure 19: Shear influence line for the shear keys in an eight-foot section NEXT-D bridge under a single-axle loading at the supports

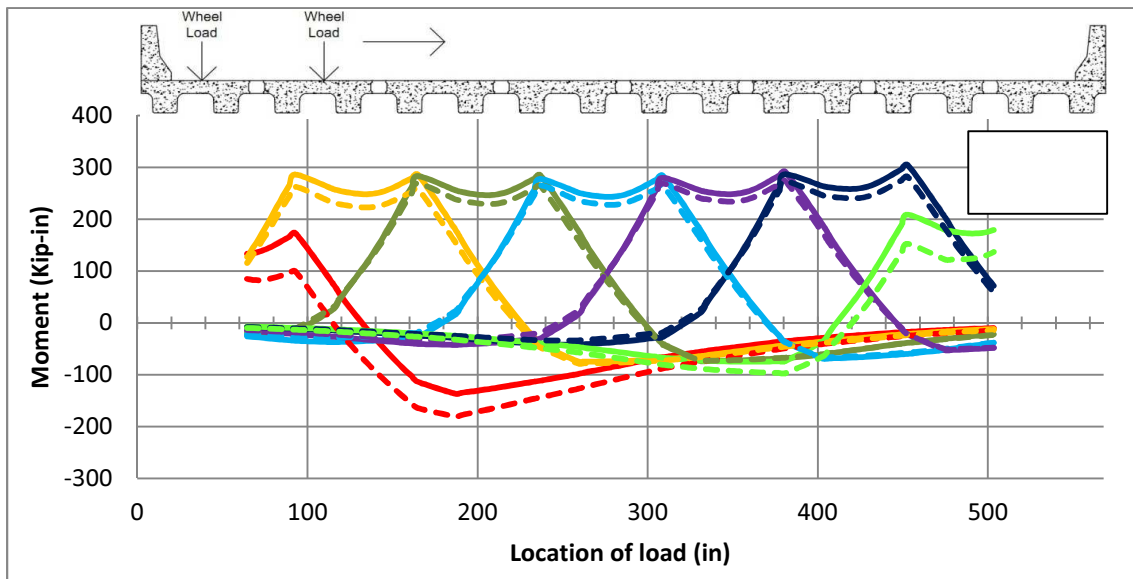


Appendix Figure 20: Moment influence line for the left side of the shear keys in an eight-foot section NEXT-D bridge under a single-axle loading at the supports

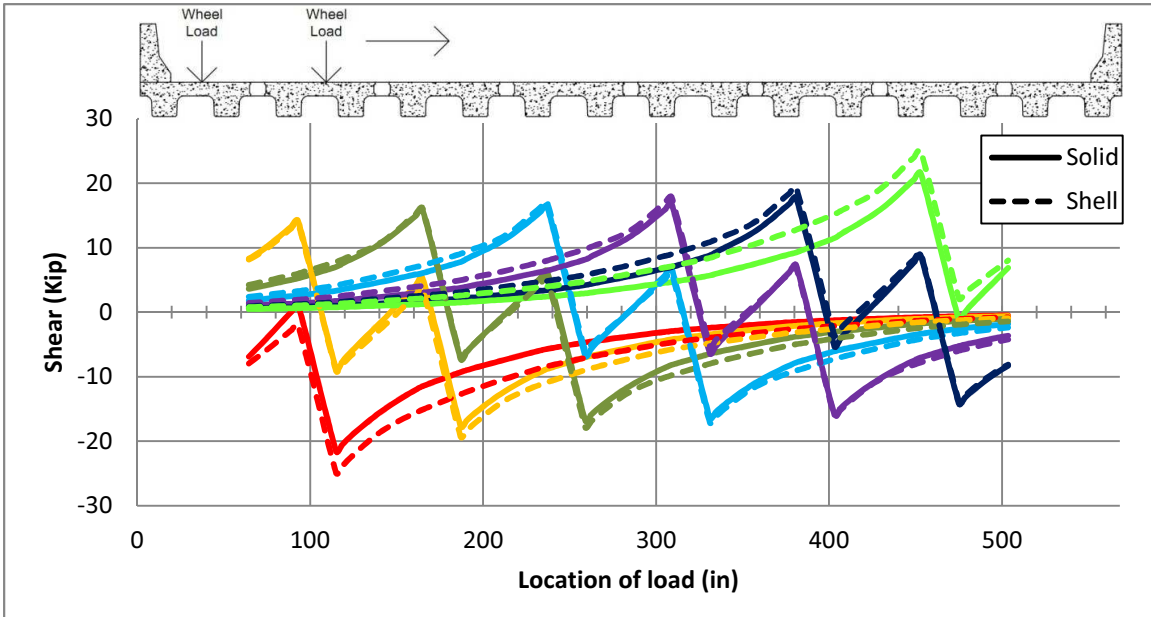
Two-Axle Influence Lines for the 6-Foot Section Bridge with Parapets



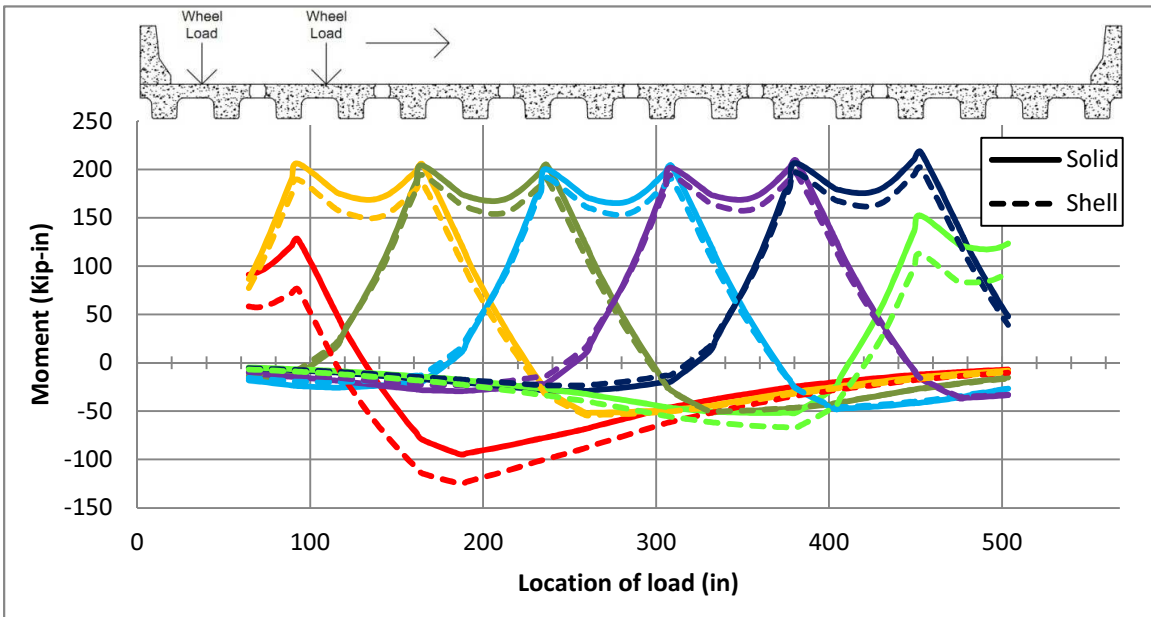
Appendix Figure 21: Shear influence line for the shear keys in a six-foot section NEXT-D bridge under a two-axle loading at mid-span



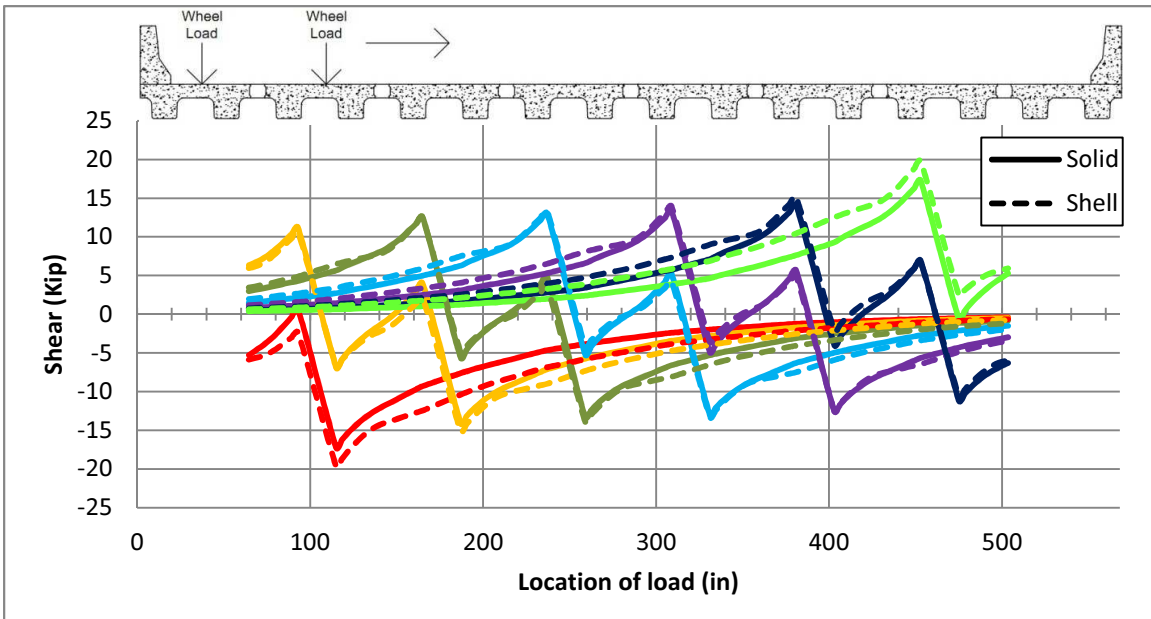
Appendix Figure 22: Moment influence line for the left side of the shear keys in a six-foot section NEXT-D bridge under a two-axle loading at mid-span



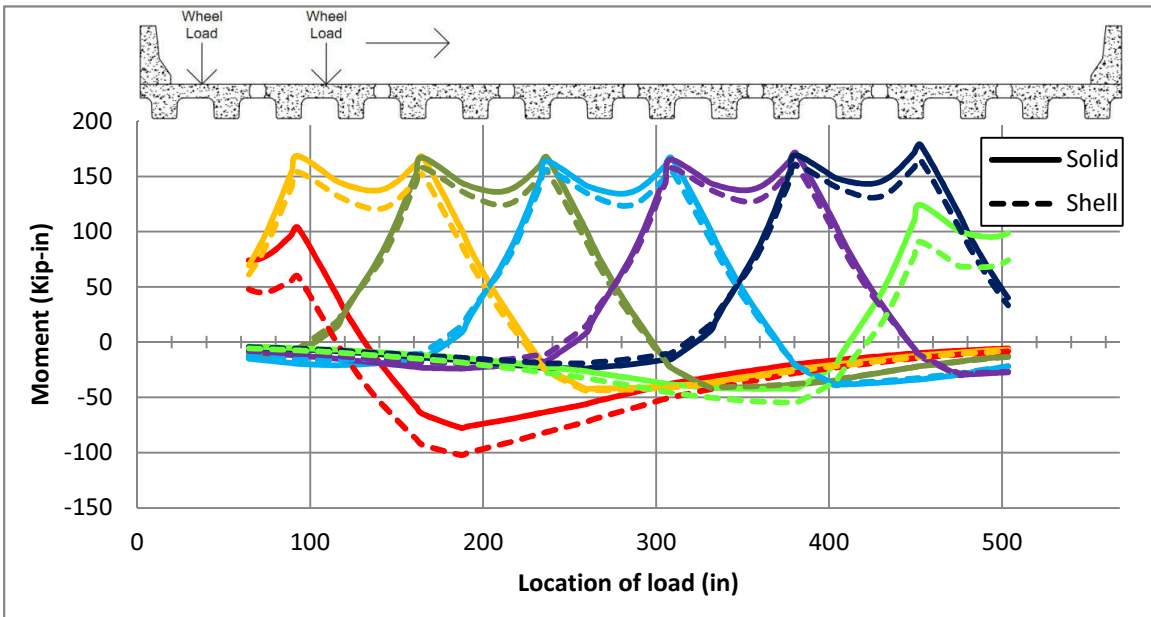
Appendix Figure 23: Shear influence line for the shear keys in a six-foot section NEXT-D bridge under a two-axe loading at quarter-span



Appendix Figure 24: Moment influence line for the left side of the shear keys in a six-foot section NEXT-D bridge under a two-axe loading at quarter-span

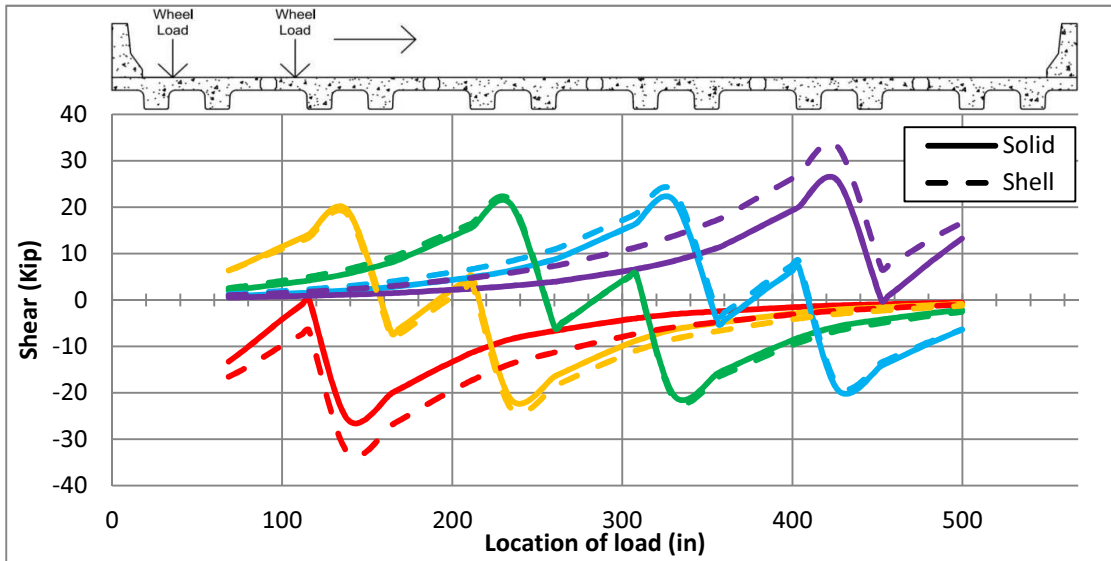


Appendix Figure 25: Shear influence line for the shear keys in a six-foot section NEXT-D bridge under a two-axle loading at the supports

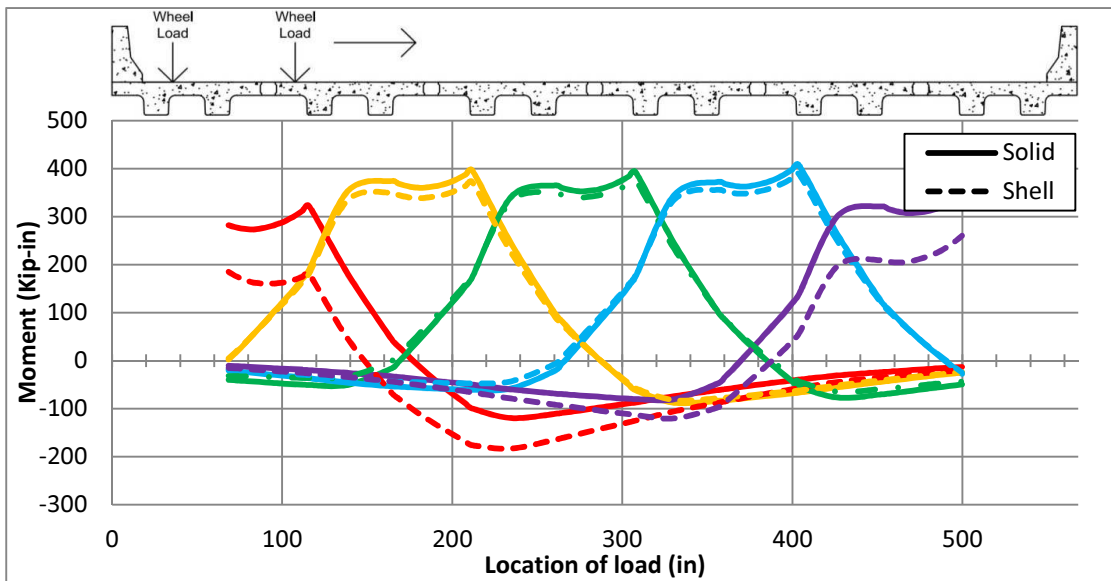


Appendix Figure 26: Moment influence line for the left side of the shear keys in a six-foot section NEXT-D bridge under a two-axle loading at the supports

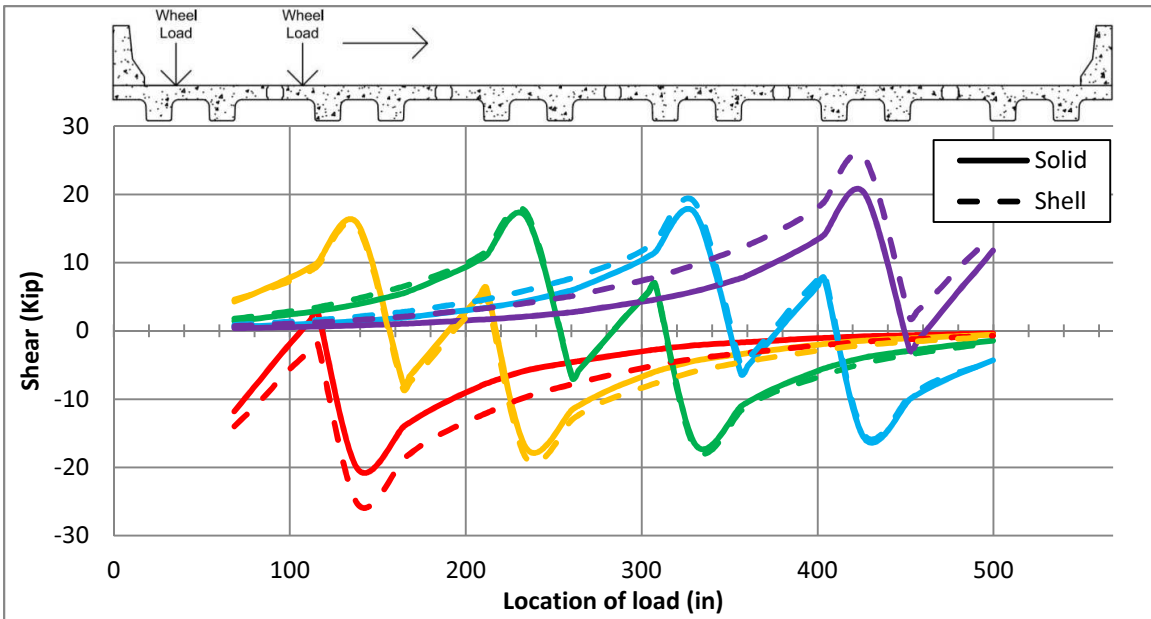
Two-Axle Influence Lines for the 8-Foot Section Bridge with Parapets



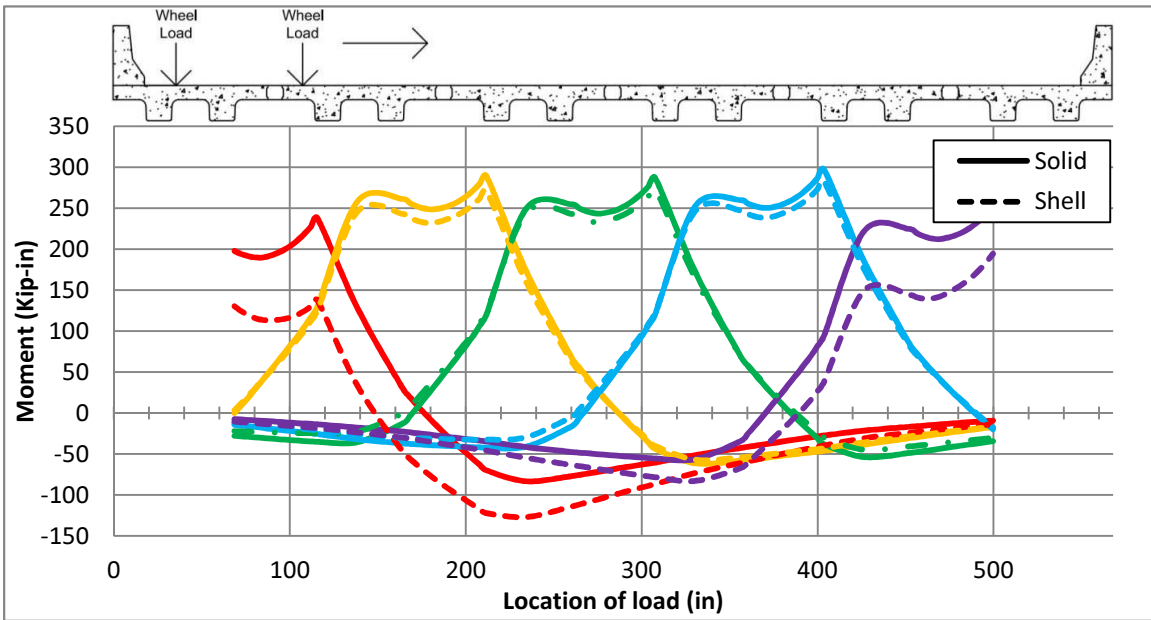
Appendix Figure 27: Shear influence line for the shear keys in an eight-foot section NEXT-D bridge under a two-axle loading at mid-span



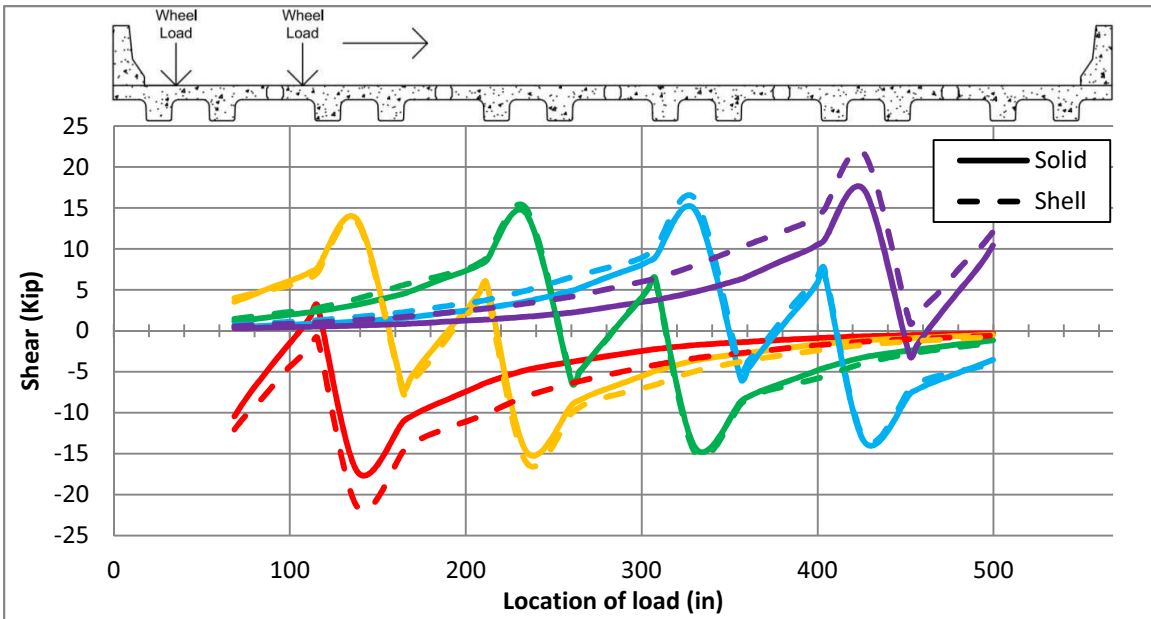
Appendix Figure 28: Moment influence line for the left side of the shear keys in an eight-foot section NEXT-D bridge under a two-axle loading at mid-span



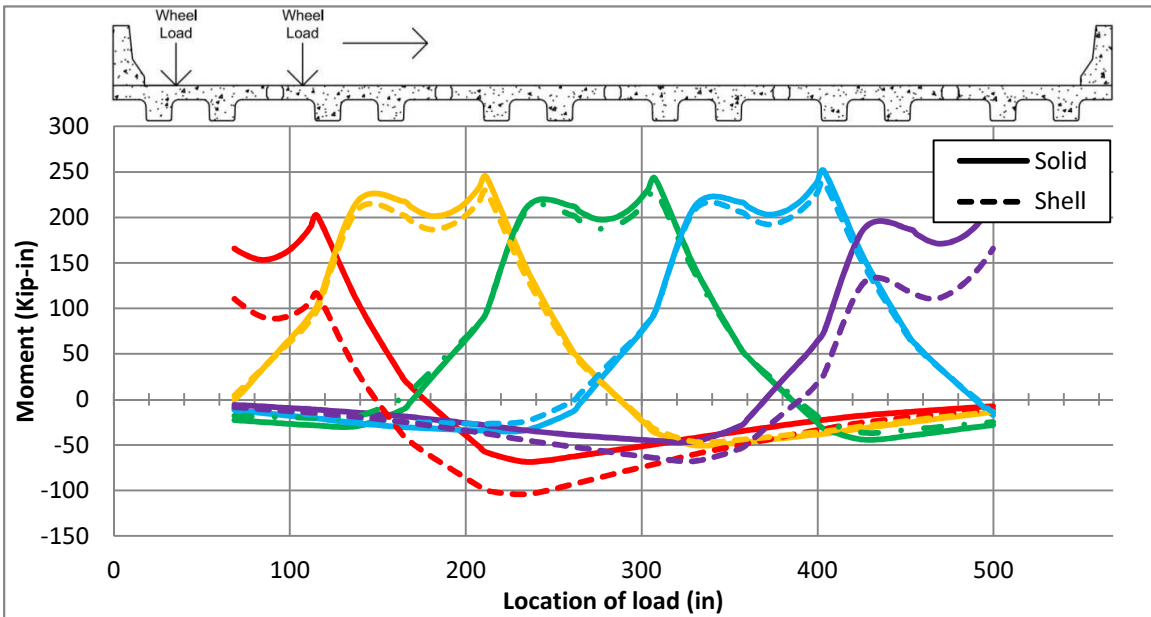
Appendix Figure 29: Shear influence line for the shear keys in an eight-foot section NEXT-D bridge under a two-axle loading at quarter-span



Appendix Figure 30: Moment influence line for the left side of the shear keys in an eight-foot section NEXT-D bridge under a two-axle loading at quarter-span

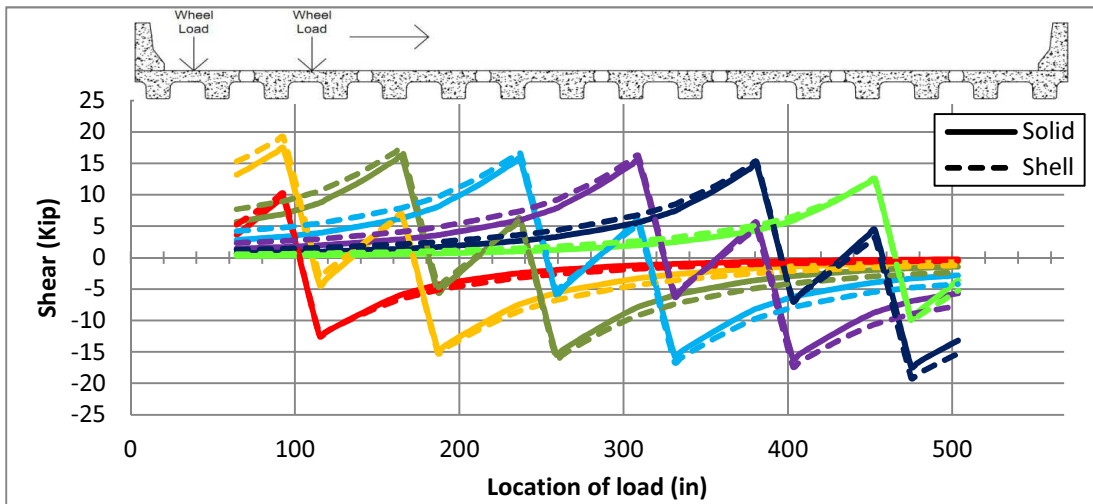


Appendix Figure 31: Shear influence line for the shear keys in an eight-foot section NEXT-D bridge under a two-axle loading at the supports

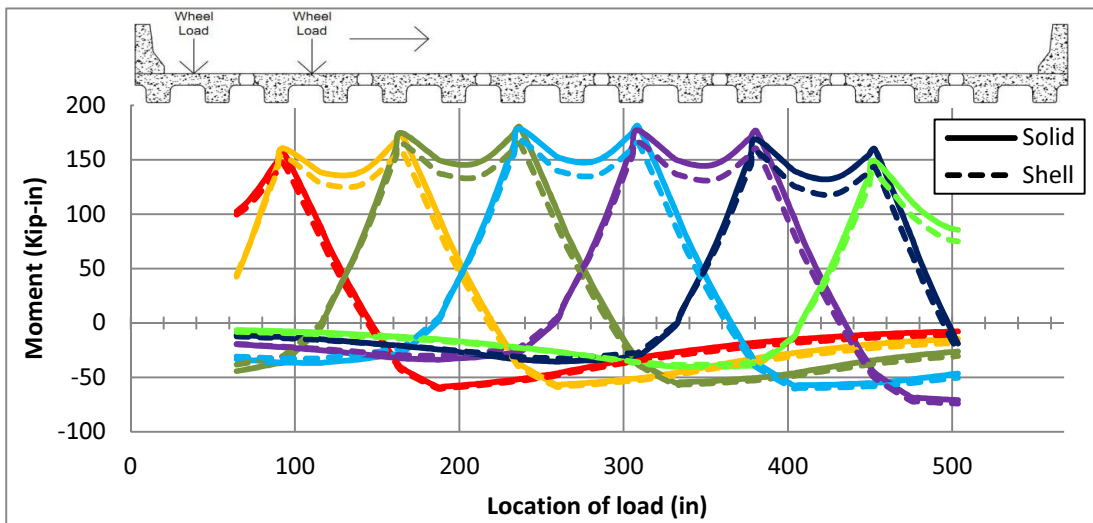


Appendix Figure 32: Moment influence line for the left side of the shear keys in an eight-foot section NEXT-D bridge under a two-axle loading at the supports

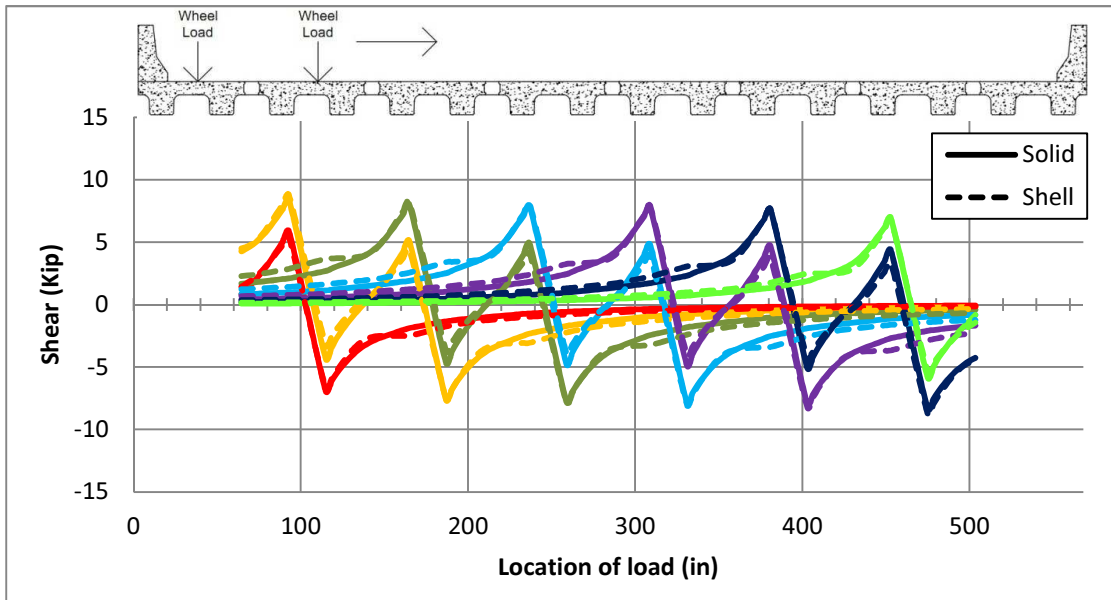
Design Tandem Influence Lines for the 6-Foot Section Bridge with no Parapets



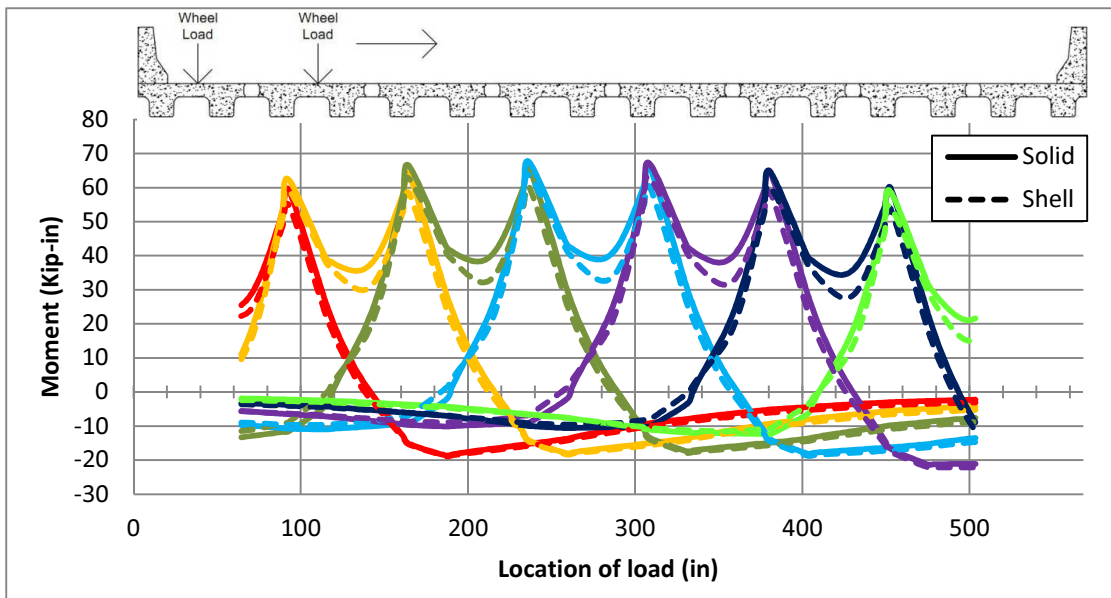
Appendix Figure 33: Shear influence line for the shear keys in a six-foot section NEXT-D bridge without parapets under a design tandem loading at quarter-span



Appendix Figure 34: Moment influence line for the left side of the shear keys in a six-foot section NEXT-D bridge without parapets under a design tandem loading at quarter-span

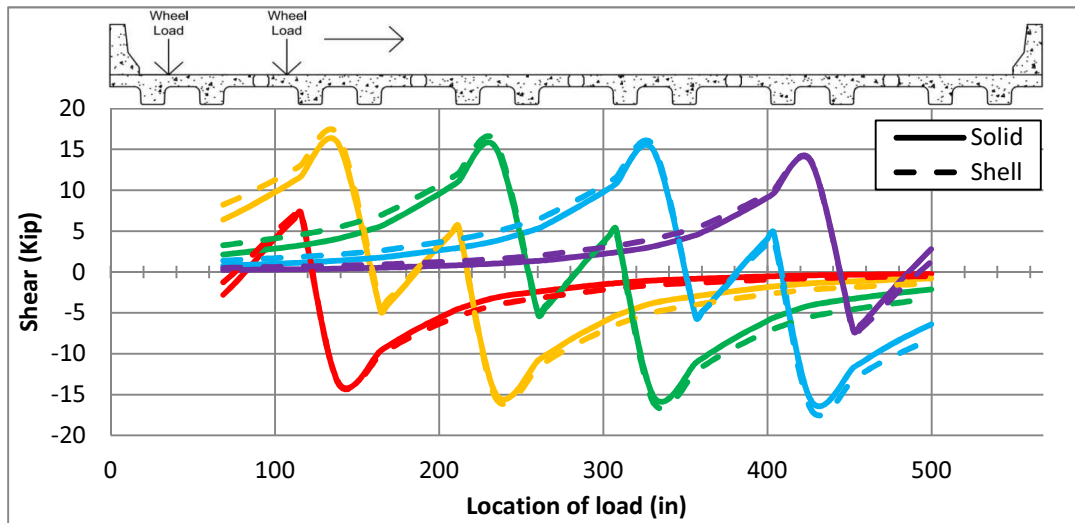


Appendix Figure 35: Shear influence line for the shear keys in a six-foot section NEXT-D bridge without parapets under a design tandem loading at the supports

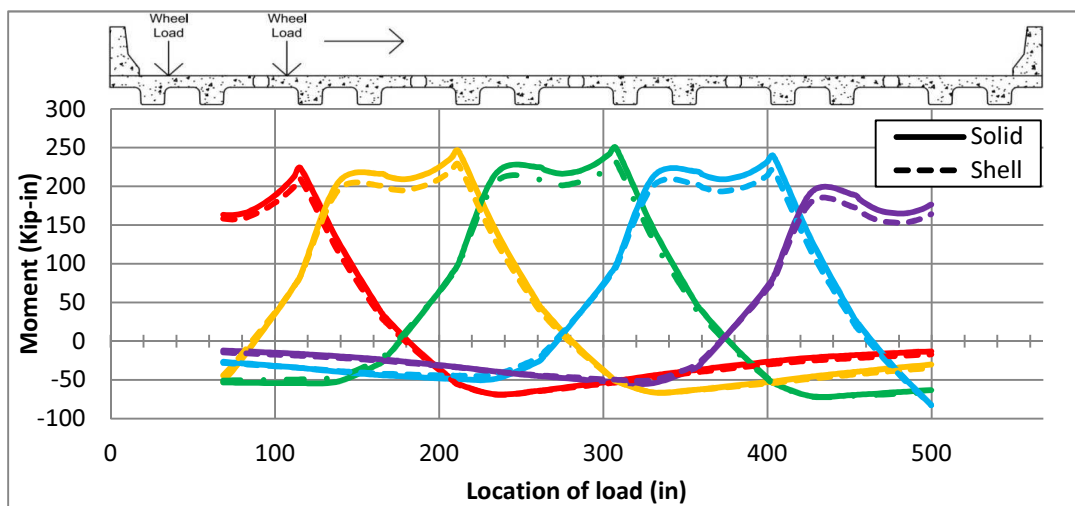


Appendix Figure 36: Moment influence line for the left side of the shear keys in a six-foot section NEXT-D bridge without parapets under a design tandem loading at the supports

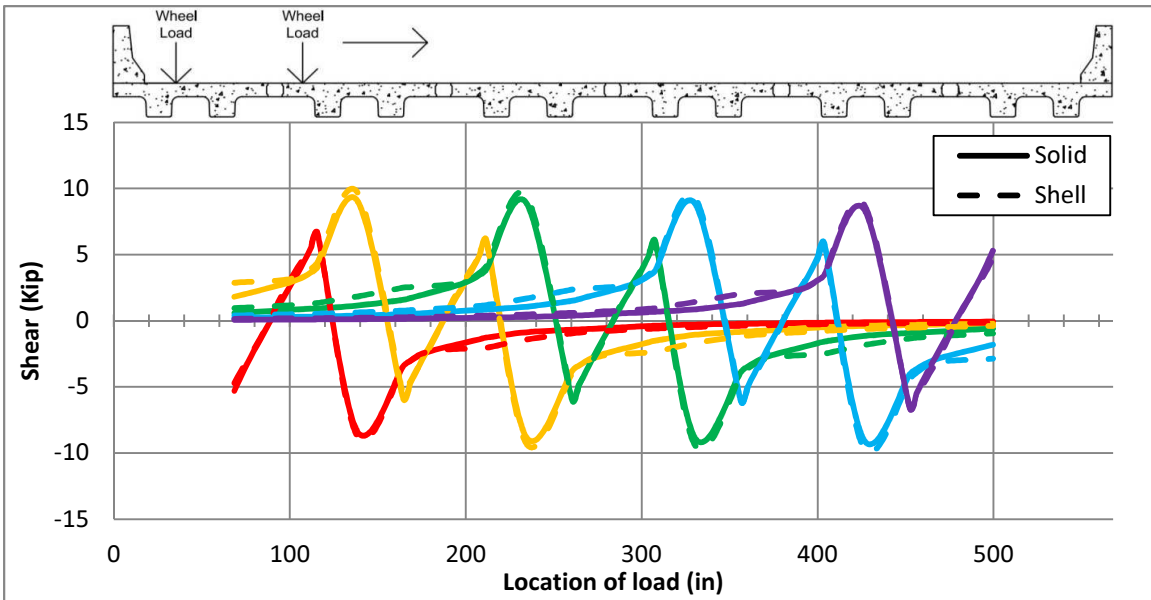
Design Tandem Influence Lines for the 8-Foot Section Bridge with no Parapets



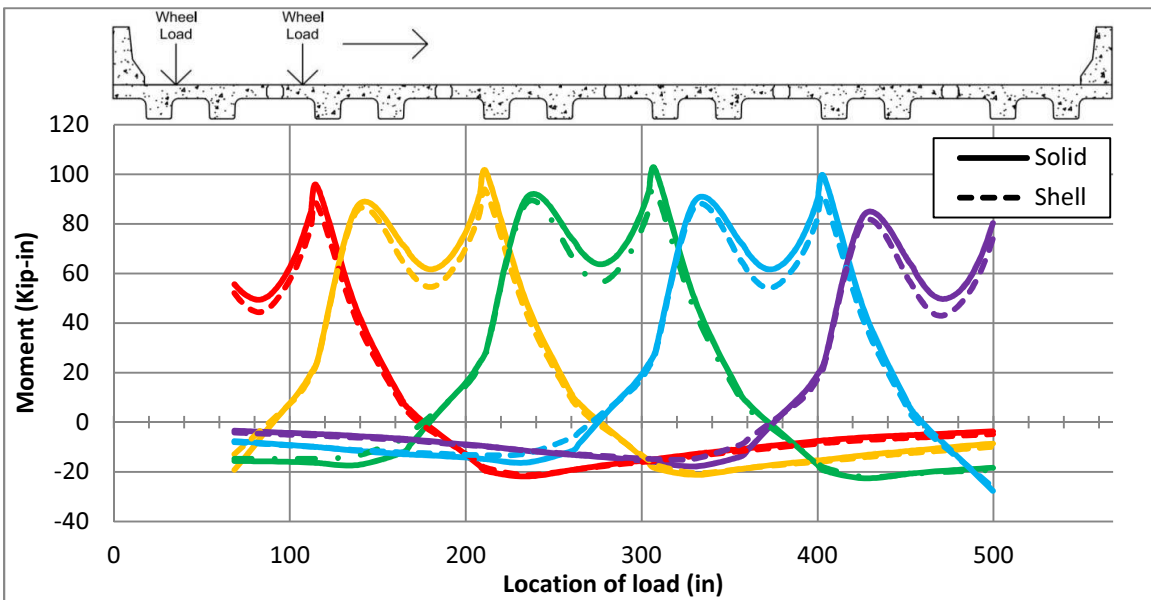
Appendix Figure 37: Shear influence line for the shear keys in an eight-foot section NEXT-D bridge without parapets under a design tandem loading at quarter-span



Appendix Figure 38: Moment influence line for the left side of the shear keys in an eight-foot section NEXT-D bridge without parapets under a design tandem loading at quarter-span

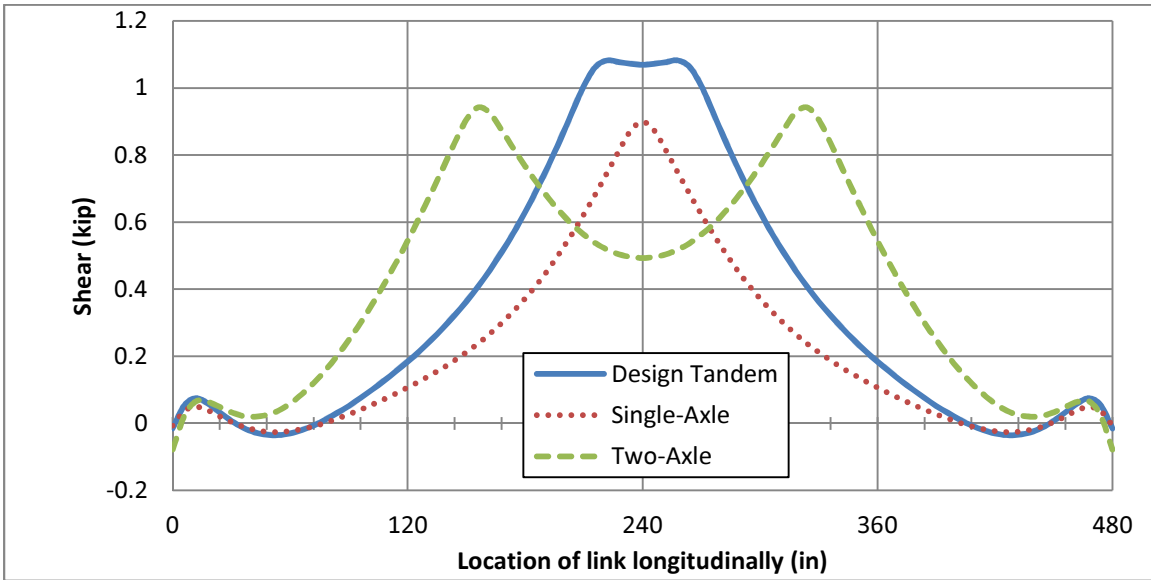


Appendix Figure 39: Shear influence line for the shear keys in an eight-foot section NEXT-D bridge without parapets under a design tandem loading at the supports

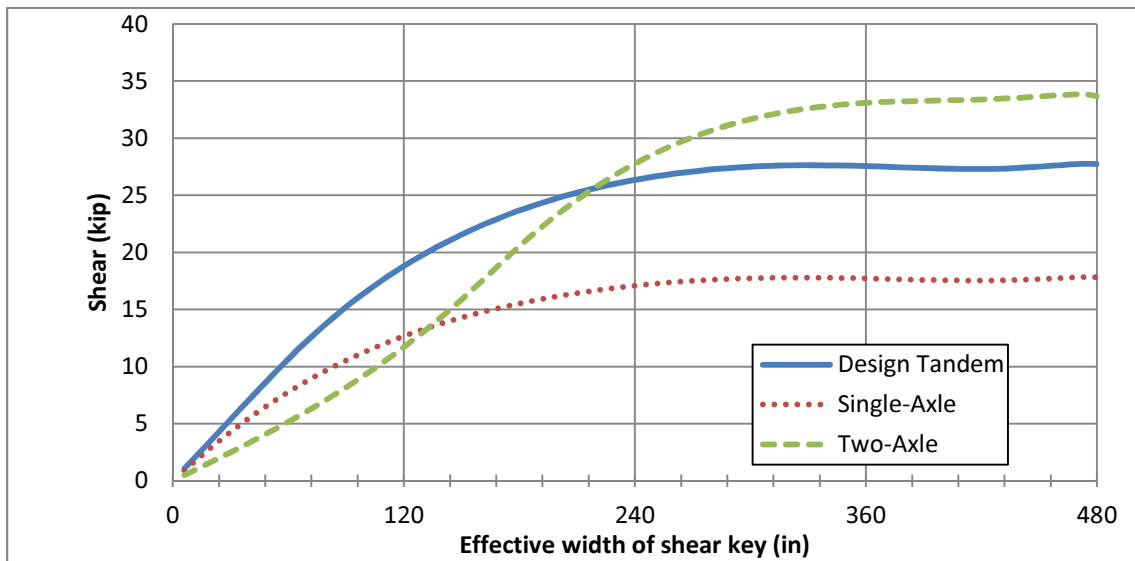


Appendix Figure 40: Moment influence line for the left side of the shear keys in an eight-foot section NEXT-D bridge without parapets under a design tandem loading at the supports

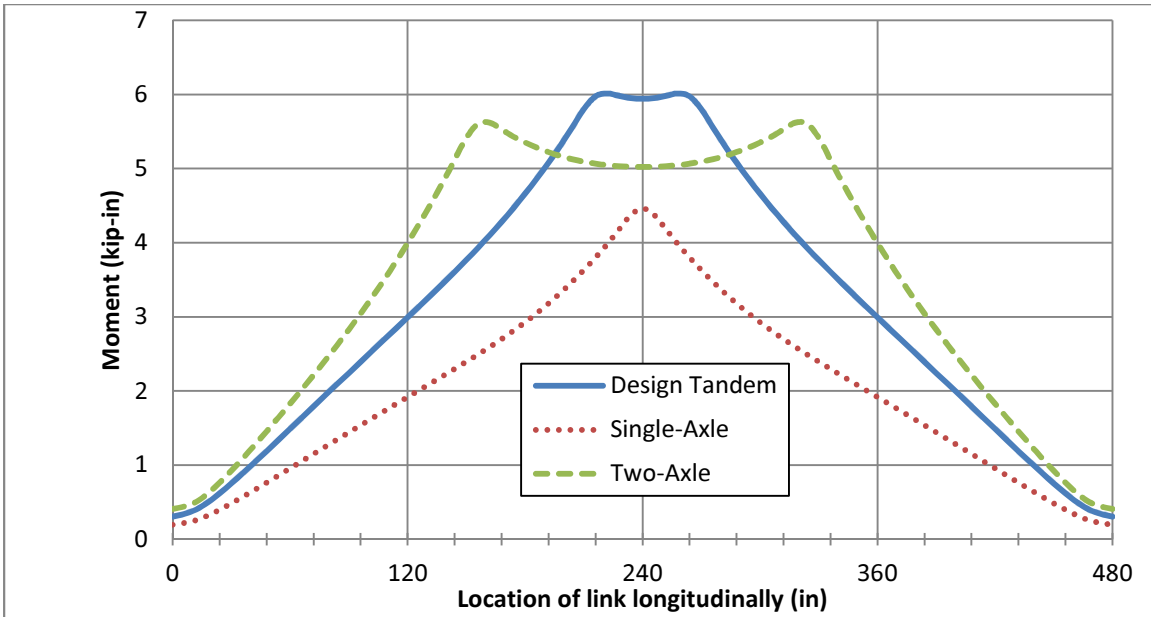
Appendix D: Demand Distribution and Accumulation Plots



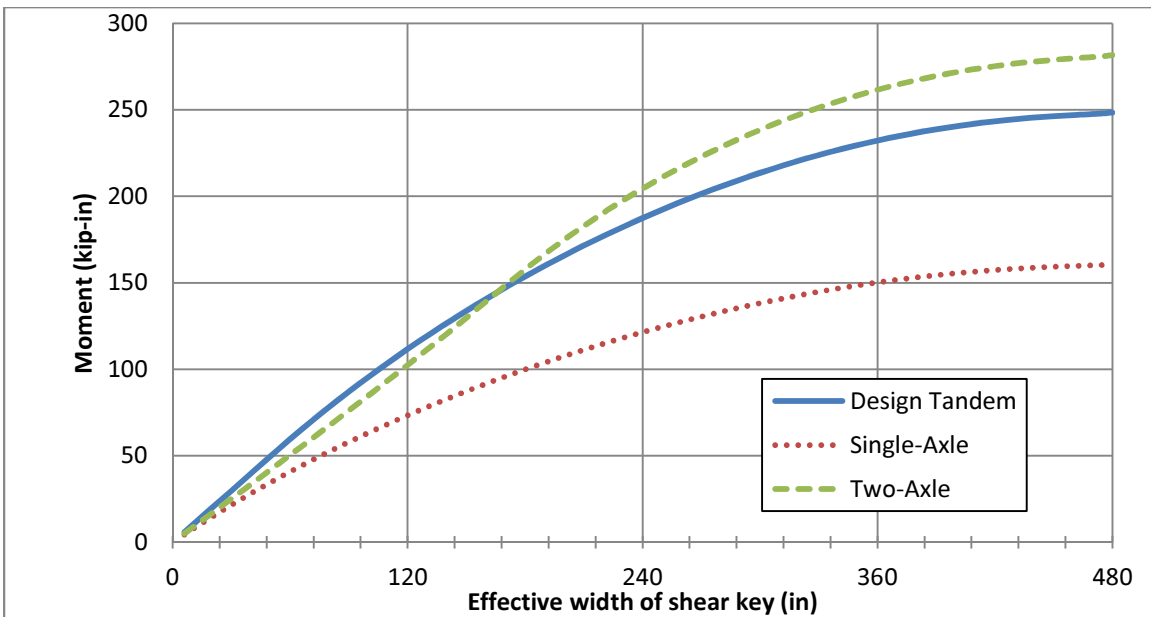
Appendix Figure 41: Shear in each shear key element of Key 7 along the length of a six-foot section NEXT-D bridge with load at the critical shear location



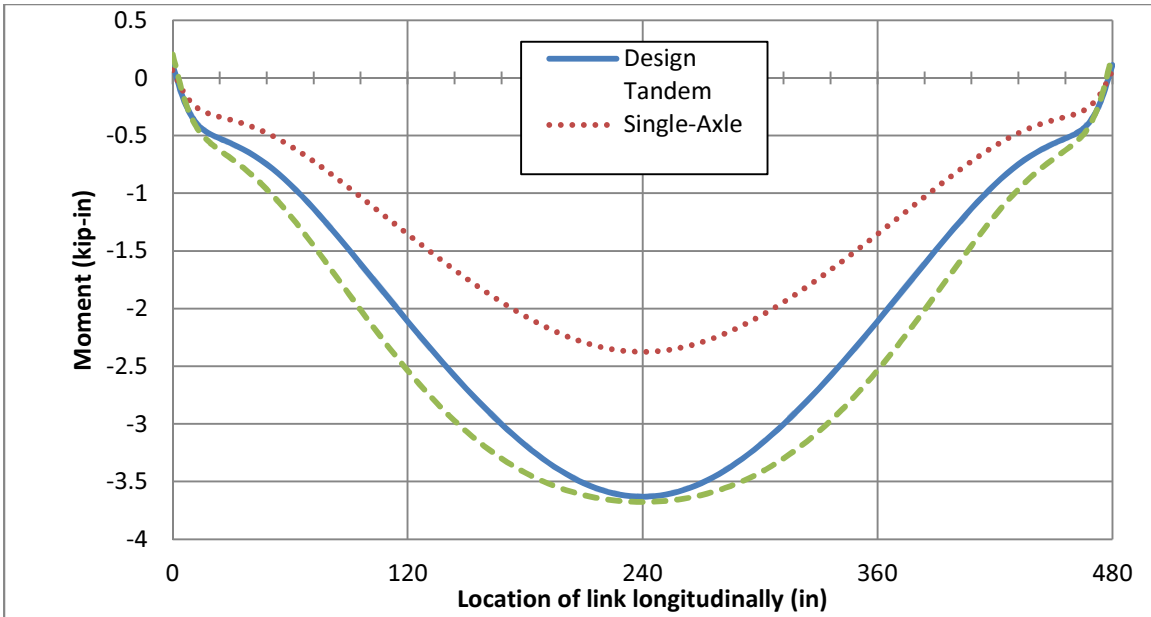
Appendix Figure 42: Shear accumulation plot for Key 7 of a six-foot section NEXT-D bridge with load at the critical shear location



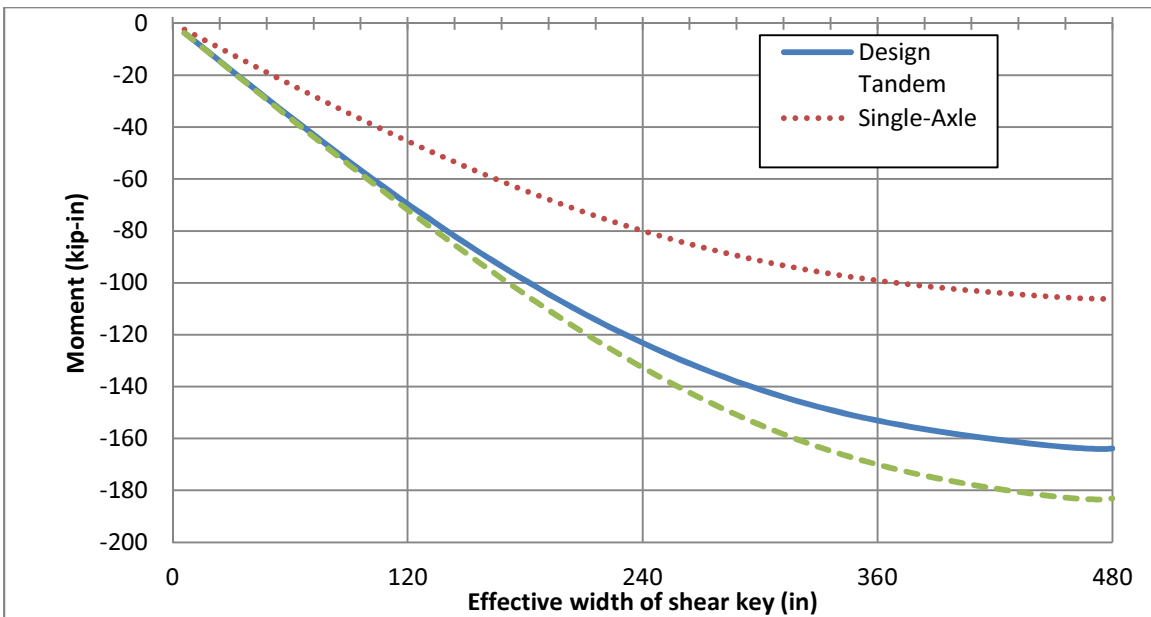
Appendix Figure 43: Moment in each shear key element of Key 6 along the length of a six-foot section NEXT-D bridge with load at the critical positive moment location



Appendix Figure 44: Moment accumulation plot for Key 6 of a six-foot section NEXT-D bridge with load at the critical positive moment location

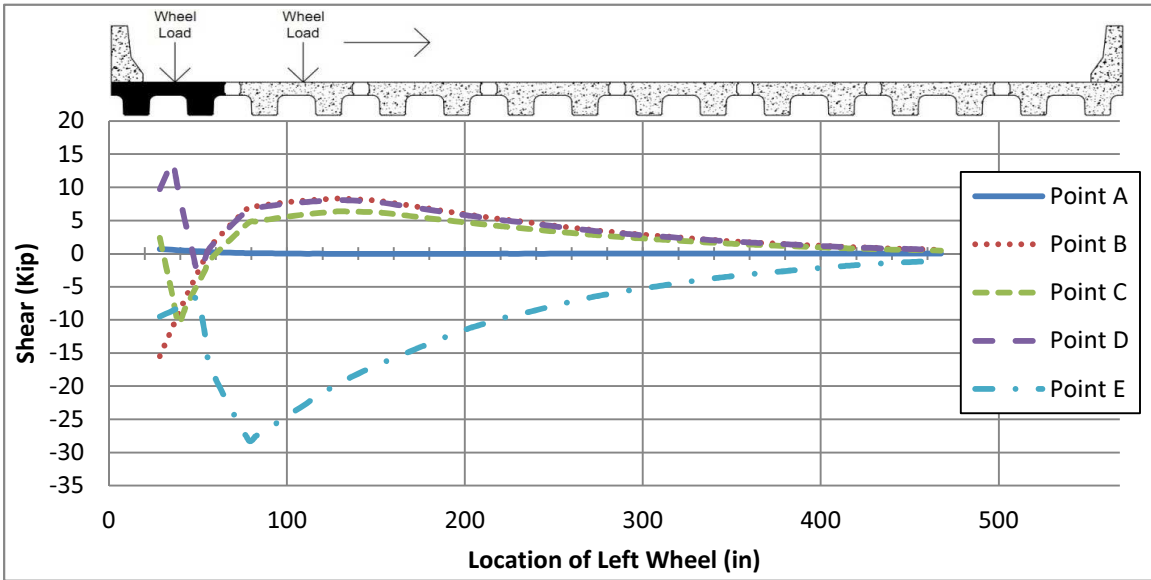


Appendix Figure 45: Moment in each shear key element of Key 7 along the length of a six-foot section NEXT-D bridge with load at the critical negative moment location

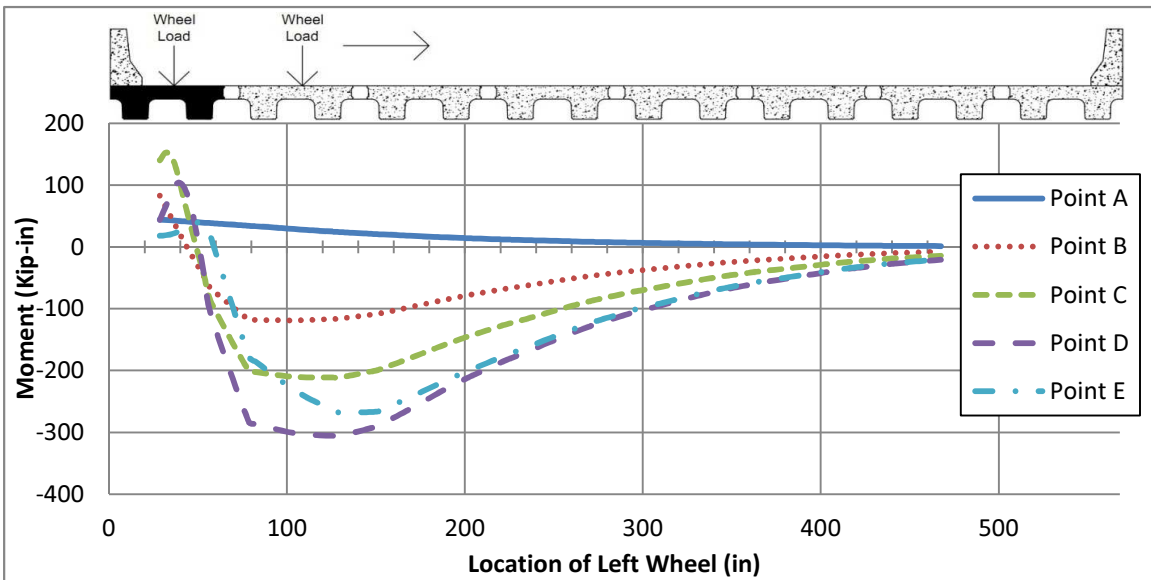


Appendix Figure 46: Moment accumulation plot for Key 7 of a six-foot section NEXT-D bridge with load at the critical negative moment location

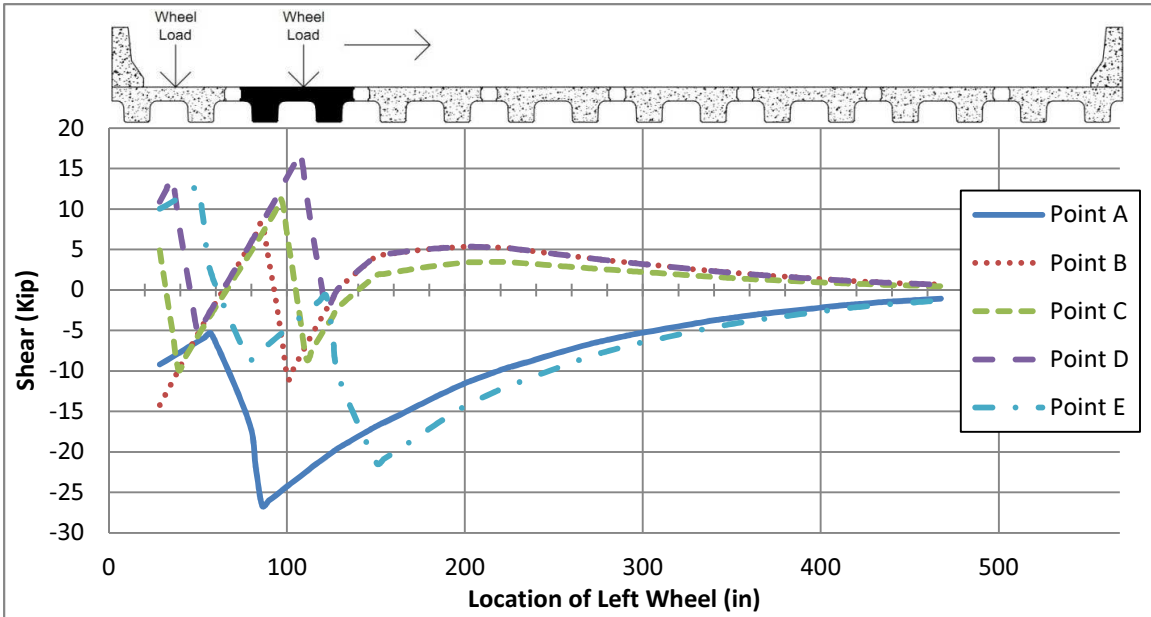
Appendix E: Bridge Deck Influence Lines



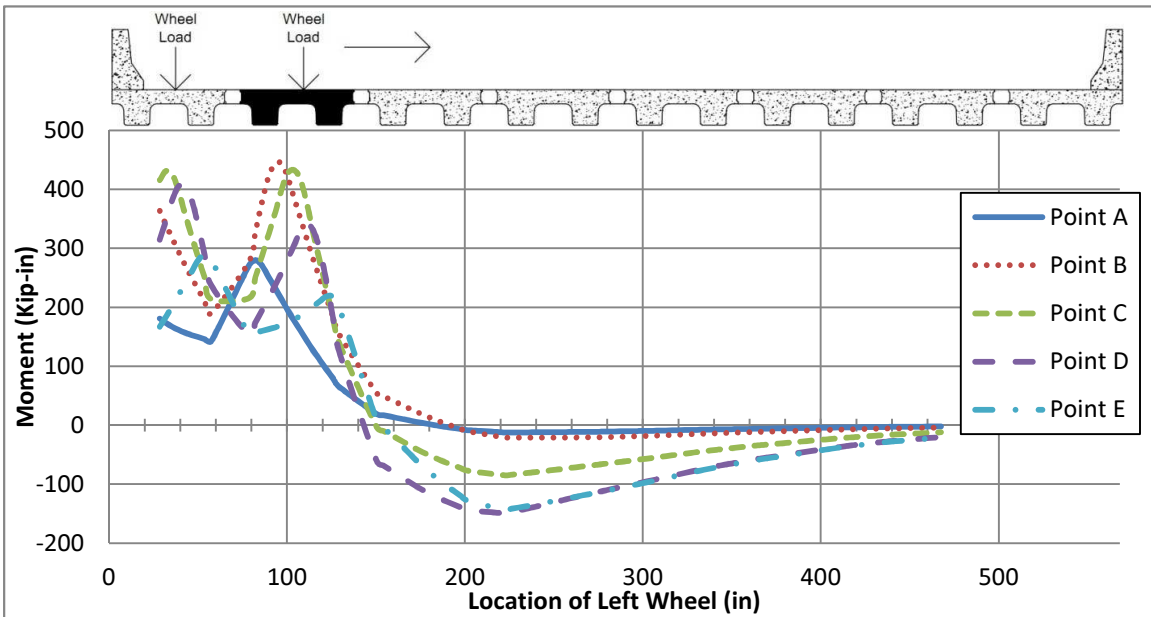
Appendix Figure 47: Shear influence line for the critical deck locations in the first beam from the left in a six-foot section NEXT-D bridge



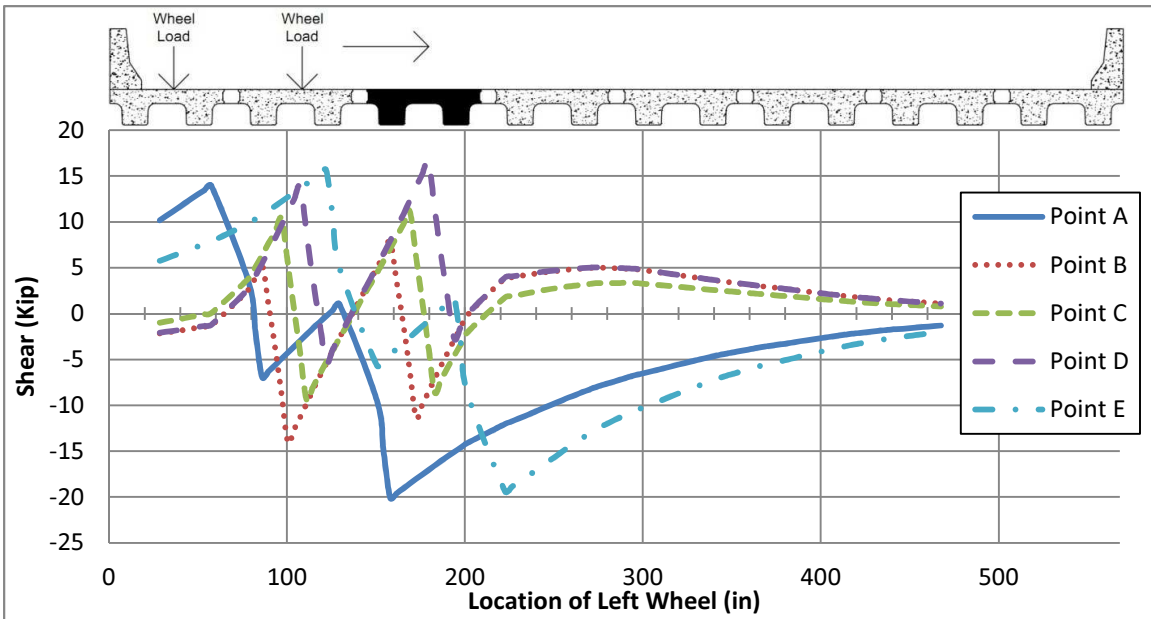
Appendix Figure 48: Moment influence line for the critical deck locations in the first beam from the left in a six-foot section NEXT-D bridge



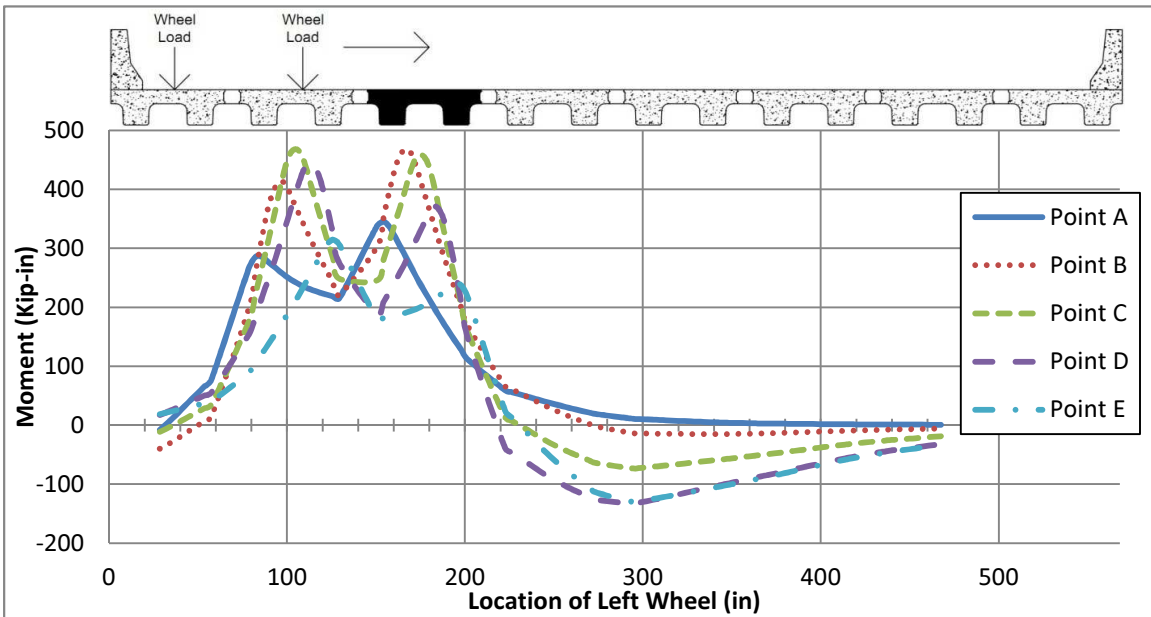
Appendix Figure 49: Shear influence line for the critical deck locations in the second beam from the left in a six-foot section NEXT-D bridge



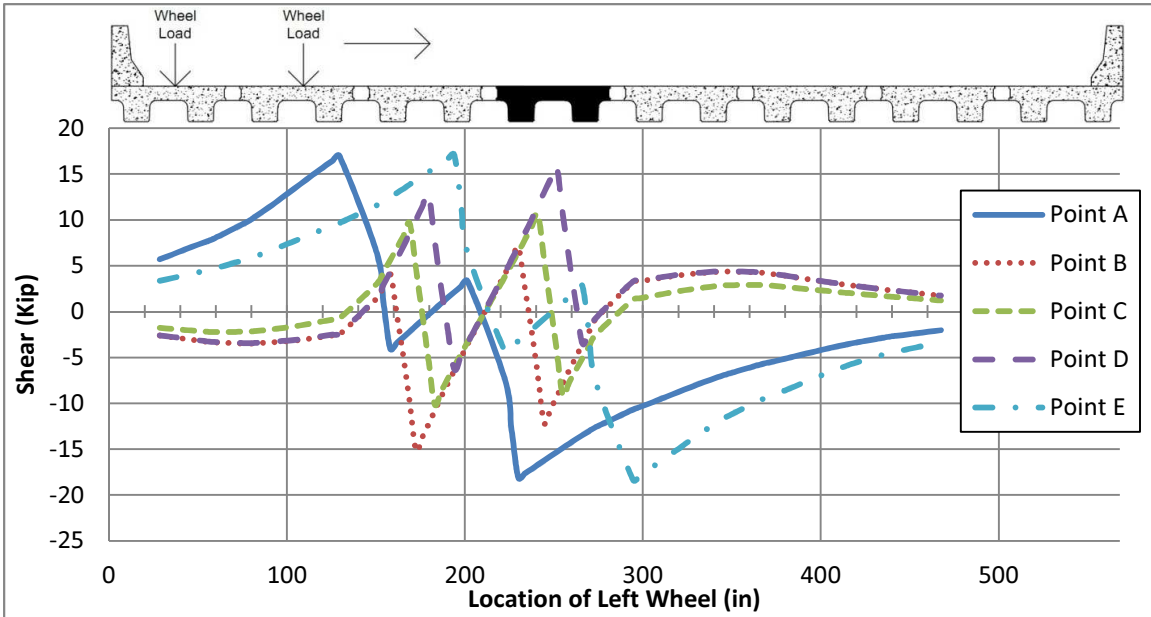
Appendix Figure 50: Moment influence line for the critical deck locations in the second beam from the left in a six-foot section NEXT-D bridge



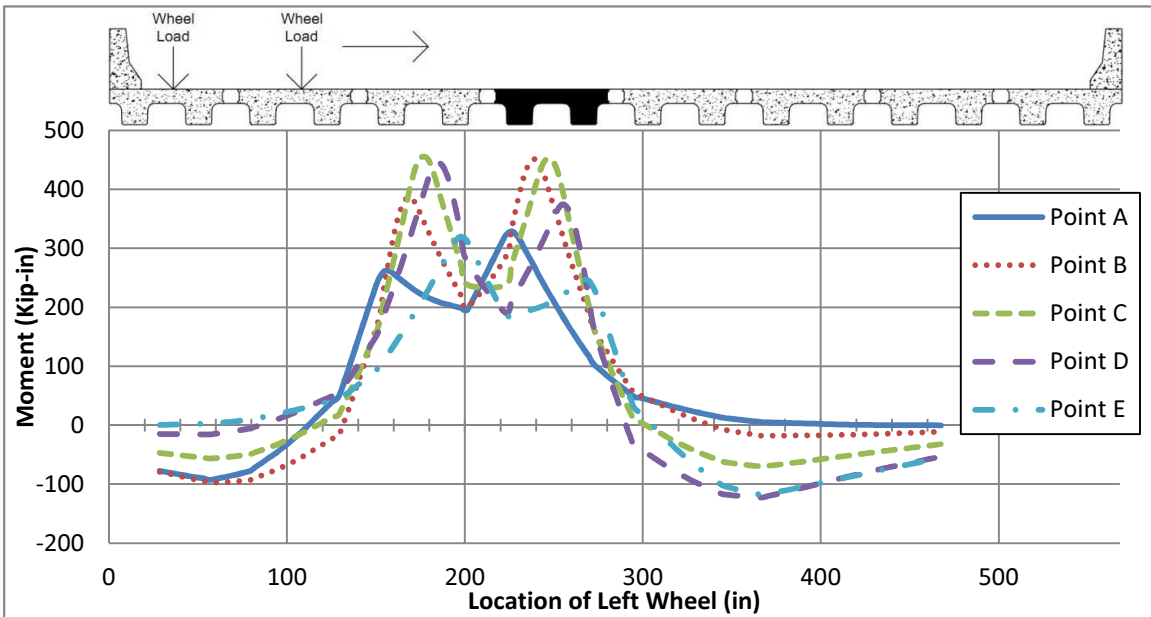
Appendix Figure 51: Shear influence line for the critical deck locations in the third beam from the left in a six-foot section NEXT-D bridge



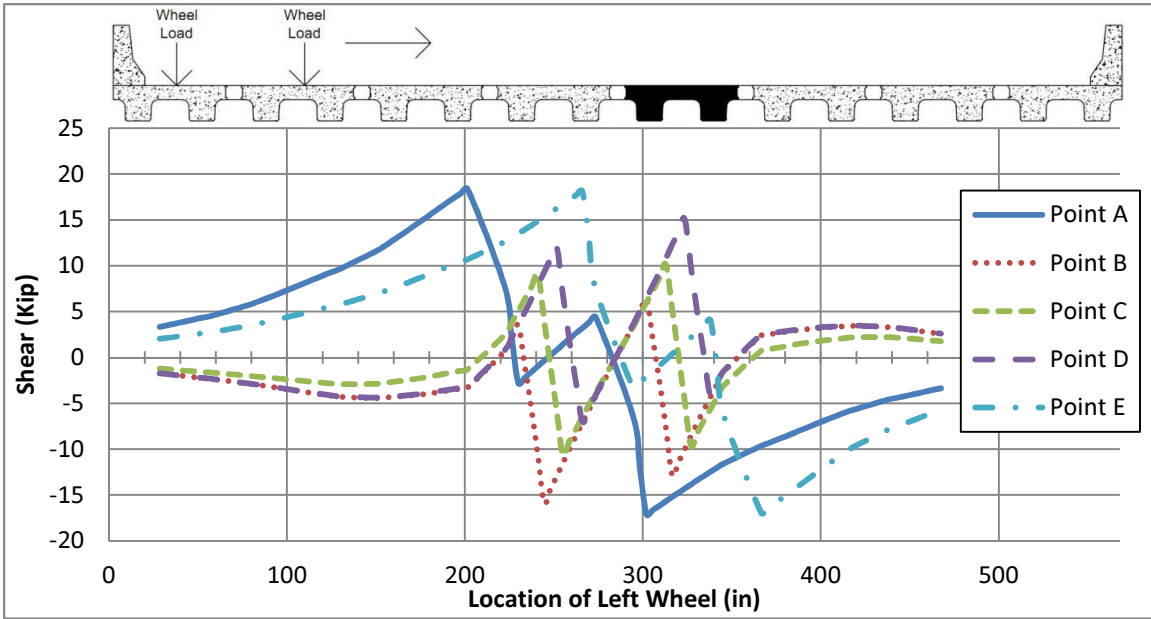
Appendix Figure 52: Moment influence line for the critical deck locations in the third beam from the left in a six-foot section NEXT-D bridge



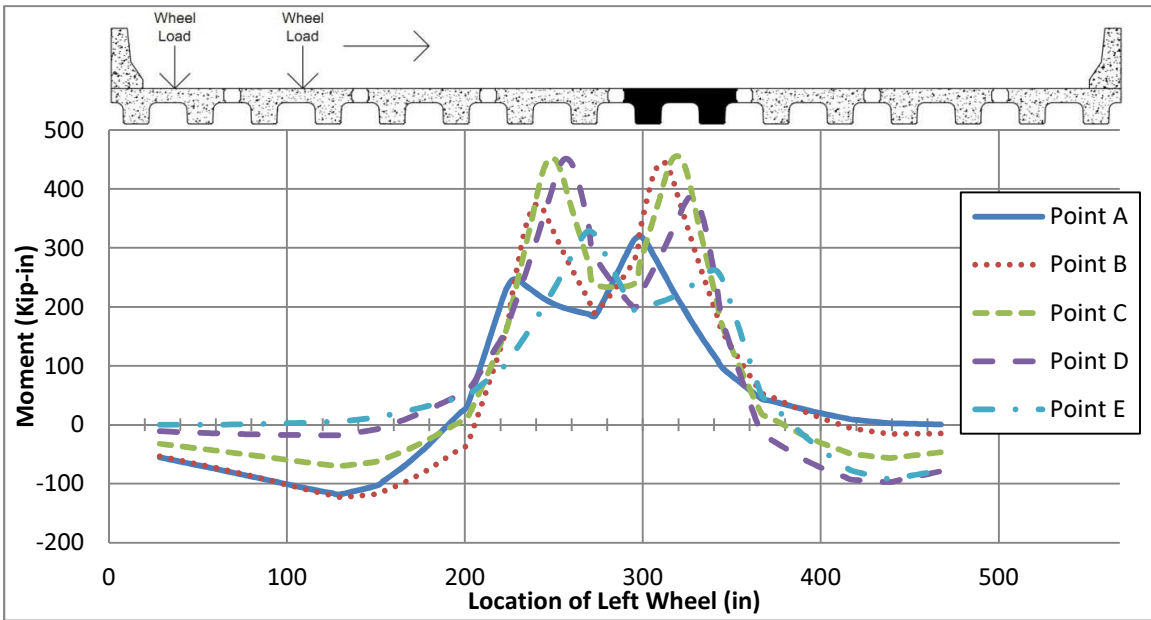
Appendix Figure 53: Shear influence line for the critical deck locations in the fourth beam from the left in a six-foot section NEXT-D bridge



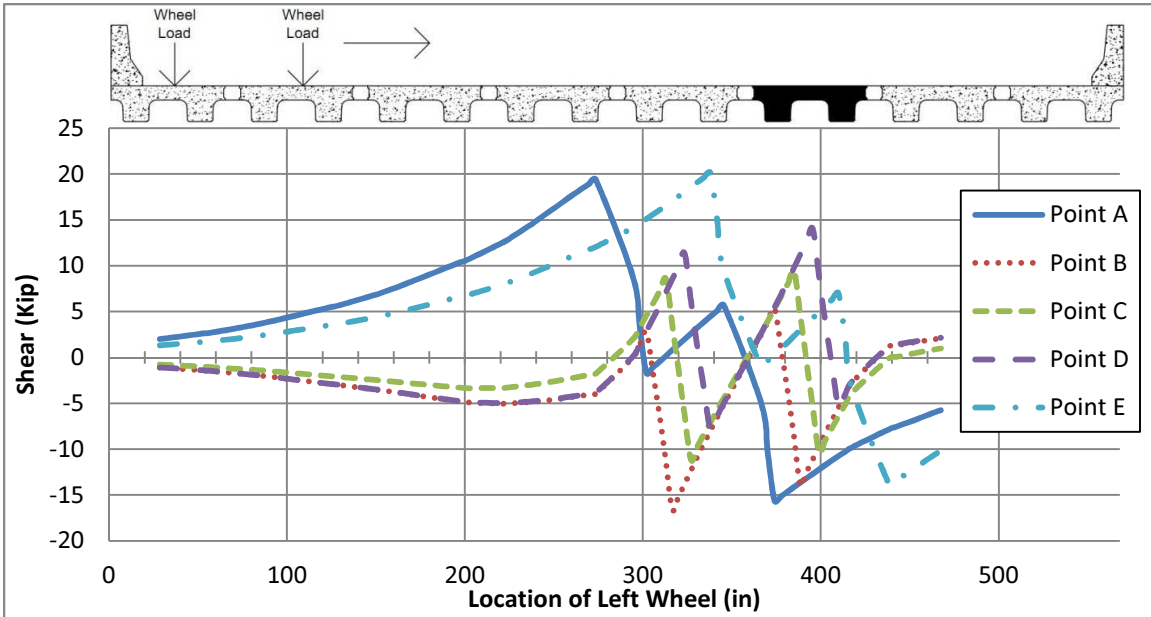
Appendix Figure 54: Moment influence line for the critical deck locations in the fourth beam from the left in a six-foot section NEXT-D bridge



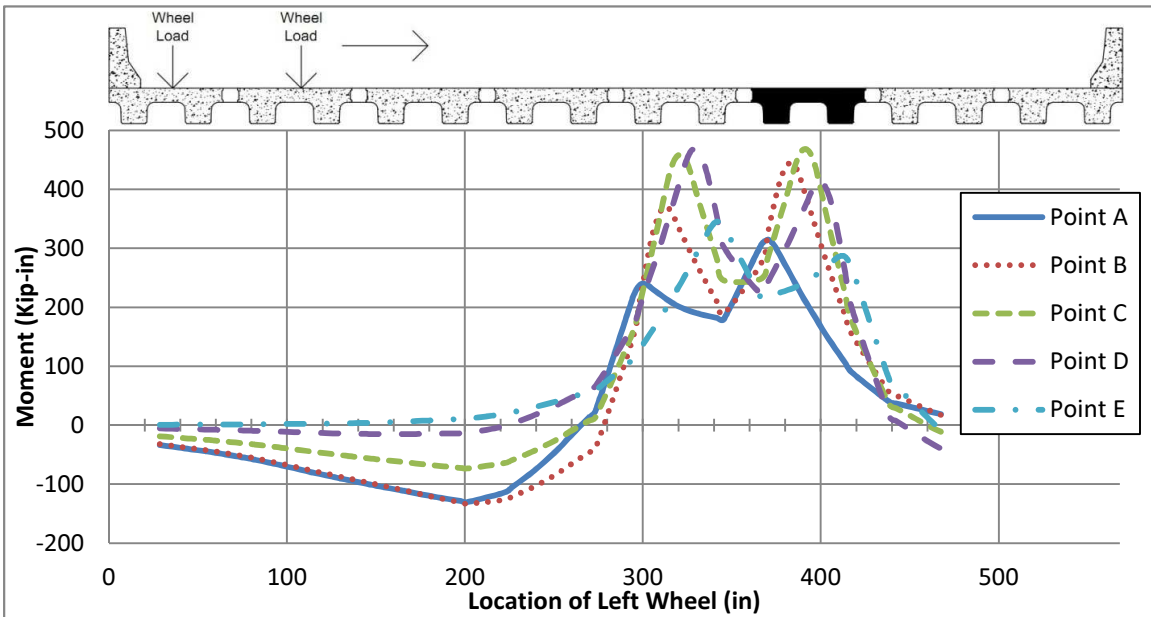
Appendix Figure 55: Shear influence line for the critical deck locations in the fifth beam from the left in a six-foot section NEXT-D bridge



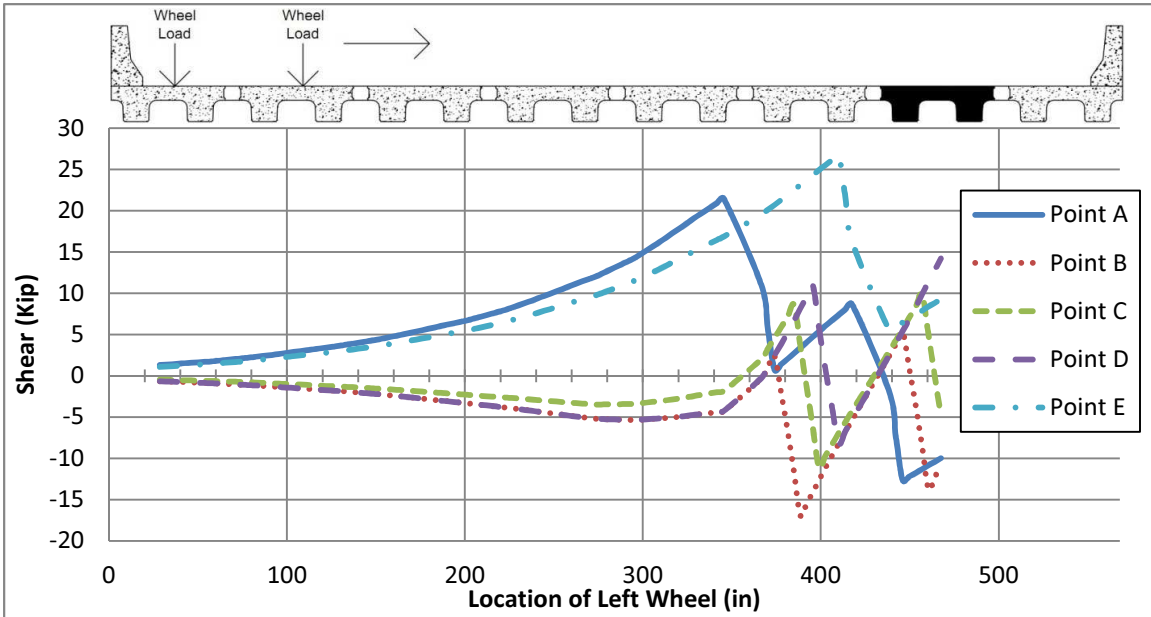
Appendix Figure 56: Moment influence line for the critical deck locations in the fifth beam from the left in a six-foot section NEXT-D bridge



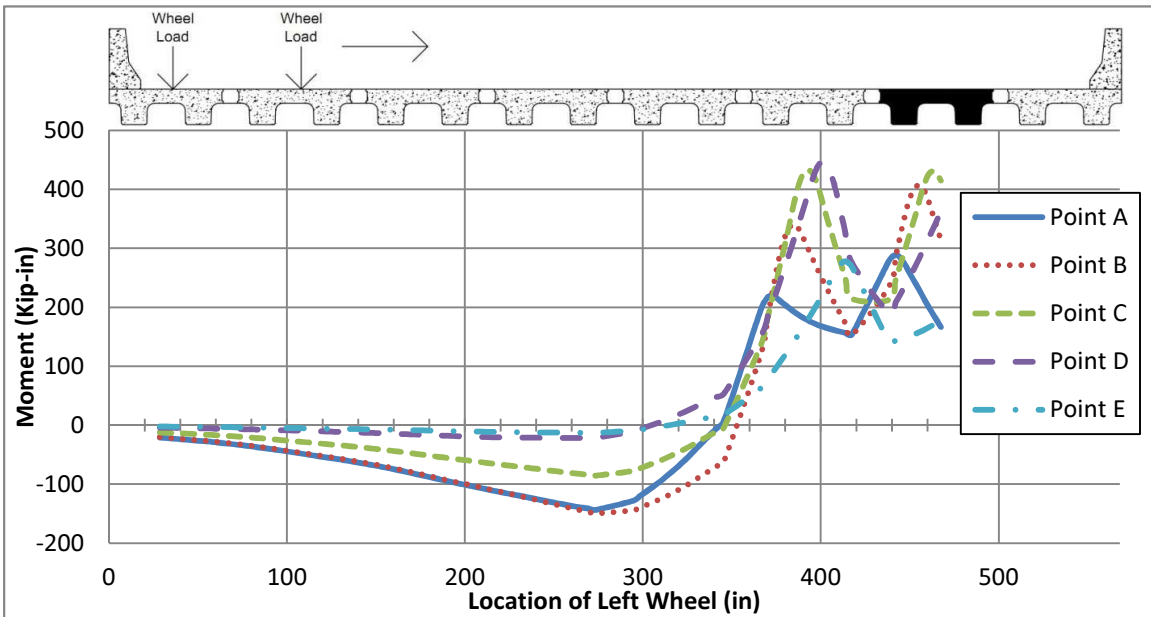
Appendix Figure 57: Shear influence line for the critical deck locations in the sixth beam from the left in a six-foot section NEXT-D bridge



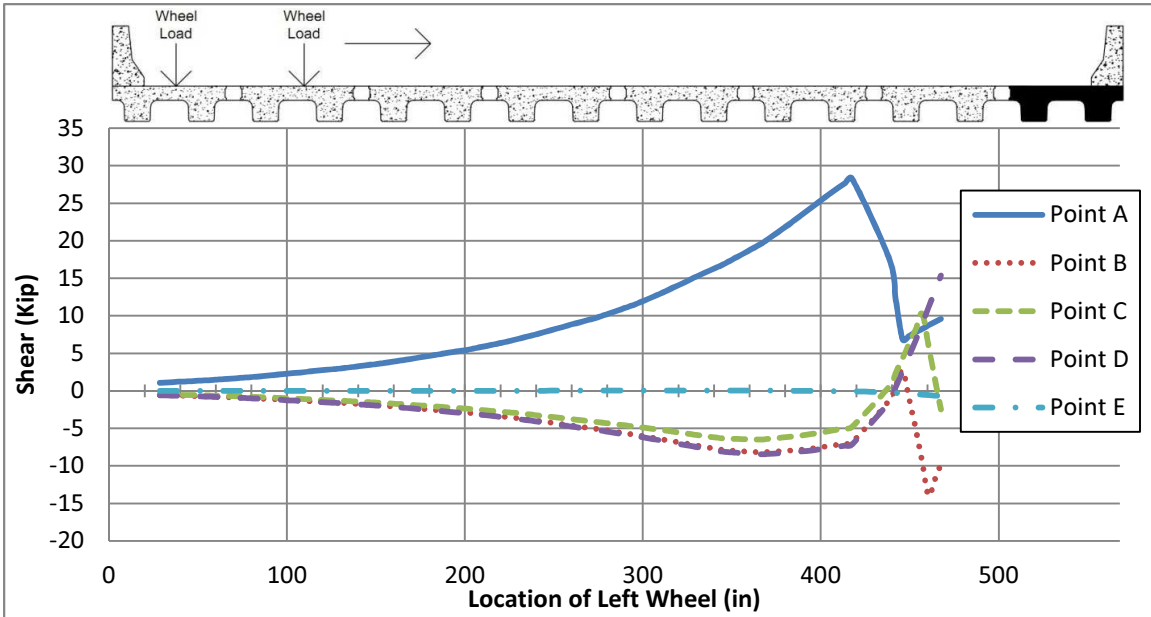
Appendix Figure 58: Moment influence line for the critical deck locations in the sixth beam from the left in a six-foot section NEXT-D bridge



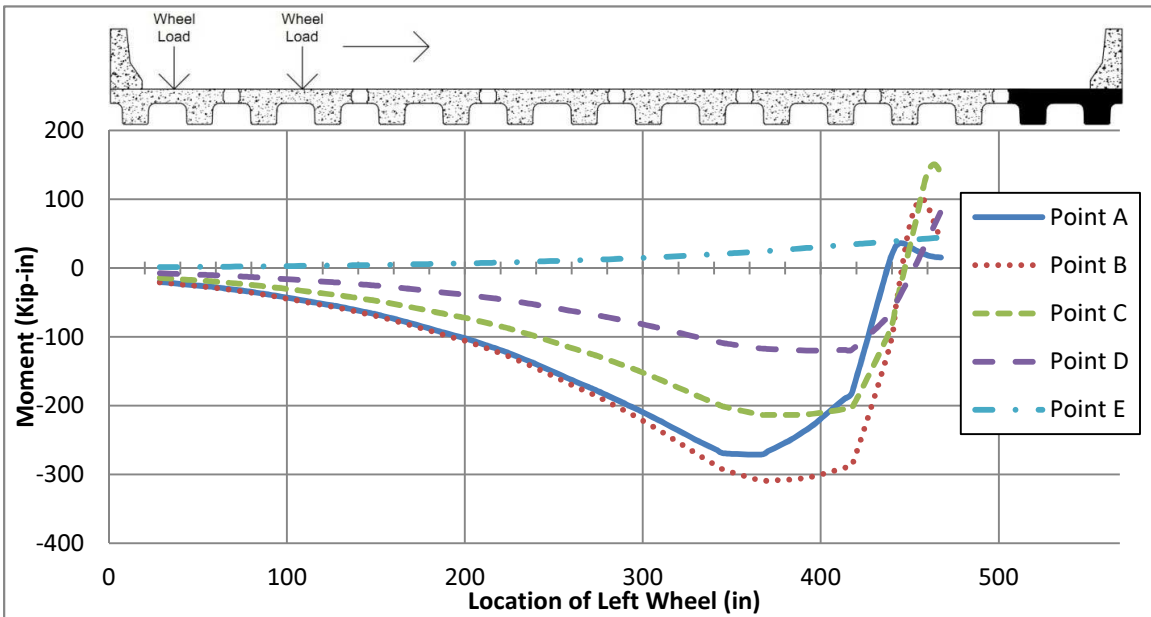
Appendix Figure 59: Shear influence line for the critical deck locations in the seventh beam from the left in a six-foot section NEXT-D bridge



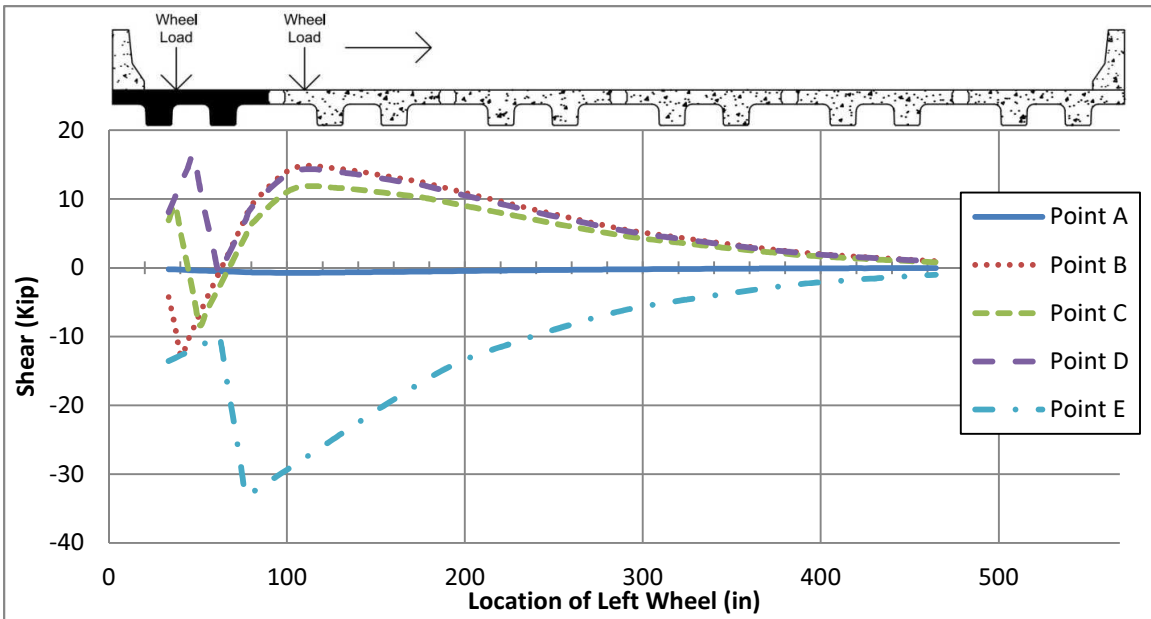
Appendix Figure 60: Moment influence line for the critical deck locations in the seventh beam from the left in a six-foot section NEXT-D bridge



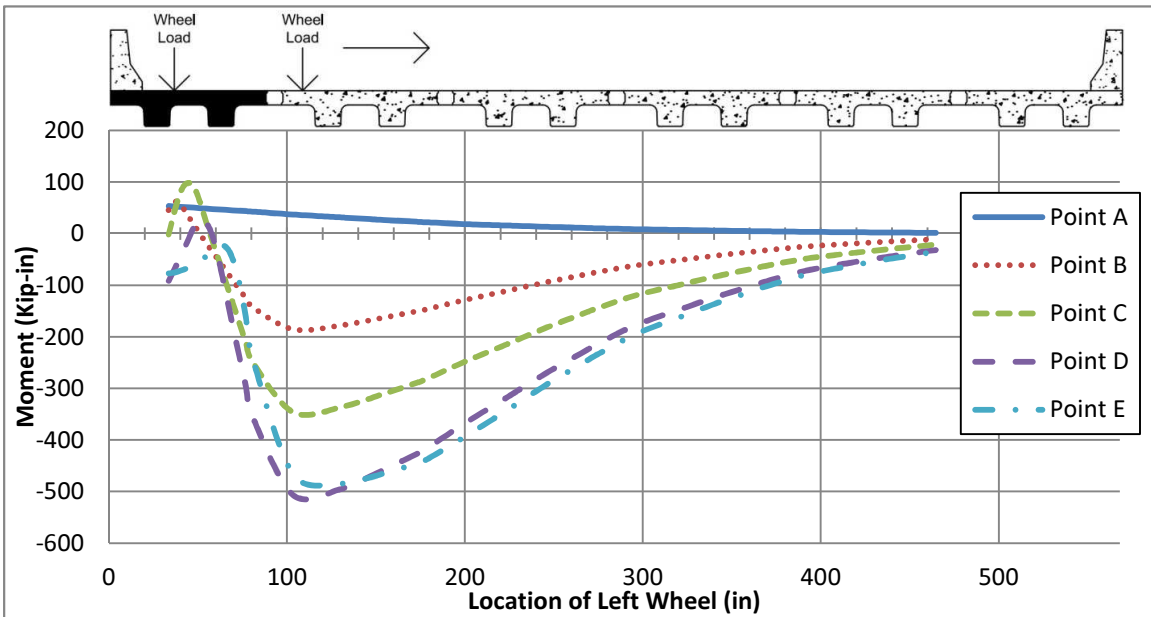
Appendix Figure 61: Shear influence line for the critical deck locations in the eighth beam from the left in a six-foot section NEXT-D bridge



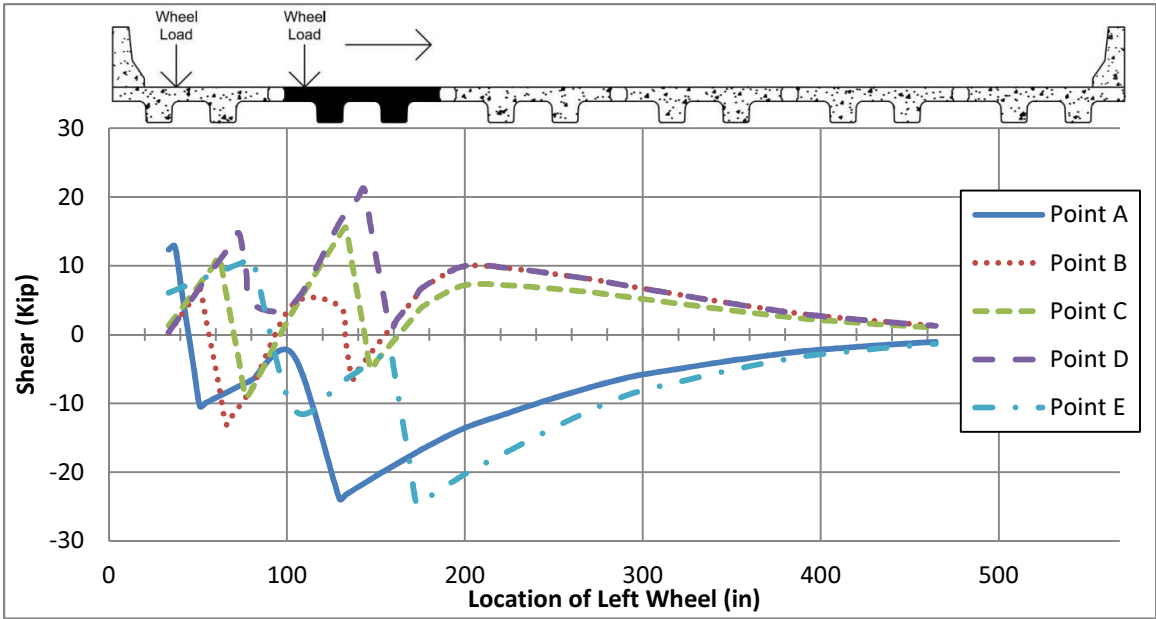
Appendix Figure 62: Moment influence line for the critical deck locations in the eighth beam from the left in a six-foot section NEXT-D bridge



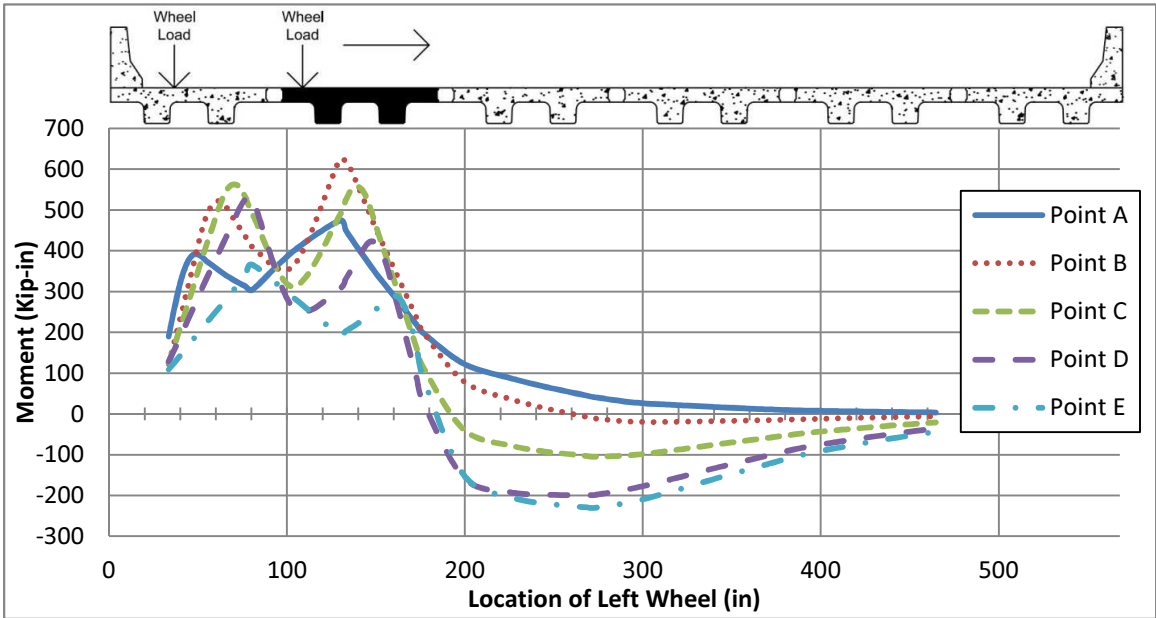
Appendix Figure 63: Shear influence line for the critical deck locations in the first beam from the left in an eight-foot section NEXT-D bridge



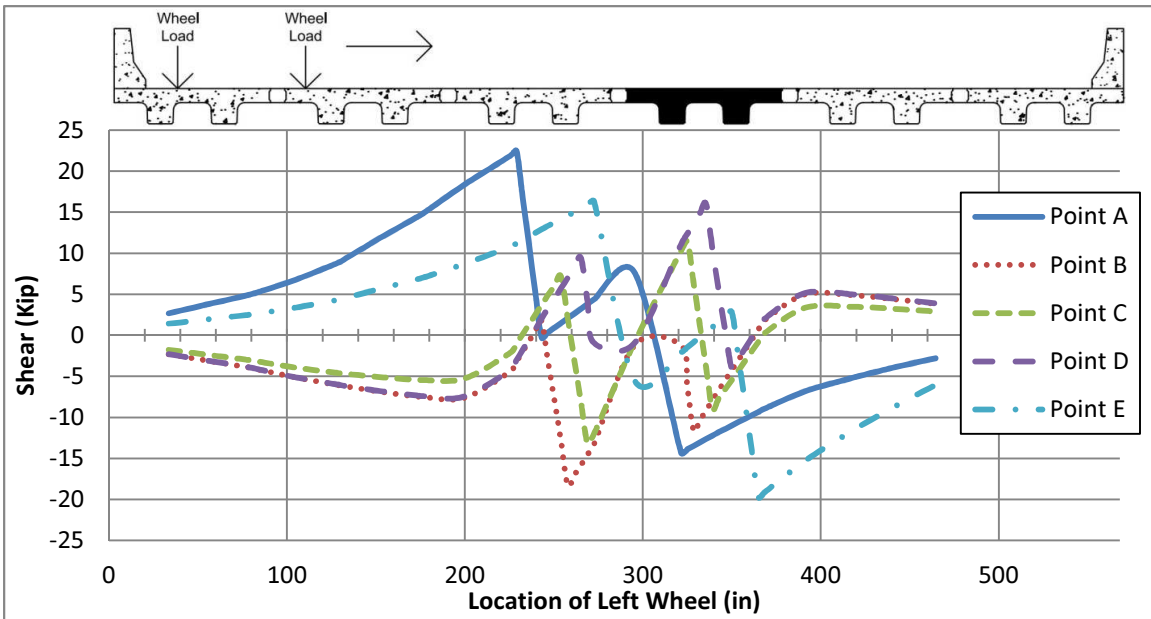
Appendix Figure 64: Moment influence line for the critical deck locations in the first beam from the left in an eight-foot section NEXT-D bridge



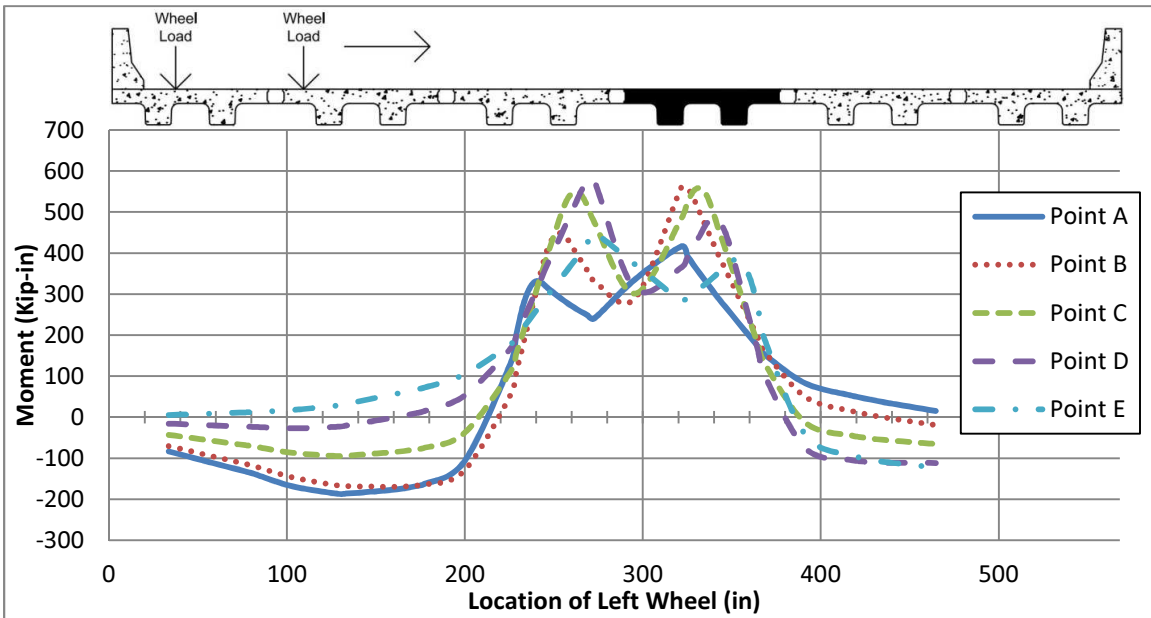
Appendix Figure 65: Shear influence line for the critical deck locations in the second beam from the left in an eight-foot section NEXT-D bridge



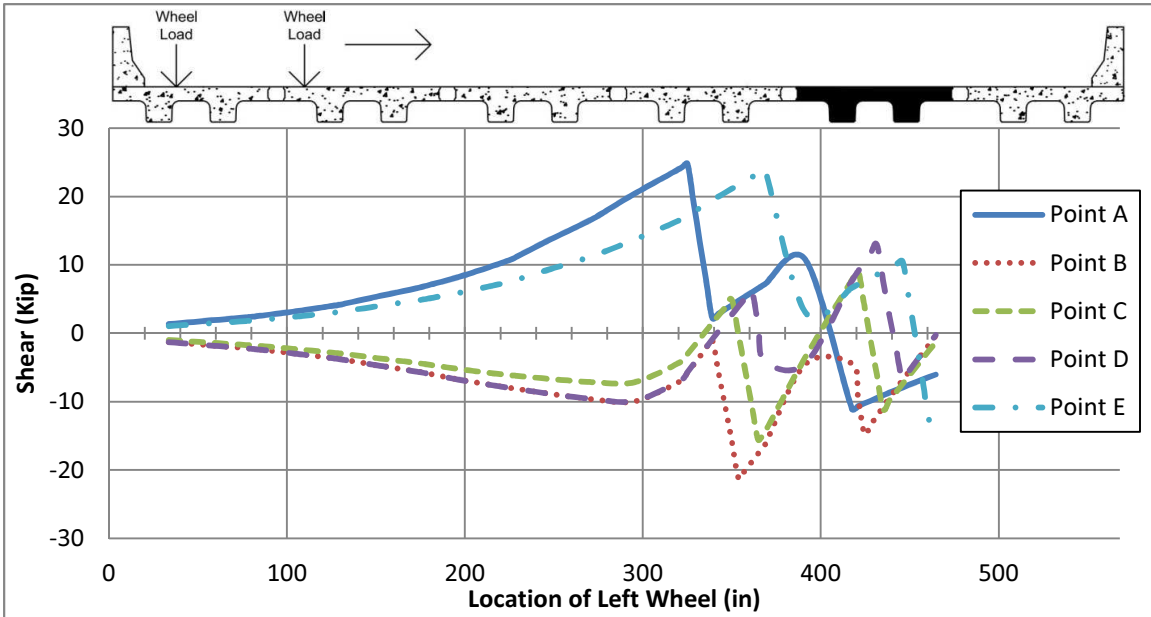
Appendix Figure 66: Moment influence line for the critical deck locations in the second beam from the left in an eight-foot section NEXT-D bridge



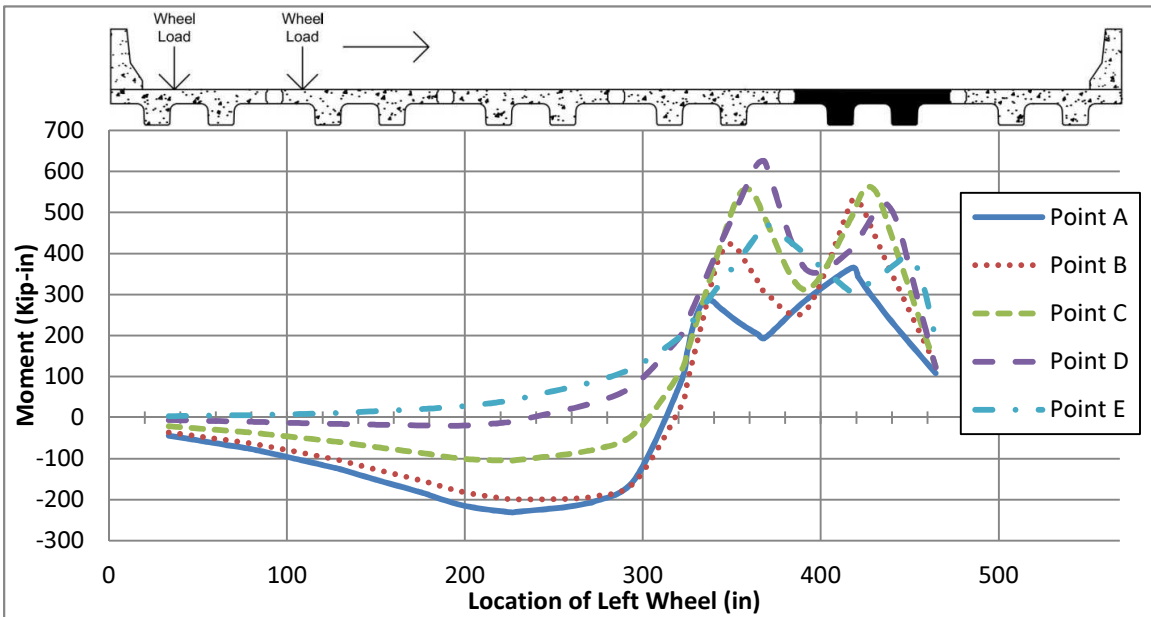
Appendix Figure 67: Shear influence line for the critical deck locations in the fourth beam from the left in an eight-foot section NEXT-D bridge



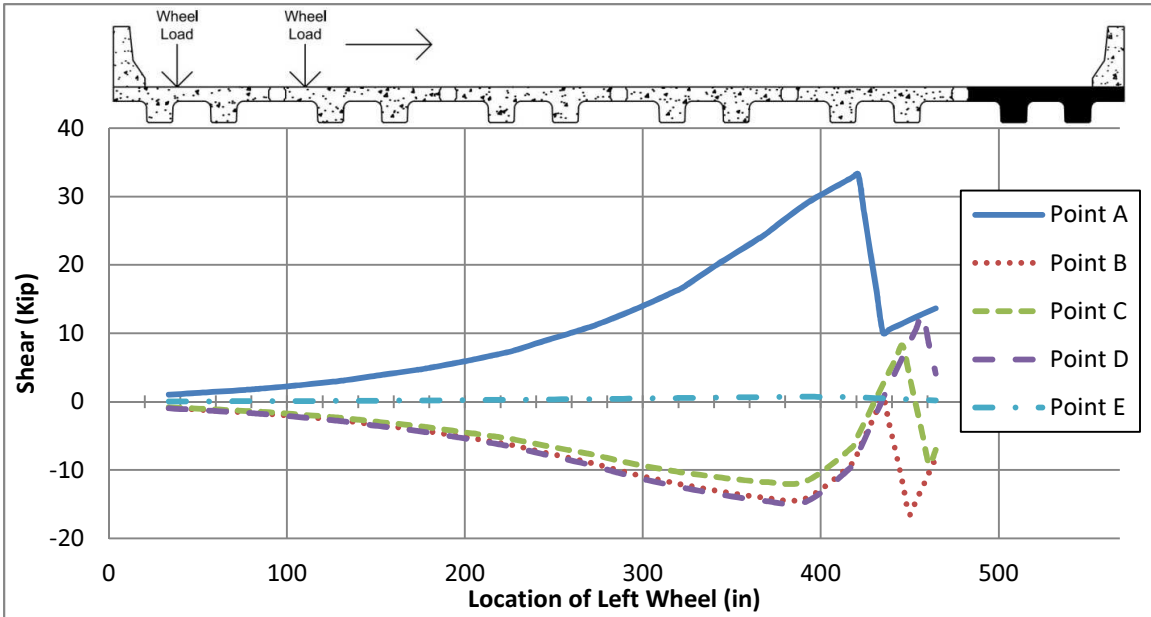
Appendix Figure 68: Moment influence line for the critical deck locations in the fourth beam from the left in an eight-foot section NEXT-D bridge



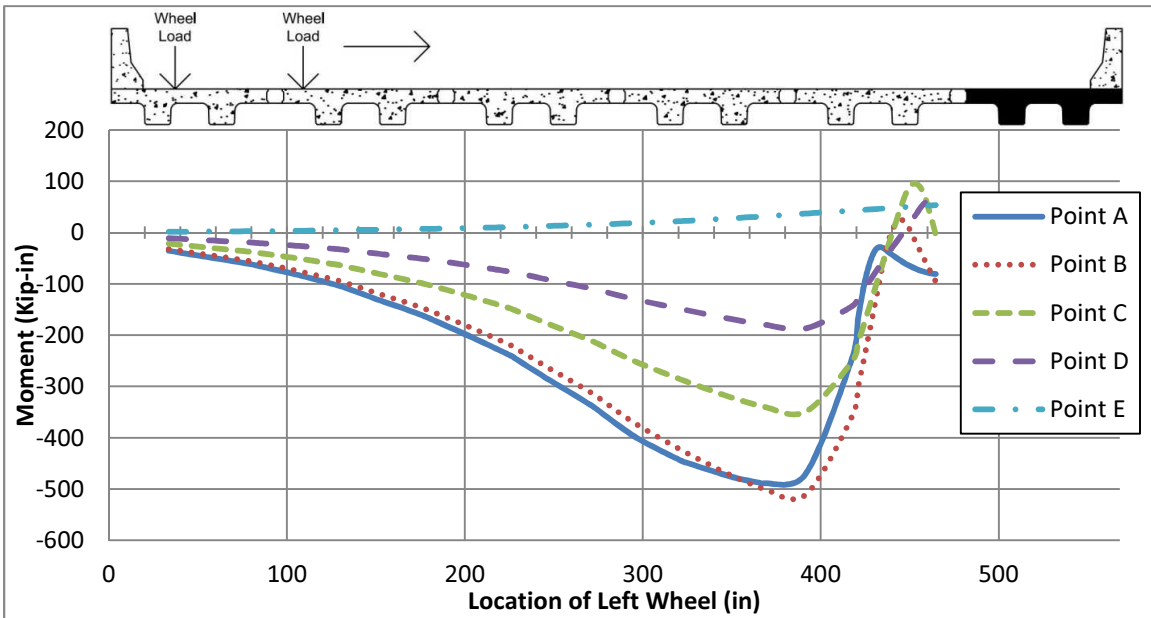
Appendix Figure 69: Shear influence line for the critical deck locations in the fifth beam from the left in an eight-foot section NEXT-D bridge



Appendix Figure 70: Moment influence line for the critical deck locations in the fifth beam from the left in an eight-foot section NEXT-D bridge



Appendix Figure 71: Shear influence line for the critical deck locations in the sixth beam from the left in an eight-foot section NEXT-D bridge



Appendix Figure 72: Moment influence line for the critical deck locations in the sixth beam from the left in an eight-foot section NEXT-D bridge

REFERENCES

- AASHTO. (2010). *AASHTO LRFD Bridge Design Specifications, 5th Ed.* American Association of State Highway and Transportation Officials, Washington, D.C.
- AASHTO Technology Implementation Group. (2002). *Prefabricated Bridges, "Get in, Get out, Stay out."* Washington, D.C.
- ANSYS, I. (2009). "ANSYS® Academic Research." 12.0.
- Computers and Structures, Inc. (2011a). *CSI Analysis Reference Manual.* Computers and Structures, Inc, Berkeley, CA.
- Computers and Structures, Inc. (2011b). "SAP2000." 15.
- CSI Wiki Knowledge Base. (2011). "CSI Wiki Knowledge Base." <<https://wiki.csiberkeley.com/display/kb/Home>> (7/10/2011).
- Culmo, M. (2011). "Face-to-Face Meeting with Michael Culmo."
- Deery, D. P. (2010). "Investigation of Northeast Extreme Tee (NEXT) D Beam Bridges as an Alternative to Precast Hollow Core Bridges: An Exploration of Appropriate Slab Design Forces." Clemson University, Clemson, SC.
- Federal Highway Administration. "General Guidelines for Refined Analysis of Deck Slabs." <<http://www.fhwa.dot.gov/bridge/lrfd/pscusappb.htm>> (11/17/2011).
- Flores Duron, A. (2011). "Behavior of the NEXT-D Beam Shear Key: A Finite Element Approach." PhD thesis, Clemson University, Clemson, SC.
- Nielson, B. G. (2011). *Matrix Structural Analysis Lecture Handouts.*
- PCI Northeast. (2010). "PCI Northeast: Northeast Extreme Tee (NEXT) Beam." <http://pcine.org/index.cfm/resources/bridge/Northeast_Extreme_Tee_Beam> (11/04, 2011).
- SCDOT. (2008). "SCDOT Parapet Details."
- Tonias, D. E., and Zhao, J. J. (2007). *Bridge Engineering.* McGraw Hill, New York, NY.